

COMPOSITE POLYSACCHARIDES AND PROTEIN HYDRO-GELS FOR
CONTROLLED RELEASE APPLICATIONS: FORMULATION,
CHARACTERIZATION AND RELEASE STUDIES

A THESIS SUBMITTED TO
THE GRADUATE SCHOOL OF NATURAL AND APPLIED SCIENCES
OF
MIDDLE EAST TECHNICAL UNIVERSITY

BY

BARIŞ ÖZEL

IN PARTIAL FULFILLMENT OF THE REQUIREMENTS
FOR
THE DEGREE OF DOCTOR OF PHILOSOPHY
IN
FOOD ENGINEERING

JANUARY 2023

Approval of the thesis:

**COMPOSITE POLYSACCHARIDES AND PROTEIN HYDRO-GELS FOR
CONTROLLED RELEASE APPLICATIONS: FORMULATION,
CHARACTERIZATION AND RELEASE STUDIES**

submitted by **BARIŞ ÖZEL** in partial fulfillment of the requirements for the degree
of **Doctor of Philosophy in Food Engineering, Middle East Technical University**
by,

Prof. Dr. Halil Kalıpçılar
Dean, Graduate School of **Natural and Applied Sciences**

Prof. Dr. Hami Alpas
Head of the Department, **Food Engineering**

Assoc. Prof. Dr. Halil Mecit Öztop
Supervisor, **Food Engineering, METU**

Assist. Prof. Dr. Özlem Aydın
Co-Supervisor, **Food Engineering, Ahi Evran University**

Examining Committee Members:

Prof. Dr. Hami Alpas
Food Engineering, METU

Assoc. Prof. Dr. Halil Mecit Öztop
Food Engineering, METU

Prof. Dr. Gülüm Şumnu
Food Engineering, METU

Prof. Dr. Kezban Candoğan
Food Engineering, Ankara University

Assoc. Prof. Dr. Emin Burçin Özvural
Food Engineering, Çankırı Karatekin University

Date: 26.01.2023

I hereby declare that all information in this document has been obtained and presented in accordance with academic rules and ethical conduct. I also declare that, as required by these rules and conduct, I have fully cited and referenced all material and results that are not original to this work.

Name, Last name : Barış Özel

Signature :

ABSTRACT

COMPOSITE POLYSACCHARIDES AND PROTEIN HYDRO-GELS FOR CONTROLLED RELEASE APPLICATIONS: FORMULATION, CHARACTERIZATION AND RELEASE STUDIES

Özel, Barış

Doctor of Philosophy, Food Engineering
Supervisor: Assoc. Prof. Dr. Halil Mecit Öztop
Co-Supervisor: Assist. Prof. Dr. Özlem Aydın

January 2023, 227 pages

Hydrogels are highly hydrophilic polymer gels with macromolecular three-dimensional networks. They can swell by absorbing and retaining large amount of water without dissolving and losing their integrity. Polysaccharides and proteins are commonly used for designing hydrogels to be used in food applications. Encapsulating bioactive agents is one of the common uses of these gels. Composite gels in which one or two polymers are blended to modulate the physicochemical properties of the gels have gained interest due to enhanced stability and release profiles. Pectin (PC), Gum Tragacanth (GT) and Xanthan Gum (XG) were the polysaccharides used for designing Whey Protein Isolate (WPI) based release systems in this study. Black carrot concentrate (BC) having a rich anthocyanin profile was encapsulated in these hydrogels. Release behaviors of the hydrogels were monitored in neutral pH phosphate buffer and simulated *in vitro* gastrointestinal tract (GIT) conditions. Nuclear Magnetic Resonance (NMR) Relaxometry was used as the main characterization technique to understand water-binding behavior of the polymers in different release media. Fourier-Transform Infrared Spectroscopy

(FTIR), Scanning Electron Microscopy (SEM), rheological and textural measurements of hydrogels were also conducted to characterize the hydrogels in detail. Polysaccharide blending retarded the release profiles in phosphate buffer ($p < 0.05$). Composite hydrogels also prevented whole release of BC in gastric phase and delivered some of the encapsulated material in intestinal phase. Especially GT and XG blended samples attained more gradual release profiles in GIT. Simple mathematical and kinetic models were used to define the release in the gel systems. In addition to controlled release experiments, BC loaded hydrogels were applied to whole-fat yogurt samples. Total phenolic contents and antioxidant capacities of the yogurt samples were monitored during four-week storage. Hydrogel blending to yogurt increased the total phenolic contents and antioxidant capacities of the samples. Hydrogels except for XG containing ones also preserved the total phenolic content and the antioxidant capacity of the yogurt during storage.

Keywords: Hydrogel, Whey Protein Isolate, Pectin, Gum Tragacanth, Xanthan Gum

ÖZ

KONTROLLÜ SALINIM AMAÇLI BİLEŞİK POLİSAKKARİT VE PROTEİN HİDROJELLERİ: FORMÜLASYON, KARAKTERİZASYON VE SALINIM ÇALIŞMALARI

Özel, Barış
Doktora, Gıda Mühendisliği
Tez Yöneticisi: Doç. Dr. Halil Mecit Öztop
Ortak Tez Yöneticisi: Dr. Öğr. Üyesi Özlem Aydın

Ocak 2023, 227 sayfa

Hidrojeller, üç boyutlu makromoleküler ve oldukça hidrofilik yapıya sahip polimerik jellerdir. Çözünmeden ve bütünlüklerini kaybetmeden yüksek miktarda su alarak şişebilirler. Gıdalarda kullanmak amacıyla protein ve polisakkaritler hidrojel tasarımlarında kullanılabilirler. Bu jellerin yaygın kullanım alanlarından biri aktif ajanların bu jeller içerisine kapsüllenmesidir. Birkaç polimerin, jelin fiziko-kimyasal özelliklerini ayarlamak için karıştırılmasıyla oluşturulan bileşik jeller, stabilite ve salım profillerini geliştirdiği için önem kazanmıştır. Bu çalışmada, pektin (PC), kitre (GT) ve ksantan sakızı (XG) polisakkaritleri, peynir altı suyu protein izolatu (WPI) temelli salım sistemleri oluşturmak için kullanılmıştır. Zengin bir antosiyanin kaynağı olan kara havuç suyu konsantresi (BC) bu hidrojellerde kapsüllenmiştir. Hidrojellerin salım davranışları, nötr pH'daki fosfat tampon çözeltisi ve simüle edilmiş mide – bağırsak sistemi (GIT) ortamlarında gözlemlenmiştir. Polimerlerin su bağlama davranışlarını değişik salım ortamlarında karakterize etmek için temel olarak Nükleer Manyetik Rezonans (NMR) relaksasyon tekniği kullanılmıştır. Hidrojelleri detaylı olarak inceleyebilmek için Fourier Dönüşümü Kızılötesi

Spektroskopisi (FTIR), Taramalı Elektron Mikroskopisi (SEM), reolojik ve dokusal ölçümler de yapılmıştır. Polisakkarit karıştırılması, protein jellerin fosfat tampon çözeltisindeki salımını yavaşlatmıştır ($p < 0.05$). Bileşik jeller ayrıca mide fazında tüm BC içeriğini serbest bırakmamış, bir miktarını yapısında tutmaya devam ederek bağırsak fazına taşımıştır. Özellikle GT ve XG içeren örnekler sindirim sisteminde daha kademeli bir salım göstermişlerdir. Salım davranışlarını belirlemek için basit matematiksel ve kinetik modellerden yararlanılmıştır. Kontrollü salım deneylerine ek olarak, BC içeren hidrojeller tam yağlı yoğurt örneklerine uygulanmıştır. Bu yoğurt örneklerinin toplam fenolik ve antioksidan içerikleri dört haftalık depolama boyunca izlenmiştir. Yoğurt örneklerine hidrojel karıştırılması, bu örneklerin toplam fenolik ve antioksidan miktarlarını arttırmıştır. XG içeren hidrojeller dışında yoğurda hidrojel karıştırılması, yoğurdun depolama süresi boyunca toplam fenolik miktarını ve antioksidan aktivitesini korumuştur.

Anahtar Kelimeler: Hidrojel, Peynir Altı Suyu İzolatı, Pektin, Kitre, Ksantan Sakızı

In memory of my beloved Grandmother Tayyibe Gemiciođlu

ACKNOWLEDGMENTS

Firstly, I am grateful to my supervisor Assoc. Prof. Dr. Halil Mecit Öztop for his guidance, encouragement and support throughout my study. He has immensely contributed to my general scientific perspective and always encouraged me to do my best. It was a privilege and pleasure for me to work with him. I also would like to thank my co-advisor Assist. Prof. Dr. Özlem Aydın for her continuous help, interest and support.

I would like to extend my gratitude to my thesis committee members Prof. Dr. Gülüm Şumnu and Prof. Dr. Kezban Candoğan for their valuable suggestions and contributions to my dissertation. I am also grateful to our department head Prof. Dr. Hami Alpas for his continuous support during my PhD. I would also like to thank Prof. Dr. Haluk Hamamci for his guidance and support.

I am truly grateful to my beloved family for their continuous, unconditional support that has allowed me to continue my doctoral studies. Therefore, I would like to express my deepest appreciation to my mother, Müjgan Özel, my father, Tarık Özel and my brother, Mert Özel.

Lastly, I would like to acknowledge Turkish Fulbright Commission PhD Dissertation Research program. I would also like to thank Prof. Dr. David Julian McClements for giving me the opportunity to work in his lab at University of Massachusetts Amherst (UMASS) for one academic year.

TABLE OF CONTENTS

ABSTRACT.....	v
ÖZ.....	vii
ACKNOWLEDGMENTS	x
TABLE OF CONTENTS.....	xi
LIST OF TABLES	xvi
LIST OF FIGURES	xxx
LIST OF ABBREVIATIONS	xxxiii
LIST OF SYMBOLS	xxxv
CHAPTERS	
1 INTRODUCTION	1
1.1 Hydrogels	1
1.1.1 Heat Induced Gelling of Proteins.....	2
1.1.2 Heating Methods	3
1.1.2.1 Conventional Heating	3
1.1.2.2 Microwave Heating	3
1.1.3 Composite Hydrogels.....	4
1.2 Biopolymers for Hydrogel Production	6
1.2.1 Whey Protein Isolate.....	7
1.2.2 Pectin.....	9
1.2.3 Gum Tragacanth.....	12
1.2.4 Xanthan Gum	15
1.3 Controlled Release Applications	19

1.3.1	Controlled Release in GIT	20
1.3.2	Food Applications	22
1.4	Black Carrot (<i>Daucus carota</i>) Concentrate	23
1.5	Characterization of Hydrogels	28
1.5.1	Low Field (LF) Nuclear Magnetic Resonance (NMR) Relaxometry	29
1.5.1.1	Transverse Relaxation Time (T ₂)	30
1.5.1.2	Self-Diffusion Coefficient (SDC)	32
1.5.2	Fourier Transform Infrared (FTIR) Spectroscopy	32
1.5.3	Scanning Electron Microscopy	33
1.5.4	Rheology and Texture Characterization	34
1.5.4.1	Rheology of Hydrogel Forming Solutions	34
1.5.4.2	Texture of Hydrogels	34
1.5.5	Release Modellings	35
1.6	Objectives of the Study	36
2	MATERIALS AND METHODS	39
2.1	Materials	39
2.2	Hydrogel Preparation	40
2.3	Release Media Preparations	41
2.3.1	Phosphate Buffer	41
2.3.2	Simulated Gastric Fluid (SGF)	41
2.3.3	Simulated Intestinal Fluid (SIF)	42
2.4	Swelling Experiments	42
2.5	Monitoring the Release of Black Carrot Concentrate (BC)	42
2.5.1	Release in Phosphate Buffer	43

2.5.2	Release in SGF	43
2.5.3	Release in SIF	43
2.6	Dielectric Measurements	44
2.7	Viscosity Measurements	44
2.8	LF NMR Relaxometry Experiments	45
2.8.1	T ₂ Measurements	45
2.8.2	SDC Measurements	45
2.9	FTIR Analysis	46
2.10	Rheology Measurements	46
2.10.1	Determination of Flow Behavior	47
2.10.2	Amplitude Tests	47
2.10.3	Frequency Sweep Tests.....	47
2.10.4	Temperature Sweep Tests	47
2.11	Texture Analysis	48
2.12	Zeta Potential Analysis	48
2.13	Sugar Composition Analysis of BC.....	48
2.14	Moisture and pH Measurements.....	49
2.15	Gel Total Acidity Measurements.....	49
2.16	Weight Loss Determination of Hydrogels in SIF	50
2.17	Soluble Protein Content Measurements.....	50
2.18	Release Behavior Modelling of Hydrogels.....	51
2.18.1	Release Modelling in Phosphate Buffer and SGF	51
2.18.2	Release Trend in SIF.....	51
2.19	SEM Analysis	52

2.20	Total Phenolic Content in Yogurt	52
2.21	Antioxidant Capacity in Yogurt	53
2.22	Statistical Analysis	54
2.23	Experimental Design	54
3	RESULTS AND DISCUSSION.....	57
3.1	Characterization of Hydrogel Solutions	57
3.1.1	Rheology Analysis.....	57
3.1.1.1	Flow Behavior Analysis	57
3.1.1.2	Amplitude Sweep Analysis	60
3.1.1.3	Frequency Sweep Analysis	62
3.1.1.4	Temperature Sweep Analysis.....	63
3.1.2	Dielectric Properties	66
3.1.3	Zeta Potential and pH Analysis	68
3.2	Controlled Release in Phosphate Buffer	70
3.2.1	Swelling Ratios.....	71
3.2.2	Release Profiles	73
3.2.3	NMR Relaxometry Analysis	79
3.2.3.1	T ₂ Analysis	79
3.2.3.2	SDC Analysis	83
3.2.4	Hardness Analysis	84
3.2.5	Release Modelling	86
3.2.6	Microstructure Analysis	87
3.3	Controlled Release in GIT	90
3.3.1	Simulated Gastric Phase	91

3.3.1.1	Release Profiles	91
3.3.1.2	NMR Relaxometry Analysis	94
3.3.1.3	Release Modelling	97
3.3.1.4	Hardness Analysis	98
3.3.1.5	FTIR Analysis.....	99
3.3.1.6	Total Acidity, pH and Moisture Analysis.....	105
3.3.2	Simulated Intestinal Phase	108
3.3.2.1	Release Profiles	108
3.3.2.2	Soluble Protein Contents in Digestion Media	112
3.3.2.3	NMR Relaxometry Analysis	115
3.3.2.4	FTIR Analysis.....	117
3.3.2.5	Hardness Analysis	122
3.3.2.6	Release Trend in SIF	124
3.3.2.7	Weight Loss of Hydrogels in SIF	126
3.3.2.8	Microstructure Analysis.....	127
3.4	Application of Hydrogels in Yogurt.....	131
4	CONCLUSIONS AND RECOMMENDATIONS	137
	REFERENCES	141
A.	Statistical Analysis.....	163
	CURRICULUM VITAE.....	225

LIST OF TABLES

TABLES

Table 2.1 Experimental design of the release and food application experiments ...	55
Table 3.1 Apparent viscosity values of Newtonian hydrogel solutions	58
Table 3.2 Flow parameters of Gum Tragacanth hydrogel solutions	59
Table 3.3 Flow parameters of Xanthan Gum hydrogel solutions.....	59
Table 3.4 Dielectric properties of hydrogel solutions	67
Table 3.5 Zeta potential values of the hydrogel forming solutions.....	68
Table 3.6 pH values of the hydrogel solutions with and without BC.....	69
Table 3.7 Viscosities of BC containing hydrogel solutions	72
Table 3.8 SDC values of CV and MW hydrogels before exposing to release medium (0 h)	83
Table 3.9 SDC values of CV and MW hydrogels (6 h).....	84
Table 3.10 Diffusion coefficients of CV and MW hydrogels	87
Table 3.11 Diffusion coefficient of hydrogels in SGF	98
Table 3.12 Total acidity values of hydrogels before and after gastric treatment ..	106
Table 3.13 Moisture increase and pH reduction ratios of hydrogels during gastric treatment.....	108
Table 3.14 Soluble protein contents of the release media after gastric digestion (SGF 2 h) and overall gastrointestinal digestion (SIF 8 h) caused by the protein losses of respective hydrogels.	114
Table 3.15 Weight loss ratios of hydrogels in SIF	127
Table 3.16 Total phenolic contents of the yogurt samples in the presence and absence of the hydrogels	131
Table 3.17 Antioxidant capacity of the yogurt samples in the presence and absence of the hydrogels	132
Table A.1 One way Analysis of Variance (ANOVA) and Tukey's comparison test for the apparent viscosity (Pa s) values of BC containing different hydrogel solutions	163

Table A.2 General linear model and Tukey’s comparison test for the apparent viscosity (Pa s) vs hydrogel solution; solution type of the C and PC hydrogel solutions	163
Table A.3 One way Analysis of Variance (ANOVA) and Tukey’s comparison test for the consistency index values (k, Pa s) of GT hydrogel solutions in the presence and absence of BC	164
Table A.4 One way Analysis of Variance (ANOVA) and Tukey’s comparison test for the flow behavior index values (n) of GT hydrogel solutions in the presence and absence of BC	165
Table A.5 One way Analysis of Variance (ANOVA) and Tukey’s comparison test for the yield stress values (Pa) of XG hydrogel solutions in the presence and absence of BC	165
Table A.6 One way Analysis of Variance (ANOVA) and Tukey’s comparison test for the consistency index values (k, Pa s) of XG hydrogel solutions in the presence and absence of BC	165
Table A.7 One way Analysis of Variance (ANOVA) and Tukey’s comparison test for the flow behavior index values (n) of XG hydrogel solutions in the presence and absence of BC	166
Table A.8 One way Analysis of Variance (ANOVA) and Tukey’s comparison test for the critical gelling temperatures (°C) of the different BC containing hydrogel solutions	166
Table A.9 One way Analysis of Variance (ANOVA) and Tukey’s comparison test for the dielectric constant values of the different BC containing hydrogel solutions and distilled water	167
Table A.10 One way Analysis of Variance (ANOVA) and Tukey’s comparison test for the dielectric loss factor values of the different BC containing hydrogel solutions and distilled water	167
Table A.11 General linear model and Tukey’s comparison test for the absolute zeta potential (mV) vs BC presence; hydrogel solution type (C, PC, GT & XG)	168

Table A.12 One way Analysis of Variance (ANOVA) and Tukey’s comparison test for the pH values of the different BC containing hydrogel solutions.....	169
Table A.13 One way Analysis of Variance (ANOVA) and Tukey’s comparison test for the pH values of the different hydrogel solutions in the absence of BC	169
Table A.14 One way Analysis of Variance (ANOVA) and Tukey’s comparison test for the pH values of the PC hydrogel solutions in the absence and presence of BC	169
Table A.15 One way Analysis of Variance (ANOVA) and Tukey’s comparison test for the pH values of the GT hydrogel solutions in the absence and presence of BC	170
Table A.16 One way Analysis of Variance (ANOVA) and Tukey’s comparison test for the pH values of the C hydrogel solutions in the absence and presence of BC	170
Table A.17 One way Analysis of Variance (ANOVA) and Tukey’s comparison test for the pH values of the XG hydrogel solutions in the absence and presence of BC	171
Table A.18 One way Analysis of Variance (ANOVA) and Tukey’s comparison test for the swelling ratios (%) of the CV hydrogels in phosphate buffer at 6 h.....	171
Table A.19 One way Analysis of Variance (ANOVA) and Tukey’s comparison test for the swelling ratios (%) of the CV hydrogels in phosphate buffer at 24 h.....	171
Table A.20 One way Analysis of Variance (ANOVA) and Tukey’s comparison test for the change in the swelling ratios (%) of the CV PC hydrogels in phosphate buffer during 24 h experiment.....	172
Table A.21 One way Analysis of Variance (ANOVA) and Tukey’s comparison test for the change in the swelling ratios (%) of the CV XG hydrogels in phosphate buffer during 24 h experiment.....	172
Table A.22 One way Analysis of Variance (ANOVA) and Tukey’s comparison test for the change in the swelling ratios (%) of the CV C hydrogels in phosphate buffer during 24 h experiment.....	173

Table A.23 One way Analysis of Variance (ANOVA) and Tukey’s comparison test for the change in the swelling ratios (%) of the CV GT hydrogels in phosphate buffer during 24 h experiment	173
Table A.24 One way Analysis of Variance (ANOVA) and Tukey’s comparison test for the viscosity values (cP) of the hydrogel solutions	174
Table A.25 One way Analysis of Variance (ANOVA) and Tukey’s comparison test for the release rates (%) of the different CV hydrogels in phosphate buffer at 24 h	174
Table A.26 One way Analysis of Variance (ANOVA) and Tukey’s comparison test for the release rates (%) of the different MW hydrogels in phosphate buffer at 24 h	175
Table A.27 General linear model and Tukey’s comparison test for the release rates (%) vs hydrogel type (C, PC, GT, XG); heating type (CV, MW) in phosphate buffer at 24 h.....	175
Table A.28 One way Analysis of Variance (ANOVA) and Tukey’s comparison test for the change in the release rates (%) of the CV PC hydrogels in phosphate buffer during 24 h experiment	176
Table A.29 One way Analysis of Variance (ANOVA) and Tukey’s comparison test for the change in the release rates (%) of the CV XG hydrogels in phosphate buffer during 24 h experiment	177
Table A.30 One way Analysis of Variance (ANOVA) and Tukey’s comparison test for the change in the release rates (%) of the CV GT hydrogels in phosphate buffer during 24 h experiment	177
Table A.31 One way Analysis of Variance (ANOVA) and Tukey’s comparison test for the change in the release rates (%) of the CV C hydrogels in phosphate buffer during 24 h experiment	178
Table A.32 One way Analysis of Variance (ANOVA) and Tukey’s comparison test for the change in the release rates (%) of the MW PC hydrogels in phosphate buffer during 24 h experiment	178

Table A.33 One way Analysis of Variance (ANOVA) and Tukey's comparison test for the change in the release rates (%) of the MW XG hydrogels in phosphate buffer during 24 h experiment.....	179
Table A.34 One way Analysis of Variance (ANOVA) and Tukey's comparison test for the change in the release rates (%) of the MW GT hydrogels in phosphate buffer during 24 h experiment.....	179
Table A.35 One way Analysis of Variance (ANOVA) and Tukey's comparison test for the change in the release rates (%) of the MW C hydrogels in phosphate buffer during 24 h experiment.....	180
Table A.36 One way Analysis of Variance (ANOVA) and Tukey's comparison test for the transverse relaxation times (T_2 , ms) of the different CV hydrogels at 0 h	180
Table A.37 One way Analysis of Variance (ANOVA) and Tukey's comparison test for the transverse relaxation times (T_2 , ms) of the different CV hydrogels in phosphate buffer at 24 h	181
Table A.38 One way Analysis of Variance (ANOVA) and Tukey's comparison test for the transverse relaxation times (T_2 , ms) of the different MW hydrogels at 0 h	181
Table A.39 One way Analysis of Variance (ANOVA) and Tukey's comparison test for the transverse relaxation times (T_2 , ms) of the different MW hydrogels in phosphate buffer at 24 h	182
Table A.40 General linear model and Tukey's comparison test for the transverse relaxation times (T_2 , ms) vs hydrogel type (C, PC, GT, XG); heating type (CV, MW) at 0 h	182
Table A.41 General linear model and Tukey's comparison test for the transverse relaxation times (T_2 , ms) vs hydrogel type (C, PC, GT, XG); heating type (CV, MW) in phosphate buffer at 24 h	183
Table A.42 One way Analysis of Variance (ANOVA) and Tukey's comparison test for the change in the transverse relaxation times (T_2 , ms) of the CV PC hydrogels in phosphate buffer during 24 h experiment.....	184

Table A.43 One way Analysis of Variance (ANOVA) and Tukey’s comparison test for the change in the transverse relaxation times (T_2 , ms) of the CV XG hydrogels in phosphate buffer during 24 h experiment	185
Table A.44 One way Analysis of Variance (ANOVA) and Tukey’s comparison test for the change in the transverse relaxation times (T_2 , ms) of the CV C hydrogels in phosphate buffer during 24 h experiment	185
Table A.45 One way Analysis of Variance (ANOVA) and Tukey’s comparison test for the change in the transverse relaxation times (T_2 , ms) of the CV GT hydrogels in phosphate buffer during 24 h experiment	186
Table A.46 One way Analysis of Variance (ANOVA) and Tukey’s comparison test for the change in the transverse relaxation times (T_2 , ms) of the MW PC hydrogels in phosphate buffer during 24 h experiment	186
Table A.47 One way Analysis of Variance (ANOVA) and Tukey’s comparison test for the change in the transverse relaxation times (T_2 , ms) of the MW XG hydrogels in phosphate buffer during 24 h experiment	187
Table A.48 One way Analysis of Variance (ANOVA) and Tukey’s comparison test for the change in the transverse relaxation times (T_2 , ms) of the MW C hydrogels in phosphate buffer during 24 h experiment	187
Table A.49 One way Analysis of Variance (ANOVA) and Tukey’s comparison test for the change in the transverse relaxation times (T_2 , ms) of the MW GT hydrogels in phosphate buffer during 24 h experiment	188
Table A.50 One way Analysis of Variance (ANOVA) and Tukey’s comparison test for the self-diffusion coefficient ($SDC \times 10^9$, m^2/s) of the different CV hydrogels at 0 h.....	188
Table A.51 One way Analysis of Variance (ANOVA) and Tukey’s comparison test for the self-diffusion coefficient ($SDC \times 10^9$, m^2/s) of the different CV hydrogels in phosphate buffer at 6 h.....	189
Table A.52 One way Analysis of Variance (ANOVA) and Tukey’s comparison test for the self-diffusion coefficient ($SDC \times 10^9$, m^2/s) of the different MW hydrogels at 0 h.....	189

Table A.53 One way Analysis of Variance (ANOVA) and Tukey’s comparison test for the self-diffusion coefficient (SDC x 10 ⁹ , m ² /s) of the different MW hydrogels in phosphate buffer at 6 h	190
Table A.54 General linear model and Tukey’s comparison test for the self-diffusion coefficient (SDC x 10 ⁹ , m ² /s) vs hydrogel type (C, PC, GT, XG); heating type (CV, MW) at 0 h.....	190
Table A.55 General linear model and Tukey’s comparison test for the self-diffusion coefficient (SDC x 10 ⁹ , m ² /s) vs hydrogel type (C, PC, GT, XG); heating type (CV, MW) in phosphate buffer at 6 h	191
Table A.56 One way Analysis of Variance (ANOVA) and Tukey’s comparison test for the change in the self-diffusion coefficient (SDC x 10 ⁹ , m ² /s) of the CV PC hydrogels in phosphate buffer during 6 h experiment.....	192
Table A.57 One way Analysis of Variance (ANOVA) and Tukey’s comparison test for the change in the self-diffusion coefficient (SDC x 10 ⁹ , m ² /s) of the CV XG hydrogels in phosphate buffer during 6 h experiment.....	193
Table A.58 One way Analysis of Variance (ANOVA) and Tukey’s comparison test for the change in the self-diffusion coefficient (SDC x 10 ⁹ , m ² /s) of the CV GT hydrogels in phosphate buffer during 6 h experiment.....	193
Table A.59 One way Analysis of Variance (ANOVA) and Tukey’s comparison test for the change in the self-diffusion coefficient (SDC x 10 ⁹ , m ² /s) of the CV C hydrogels in phosphate buffer during 6 h experiment.....	194
Table A.60 One way Analysis of Variance (ANOVA) and Tukey’s comparison test for the change in the self-diffusion coefficient (SDC x 10 ⁹ , m ² /s) of the MW PC hydrogels in phosphate buffer during 6 h experiment.....	194
Table A.61 One way Analysis of Variance (ANOVA) and Tukey’s comparison test for the change in the self-diffusion coefficient (SDC x 10 ⁹ , m ² /s) of the MW XG hydrogels in phosphate buffer during 6 h experiment.....	195
Table A.62 One way Analysis of Variance (ANOVA) and Tukey’s comparison test for the change in the self-diffusion coefficient (SDC x 10 ⁹ , m ² /s) of the MW GT hydrogels in phosphate buffer during 6 h experiment.....	195

Table A.63 One way Analysis of Variance (ANOVA) and Tukey’s comparison test for the change in the self-diffusion coefficient (SDC x 10 ⁹ , m ² /s) of the MW C hydrogels in phosphate buffer during 6 h experiment	196
Table A.64 One way Analysis of Variance (ANOVA) and Tukey’s comparison test for the hardness values (N) of the different CV hydrogels at 0 h	196
Table A.65 One way Analysis of Variance (ANOVA) and Tukey’s comparison test for the hardness values (N) of the different CV hydrogels in phosphate buffer at 24 h.....	197
Table A.66 One way Analysis of Variance (ANOVA) and Tukey’s comparison test for the change in the hardness values (N) of the CV PC hydrogels in phosphate buffer during 24 h experiment	197
Table A.67 One way Analysis of Variance (ANOVA) and Tukey’s comparison test for the change in the hardness values (N) of the CV XG hydrogels in phosphate buffer during 24 h experiment	198
Table A.68 One way Analysis of Variance (ANOVA) and Tukey’s comparison test for the change in the hardness values (N) of the CV GT hydrogels in phosphate buffer during 24 h experiment	198
Table A.69 One way Analysis of Variance (ANOVA) and Tukey’s comparison test for the change in the hardness values (N) of the CV C hydrogels in phosphate buffer during 24 h experiment	199
Table A.70 One way Analysis of Variance (ANOVA) and Tukey’s comparison test for the diffusion coefficient values (m ² /s) of the different CV hydrogels in phosphate buffer.....	199
Table A.71 One way Analysis of Variance (ANOVA) and Tukey’s comparison test for the diffusion coefficient values (m ² /s) of the different MW hydrogels in phosphate buffer.....	200
Table A.72 One way Analysis of Variance (ANOVA) and Tukey’s comparison test for the diffusion coefficient values (m ² /s) of the CV and MW C hydrogels in phosphate buffer.....	200

Table A.73 One way Analysis of Variance (ANOVA) and Tukey’s comparison test for the diffusion coefficient values (m^2/s) of the CV and MW PC hydrogels in phosphate buffer	201
Table A.74 One way Analysis of Variance (ANOVA) and Tukey’s comparison test for the diffusion coefficient values (m^2/s) of the CV and MW GT hydrogels in phosphate buffer	201
Table A.75 One way Analysis of Variance (ANOVA) and Tukey’s comparison test for the diffusion coefficient values (m^2/s) of the CV and MW XG hydrogels in phosphate buffer	202
Table A.76 One way Analysis of Variance (ANOVA) and Tukey’s comparison test for the cumulative release rates (%) of the CV hydrogels in GIT (8 h)	202
Table A.77 One way Analysis of Variance (ANOVA) and Tukey’s comparison test for the cumulative release rates (%) of the CV hydrogels in SGF (2 h)	202
Table A.78 One way Analysis of Variance (ANOVA) and Tukey’s comparison test for the transverse relaxation times (T_2 , ms) of the different CV hydrogels before gastric treatment	203
Table A.79 One way Analysis of Variance (ANOVA) and Tukey’s comparison test for the transverse relaxation times (T_2 , ms) of the different CV hydrogels after gastric treatment (2 h)	203
Table A.80 One way Analysis of Variance (ANOVA) and Tukey’s comparison test for the change in the transverse relaxation times (T_2 , ms) of the CV PC hydrogels in SGF during 2 h experiment	204
Table A.81 One way Analysis of Variance (ANOVA) and Tukey’s comparison test for the change in the transverse relaxation times (T_2 , ms) of the CV XG hydrogels in SGF during 2 h experiment	204
Table A.82 One way Analysis of Variance (ANOVA) and Tukey’s comparison test for the change in the transverse relaxation times (T_2 , ms) of the CV C hydrogels in SGF during 2 h experiment	205

Table A.83 One way Analysis of Variance (ANOVA) and Tukey’s comparison test for the change in the transverse relaxation times (T_2 , ms) of the CV GT hydrogels in SGF during 2 h experiment.....	205
Table A.84 One way Analysis of Variance (ANOVA) and Tukey’s comparison test for the self-diffusion coefficients (SDC, m^2/s) of the different CV hydrogels before gastric treatment.....	206
Table A.85 One way Analysis of Variance (ANOVA) and Tukey’s comparison test for the self-diffusion coefficients (SDC, m^2/s) of the different CV hydrogels after gastric treatment (2 h).....	206
Table A.86 One way Analysis of Variance (ANOVA) and Tukey’s comparison test for the change in the self-diffusion coefficients (SDC, m^2/s) of the CV PC hydrogels in SGF during 2 h experiment.....	207
Table A.87 One way Analysis of Variance (ANOVA) and Tukey’s comparison test for the change in the self-diffusion coefficients (SDC, m^2/s) of the CV XG hydrogels in SGF during 2 h experiment.....	207
Table A.88 One way Analysis of Variance (ANOVA) and Tukey’s comparison test for the change in the self-diffusion coefficients (SDC, m^2/s) of the CV GT hydrogels in SGF during 2 h experiment.....	208
Table A.89 One way Analysis of Variance (ANOVA) and Tukey’s comparison test for the change in the self-diffusion coefficients (SDC, m^2/s) of the CV C hydrogels in SGF during 2 h experiment.....	208
Table A.90 One way Analysis of Variance (ANOVA) and Tukey’s comparison test for the diffusion coefficient values (m^2/s) of the CV hydrogels in SGF (2 h).....	208
Table A.91 One way Analysis of Variance (ANOVA) and Tukey’s comparison test for the hardness values (N) of the CV hydrogels after gastric treatment (2 h).....	209
Table A.92 One way Analysis of Variance (ANOVA) and Tukey’s comparison test for the total acidity values (g citric acid/100 g gel) of the CV hydrogels before gastric treatment	209

Table A.93 One way Analysis of Variance (ANOVA) and Tukey’s comparison test for the total acidity values (g citric acid/100 g gel) of the CV hydrogels after gastric treatment (2 h)	210
Table A.94 One way Analysis of Variance (ANOVA) and Tukey’s comparison test for the reduction of the pH (%) of the CV hydrogels in SGF during 2 h experiment	210
Table A.95 One way Analysis of Variance (ANOVA) and Tukey’s comparison test for the increase of the moisture content (%) of the CV hydrogels in SGF during 2 h experiment	211
Table A.96 One way Analysis of Variance (ANOVA) and Tukey’s comparison test for the increase in the release rates (%) of the CV hydrogels in SIF (2 h) with respect to their final release rates after gastric treatment.....	211
Table A.97 One way Analysis of Variance (ANOVA) and Tukey’s comparison test for the increase in the release rates (%) of the CV hydrogels in SIF (4 h) with respect to their final release rates after gastric treatment.....	212
Table A.98 One way Analysis of Variance (ANOVA) and Tukey’s comparison test for the increase in the release rates (%) of the CV hydrogels in SIF (6 h) with respect to their final release rates after gastric treatment.....	212
Table A.99 One way Analysis of Variance (ANOVA) and Tukey’s comparison test for the soluble protein contents (mg BSA/mL) of the CV hydrogel containing SGF release media at the end of the gastric treatment.....	213
Table A.100 One way Analysis of Variance (ANOVA) and Tukey’s comparison test for the soluble protein contents (mg BSA/mL) of the CV hydrogel containing SIF release media at the end of the intestinal treatment.....	213
Table A.101 One way Analysis of Variance (ANOVA) and Tukey’s comparison test for the transverse relaxation times (T_2 , ms) of the CV hydrogels after SIF treatment (6 h)	214
Table A.102 One way Analysis of Variance (ANOVA) and Tukey’s comparison test for the change in the transverse relaxation times (T_2 , ms) of the CV C hydrogels during SIF treatment (6 h)	214

Table A.103 One way Analysis of Variance (ANOVA) and Tukey’s comparison test for the change in the transverse relaxation times (T_2 , ms) of the CV PC hydrogels during SIF treatment (6 h).....	215
Table A.104 One way Analysis of Variance (ANOVA) and Tukey’s comparison test for the change in the transverse relaxation times (T_2 , ms) of the CV GT hydrogels during SIF treatment (6 h).....	215
Table A.105 One way Analysis of Variance (ANOVA) and Tukey’s comparison test for the change in the transverse relaxation times (T_2 , ms) of the CV XG hydrogels during SIF treatment (6 h).....	216
Table A.106 One way Analysis of Variance (ANOVA) and Tukey’s comparison test for the hardness values (N) of the CV hydrogels after SIF treatment (6 h).....	216
Table A.107 One way Analysis of Variance (ANOVA) and Tukey’s comparison test for the change in the hardness values (N) of the CV PC hydrogels during SIF treatment (6 h).....	217
Table A.108 One way Analysis of Variance (ANOVA) and Tukey’s comparison test for the change in the hardness values (N) of the CV XG hydrogels during SIF treatment (6 h).....	217
Table A.109 One way Analysis of Variance (ANOVA) and Tukey’s comparison test for the change in the hardness values (N) of the CV GT hydrogels during SIF treatment (6 h).....	218
Table A.110 One way Analysis of Variance (ANOVA) and Tukey’s comparison test for the change in the hardness values (N) of the CV C hydrogels during SIF treatment (6 h).....	218
Table A.111 One way Analysis of Variance (ANOVA) and Tukey’s comparison test for the weight loss values (%) of the CV hydrogels during 6h SIF treatment.....	218
Table A.112 One way Analysis of Variance (ANOVA) and Tukey’s comparison test for the total phenolic contents (mg Gallic acid/mL sample) of the yogurt samples at the end of the first week of the storage	219

Table A.113 One way Analysis of Variance (ANOVA) and Tukey’s comparison test for the total phenolic contents (mg Gallic acid/mL sample) of the yogurt samples at the end of the fourth week of the storage	219
Table A.114 One way Analysis of Variance (ANOVA) and Tukey’s comparison test for the antioxidant capacities (mg Trolox/mL sample) of the yogurt samples at the end of the first week of the storage	220
Table A.115 One way Analysis of Variance (ANOVA) and Tukey’s comparison test for the antioxidant capacities (mg Trolox/mL sample) of the yogurt samples at the end of the fourth week of the storage	220
Table A.116 One way Analysis of Variance (ANOVA) and Tukey’s comparison test for the change in the total phenolic contents (mg Gallic acid/mL sample) of the CV C hydrogel containing yogurt samples during storage (1 – 4 weeks)	221
Table A.117 One way Analysis of Variance (ANOVA) and Tukey’s comparison test for the change in the total phenolic contents (mg Gallic acid/mL sample) of the CV PC hydrogel containing yogurt samples during storage (1 – 4 weeks)	221
Table A.118 One way Analysis of Variance (ANOVA) and Tukey’s comparison test for the change in the total phenolic contents (mg Gallic acid/mL sample) of the CV GT hydrogel containing yogurt samples during storage (1 – 4 weeks).....	221
Table A.119 One way Analysis of Variance (ANOVA) and Tukey’s comparison test for the change in the total phenolic contents (mg Gallic acid/mL sample) of the CV XG hydrogel containing yogurt samples during storage (1 – 4 weeks)	222
Table A.120 One way Analysis of Variance (ANOVA) and Tukey’s comparison test for the change in the total phenolic contents (mg Gallic acid/mL sample) of the yogurt samples with no blended hydrogel during storage (1 – 4 weeks)	222
Table A.121 One way Analysis of Variance (ANOVA) and Tukey’s comparison test for the change in the antioxidant capacities (mg Trolox/mL sample) of the CV C hydrogel containing yogurt samples during storage (1 – 4 weeks).....	223
Table A.122 One way Analysis of Variance (ANOVA) and Tukey’s comparison test for the change in the antioxidant capacities (mg Trolox/mL sample) of the CV PC hydrogel containing yogurt samples during storage (1 – 4 weeks).....	223

Table A.123 One way Analysis of Variance (ANOVA) and Tukey’s comparison test for the change in the antioxidant capacities (mg Trolox/mL sample) of the CV GT hydrogel containing yogurt samples during storage (1 – 4 weeks)	223
Table A.124 One way Analysis of Variance (ANOVA) and Tukey’s comparison test for the change in the antioxidant capacities (mg Trolox/mL sample) of the CV XG hydrogel containing yogurt samples during storage (1 – 4 weeks)	224

LIST OF FIGURES

FIGURES

Figure 1.1. Hydrogel network junction sites (Ullah et al., 2015).....	2
Figure 1.2. Conventional vs Microwave heating mechanisms (Gude et al., 2013)...	4
Figure 1.3. Gelation of protein – polysaccharide systems (Le et al., 2017).....	5
Figure 1.4. Schematic representation of protein denaturation (Vantaraki, 2019)	8
Figure 1.5. HMP vs LMP chemical structures (Fuchsman, 1980)	10
Figure 1.6. Protonation and ionization of HMP carboxyl groups at different pH values (Guo & Kaletunç, 2016).....	11
Figure 1.7. A section (bassorin) of GT molecular structure (Gavlighi et al., 2013)	13
Figure 1.8. Chemical structure of XG molecule (García-Ochoa et al., 2000).....	16
Figure 1.9. Chlorogenic acid (Rein, 2005)	24
Figure 1.10. Cyanidin-3-xylosyl-glucosyl-galactoside (Rein, 2005)	25
Figure 1.11. Chemical structures of coumaric, sinapic and ferulic acids (Rein, 2005)	26
Figure 1.12. Chemical structures of cyanidin, delphinidin and petunidin.....	27
Figure 1.13. Representation of magnetization relaxation in z direction after the removal of RF excitation	29
Figure 1.14. A representative exponential transverse relaxation of a sample	31
Figure 3.1. Flow curves of hydrogel solutions in the presence and absence of BC: A: Control, B: Pectin, C: Gum Tragacanth, D: Xanthan Gum.....	60
Figure 3.2. Amplitude sweep test graph of BC containing XG hydrogel solutions	61
Figure 3.3. Frequency dependence of storage and loss moduli of xanthan hydrogel solutions: A: in the presence of BC, B: in the absence of BC and frequency dependence of complex viscosity of xanthan hydrogel solutions: C: in the presence of BC, D: in the absence of BC	62
Figure 3.4. Temperature dependence of storage and loss moduli of A: Control, B: Pectin, C: Gum Tragacanth, D: Xanthan Gum hydrogel solutions, in the presence of BC.....	65

Figure 3.5. Temperature dependence of storage and loss moduli of A: Control, B: Pectin, C: Gum Tragacanth, D: Xanthan Gum hydrogel solutions, in the absence of BC	66
Figure 3.6. Swelling ratio profiles of conventionally heated hydrogels (0 – 24 h)	71
Figure 3.7. Release profiles of conventionally heated hydrogels (0 – 24 h).....	75
Figure 3.8. Release profiles of microwave heated hydrogels (0 – 24 h).....	77
Figure 3.9. T ₂ profiles of conventionally heated hydrogels.....	80
Figure 3.10. T ₂ profiles of infrared assisted microwave heated hydrogels.....	82
Figure 3.11. Hardness profiles of hydrogels in phosphate buffer	86
Figure 3.12. SEM images of hydrogels: A: CV C, B: MW C, C: CV PC, D: MW PC, E: CV XG, F: MW XG, G: CV GT, H: MW GT.....	89
Figure 3.13. Cumulative release profiles of hydrogels in GIT (0 – 2 h gastric phase, 2 – 8 h intestinal phase)	91
Figure 3.14. Release profiles of hydrogels in SGF	93
Figure 3.15. T ₂ profiles of hydrogels in SGF.....	96
Figure 3.16. SDC profiles hydrogels in SGF	97
Figure 3.17. Hardness profiles of hydrogels in SGF	99
Figure 3.18. FTIR spectra of dry powders, hydrogels before SGF treatment (0 h) and hydrogels after 2 h SGF treatment: A: Control, B: Pectin, C: Gum Tragacanth, D: Xanthan Gum	105
Figure 3.19. BC release rate increase (%) of hydrogels during 6 h SIF treatment with respect to their final release rates after 2 h SGF treatment	109
Figure 3.20. T ₂ profiles of hydrogels in SIF (0 h: T ₂ after SGF digestion, 6 h: T ₂ after the 6 h SIF digestion subsequent to SGF digestion)	117
Figure 3.21. FTIR spectra of hydrogels after 2 h SGF digestion (2 h SGF) and 8 h gastrointestinal digestion (2 h SGF + 6 h SIF treatment) (8 h SIF): A: Control, B: Pectin, C: Gum Tragacanth, D: Xanthan Gum	122
Figure 3.22. Hardness profiles of hydrogels in gastrointestinal digestion: 0 h: Before any treatment, 2 h: After SGF treatment, 8 h: After gastrointestinal digestion (2 h SGF + 6 h SIF).....	124

Figure 3.23. Release trends of hydrogels in SIF 126

Figure 3.24. SEM images of hydrogels: A: Only SGF treated C, B: SGF + SIF treated C, C: Only SGF treated PC, D: SGF + SIF treated PC, E: Only SGF treated GT, F: SGF + SIF treated GT, G: Only SGF treated XG, H: SGF + SIF treated XG 130

LIST OF ABBREVIATIONS

ABBREVIATIONS

ATR	attenuated total reflectance
BC	black carrot extract
BSA	bovine serum albumin
C	control hydrogel
CV	conventional heating
CV C	control hydrogel produced by conventional heating
CV GT	gum tragacanth hydrogel produced by conventional heating
CV PC	pectin hydrogel produced by conventional heating
CV XG	xanthan gum hydrogel produced by conventional heating
DPPH	2,2-diphenyl-1-picrylhydrazyl
FTIR	Fourier transform infrared
GAE	gallic acid equivalent
GIT	gastrointestinal tract
GT	gum tragacanth
HMP	high esterified pectin
HPLC	high performance liquid chromatography
IR	infrared heating
LF NMR	low field nuclear magnetic resonance
LMP	low esterified pectin

LVE	linear viscoelastic region
MW	infrared assisted microwave heating
MW C	control hydrogel produced by microwave heating
MW GT	gum tragacanth hydrogel produced by microwave heating
MW PC	pectin hydrogel produced by microwave heating
MW XG	xanthan gum hydrogel produced by microwave heating
o/w	oil-in-water emulsion
PC	pectin
RF	radio frequency
SDC	self-diffusion coefficient
SEM	scanning electron microscope
SGF	simulated gastric fluid
SIF	simulated intestinal fluid
SR	swelling ratio
TA	total acidity
TPA	texture profile analysis
WPI	whey protein isolate
XG	xanthan gum
β -Lg	β -lactoglobulin
α -LA	α -lactalbumin

LIST OF SYMBOLS

SYMBOLS

Al	aluminum
C	carbon
Ca ²⁺	calcium cation
cm	centimeter
cP	centipoise
Cu	copper
D	effective diffusion coefficient
E	equivalent acidity
f	solution factor
Fe	iron
g	gram
<i>g</i>	gravity force
GHz	gigahertz
H	hydrogen
h	hour
<i>h</i>	height of the sample
HCl	hydrochloric acid
H ₂ SO ₄	sulfuric acid
Hz	hertz

k	consistency index
K ⁺	potassium cation
kDa	kilodalton
keV	kiloelectron volt
KH ₂ PO ₄	potassium phosphate
M	molarity
<i>M</i>	amount of gel titrated
mg	milligram
Mg ²⁺	magnesium cation
MHz	megahertz
min	minute
mL	milliliter
mm	millimeter
M _t	amount of diffusing agent at time t
M _∞	amount of release at long times
mV	millivolt
N	nitrogen
n	flow behavior index
NaCl	sodium chloride
NaOH	sodium hydroxide
nm	nanometer
O ₂	oxygen

Pa	Pascal
Pa s	Pascal second
pH	potential of hydrogen
pI	isoelectric point
pKa	ionization constant
ppm	part per million
R	radius of the sample
rpm	revolution per minute
Sn	tin
T	Tesla
$\tan \delta$	loss tangent
T/m	tesla per meter
T_2	transverse relaxation time (spin-spin relaxation time)
V	volume
W	watt
w_0	initial gel weight
w_t	weight of the gel at a defined time
w_{2h}	weight of the hydrogel after gastric digestion
w_{8h}	weight of the hydrogel after the gastrointestinal digestion
$^{\circ}\text{C}$	degree Celsius
ε'	dielectric constant
ε''	dielectric loss factor

G'	storage modulus (elastic modulus)
G''	loss modulus (viscous modulus)
μl	microliter
μm	micrometer
μs	microsecond
γ	ratio of the volume of the solution to the volume of the hydrogel
τ_0	yield stress

CHAPTER 1

INTRODUCTION

1.1 Hydrogels

Hydrogels are three-dimensional polymer networks having ability to retain large amount of water in their hydrophilic internal structures (Ahmed, 2015; Ullah et al., 2015). Both synthetic and natural polymers could be used to produce hydrogels (Argin et al., 2014). However, natural grade hydrogels are gaining more importance than the synthetic ones due to their several advantages including higher water absorption capacity and their biodegradable character. Physical or chemical cross-linking of the used polymers is needed to produce hydrogel systems. If the polymer network is chemically cross-linked, the junction zones of the polymers become permanent while physically cross-linked networks have transient junction zones. These transient junction zones may arise from physical interactions such as hydrogen bonding, ionic interactions, hydrophobic associations and polymer chain entanglements (Ahmed, 2015).

Hydrogels can be utilized in many industrial and reseach fields such as pharmaceutical, biomedical, agricultural and food applications. Each production method provides hydrogels with different characteristics. Hydrogel production techniques for food applications are limited mostly due to safety reasons. Therefore, food grade polymers including proteins and polysaccharides like starch, alginate, chitosan and pectin have been used to produce hydrogels for food applications, recently (Lu et al., 2015; Mun et al., 2015; Si et al., 2009; Wichchukit et al., 2013).

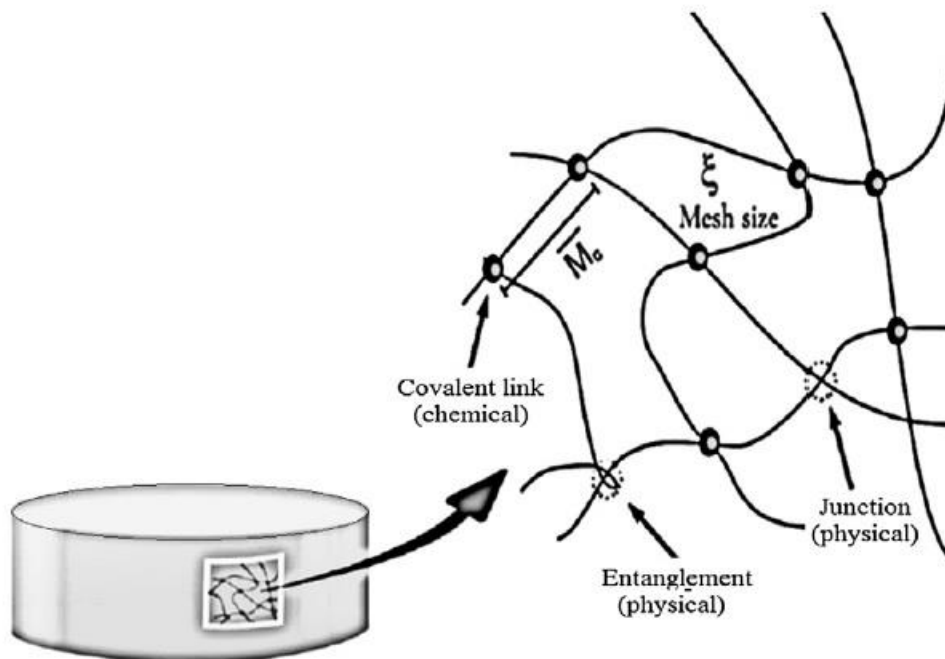


Figure 1.1. Hydrogel network junction sites (Ullah et al., 2015)

Food grade hydrogels are generally produced by cross-linking processes mostly induced by ionic and polymer interactions. Cold-set gelling and heat induced gelling methods are the two common examples for such mechanisms. Cold-set gelling utilizes ionic interactions whereas heat induced gelling mostly depends on interactions between the polymers constituting the hydrogel network (Mession et al., 2015). Protein based heat induced hydrogels are gaining interest since molecular structures of proteins change upon heating which is defined as denaturation (Fathi et al., 2018).

1.1.1 Heat Induced Gelling of Proteins

Proteins undergo a conformational transition when heated above their thermal denaturation temperatures. Each protein has its unique thermal denaturation temperature and behavior. Plant based pea and soy proteins as well as animal based

proteins such as whey protein isolate (WPI) are widely used for hydrogel production (Fathi et al., 2018). Thermal denaturation of proteins promotes more hydrophobic reactions and decreases the protein solubility (Munialo et al., 2016). This may create a gel structure enabling water absorption and retention within the gel matrix. Gel characteristics strongly depend on the physico-chemical characteristics of the used protein. In this study, two heating methods namely conventional heating (CV) and Infrared Assisted Microwave Heating (MW) were used to obtain hydrogels.

1.1.2 Heating Methods

1.1.2.1 Conventional Heating

Conventional heating can be achieved by conduction or convection. Oven and furnace systems utilize heat convection mechanisms whereas water boilers provide energy transfer via conduction. In this study, hydrogel solutions were heated in a water bath. Thus, conventional heating was based on heat transfer by means of conduction. This type of heating provides a heat flow from outside to inside of the food material which can be time and energy consuming. However, a stable heating could be achieved after reaching the equilibrium in the system (Ozel, Cikrikci, et al., 2017).

1.1.2.2 Microwave Heating

Microwave heating could be considered as an alternative way for gelation. Microwaves are oscillating electromagnetic waves in the frequency range of 300 MHz and 300 GHz on the material, causing an instantaneous heat generation due to the polarization of the chemical constituents in the material (Liu & Kuo, 2011). Microwave heating has some advantages over CV. For instance, microwave heating provides faster heating with more energy efficient process (Gude et al., 2013). Precise process control and selective heating properties of microwave heating is

widely used by the food industry (Turabi et al., 2010). However, there exists less time for the formation of three-dimensional gel matrix during microwave heating which could affect the gel properties. Microwave heating may induce weaker and coagulate-like gel structures for protein based systems (Gustaw & Mleko, 2007). Near infrared heating (IR) could be combined with microwave heating to increase the control on the moisture transport by increasing heating rate (Turabi et al., 2010). Studies on WPI and soy protein isolate gelation by microwave heating showed that this heating method affects the gelation mechanism and final gel structure. Comparison of conventional and microwave gelation of WPI in different pH conditions revealed different results (Gustaw & Mleko, 2007). Microwave heating also had distinct impacts on the microstructural and rheological properties of soy protein isolate gels (Liu & Kuo, 2011). Therefore, IR was combined with microwave heating in this study.

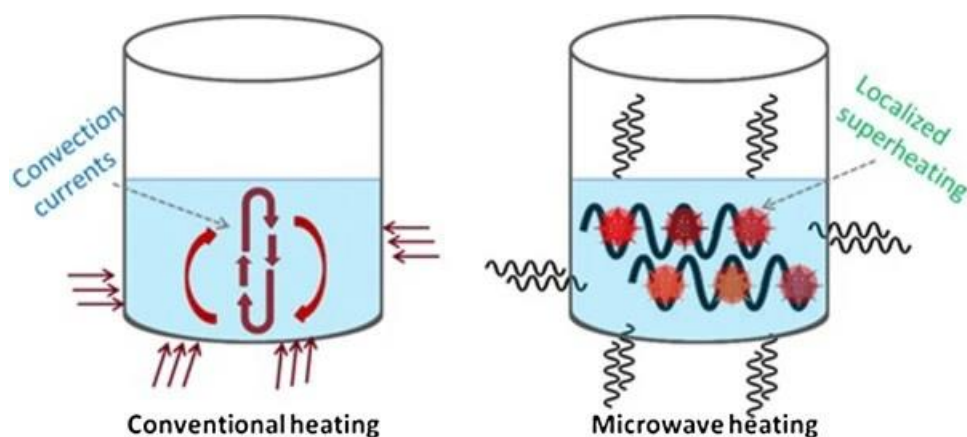


Figure 1.2. Conventional vs Microwave heating mechanisms (Gude et al., 2013)

1.1.3 Composite Hydrogels

Utilization of synergistic interactions between various polymers in order to modulate hydrogel characteristics has been implemented in the literature. Protein and

polysaccharide blending is one of the preferred techniques reported to alter the functional properties of gel systems (Betz & Kulozik, 2011a; Betz et al., 2012; Mun et al., 2015; Petzold et al., 2014; Zhang, Decker, & McClements, 2014). Functional and microstructural characteristics of WPI based hydrogels could also be modulated by gum blending to such systems. Interactions between WPI and a polysaccharide may promote new features for hydrogels which could be used to implement novel applications (Zand-Rajabi & Madadlou, 2016).

Nature of interactions between polymers (attractive or repulsive) leads to different behaviors like associative phase separation or co-solubility forming soluble/insoluble complexes. Resulted complexes demonstrate unique functional properties other than the individual protein and polysaccharides used (Shiroodi et al., 2012). Some of the factors influencing the hydrogel properties are nature of the biopolymer, protein to polysaccharide ratio, biopolymer concentration and ionic strength of the mixed biopolymer solution (Le et al., 2017).

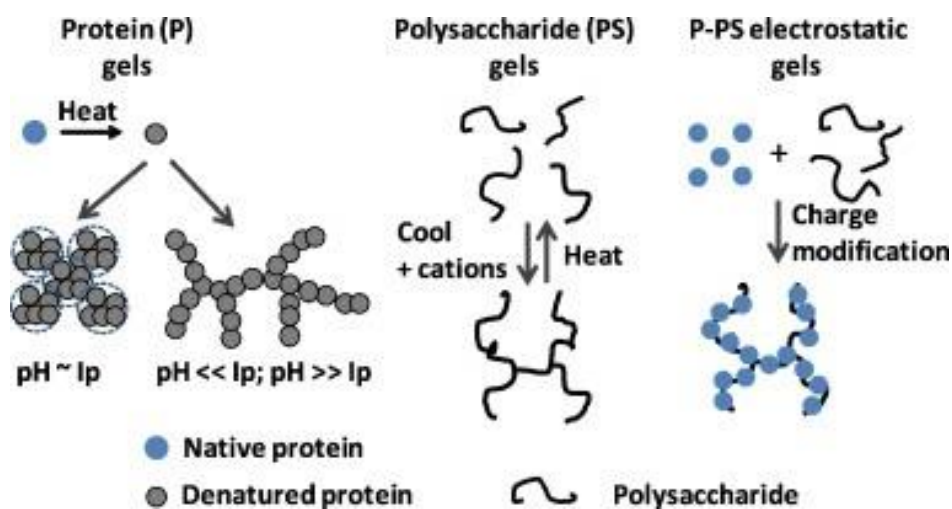


Figure 1.3. Gelation of protein – polysaccharide systems (Le et al., 2017)

Protein – anionic polysaccharide based hydrogels can be achieved via electrostatic complexation. These hydrogels are produced at ambient temperature (Zhang, Zhang, Chen, Tong, & McClements, 2015). Introduction of a cation such as Ca^{2+} to the biopolymer mixture at neutral pH creates a three – dimensional network since both the protein and polysaccharide used are negatively charged at this pH (Barbut & Foegeding, 1993). However, sizes of the native proteins are relatively smaller than their denatured state and this may lead to a decrease in the protein incorporation into the gel matrix. Therefore, a globular protein source should be pre – denatured before complexing with a polysaccharide at ambient temperature (Bryant & McClements, 1998). Additionally, any bioactive agent to be encapsulated in such hydrogels could be excessively lost through the gel matrix which would also reduce the encapsulation efficiency. In order to prevent such problems, an excessive use of cross-linking agent may be needed and this would have an unwanted influence on the encapsulated sensitive material. On the other hand, heat induced gelation of protein – polysaccharide biopolymer solutions can decrease the preparation steps such as pre – denaturation of protein and produce more abundant interactions between the polymers. Unfolding of the protein during heating produces more interaction sites between the polymers including hydrogen bondings and steric interactions as well as the electrostatic interactions which is the main driving force in electrostatic complexations taking place at ambient temperature (Munialo et al., 2016). If the material intended to be encapsulated is resistant to heat, heat induced biopolymer hydrogels offer a reasonable alternative way for delivery system preparations. Since the cross-linking mechanism will be different in this case, a variety of new complexes and different combinations could be produced (Doublier et al., 2000).

1.2 Biopolymers for Hydrogel Production

Natural biodegradable polymers including proteins and polysaccharides could be used to produce hydrogels in food industry. In this study, WPI based heat induced

hydrogels were produced by blending PC, GT and/or XG polysaccharides to WPI, separately.

1.2.1 Whey Protein Isolate

WPI is an animal based protein with functional attributes including surface activity, gelling ability and high interacting capability due to its functional groups located on the molecular surface (McClements & Gumus, 2016). Whey proteins are generally very suitable candidates for thermal denaturation to produce hydrogels (Gunasekaran et al., 2007). WPI molecules experience a thermal denaturation to create a three – dimensional network above 70 °C. Unfolding of the native whey proteins above the denaturation temperature reveals their non-polar residues on the molecule surface and induces aggregation reactions to form a spatial gel network (Munialo et al., 2016). WPI has some advantages over some of the other animal and plant based proteins that could be thermally denatured to obtain hydrogels. For instance, casein is a more heat resistant protein which requires higher temperatures than WPI to denature and change its conformation (Munialo et al., 2016). Difficulties in the extraction of soy proteins due to possible loss of functionalities, excess purification requirements of gelatin and high water soluble surface characteristics of pea proteins, put forward whey proteins as a convenient choice for designing hydrogels by heat induced gelation (Fathi et al., 2018).

WPI contains globular proteins such as β -lactoglobulin (β -Lg), α -lactalbumin (α -LA) and bovine serum albumin (BSA). These proteins also contribute to heat induced gelling of WPI (Takagi et al., 2003). β -Lg and α -LA constitutes the 65 % (w/w) and 25 % (w/w) of the WPI molecule, respectively (Shiroodi et al., 2015). Due to its large amount and specific characteristics, β -Lg dominates the gelling mechanism of WPI (Hoffman & Van Mil, 1999). In contrast to β -Lg, α -LA cannot polymerize by itself when heated above 70 °C (De la Fuente et al., 2002). Addition of β -Lg allows interactions between α -LA and itself through disulfide bridges. Heating of α -LA, β -Lg and BSA accelerates aggregation rate thus promotes a synergistic effect on

aggregation (Havea et al., 2001). Thermal heat induced denaturation steps of β -Lg mainly consists of initial denaturation (unfolding) and subsequent aggregation stages (Prabakaran & Damodaran, 1997). Firstly, β -Lg existing mainly as a dimer at room temperature and physiological pH, dissociates into monomers. Upon heating above 60 °C, some conformational changes such as unfolding of the molecules via exposure of the buried hydrophobic and thiol groups are observed. Afterwards, irreversible aggregation reactions begin to take place. At this stage, noncovalent reactions (electrostatic and hydrophobic interactions, hydrogen bonding) between the exposed groups trigger physical aggregation. Additionally, chemical aggregation between the dissociated monomers with thiol-disulfide exchange reactions also contributes to the overall aggregation process (Hoffman & Van Mil, 1999; Verheul et al., 1998).

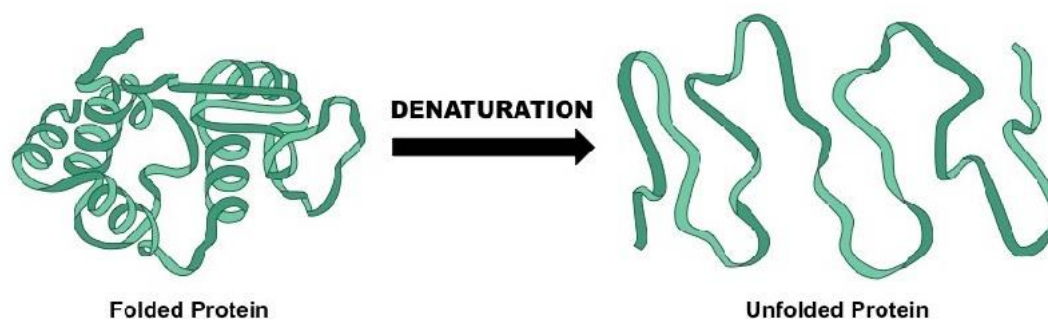


Figure 1.4. Schematic representation of protein denaturation (Vantaraki, 2019)

Characteristics of hydrogels formed by heating of WPI are strongly dependent on the heating conditions. Temperature of the denaturation process, pH of the WPI solution, initial WPI concentration and the ionic strength of the heated medium determine the physical properties of the obtained hydrogels (Britten & Giroux, 2001; Dissanayake, Ramchandran, Donkor, & Vasiljevic, 2013; Li, Ye, Lee, & Singh, 2013). When pH of the heated medium is increased especially above 7.0 during gelling, free thiol reactivity is also increased thus thiol-disulfide exchange reaction rates (covalent interactions) are enhanced. On the other hand, at high temperatures (above 90 °C),

contribution of noncovalent interactions to β -Lg aggregation predominates the mechanism (De la Fuente et al., 2002). High salt concentrations during heating decelerates the initial denaturation of β -Lg by making β -Lg less soluble but increases the subsequent aggregation rate due to the reduced intramolecular electrostatic repulsions through charge screening (Roefs & De Kruif, 1994; Xiong et al., 1993). All these conditions induce different physical attributes, therefore different physico-chemical features for the developed WPI hydrogels (Ju & Kilara, 1998).

1.2.2 Pectin

PC is a natural heteropolysaccharide primarily found in cell walls in most plants (Ventura & Bianco-Peled, 2015). This biodegradable polymer has an anionic character mostly due to its covalently linked linear $\alpha - (1 - 4) - D -$ galacturonic acid units having a pKa around 3.0. Galacturonic acid units comprises the 70 % of the PC structure as the main backbone and the rest is composed of partially methoxylated carboxyl group containing side units (Ralet et al., 2011). $\alpha - (1 - 2) - L -$ rhamnose units are interspersed along the homogalacturonic regions of PC. Hydrophilic neutral sugar units (xylose, galactans, arabenes) are carried by the $\alpha - L -$ rhamnopyranosyl residues imparting a hydrophilic character to the PC molecule (Yildiz, 2010). Presence of hydroxyl and carboxylate groups in PC molecular structure increases the hydrophilicity of the polysaccharide (Guo & Kaletunç, 2016). At pH values above its pKa (~ 3.0), negatively charged PC side chains promote polymer chain extensions induced by charge repulsions. This may lead to water absorption into the biopolymer matrix depending on the surrounding medium properties (Belscak-Cvitanovic et al., 2015). Physico-chemical properties of PC allow its use in food industry as a gelling agent, thickener and stabilizer (Mohnen, 2008).

PC can be found in different states according to the degree of esterification of its carboxyl groups. When a high number of PC carboxyl groups are esterified with methanol, this class of pectin is defined as high-esterified pectin (HMP). A low

number of carboxyl group esterification reveals low-esterified pectin (LMP). HMPs generally have a methoxyl content higher than 7 % whereas LMPs have lower than 7 %. Additionally, degree of esterification for HMP is more than 50 % (typically 55 – 75 %) while LMP has lower than 50 % with an average around 20 – 45 % esterification (Wüstenberg, 2015). Despite having a dominant homogalacturonic backbone, HMPs and LMPs have some differences in their physico-chemical properties. For instance, HMP is cold water soluble but LMP is only soluble in cold water if Na^+ or K^+ salts present. They also have different gelling abilities. HMP gels at acidic environment in the presence of sugar in the gelling environment. LMP, on the other hand, requires Ca^{2+} ions for gelation. Therefore, LMP is suitable for cold gelation process via egg – box model whereas HMP requires high soluble solid content to undergo gelation (Guo & Kaletunç, 2016). When heated at high temperatures, HMP can produce thermo – irreversible gels especially at pH values below 3.5. At higher pH values HMP imparts viscosity to the solution (Wüstenberg, 2015). Because of the predisposition of HMP to heat induced gelling, HMP was used in this study.

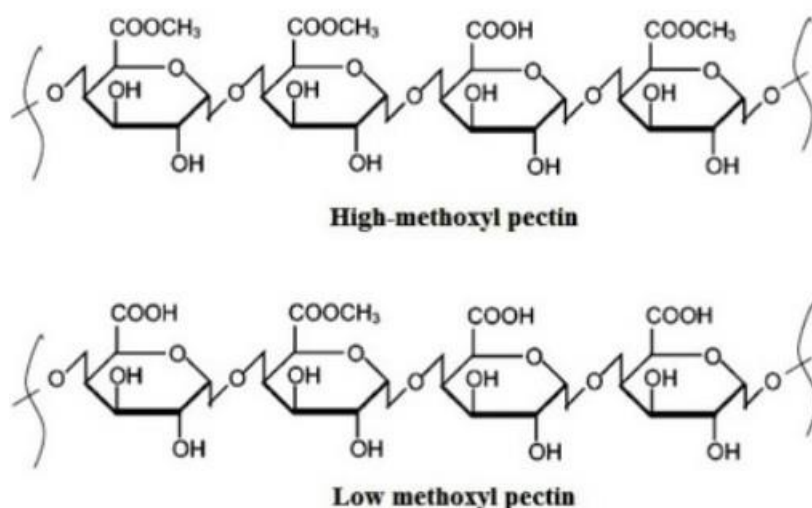


Figure 1.5. HMP vs LMP chemical structures (Fuchsman, 1980)

PC is abundantly used in food industry. Controlling the moisture content and regulating the texture of foods are some of the uses of PC. Since PC is a highly hydrophilic polymer, it requires at least 3 % (w/w, w/v) concentration to permanently increase the solution viscosity (Wüstenberg, 2015). Industrial applications of HMP and LMP are also different due to their distinct characteristics. HMP is used to provide structural stability to sugary products such as confectionaries and jams. Some fruit beverages and acidified dairy drinks may contain HMP as a non – gelling stabilizer. When used in bread and frozen dough, HMP can retain moisture and provide softness to these products which could ensure freeze – thaw stability. LMP is generally used for fruit formulations for yogurt and some cold milk products. LMP is also a fat substitute in some low – fat foods such as dairy and meat products (Mohnen, 2008).

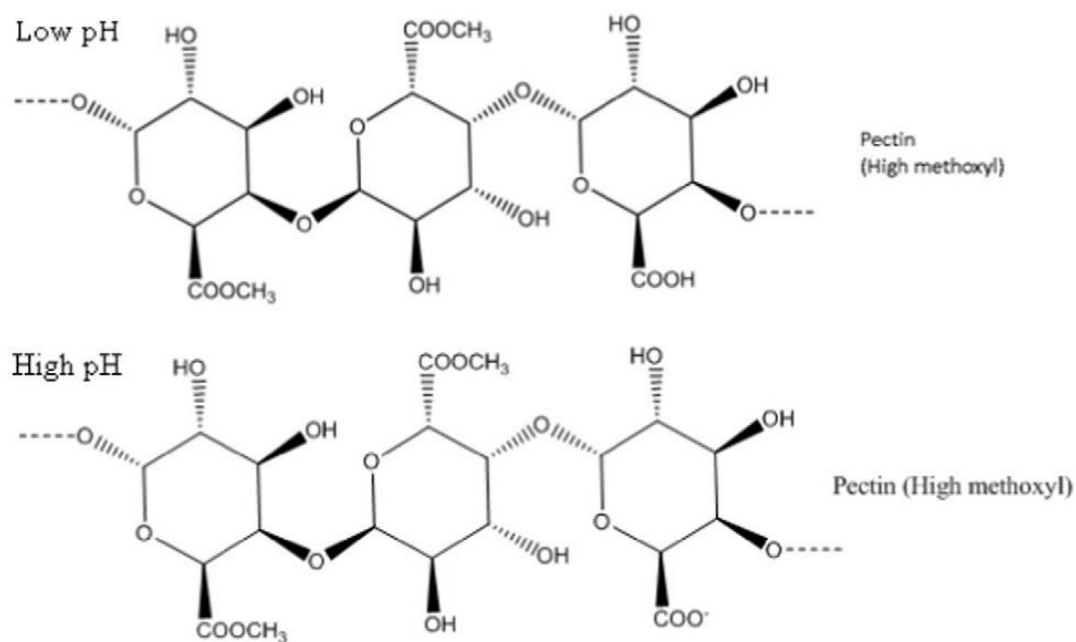


Figure 1.6. Protonation and ionization of HMP carboxyl groups at different pH values (Guo & Kaletunç, 2016)

1.2.3 Gum Tragacanth

GT is a hydrophilic, branched and anionic polysaccharide with a pKa around 3.0 (Mostafavi et al., 2016). Molecular weight of GT is about 850 kDa (Nur et al., 2016). Trunk of *Astragalus* is the source of this complex exudate. Species are mostly grown in Turkey, Syria and Iran. Galacturonic acid groups in the polysaccharide structure are the main reason for the negative charge character of GT over a wide pH range (Wüstenberg, 2015). GT is a physical mixture of two components namely tragacanthin and bassorin. Tragacanthin constitutes the water – soluble part whereas bassorin accounts for the water – insoluble (swellable) part of the gum (Aspinall & Baillie, 1963). Composition of our GT sample comprises of 60 % (w/w) tragacanthin and 40 % (w/w) bassorin which is compatible with the previous reports (Ozel et al., 2020). Tragacanthin provides the liquid character of GT and it is also described as arabinogalactan fraction with neutral and highly branched structure having D – galactose, L – arabinose and D – galacturonic acid residues mostly esterified with methanol (Gavlighi et al., 2013). Repeating D – galactose units of tragacanthin are branched with L – arabinofuranose chains. These arabinose units constitute the majority of the structure. Presence of protein (3 – 4 %, w/w), starch and cellulosic residues in tragacanthin fraction contributes to the colloidal and emulsifying properties of GT. On the other hand, gelling and swelling abilities of GT come from its bassorin or tragacanthic acid fraction. Bassorin is a complex, pectic component. D – galacturonic acid, D – xylose, L – fucose, L - rhamnose and D – galactose residues constitute the bassorin structure. (1 – 4) – linked – α – D – galacturonic acid chains provide bassorin its pectic backbone structure and the main bassorin properties such as viscosity (Balaghi et al., 2011). High molecular weight D – galactose side chains are also responsible for the viscous properties of the gum. Short side chains like D – xylose and L – fucose are linked to the main backbone. K^+ , Ca^{2+} and Mg^{2+} cations are usually associated with the bassorin fraction. There may be some compositional differences between GT products produced from various origins. Tragacanthin and bassorin fractions may possess distinctions in their uronic

acid and methoxyl contents which yield compositional differences in GT structures (Wüstenberg, 2015).

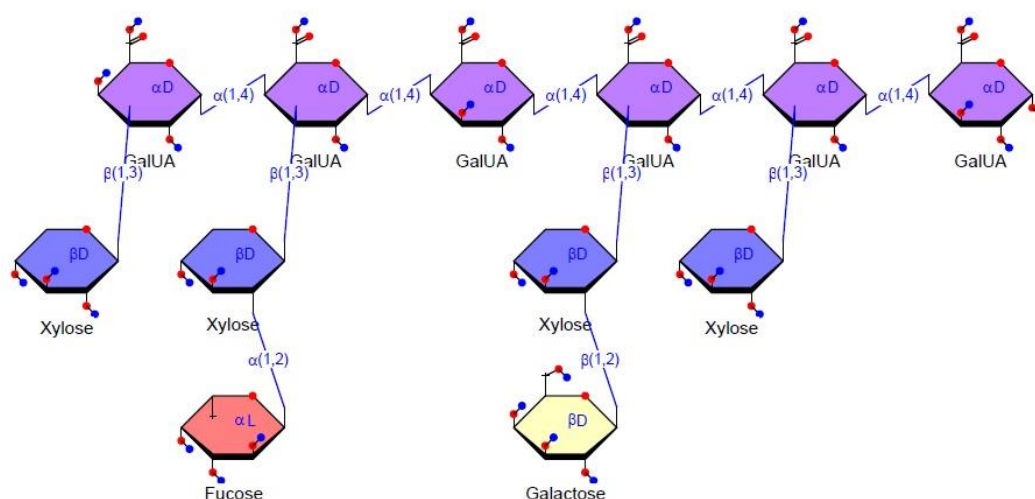


Figure 1.7. A section (bassorin) of GT molecular structure (Gavlighi et al., 2013)

GT can hydrate and form viscous solutions both in cold and hot water. Viscosity of GT solutions determine the main quality of the used GT product. GT is stable over a wide pH range (2.0 – 10.0) but the maximum stability is observed between the pH of 4.0 and 8.0 (Gavlighi et al., 2013). Solutions prepared with this gum are usually acidic. 1 % (w/w) GT solution gives an acidic pH (4.0 – 6.0). Since GT preserves its stability even at extreme pH's as low as 2.0, GT is considered as a highly acid resistant polysaccharide. Storage of a GT solution for one day at room temperature is enough for viscosity to fully develop. If the initial water temperature is increased, hydration time for GT could be reduced. Even at low concentrations down to 0.5 % (w/w, w/v) GT solutions demonstrate a shear – thinning character. However, aqueous GT dispersions having concentrations more than 2 % (w/w, w/v) form a soft gel – like thick pastes (Wüstenberg, 2015).

GT is renowned for its emulsification ability for oil – in – water (o/w) emulsions. Especially in acidic o/w emulsions, GT can exhibit extensive surface active properties. GT concentration less than 0.25 % is sufficient to facilitate emulsification via rapidly lowering the surface tension of water in the emulsion system (Balaghi et al., 2010). Thickening of the aqueous phase mostly due to bassorin and lowering the oil – water interfacial tension by the help of tragacanthin are the two main mechanisms performed by GT in these systems. GT can also maintain viscosity at low pH's. Therefore, GT is widely facilitated in salad dressings and acidified sauces in order to maintain the viscosity of these products during storage (Balaghi et al., 2010; Gavlighi et al., 2013).

GT is generally used as stabilizer, thickener, emulsifier and suspending or gelling agent in food industry. Some of the food products in which GT is used are salad dressings, icings, confectionary, citrus oil emulsions, condiments, bakery emulsions, ice creams, sherbets, oil containing flavor emulsions, fruit based fillings, soft drinks and desserts (Wüstenberg, 2015). Long shelf life providing property of GT makes it convenient for a wide range of food products. Producing a creamy mouth – feel with a pourable character of GT makes it an appropriate candidate for products requiring flavor release in the mouth (Phillips & Williams, 2009). In order to suspend the pulp in fruit beverages GT could also be used. GT ensures the settling of fruit particles and provides the desired body. GT acts as a water binder in icings and provides a creamy taste to the product with a smooth texture. GT could reduce the dairy cream fat extensively without changing the sensory properties of the product (Wüstenberg, 2015).

Stabilization mechanisms of GT include steric repulsion forces, residual surface activity, increase of the emulsion viscosity and electrostatic interactions (Balaghi et al., 2011). Ability of GT to maintain steric repulsions in a wide pH range contributes to overall stabilizing characteristic of GT blended products. Additionally, GT stabilizes the beverage emulsions mostly by reducing the interface surface activity via its surface active residuals and enhancing the continuous phase viscosity by its water swellable regions (Rezvani et al., 2012). GT stabilizes some dairy products

with electrostatic interactions. GT provides a highly negatively charged environment mainly by the negatively charged carboxylic groups of galacturonic acid chains. This electrostatic interaction capability of GT allows for creating polysaccharide – protein complexes. Anionic polymers like GT can interact with the positively charged patches on the protein surfaces (Muhammadifar et al., 2007). Therefore, protein – polysaccharide complexes could be utilized to enhance emulsion stabilization. Whey and casein proteins are some of the examples that were combined with polysaccharides for such purposes (Garti & Reichman, 1993; Owens et al., 2018). Possibility of electrostatic interactions between anionic polysaccharides and proteins under convenient pH and ionic strength conditions, makes it also feasible to produce hydrogels for some other applications. For instance, β -Lg could associate with many anionic polymers including PC (Sperber et al., 2009). Despite the frequently used polysaccharides such as alginate, PC and carrageenan, GT has not been extensively studied in protein based hydrogel formulations. Thus, GT was chosen as another polysaccharide to be blended with WPI to obtain hydrogels in this study.

1.2.4 Xanthan Gum

XG is an anionic natural heteropolysaccharide and produced mainly by *Xanthomonas campestris* species during fermentation. Bacterial cultures aerobically ferment the glucose or sucrose solutions in the fermentation vessel to produce XG which has high viscosity (Wüstenberg, 2015). Chemical structure of XG presents a long and branched structure. The long cellulosic backbone of XG consists of (1 – 4) linked β – D – glucose units. Alternating trisaccharide side chains are linked to this cellulosic backbone. Glucuronic and pyruvic acids are present in the side chains. Two D – mannose units and a D – glucuronic acid between the mannose units constitute the trisaccharide chain with small modifications. Generally, the D – mannose unit directly connected to the main backbone, possesses an acetyl group. A pyruvic acid residue can be found in the one half of the terminal D – mannose units

(García-Ochoa et al., 2000). These carboxyl groups in the side chains impart an anionic character to the polysaccharide (Zhang, Zhang, & Vardhanabhuti, 2014).

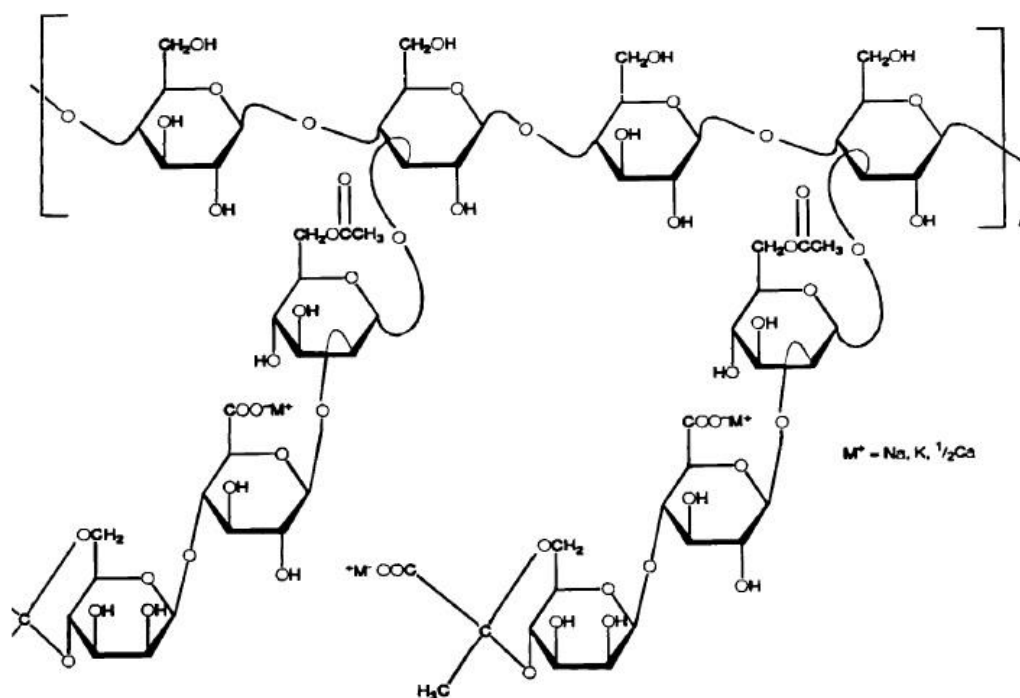


Figure 1.8. Chemical structure of XG molecule (García-Ochoa et al., 2000)

Trisaccharide side chains of XG are closely aligned with the main polymer backbone and this induces a stiff molecular conformation. Thus, XG molecule may adopt a double – stranded helix conformation in its native state. When exposed to external stimuli, molecular conformation of XG alters and adjusts itself to the new conditions. Adjustments of the new conformations are originated from the intra- and inter-molecular interactions of XG molecules. Transformation from a rigid helical – coil structure into flexible coils is a typical example for the change in the XG conformational behavior in solutions (Zasytkin et al., 1996). pH and ionic strength

of the solution affect the physical properties of XG and determine its stability in the solution (Mikac et al., 2010).

XG is water soluble at room temperature. Even at colder temperatures, XG can be dissolved in water up to 0.5 % (w/v) concentration. XG solutions generally display an opaque appearance. Increasing the stirring speed assists the dispersion and dissolution of XG in water. High ionic strength delays the hydration of XG (Wüstenberg, 2015). Average molecular weight of XG is around (~ 2000 kDa) which is a high value compared to many other biodegradable polymers. The high molecular weight, branched chemical structure and polyelectrolyte nature (pKa ~ 2.8) of XG makes it a good stabilizing agent for food formulations (Zasytkin et al., 1996). Side chains of XG interact with the cellulosic main backbone in solutions. Wrapping of these side chains around the cellulosic long chain protects the main backbone and increases the stability of XG to adverse conditions. Temperature, on the other hand, may induce some conformational transitions in the XG chemical structure. By the increase in the temperature, rigid – ordered state of XG molecules becomes more disordered and flexible. Low ionic strength promotes the ordered – rigid conformation of XG molecules so viscosity increase could be lower when XG solutions are heated to elevated temperatures at low salt concentrations (Wüstenberg, 2015).

Viscosity enhancing effect is the most distinct feature of XG. Even at very low concentrations (<1%), XG increases the solution viscosity, abruptly (Fabek et al., 2014). Therefore, XG is used as a thickener in the food industry. Viscous XG solutions demonstrate a pseudoplastic flow behavior. Except for the flow rate, temperature, gum and salt concentration and pH affect the viscosity of XG containing solutions. Especially above 0.5 % (w/v) concentration, XG solutions show weak gel visco-elastic properties (Phillips & Williams, 2009). Despite some changes in XG molecular conformation, XG solutions are extremely stable during heating. Even presence of salts and acids cannot diminish the extreme stability of XG solutions to heating despite the intermolecular interaction strengthening effect of salts for XG solutions (Braga et al., 2006). A slight decrease in the viscosity of

the XG solution could be recovered upon cooling. Another major characteristic of XG is the pH stability over a very wide range (pH 3 – 10) (Fabek et al., 2014). XG is more stable than most of the other thickeners used in the food industry for similar purposes. XG can be directly dissolved in acidic solutions and it is compatible with most organic acids. Independence from pH for a wide range makes XG a favorable thickener to be used in sauces, dressings and cakes. Furthermore, XG also shows a remarkable resistance to enzymes including most proteases, cellulases and amylases (Wüstenberg, 2015).

Dressings and sauces are the two most popular application areas for XG. When used in cake formulations, XG can provide and maintain volume. XG incorporates added fruit and chocolate particles in cakes very well so that sedimentation in cakes is prevented during baking. Cakes having XG in formulations are less prone to lose freshness during storage (Phillips & Williams, 2009). In order to reduce syneresis and maintain the initial gel texture, XG is added to dairy desserts (Shiroodi et al., 2015). Addition of XG to such food products help maintain the desired body and particle distribution in these products. Besides its sole application to variety of food formulations, XG can also be used synergistically with some other polysaccharides and proteins. Galactomannans including guar gum, cassia gum and locust bean gum show some synergistic effect with XG. When used together with these galactomannans, XG increase the viscosity of the formulations. Locust bean gum and cassia gum are also blended with XG for gelling purposes. Glucomannans such as konjac gum can also be used with XG to increase the viscosity. A heating and cooling process forms elastic gels for konjac – XG mixtures (Wüstenberg, 2015). In addition to some polysaccharides, XG interacts with WPI and may indicate synergistic effect. Solutions containing XG and native WPI can form homogenous solutions suggesting strong interactions between the two polymers. In the absence of any additional salt, XG and heat denatured WPI are not very compatible with each other and their solution may undergo a phase separation. However, presence of salt even at low concentrations induce cold – gelling for these systems (Bryant & McClements, 2000). Moreover, heating of XG – WPI mixtures creates more

interaction possibilities between the two polymers and generally soft gels are created (Li, Ould Eleya, & Gunasekaran, 2006). Molecular conformations and physico – chemical properties of XG and WPI prevent formation of a highly elastic gel but still the combination of these polymers presents a considerable alternative for such applications (Bryant & McClements, 2000).

1.3 Controlled Release Applications

Food grade hydrogels are widely employed for controlled release of encapsulated bioactive agents since they have suitable healthy characteristics such as biodegradability, biocompatibility and non-toxicity (Ahmed, 2015). Controlled release ensures the protection of the encapsulated bioactive agent from the environmental conditions via releasing the active agent at a specific site with a specific rate so that the sensitive agent could be delivered into the selected food or human GIT system with a minimum damage (Abaee, Mohammadian, & Jafari, 2017; Zhang, Zhang, & McClements, 2017). Encapsulated delivery systems attract great attention for the delivery of bioactive components and therapeutic drugs in food technology, biotechnology and medicine (Belscak-Cvitanovic et al., 2015). Combination of proteins and polysaccharides is of high interest for production of novel hydrogels for release purposes. Different polysaccharides may interact with the protein network during hydrogel production which would enable the producer to gain control over the manipulation of the release systems (Argin et al., 2014).

Protein based delivery systems for encapsulation of bioactive compounds have gained growing interest in recent years. Proteins from various sources such as whey and casein from milk, gelatin from meat, soy and pea proteins from plants have been used for the delivery of sensitive food ingredients with remarkable nutritional and functional properties (Fathi et al., 2018). The functional attributes of proteins including surface activity, gelling ability and high interacting capability of the functional groups located on their surfaces, offer a great opportunity for the delivery of bioactive agents (McClements & Gumus, 2016). Thermal denaturation of proteins

is widely utilized to form hydrogels for such delivery purposes and one of the most suitable proteins are whey proteins (Gunasekaran et al., 2007).

An important factor affecting the encapsulation hence the release characteristics of WPI hydrogels is the polymer blending to these hydrogels during gelation (Jones & McClements, 2010; Turgeon & Beaulieu, 2001; Zand-Rajabi & Madadlou, 2016; Zhang et al., 2014). Production and characterization of alginate added WPI based hydrogels were thoroughly examined as bioactive agent carriers in various controlled release systems (Chen & Subirade, 2006; Gbassi, Vandamme, Yolou, & Marchioni, 2011; Hébrard et al., 2010; Nogueira, Prata, & Grosso, 2017). Besides alginate; PC and XG polysaccharides were mainly used for the incorporation into particularly chitosan containing polyelectrolyte complexes (Argin et al., 2014; Ventura & Bianco-Peled, 2015). Furthermore, PC, XG and GT blended composite WPI hydrogels have also gained interest for such delivery purposes (Ozel et al., 2020; Ozel et al., 2017; Santipanichwong, Suphantharika, Weiss, & McClements, 2008; Zhang et al., 2014). Further investigations on the effects of blending these polymers into WPI based hydrogel formulations and detection of their possible synergistic effects on bioactive compound delivery systems in different release media are, therefore, at utmost importance.

1.3.1 Controlled Release in GIT

Foods consumed by human beings follow a gastrointestinal path including mouth, stomach and intestine phases. After ingestion of a food material, stomach and intestinal phases determine the bioavailability of the nutrient (McClements, 2017). Absorption rate of the nutrients through the intestinal wall could be manipulated by encapsulation of the nutrient in an active agent carrier which would induce a controlled release throughout the GIT (Dima et al., 2020). Human GIT has some factors influencing the digestion of sensitive nutraceuticals. These physicochemical and physiological factors including pH, presence of enzymes and other chemical constituents in the gastrointestinal fluids affect the digestion process thus the

bioavailability of the ingested nutraceuticals (Peanparkdee & Iwamoto, 2020). Therefore, encapsulation of the bioactive agents prevents these compounds from fast and excessive biochemical degradation in GIT. Bioaccessibility and bioavailability of the ingested nutraceutical depend on some endogenous and exogenous factors. Endogenous factors consist of release rate, dissolution of the compounds in the gastrointestinal fluids and absorption of the bioactive material by the epithelial layer whereas exogenous factors include the physicochemical properties of the ingested material, food matrix used and any type of food processing and storage before the digestion (Dima et al., 2020).

Plant polyphenols are one of the bioactive compounds that are very sensitive to aggressive GIT conditions (McClements, 2017). During gastrointestinal digestion, polyphenols may undergo some structural changes that would reduce their stability (Cilla et al., 2009). Simulated gastric digestion reduces the recovery of plant phenolics in the presence of pepsin. Therefore, major loss of phenolic compounds and anthocyanins takes place in simulated gastric fluid (SGF) (Peanparkdee & Iwamoto, 2020). Intestine phase also has some drawbacks for polyphenol recovery. Polyphenols including anthocyanins and phenolic acids are unstable in the mild alkaline environment of simulated intestinal fluid (SIF) (Tagliacruzchi et al., 2010). Degradation of these compounds in intestine phase is a quite common phenomenon (Liang et al., 2012). Consequently, in order to avoid low absorption and bioavailability of polyphenols in GIT, encapsulating them in a food grade hydrogel could be implemented.

In vitro gastrointestinal digestion studies are considered as predictive substitutes for *in vivo* studies. *In vitro* digestion estimates the pre – absorptive events including stability and bioaccessibility of a nutrient from a food matrix (Thakur et al., 2020). For this reason, determination of the release behavior of the ingested compound for its subsequent availability for absorption in the intestine was the main purpose of this study. The overall evaluation of the digestion including the bioavailability of the nutrient which defines the systematic circulation of the ingested nutrient and its utilization in physiological functions is out of the scope of this study. For such

evaluations and validation of *in vitro* gastrointestinal studies, *in vivo* gastrointestinal digestion experiments should be conducted (Cardoso et al., 2015). Although *in vitro* gastrointestinal studies offer a limited assessment for gastrointestinal models due to some hindrances such as static digestion process, these studies provide valuable and practical information for respective human and animal gastrointestinal models which are difficult to set up (Bouayed et al., 2011). Moreover, evaluation of *in vitro* models could be correlated with human and animal models (Biehler & Bohn, 2010).

1.3.2 Food Applications

Microcapsules, nanocapsules and hydrogels are used to encapsulate bioactive compounds for food applications. Plant polyphenols are among those compounds loaded in these matrices and implemented into the food products in order to enhance the bioaccessibility of the release material. Researchers have reported that encapsulated plant polyphenols provide greater benefits than polyphenols that are not encapsulated in the food products. When a bioactive carrier is introduced into a food matrix, the active agent is gradually released into the product so that the activity of the released agent is preserved during storage. These applications also provide higher stability of the encapsulated compound during gastrointestinal digestion. Some of the examples for such applications are dairies, beverages, confectionaries, meat and fish products (Peanparkdee & Iwamoto, 2020).

Altin et al. (2018) prepared a drinking yogurt beverage formulation including cocoa hull waste extract. They observed a higher stability of the phenolic compounds after *in vitro* digestion when cocoa hull waste extract was introduced into the product after encapsulation in chitosan coated liposomes (Altin et al., 2018). Encapsulation of Roselle in gelatin confectionary gum and incorporation of encapsulated cinnamon particles in white chocolate reduced the release rates of phenolic compounds thus increased their stability during *in vitro* gastrointestinal digestion (Muhammad et al., 2018; Villanueva-Carvajal et al., 2013). In dairy products, positive effects of encapsulation can also be observed. When encapsulated green tea catechins were

incorporated into a hard low-fat cheese, it was found that encapsulation protected the green tea antioxidants in low-fat cheese before the delivery of the cheese into the digestive system. Moreover, after *in vitro* digestion, antioxidant potential originated from consumption of cheese was enhanced by this application (Rashidinejad et al., 2016). Curcumin nanoemulsion prepared with sodium caseinate was incorporated into an ice cream formulation. This system showed a high encapsulation efficiency and high stability against processing conditions. Encapsulated curcumin emulsions were also found to be stable especially in gastric phase (Kumar et al., 2016).

Number of application areas for encapsulation of nutraceuticals can be increased but some applications were mentioned. Literature studies show that there are many techniques to produce bioactive carriers and achieve encapsulation. Encapsulation technique, carrier material used, type of the encapsulated material and release medium determine the bioaccessibility and stability of the encapsulated agent (Peanparkdee & Iwamoto, 2020). In this study, WPI based polymer gels were loaded with BC to manipulate the release rate and increase the stability of BC polyphenols in gastrointestinal conditions. Furthermore, these BC containing hydrogels were incorporated into yogurt to develop a phenolic – enriched product.

1.4 Black Carrot (*Daucus carota*) Concentrate

BC is a rich source of polyphenols (Akhtar et al., 2017). Phenolic compounds are composed of aromatic rings with an attached hydroxyl group. Phenolics are present in plants and they play a crucial role in human nutrition (Naczki & Shahidi, 2004). Polyphenols can be divided into two major groups namely flavonoids and non-flavonoids. Non-flavonoids contain mainly phenolic acids. Flavonoids include anthocyanins, flavones, flavanones, flavonols and flavanols (Akhtar et al., 2017). Flavonoids are reported to have a protective role against several degenerative diseases such as diabetes, cancer, oxidative stress, neuro – degeneration and cardiovascular diseases (Arts & Hollman, 2005; Graf et al., 2005; Metzger & Barnes, 2009). Black carrot differs from most of the other plant flavonoid sources with its

high anthocyanin content (1.75 g/kg) and remarkable anthocyanin profile (Kirca, Ozkan, & Cemeroglu, 2006). Anthocyanins have antioxidant properties (Thakur et al., 2020). Due to its high total phenolic concentration and rich anthocyanin profile, BC has a high antioxidant capacity (Kammerer et al., 2004). Antioxidant capacity of BC is at least ten fold higher than orange carrot juice. Obviously, intense and remarkable anthocyanin content of BC provides a high antioxidant activity (Kirca et al., 2006). Besides anthocyanin compounds, some non –anthocyanin phenolic compounds such as phenolic acids are also present in BC and contribute to the antioxidant properties of BC. Among them, chlorogenic acid is found as the major phenolic in BC. Generally, high chlorogenic acid content of BC is mainly responsible for its antioxidant activity (Cemeroglu, 2010).

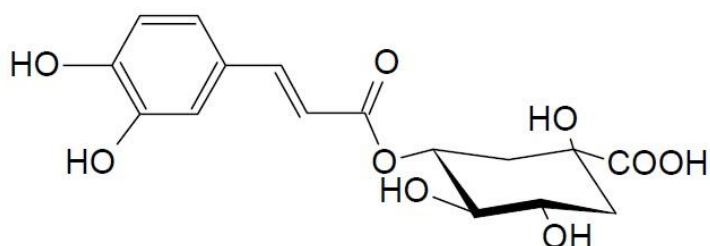


Figure 1.9. Chlorogenic acid (Rein, 2005)

Major anthocyanins of BC are mainly cyanidin based ones such as cyanidin-3-xylosyl-glucosyl-galactoside, cyanidin-3-xylosyl-galactoside and coumaric, ferulic and sinapic acid derivatives of cyanidin-3-xylosyl-glucosyl-galactoside. More than half of the BC anthocyanins are in acylated forms and the predominant anthocyanin is cyanidin-3-xylosyl-feruloyl-glucosyl-galactoside (Kamiloglu et al., 2017).

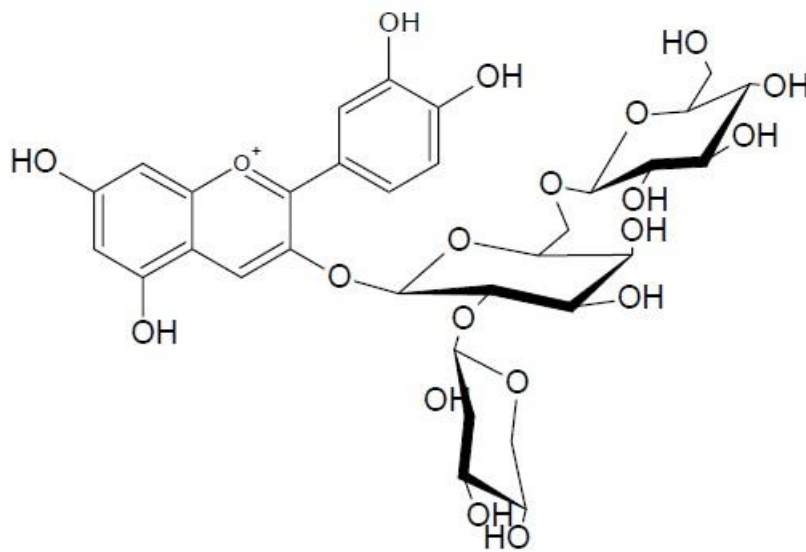


Figure 1.10. Cyanidin-3-xylosyl-glucosyl-galactoside (Rein, 2005)

Chemical structures of acyl groups that are bound to anthocyanins affect the stability of the anthocyanins. Non-acylated anthocyanins are more susceptible to temperature and pH changes. An acyl group is covalently bonded to glycosyl group of an anthocyanin. Thus, acylated anthocyanins have covalent bonds in their structures whereas non-acylated anthocyanins have hydrogen bonding and hydrophobic interactions. The energy needed to disrupt a covalent bond is approximately 17 times higher than the energy needed to disrupt a hydrogen bond. Consequently, acylated anthocyanins are more stable with respect to non-acylated ones (Kammerer et al., 2003). Since BC anthocyanins are mostly in acylated form and they undergo enhanced co-pigmentation by acylated anthocyanins, BC anthocyanins have a high stability (Esatbeyoglu et al., 2016).

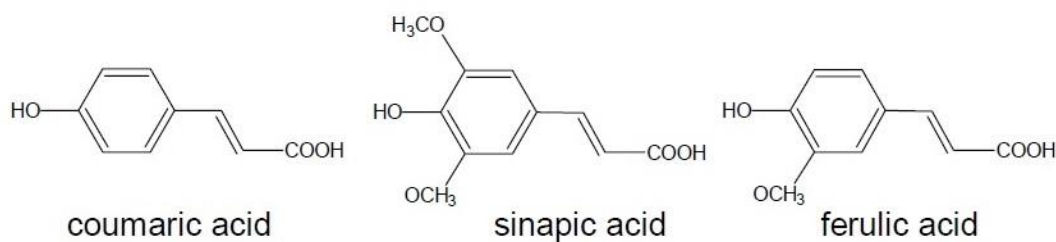


Figure 1.11. Chemical structures of coumaric, sinapic and ferulic acids (Rein, 2005)

BC anthocyanins are more stable over a wide pH range and at elevated temperatures. They show good stability at pH's between 2.5 – 4.0 but as pH increases above 4.0, anthocyanin stability decreases (Ersus Bilek et al., 2017; Kammerer et al., 2004). Kirca et al. (2006) reported that BC anthocyanins had high stability in apple and grape juices even at 90 °C (Kirca et al., 2006). Although acylated anthocyanins exert good stability characteristics, type and chemical structure of the organic acid esterified to anthocyanins determine the degree of stability of that acylated compound. Organic acids forming an ester bond with glycosyl units of anthocyanins could be an aromatic phenolic acid, an aliphatic dicarboxylic acid or even a combination of those (Cabrita et al., 2000). Anthocyanins acylated with aromatic acyl groups are more stable than the ones acylated with aliphatic acyl groups. Reason for this phenomenon is the presence of methoxy groups in the phenolic acid structures. Methoxy groups are believed to increase the stability of the phenolic acids and number of these groups affect the stability of such structures. Ferulic acid has one methoxy group whereas sinapic acid has two methoxy groups. Coumaric acid, on the other hand, does not possess any methoxy group in its structure (Stintzing & Carle, 2004).

Anthocyanin pigments are water soluble and they give black carrots their purple color (Yildiz, 2010). Therefore, commercial BC anthocyanins are widely used as natural food colorants in food industry (Downham & Collins, 2000). There is a great attention in food industry for natural food colorants instead of synthetic ones. The high temperature, light and pH stability of BC anthocyanins makes it a good

candidate to be used as colorant in beverages, jellies, confectionaries, syrups and canned products. Moreover, food materials containing BC pigments possess some health benefits (Montilla et al., 2011).

Anthocyanins can form complexes with metals such as Mg, Fe, Cu, Sn and Al to produce stable and intense colored compounds (Markakis, 1982). These anthocyanin – metal complexes stabilize the color of fruit and vegetable products. Cyanidin is the main anthocyanidin in BC and the presence of two hydroxyl groups in its B ring makes chelating possible with metals (Osawa, 1982). Only cyanidin, delphinidin and petunidin anthocyanidins can form chelates with metals since they are the ones carrying more than one free hydroxyl group in their B rings (Williams & Hrazdina, 1979).

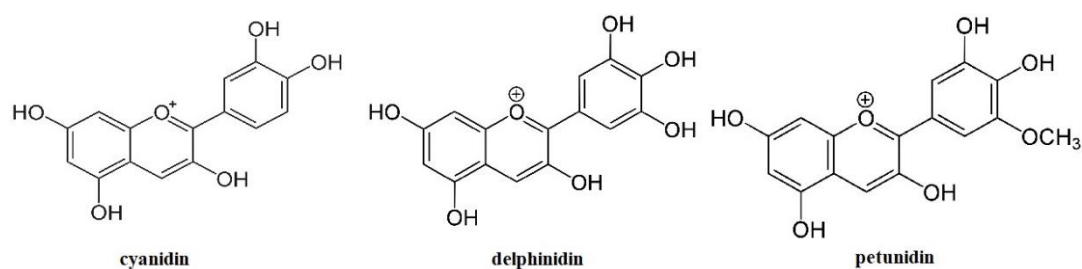


Figure 1.12. Chemical structures of cyanidin, delphinidin and petunidin

Despite the relatively higher stability to environmental conditions compared to other plant phenolics, black carrot phenolics are also susceptible to some processing conditions and external factors. Thermal degradation of black carrot anthocyanins follows first order kinetics in natural fruit juices and nectars. Ascorbic acid increases the degradation rate of anthocyanins. So, black carrot anthocyanins have more stability in apple and grape juices at high temperatures since these juices contain much lower amount of ascorbic acid. Consequently, black carrot anthocyanins show the lowest stability in orange juice (Kirca & Cemeroglu, 2003). In addition, *in vitro*

gastrointestinal digestion of BC indicated lower total phenolic content (Bouayed et al., 2011). Kamiloglu et al. (2015) demonstrated that total phenolic contents of black carrot jams and marmalades were significantly lowered in gastrointestinal digestion conditions (Kamiloglu et al., 2015b). Total polyphenol contents further decreased during transition from the acidic gastric environment to mildly alkaline intestinal medium. Anthocyanins are highly unstable especially at intestinal pH (McDougall et al., 2005; Tagliazucchi et al., 2010). Therefore, encapsulation BC in delivery matrices is necessary particularly for gastrointestinal digestion. There are some studies showing that microencapsulation of phenolics by using protein hydrogels is a promising method (Betz et al., 2012; Betz & Kulozik, 2011b). High temperature stability of black carrot anthocyanins enable their encapsulation in heat induced WPI hydrogels for controlled release purposes. Additionally, at high concentrations, anthocyanins may increase their stability through their self-association in thermally generated whey protein gel matrices (Betz & Kulozik, 2011b; Naczki, Grant, Zadernowski, & Barre, 2006). Encapsulated active agents in polymer networks were used for nutraceutical delivery systems before and BC could also be used for such purposes (Pakzad et al., 2013).

Encapsulation efficiency of phenolics depends on phenolic concentration and encapsulating polymer amount. Generally, a high encapsulating material presence increases the stability of the encapsulated phenolics during storage (Çam et al., 2014). Additionally, carbohydrate and protein containing encapsulating materials demonstrate an effective encapsulation (Kuck & Noreña, 2016). Therefore, in this study, PC, GT and XG polymers were blended with WPI to achieve suitable BC carriers and manipulate the release of BC in different release media.

1.5 Characterization of Hydrogels

Physicochemical characterization of hydrogels is important to understand the dynamics affecting the release behaviors of the bioactive agent loaded hydrogels. LF NMR, FTIR spectroscopy, SEM, texture and rheology measurements were the main

experiments conducted for the physicochemical characterization of the hydrogels in this study. Simple mathematical and kinetic release modellings were also used for hydrogel characterization.

1.5.1 Low Field (LF) Nuclear Magnetic Resonance (NMR) Relaxometry

NMR relaxometry is a non-invasive and non-destructive method that can be used to analyze the internal compositions of foods (Kirtil & Oztop, 2016a). LF ^1H NMR presents a practical way to measure proton relaxation in the complex food systems (Oztop et al., 2012). Working principle of NMR Relaxometry includes the use of a radio frequency (RF) pulse. Sample is placed between magnets creating static magnetic field. The applied RF pulse then creates a temporary disturbance within the sample. When the RF pulse is removed, relaxation of the excited signal is monitored and recorded. This information can be used to differentiate distinct samples (Kirtil & Oztop, 2016a).

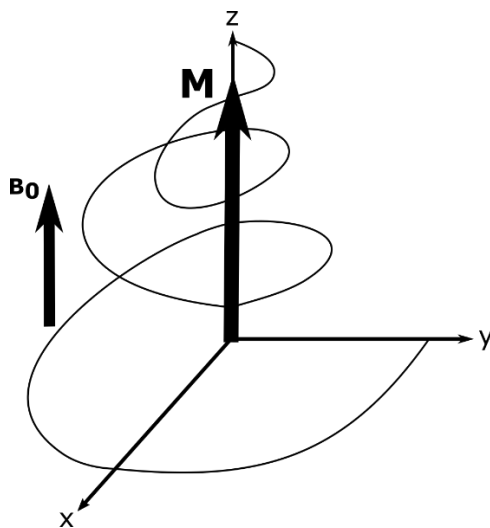


Figure 1.13. Representation of magnetization relaxation in z direction after the removal of RF excitation

1.5.1.1 Transverse Relaxation Time (T_2)

Hydrogen is abundantly found in organic samples. The odd nucleon number of hydrogen is suitable to get a net nuclear magnetization moment which enables characterization of water and oil containing samples by NMR Relaxometry. Magnetic moments of protons of a sample could be either in the same or in the opposite direction with the external magnetic field. Thus, a net magnetic is generated in the sample (in z direction) which is called as longitudinal magnetization. However, these protons make precession at the same frequency under the strength of the external magnetization. The resulting magnetization on the xy plane is defined as transverse magnetization. Due to the out of phase precession of protons, net magnetization on the xy plane becomes zero. In order to create a net magnetization on the xy plane an RF pulse is needed. When an RF pulse is applied, some of the net magnetization along the z axis is tipped onto the xy plane. As longitudinal magnetization declines transverse magnetization rises. After RF pulse is removed, in-phase protons in the transverse plane turn back to their initial states. This is called transverse or spin-spin relaxation. Consequently, the time it takes for the generated transverse magnetization to decay to zero after the removal of RF pulse is described as transverse relaxation time (T_2) (Hashemi et al., 2010; Kirtil & Oztop, 2016a).

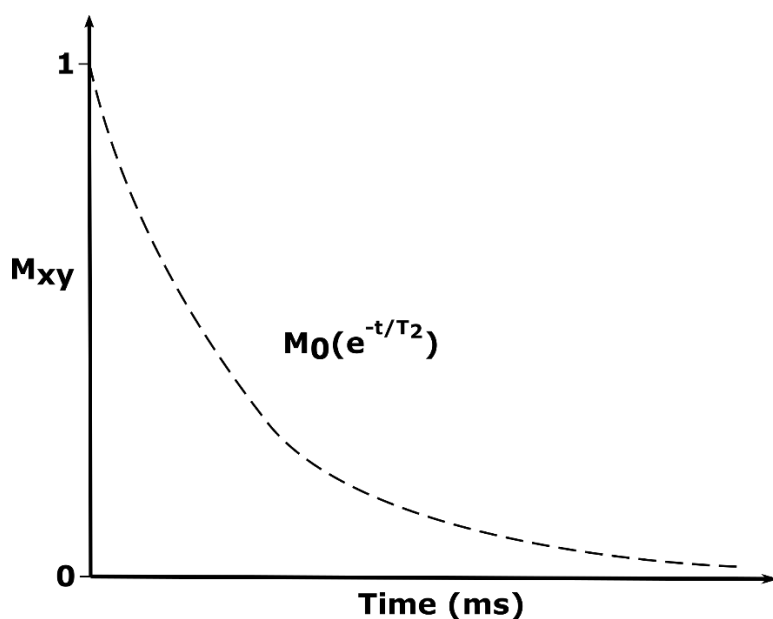


Figure 1.14. A representative exponential transverse relaxation of a sample

Proton relaxation represents the overall sample analyzed since signals come from all protons in a sample. The obtained NMR signal can give information about the internal structure of a sample due to the mobility and distribution of protons within the sample. T_2 defines the effectiveness of the energy transfer between neighboring spins. Therefore, materials having closely packed molecular structures such as solids attain shorter T_2 whereas materials having larger distances between their neighboring spins such as water have longer T_2 (Hashemi et al., 2010). Based on this idea, transverse relaxation experiments are used as an alternative method to monitor swelling and release behaviors of polymer matrices and hydrogels. This technique allows identification of water distribution within the hydrogels. Moreover, molecular interactions of the polymers constituting the respective hydrogel including polymer – polymer and polymer – water interactions could also be investigated by transverse relaxation parameters of NMR relaxometry (Oztop et al., 2012; Williams, Oztop, Mccarthy, Mccarthy, & Lo, 2011). T_2 enables the characterization of changes in the

mobility of protons and conformations of biopolymer chains in various media (Oztop et al., 2014).

1.5.1.2 Self-Diffusion Coefficient (SDC)

Self-diffusion coefficient (SDC) is calculated from the direct measurement of the mobility of water molecules within a food material (Hashemi et al., 2010). The direct SDC measurement can be used to get more specific findings about the water protons within a sample. There are many protons that are located in different materials besides the water in a hydrogel sample such as macromolecular surroundings. These proton populations can also contribute to the proton relaxation in the overall system and affect T_2 . Thus, SDC measurements can give more information about water mobility in a sample from a macroscopic scale (Salami et al., 2013). For instance, presence and type of the polymers in a hydrogel system influence the SDC of water (Manetti et al., 2004). Therefore, differences in the types of hydrogels and release media are expected to reveal distinct results for SDC of water which could be utilized for hydrogel characterization.

1.5.2 Fourier Transform Infrared (FTIR) Spectroscopy

FTIR technique is based on obtaining an infrared spectrum of a tested sample through absorption or emission. Applied infrared radiation could be absorbed or transmitted through the sample. In most cases, some of the radiation is absorbed and the remaining radiation is transmitted through the sample. Collected signal at the detector presents a spectrum which could be called as molecular fingerprint of the sample (Berthomieu & Hienerwadel, 2009). FTIR spectroscopy is able to detect distinct chemical structures and interactions since each of these structures produces different spectral fingerprints. Therefore, it has been extensively used for structural composition analysis of food components (Dong et al., 1996; Ebrahimi et al., 2016). One important example is the analysis of secondary structural compositions and

conformational changes of proteins (Arrondo et al., 1993). Chemical structures and bond stretchings in polysaccharides can also be detected by FTIR spectroscopy. Presence of carboxylic acids and glycosidic bonds induces changes in the IR spectrum and may be associated with polysaccharide existence in the system (Cai et al., 2010). Consequently, hydrogels containing WPI and various polysaccharides were suitable for FTIR spectroscopy characterization in this study.

1.5.3 Scanning Electron Microscopy

SEM provides higher magnification and better resolution than conventional optical microscope. Electron microscopy utilizes the acceleration of electrons to high energies (2 – 1000 keV). By this way, the wavelength of the imaging radiation is decreased. The sent high-energy beam interacts with the atoms in the sample. If the sample is thick enough, electrons are not transmitted through the sample and a signal is generated. This signal is induced via excited atoms in the specimen by the electron beam. Emitted electrons are collected by an electron detector. From this information, surface topography and even composition of the sample could be analyzed (Vernon-Parry, 2000). Agricultural products can be examined by SEM. Although SEM measurements require dry samples, hydrated food samples could also be analyzed by SEM after freeze-drying. High fat food samples are also among the materials that have been observed by SEM technique (Kalab et al., 1995). Moreover, SEM has been used to identify and analyze the polysaccharide, protein and gel-emulsion systems (Krstonošić, Dokić, Nikolić, & Milanović, 2015; Ozel et al., 2020; Wang et al., 2018). Visualization of polymer interactions and structural changes in microscale enabled detailed characterization of such systems.

1.5.4 Rheology and Texture Characterization

1.5.4.1 Rheology of Hydrogel Forming Solutions

Rheology examines the responses of the materials in terms of deformation under applied forces or stresses. Rheological properties of a food material reflect the deformation and the flow of that material in the presence of a stress. Rheological properties of foods determine the product quality and required process conditions to produce that specific product (Sahin & Sumnu, 2006). Rheological characterization of solutions from which the hydrogels are formed is important since the rheology of the solutions shapes the physical characteristics of the respective hydrogels (Taherian et al., 2017). Flow character of a hydrogel solution can give an idea about the physical interactions taking place within the sample (Abbastabar et al., 2015). Our hydrogels contain protein, polysaccharides, BC and water. Distinct flow behaviors could be attributed to structure of the polymers, their degree of interactions and extent of molecular entanglements in the system. For this purpose, shear rate ramp measurements could be conducted. Solutions having a linear viscoelastic region (LVE) can also be subjected to frequency and temperature sweep tests. These tests reveal information about the storage and loss moduli of the tested solutions. In this way it could be determined whether the sample possesses viscous or solid-like character (Doucet et al., 2001).

1.5.4.2 Texture of Hydrogels

One of the most important quality parameters of foods is texture. Textural properties of food materials comprise hardness, adhesiveness, cohesiveness, springiness e.g. and can be analyzed by a texture analyzer. Among the aforementioned properties, hardness is one of the most common textural properties in order to define a food product. Hardness is simply expressed as firmness of the product. Puncture and texture profile analysis (TPA) are used to determine the hardness of a food material.

Some dairy or meat products, vegetables, fruits and gels are suitable for hardness measurements. Working principle of TPA is based on simulation of the chewing action of teeth by compressing a piece of food material twice. Usually, 80 % of the length of the food material is compressed during the hardness measurements (Sahin & Sumnu, 2006). TPA produces a force curve as a function of time. Here, hardness is defined as the peak force generated against the resistance during the first compression cycle (Sahin & Sumnu, 2006; Zand-Rajabi & Madadlou, 2016).

Hardness is an important texture property in terms of hydrogel characterization (Wichchukit et al., 2013). Since hydrogels are mostly used for bioactive agent encapsulation and controlled release purposes, endurance of these hydrogels in adverse conditions is an important parameter. Ionic strength, pH, presence or absence of an enzyme etc. in release media induce different changes in hydrogels having different hardness properties. For instance, a hard hydrogel matrix may provide smaller pores for the hydrogel which would reduce the penetration depth of the digestive enzymes into the gel matrix. Such hydrogels are expected to remain intact and resist digestion under these conditions (Guo, Bellissimo, & Rousseau, 2017). Final hardness value of a hydrogel after exposure to a release medium may present an idea about the degree of cross-linking within the hydrogel during the experiment. Liang et al. (2020) stated that cross-linking increased the hardness of whey protein emulsion gels (Liang et al., 2020). Release rate of encapsulated material from a hydrogel in a release medium is also affected by the gel strength (Ozel et al., 2020). Therefore, hardness characterization of hydrogels provides valuable information for the manipulation of the release behaviors in GIT and various release media.

1.5.5 Release Modellings

Understanding the release mechanism of a controlled release system is crucial in terms of optimization of the release phenomenon. Release of active agents from gels could be explained by diffusion, swelling – shrinkage and chemical mechanisms (Je Lee & Rosenberg, 2000). When hydrogels are placed in a solvent, they usually swell

owing to the penetration of hydrophilic solvent into the gel matrix due to the relaxation in the polymer structure. However, each gel formulation and release medium characteristics produces different swelling behaviors (Siepmann & Peppas, 2001). When swelling has no or very little effect on diffusion, diffusion controlled release could be expressed by Fick's law of diffusion. Swelling controlled release occurs on the condition that mass transfer of active compound is faster than swelling of the gel (Oztop et al., 2014). Both diffusion and swelling related mechanisms may affect the release behavior. Models taking into account both diffusion by Brownian motion and polymer relaxation to predict the molecule release may require several modeling iterations and considered as rigorous methods (Lin & Metters, 2006). Diffusion coefficient could be examined in terms of molecular motions. Such Brownian motion could arise from random motion of particles. This random motion is then connected to diffusion (Cussler, 2009).

In chemically controlled systems, reactions occur within the delivery matrix such as cleavage of polymer chains via enzymatic or hydrolytic degradation, during the release of encapsulated substance (Lin & Metters, 2006). In such cases, erosion of the polymer matrix may take place which would change the hydrogel dimensions during the release process (Fathi et al., 2018). Since release behavior of these hydrogels would be irregular under these conditions, simple kinetic models could be used to identify the release behavior instead of using a fitting release model. Erosion of hydrogels is usually encountered in the intestine phase of gastrointestinal digestion (Chen & Subirade, 2006).

1.6 Objectives of the Study

The primary objective of this study was to demonstrate that WPI-based hydrogels could be used to design hydrogel systems for controlled release purposes. Another important objective was to prove that the release behavior of such hydrogels could be manipulated by addition of different types of polysaccharides. It was also hypothesized that the type and condition of the release medium was effective on the

physicochemical properties and release behaviors of the hydrogels. The results of the controlled release of BC experiments in phosphate buffer and simulated gastrointestinal fluids confirmed these claims. Another core objective of the study was the use of TD NMR relaxometry as a nondestructive analysis technique. TD NMR relaxometry parameters such as T_2 and SDC have been found to contribute to the understanding of physicochemical changes and polymer-water/polymer-encapsulated agent interactions within hydrogels. Produced hydrogels were also applied to a real food formulation (yogurt) in order to show that these hydrogels could be successfully used for food formulations. The most important objectives of this study could be summarized as follows:

- To design and demonstrate that heat-induced WPI-based hydrogels could be used for encapsulation and controlled release of BC
- To demonstrate that blending additional polysaccharides to WPI could be used to manipulate the swelling and release characteristics of the hydrogels
- To show that heating type (MW and conventional heating) affects the release behaviors of the hydrogels
- To understand the effects of different release media on the physicochemical properties and release behaviors of the hydrogels
- To show that TD NMR relaxometry was an effective nondestructive tool to monitor the physicochemical changes within the hydrogels during the controlled release of the hydrogels
- To analyze the rheological properties of hydrogel solutions and textural characteristics of hydrogels and correlate these characteristics with the macro properties (release behaviors) of the produced hydrogels
- To show the use of FTIR spectroscopy, zeta potential, dielectric, pH, total acidity, moisture, soluble protein content, SEM and total phenolic content/antioxidant capacity measurements for characterization of hydrogels
- To demonstrate the potential of the application of BC loaded hydrogels to maintain the total phenolic content and antioxidant capacity of yogurt samples

CHAPTER 2

MATERIALS AND METHODS

2.1 Materials

WPI was purchased from Hardline Nutrition (Kavi Food Ltd. Co., Istanbul, Turkey). Protein content of WPI was determined by Kjeldahl method as 88.5 % (w/w). Polysaccharides PC (Product Code: GP 1507, FMC, Italy S.R.L.) and GT from *Astragalus gummifier* Labillardiere (Product Code: TRA5183, Thew Arnott & Co. Ltd, Deeside, United Kingdom) and XG from *Xanthomonas campestris* were the blended polysaccharides. PC is a high methoxyl pectin extracted from citrus peel and has an esterification degree of 64 – 68 %. XG was purchased from a local company (Smart Kimya Tic. ve Danismanlik Ltd. Sti., Izmir, Turkey). Sodium azide was used to protect hydrogels from microbial activity (Merck KgaA, Darmstadt, Germany). Compositional analysis of GT revealed 60 % tragacanthin and 40 % bassorin (w/w) in GT. BC was kindly provided by Targid A.S. (Targid Agriculture Co., Inc., Icel, Turkey). Total phenolic content of BC was measured as 20.59 mg of Gallic Acid Equivalent (GAE) / g sample by Folin – Ciocalteu method (Arab et al., 2011). Antioxidant capacity of BC was found as 1.93 mg 2,2-diphenyl-1-picrylhydrazyl (DPPH) / g sample by DPPH radical scavenging method (Wang, Gao, Zhou, Cai, & Yao, 2008). Disodium and monosodium phosphates were used to prepare the phosphate buffer at pH 7.0 (Na_2HPO_4 , NaH_2PO_4 , Sigma-Aldrich Co., St. Louis, MO). Pepsin and pancreatin enzymes, sodium chloride (NaCl) and hydrochloric acid (HCl) were used in gastrointestinal experiments (Sigma-Aldrich Co., St. Louis, MO). Additionally, monobasic potassium phosphate (KH_2PO_4) was used in SIF solutions and sodium azide was included in all release media as an antimicrobial agent (Merck KgaA, Darmstadt, Germany). Yogurt was chosen as the product for the food application of hydrogels. Full-fat yogurt was purchased from a local company (Eker

Süt Ürünleri Gıda San. ve Tic. A.S.) and total phenolic content – antioxidant capacity measurements were performed.

2.2 Hydrogel Preparation

All hydrogel formulations include WPI 15 % (w/w), a blended polysaccharide (PC, GT or XG) 0.5 % (w/w), BC 4 % (w/w) and sodium azide 0.02 % (w/w). The remaining portion is distilled water. Amounts of WPI, polysaccharides and BC were determined and optimized by preliminary experiments. WPI solutions and polysaccharide – BC including solutions were stirred at 15,000 rpm for 2 min with Ultra Turrax T-18 (IKA Corp., Staufen, Germany), separately. Then, these mixtures were mixed and stirred overnight at room temperature. XG solutions were centrifuged at 715 g for 2 min prior to mixing with WPI solutions in order to remove air bubbles formed in the XG solutions (Hanil Science Industrial Co., Ltd., Incheon, Korea). After overnight stirring, hydrogel solutions having pH values ranging between 5.66 and 5.89 were poured into cylindrical tubes with 1.5 cm outer diameter and 5 cm length. Gelation of the solutions is achieved either by conventional heating (CV) or Infrared Assisted Microwave heating (MW). For CV, glass tubes containing hydrogel solutions were immersed in water bath and heated at 90 °C for 30 min (Wisd, Wertheim, Germany). After 30 min of heating, tubes were immersed in ice bath for 15 min. MW was implemented by a IR-assisted-microwave oven consisting of two upper and one lower halogen lamp, a turntable and a microwave source (General Electric Comp., Louisville, KY, USA). Cavity size of the oven consists of 21 cm height, 48 cm length and 33 cm height. The microwave power of the oven is 706 W which was determined by IMPI 2-1 test (Buffler, 1993). IR was combined with microwave heating to reduce the instantaneous internal heat generation in the samples. Upper and lower halogen lamps (1500 W, each) was adjusted to 40 % power level, as IR source. Microwave power was adjusted to 50 %. MW was applied to samples for 2.5 min which was the minimum sufficient time for the gelation of samples in the microwave oven. Instead of cylindrical tubes used in CV, beakers

having large cross-sectional area (9.5 cm diameter) was used in MW. By this way, overflowing of the solutions from the cylindrical tubes was prevented. After gelation of the solutions in the beaker under MW, beakers were immersed in ice bath for immediate cooling for 15 min. Following gelation either by CV or MW, gels were cut into 1.3 cm diameter cylindrical shapes with 2 cm length (Oztop et al., 2010). Samples produced by both CV and MW were used and compared in phosphate buffer release experiments. Since hydrogels produced by MW were not suitable for gastrointestinal digestion conditions due to their physical characteristics, only hydrogels produced by CV were used in GIT release experiments and food application.

2.3 Release Media Preparations

2.3.1 Phosphate Buffer

Release behaviors of MW and CV samples were compared in phosphate buffer having neutral pH. The reason for using neutral pH phosphate buffer was to mainly focus on the effect of heating type on the formation of biopolymer complexes rather than pH alteration and enzyme effects. Phosphate buffer was prepared by mixing disodium and monosodium phosphates in distilled water and pH was adjusted to neutral pH (7.0).

2.3.2 Simulated Gastric Fluid (SGF)

SGF represents the stomach phase of the *in vitro* GIT studies. The method presented by Sarkar et al. (2009) was used to prepare SGF (Sarkar et al., 2009). Pepsin enzyme (3.2 % w/v) and NaCl (2% w/v) were present in the final mixture. HCl – distilled water was mixed with pepsin – NaCl solution to obtain SGF. Final pH was adjusted to 1.2 by 0.2 N HCl and 0.2 N sodium hydroxide (NaOH) solutions.

2.3.3 Simulated Intestinal Fluid (SIF)

SIF represents the intestine phase of the *in vitro* GIT studies. SIF was prepared as described in the United States Pharmacopoeia (24th Edition, p 2236). Final mixture contained pancreatin enzyme (10 % w/v) and KH₂PO₄ (6.8 % w/v). After completing the solution volume with distilled water, final pH was adjusted to 6.8 by 0.2 N NaOH and 0.2 N HCl solutions.

2.4 Swelling Experiments

Swelling experiments were only applicable to release studies in phosphate buffer. Hydrogels did not show swelling in gastrointestinal conditions. Additionally, gels produced by MW could not maintain their shapes in the swelling medium and they were also unsuitable for swelling calculations. Only hydrogels produced by CV were subjected to swelling experiments in phosphate buffer. Cylindrical gels were placed in plastic mesh baskets and immersed into 150 mL buffer solution. They were allowed to swell at room temperature up to 24 h. The swollen gels were periodically (0.5, 1, 2, 3, 4, 5, 6 and 24 h) removed from the baskets, blotted with filter paper to remove excess water and weighed immediately. 8 sets of hydrogels were used for these measurements so that each gel was used once for swelling calculation. Then, swelling ratio was calculated according to Equation (1),

$$\text{Swelling Ratio (\%)} = \frac{W_t - W_0}{W_0} \times 100 \quad (1)$$

where W_t is the weight of the gel at the defined time, W_0 is the initial gel weight.

2.5 Monitoring the Release of Black Carrot Concentrate (BC)

All cylindrical hydrogels (1.3 cm diameter, 2 cm length) were immersed in respective 40 mL release medium. A UV – visible spectrophotometer (Mecasys Co.

Ltd., Korea) was used to monitor the release of BC from hydrogels in each release medium.

2.5.1 Release in Phosphate Buffer

Gels prepared by CV and MW were immersed in 40 mL phosphate buffer stirring at 80 rpm. 4 mL of buffer solution was withdrawn from the medium at determined time intervals (0.5, 1, 2, 3, 4, 5, 6 and 24 h) and absorbance was measured at 530 nm. After measurement, taken aliquots were put back into the medium to keep the medium volume constant. A calibration curve was prepared using predetermined amounts of BC and recording respective absorbance value ($y=7.5704x - 4E-5$ where y and x represented absorbance and g BC/40 g buffer, respectively). In preliminary experiments, BC was exposed to heating conditions used in this study to assess the stability of BC with respect to temperature. The color of BC was found to be stable within the temperature and time intervals of the heating process.

2.5.2 Release in SGF

Gels prepared only by CV were immersed in 40 mL SGF stirring at 80 rpm and 37 °C. 4 mL of aliquots were taken at determined time intervals (5, 10, 20, 30, 45, 60, 75, 90, 105 and 120 min), measured at 530 nm and then put back into medium (Bateman et al., 2011). Calibration curve was the same as the one used in phosphate buffer experiments ($y=7.5704x - 4E-5$ where y and x represented absorbance and g BC/40 g SGF, respectively). Temperature was kept constant at 37 °C throughout the release in SGF in order to imitate the *in vitro* human gastric conditions.

2.5.3 Release in SIF

Simulated *in vitro* gastric and intestinal digestions were performed consecutively. After 2 h gastric digestion, gels were removed from SGF and immediately immersed

in SIF. SIF was previously brought to 37 °C and stirred at 80 rpm. pH of the SIF was adjusted to 6.8 prior to experiment. Release in SIF was monitored for 6 h and 2.5 mL of aliquots were withdrawn from the medium in 1 h intervals and again poured back into the medium to keep the volume constant. A wavelength of 545 nm was used for the absorbance measurements. A new calibration curve was prepared for BC release in SIF ($y=6.2821x - 7.2E-3$ where x and y represented g BC/40 g SIF and absorbance, respectively) (Takagi et al., 2003). Temperature was kept constant for better simulation of the human intestine conditions.

2.6 Dielectric Measurements

Dielectric properties (dielectric constant, ϵ' and dielectric loss factor, ϵ'') of hydrogel solutions affect the gelling behavior and the resulting hydrogel properties under microwave heating. Thus, dielectric properties of hydrogel solutions were determined by Agilent 85070E open-ended coaxial probe system connected to an Agilent E8362B Vector Network Analyzer (Agilent Technologies ES061B ENA Series Network Analyzer, USA).

2.7 Viscosity Measurements

Following overnight stirring of hydrogel solutions for full hydration of the polymers, viscosities of all gel solutions were measured with Sinewave Vibro Viscometer SV-10/SV-100 (A&D Company Limited, Japan). Viscometer has two viscosity detecting gold covered sensor plates oscillating in opposite directions. Sensor plates have a low frequency of 30 Hz and an amplitude of less than 1 mm. Samples were stabilized at 20 °C before the measurements.

2.8 LF NMR Relaxometry Experiments

Transverse relaxation ^1H (T_2) and self-diffusion coefficient (SDC) measurements of hydrogels were performed by a 0.32 T benchtop NMR spectrometer equipped with a 16 mm probe (Spin Track SB4, Mary El, Russian Federation). All T_2 and SDC measurements were conducted at room temperature (~ 20 °C). In order to obtain sufficient signal to noise ratio, hydrogels were cut longitudinally at 1.2 cm length and placed into the test tubes. Gastrointestinal digestion experiments were performed at 37 °C, however the RF probe could not be heated to 37 °C. Therefore, these samples were left to equilibrate with the room temperature before measurements.

2.8.1 T_2 Measurements

Carr-Purcell-Meiboom-Gill (CPMG) sequence was used to determine the T_2 of fresh hydrogels and phosphate buffer, SGF and SIF treated samples. Decay curves were best described by monoexponential fitting. Sequence parameters were 400 echoes with 1 ms echo time, 3000 ms repetition time (to assure complete recovery of the longitudinal magnetization) and 64 scans. T_2 of CV and MW treated hydrogels were monitored in phosphate buffer at determined time intervals (0, 2, 4, 6 and 24 h). During 2h of SGF treatment, T_2 of the samples were measured every 30 min (0, 0.5, 1, 1.5, 2 h). Before SIF treatment, T_2 of hydrogels were measured right after SGF exposure. Then, SIF T_2 measurements were performed in 2 h intervals (2, 4 and 6 h in SIF release).

2.8.2 SDC Measurements

SDC values of hydrogels in phosphate buffer and SGF release experiments were determined. SDC values of SIF treated samples were not measured because of the erosive nature of SIF. Stimulated spin echo (SSE) pulse sequence was used for SDC measurements. SSE had three $22 \mu\text{s}$, 90° pulses with 2 ms between the first and

second pulses whereas there was 60 ms between the second and third pulses. Acquisition time was 500 μ s. Pulsed gradient field duration was 1 ms with 1.66×10^{-2} T/m gradient strength. SDC of hydrogels in phosphate buffer was measured for 0 and 6 h of the experiment. In SGF, SDC of hydrogels were measured for 0 and 2 h of the release experiment.

2.9 FTIR Analysis

FTIR absorption spectra of hydrogels were analyzed by IR Affinity-1 Spectrometer with attenuated total reflectance (ATR) attachment (Shimadzu Corporation, Kyoto, Japan). FTIR analysis was applied to fresh hydrogels and hydrogels exposed to gastrointestinal digestion. By this way, effects of digestive enzymes on hydrogel physicochemical characteristics during release in GIT could be analyzed. Prior to FTIR analysis, hydrogels were frozen at -20 °C and then freeze-dried (Zhejiang Value Mechanical & Electrical Products Co. Ltd., Wenling City, China) for 2 days. Freeze-dried samples were then ground to powder form. Absorbance measurements were recorded between $4000 - 500$ cm^{-1} with 4 cm^{-1} resolution and 32 scans. In addition to fresh (before digestion), SGF and SIF treated hydrogels, FTIR spectra of dry powder forms of WPI and the blended polysaccharides were also obtained.

2.10 Rheology Measurements

Flow behaviors of hydrogel solutions in the presence and absence of BC were determined in order to understand the effect of hydrogel forming solution rheology on resulting hydrogel physical properties. For the solutions having a LVE in the desired strain level, frequency sweep measurements were conducted. Temperature sweeps were performed for all hydrogel solutions. Measurements were performed by a cup-and-bob (C25 DIN) dynamic rheometer (Kinexus Dynamic Rheometer, Malvern, U.K.).

2.10.1 Determination of Flow Behavior

Shear rate ramp experiments were done to determine the flow behaviors of the samples. Shear stress values were recorded for respective varying shear rates (0.1 – 100 s⁻¹). 2 min total ramp time with 20 sample points were used. Tests were conducted at 25 °C.

2.10.2 Amplitude Tests

Amplitude tests were performed at a fixed frequency of 1 Hz with varying strains (0.1 – 100 %) in order to determine the LVE of the samples. In these measurements storage (G') and loss (G'') moduli were recorded. Tests were conducted at 25 °C.

2.10.3 Frequency Sweep Tests

Frequency sweep test was performed only for XG solutions (both in the presence and absence of BC) since only XG hydrogel solutions had a LVE. Measurements were conducted between 10 and 1 Hz at 1 % constant strain. The constant strain was chosen from the LVE of XG solutions determined by amplitude test. G' and G'' were recorded. Tests were conducted at 25 °C.

2.10.4 Temperature Sweep Tests

Temperature sweep measurements were performed for all hydrogel solutions at 1 Hz fixed frequency and 1 % target shear strain. Records were collected between temperatures of 55 and 85 °C which was determined by preliminary trials. Initially, a hydrogel solution sample was loaded into the reservoir at 25 °C and then heated to 55 °C before the experiment starts. After reaching the equilibrium at 55 °C, the sample was started to be heated with the ramp rate of 5 °C/min up to 85 °C. G' and G'' were recorded in this range.

2.11 Texture Analysis

A texture analyzer equipped with a 50 N load cell and 1 cm diameter cylindrical stainless – steel probe (TA Plus Lloyd Instruments, U.K.) was used to measure hardness values of the freshly produced, phosphate buffer, SGF and overall digestion (SGF – SIF) treated hydrogels. Cylindrical hydrogels were subjected to compression test with the preload stress and stress speed of 0.1 N and 100 mm/min, respectively. The test extension rate was 100 mm/min. Two compression cycles were performed with 0.68 cm first extension and 0 cm second extension. Hardness is defined as the maximum force generated in resistance to the first compression of the sample (Zand-Rajabi & Madadlou, 2016).

2.12 Zeta Potential Analysis

Zeta potentials of the all hydrogels solutions (with and without BC) were measured by photon correlation spectroscopy (PCS) using a Malvern Zetasizer instrument (Malvern Nano ZS90, Malvern Instruments Ltd., Worcestershire, U.K.) present in METU Central Laboratory. Hydrogel solutions had dispersant refractive index and dispersant dielectric constant of 1.33 and 78.5, respectively. All solutions were diluted in a 1/10 ratio before the measurements. Smoluchowski approximation was used by the instrument to calculate the zeta potential values (Kaszuba et al., 2010).

2.13 Sugar Composition Analysis of BC

High-Performance Liquid Chromatography (HPLC) analysis was performed to determine the sugar composition of BC. For this purpose, HPLC (Agilent Technologies) equipped with ROA organic column, 300 mm × 7.8 mm (Phenomenex Inc.) at a constant temperature of 55 °C and a refractive index detector at 35 °C RID temperature with 10 μ l sample injection and 0.6 mL/min flow rate of mobile phase, 0.05 M H₂SO₄ was used. Prior to HPLC measurements, 1 mL of the

hydrogel solutions were centrifuged at 22780 *g* for 5 min by a laboratory type centrifuge (Mikro 220 R, Hettich Lab Technology, Germany). Then the supernatant of the sample was collected and diluted. Finally the diluted sample was passed through 0.45 μm filter. After the analysis, 284.4 g/L sucrose, 145.9 g/L glucose and 129.0 g/L fructose were found in BC.

2.14 Moisture and pH Measurements

Moisture content of fresh and SGF treated samples were analyzed by an Infrared Moisture Analyzer (Radwag, MAC 50, Poland). pH of the same set of samples was also measured by a pH probe (HALO Glass Body Refillable pH Electrode – HI11312, Hanna Instruments, RI, U.S.).

2.15 Gel Total Acidity Measurements

Acidic conditions impart distinct physicochemical characters to hydrogels. Thus, the total titratable acidity contents of the hydrogels (before and after SGF treatment) were determined. Initially, gels were crushed in distilled water via Ultra Turrax T-18 (IKA Corp., Staufen, Germany) at 15,000 rpm for 2 min and then resulting solutions were titrated with 0.1 N NaOH up to pH 7.0. The following equation was used to calculate the total titratable acidity (Cemeroglu, 2010),

$$T.A. = \frac{V \times f \times E}{M} \times 100 \quad (2)$$

where *V* denotes the consumed amount of 0.1 N NaOH in mL during titration, *f* is defined as the solution factor corresponding to 1.0 in this case since the normality of the NaOH solution used was exactly 0.1, *E* is the equivalent acidity amount in terms of dry citric acid (g) which is 0.006404 for 1 mL 0.1 N NaOH and finally *M* is the amount of the gel that was titrated in gram (Cemeroglu, 2010).

2.16 Weight Loss Determination of Hydrogels in SIF

All hydrogels eroded to some extent in SIF. Therefore, weights of the samples were measured before and after SIF treatment. Weight loss ratios were calculated as in Eq. (3),

$$\text{Weight Loss (\%)} = \frac{W_{2h} - W_{8h}}{W_{2h}} \times 100 \quad (3)$$

where W_{2h} is the weight of the sample after SGF treatment and W_{8h} denotes the final weight of the sample after the complete gastrointestinal digestion (2h SGF and subsequent 6h SIF treatments).

2.17 Soluble Protein Content Measurements

Protein loss is inevitable under *in vitro* gastrointestinal digestion conditions having digestive enzymes. Protein contents of both SGF and SIF media were determined according to the method described by Lowry, Rosebrough, Farr, and Randall (1951) in order to measure the protein loss from hydrogels during digestion (Lowry et al., 1951). This method is mainly based on the reaction of proteins with copper ions at alkaline conditions. For the determination of protein content in release media, a calibration curve was prepared by the dilution of 1 mg/mL BSA stock solution in different ratios by distilled water ($y = 1.6854x + 0.1027$, where x and y represent BSA mg/mL and absorbance value, respectively). Since the enzyme concentrations were constant for respective digestion media, effects of enzymes on soluble protein content measurements in each digestion medium were considered constant.

2.18 Release Behavior Modelling of Hydrogels

2.18.1 Release Modelling in Phosphate Buffer and SGF

The effective diffusion coefficient of BC release from phosphate buffer and SGF treated cylindrical hydrogels were calculated by the combination of the mass transport equation for diffusion in an infinite plane and an infinite cylinder in a stirred solution of limited volume. Product rule was used to combine these two equations. The conditions of the product type solution were satisfied with the solution for the finite cylinder geometry (Crank, 1975),

$$\frac{M_t}{M_\infty} = 1 - \left(\sum_{m=1}^{\infty} \frac{4\gamma(1+\gamma)}{4+4\gamma+\gamma^2 q_m^2} \exp\left(-\frac{Dq_m^2}{R^2} t\right) \right) \cdot \left(\sum_{n=1}^{\infty} \frac{2\gamma(1+\gamma)}{1+\gamma+\gamma^2 p_n^2} \exp\left(-\frac{4Dp_n^2}{h^2} t\right) \right) \quad (4)$$

In Eq. (4), M_t defines the amount of diffusing agent at time t and M_∞ defines the release at long times. The radius and height of the sample were denoted as R and h , respectively. The ratio of the volume of the solution to the volume of the sample was represented as γ . D is the effective diffusion coefficient whereas q_m values are the nonzero positive roots of,

$$\gamma q_m J_0(q_m) + 2J_1(q_m) = 0 \quad (5)$$

and p_n values are the nonzero positive roots of,

$$\tan(p_n) = -\gamma p_n \quad (6)$$

J_0 and J_1 are the Bessel functions of order zero and order one, respectively. Diffusion coefficients were calculated by MATLAB *Isqnonlin* function and experimental results were fitted to Eq. (4).

2.18.2 Release Trend in SIF

Hydrogels exposed to SIF exerted remarkable changes in the gel dimensions. Additionally, release rates showed fluctuations during SIF treatment. Thus, Fick's

law of diffusion could not be used for modelling of BC release from the hydrogels in simulated intestinal digestion conditions. Consequently, release data of hydrogels in SIF were plotted in the form of M_t/M_∞ vs time (h) to collect information on the unusual release behaviors of hydrogels in SIF. M_t denotes the measured amount of BC (g) in SIF at time t, M_∞ is the amount of BC in SIF at equilibrium.

2.19 SEM Analysis

Samples were firstly refrigerated for 48 h and then freeze dried (Christ, Alpha 2 – 4 LD Plus, Germany) before SEM analysis. Freeze dried gels were gold sputtered and then analyzed with a SEM (FEI Nova NanoSEM 430, Oregon, USA). Images were captured at an accelerating voltage of 5 – 20 kV. Analyses were conducted at Metallurgical and Materials Engineering Laboratory of METU, Ankara, Turkey.

2.20 Total Phenolic Content in Yogurt

CV hydrogels were sliced and put into 40 g yogurt samples. Total phenolic contents in yogurt samples were measured from the first week until the fourth week of the storage at refrigeration temperature (4 °C). Total phenolic contents of control samples (only yogurt containing samples) and hydrogel containing samples were compared for the first and the fourth weeks of the storage. Folin – Ciocalteu method was used for the total phenolic measurements (Krawitzky et al., 2014). Firstly, 100 mg aliquots from control and hydrogel containing yogurt samples were taken and dissolved in 1 mL ethanol:acetic acid:water (50:8:42) mixture at a ratio of 1:4 (g/mL). Resulting mixtures were agitated by a vortex (Daihan Scientific Co., Ltd., Korea). Then, a micro filter (Gema Medical Filter, Spain) with 45 μ m pore size was used to filter the mixture into the aluminum foil covered glass tubes preventing the mixture from the light exposure. After placing 500 μ l samples into the tubes, 2.5 mL Folin – Ciocalteu reagents (0.1 N) were added on the samples. Tubes were vortexed and kept at room temperature for 5 min in a dark place. 2 mL of sodium carbonate

(7.5 %, w/v) was added to each tubes. Tubes were vortexed and kept again at room temperature for 60 min in a dark place. In order to quantify the phenolic compounds, absorbance values of the mixtures were determined by spectrophotometric method at 760 nm (Mecasys Co. Ltd., Korea). For the blank measurements, a mixture containing 2 mL sodium carbonate, 2.5 mL diluted Folin – Ciocalteu reagent and 500 μ l ethanol:acetic acid:water solutions were used. Absorbance values of gallic acid equivalence (GAE) at different concentrations of gallic acid (ppm) in ethanol:acetic acid:water mixture (50:8:42) were recorded for the preparation of the calibration curve ($y=0.0013x - 0.0052$ where x and y represented mg GAE/L and absorbance, respectively). The total phenolic contents of the samples were determined as mg gallic acid equivalence (GAE)/mL.

2.21 Antioxidant Capacity in Yogurt

Antioxidant values of the same set of samples in yogurt were also measured as described in the study of Brand-Williams et al. (1955) and these values were compared for the four-week storage period at 4 °C (Brand-Williams et al., 1995). 100 mg of aliquots were taken from the control and hydrogel containing yogurt samples and dissolved in ethanol:acetic acid:water (50:8:42) mixture in a ratio of 1:4 (g/mL). 2.5 mL glass tubes containing the mixtures were vortexed and kept for 1 h to ensure complete extraction of antioxidants. Then, micro filters were used to filter the mixtures. Aluminum foil covered glass tubes containing 100 μ l extracts were mixed with 3.9 mL 25 ppm DPPH solution in methanol. These samples were then vortexed and kept still for 1 h. Then, absorbance values were recorded at 517 nm by UV – VIS spectrophotometer (Mecasys Co. Ltd., Korea). Absorbance values of 100 μ l methanol and 3.9 mL DPPH solution mixtures were also measured at 517 nm to detect the percentage inhibition of DPPH of different samples. Methanol was used as a blank for these measurements. The formula given below was used to determine the percentage inhibition of DPPH of samples,

$$\text{Inhibition DPPH \%} = \frac{A_0 - A_s}{A_0} \times 100 \quad (7)$$

where A_0 represents the absorbance of the solution containing 3.9 mL DPPH and 100 μl 95% methanol at 517 nm, A_s denotes the absorbance of the yogurt sample after 1 h at 517 nm. Additionally, Eq. (7) was also used to calculate the percentage inhibition of DPPH of trolox samples at different concentrations. This time A_s indicates the absorbance of the solution containing 3.9 mL DPPH solution and 100 μl Trolox. Based on Trolox measurements, a calibration curve was prepared curve ($y=0.3922x - 2.8244$ where x and y represented mg Trolox/L and percentage inhibition of DPPH, respectively). By using this standard curve, antioxidant capacity values of the yogurt samples in the absence and presence of hydrogels were displayed as mg Trolox/mL sample.

2.22 Statistical Analysis

Analysis of variance (ANOVA) was performed to determine the differences between the measurements. Tukey's test with 5 % significance level ($p < 0.05$) was used to compare the means of the measurements using MINITAB (version 16).

2.23 Experimental Design

The experimental design of the controlled release and food application studies is summarized in the following table.

Table 2.1 Experimental design of the release and food application experiments

	<i>Factors</i>	<i>Levels</i>	<i>Responses</i>
Phosphate buffer	Heating type	MW heating	Swelling ratio
		CV heating	Release ratio
	Polymer blending	C (no polysac.)	T ₂
		PC (0.5% w/w)	SDC
		GT (0.5% w/w)	Hardness
	XG (0.5% w/w)	Release modelling SEM images	
GIT digestion	Polymer blending	C (no polysac.)	Release ratio
		PC (0.5% w/w)	T ₂
		GT (0.5% w/w)	SDC
		XG (0.5% w/w)	Release modelling Hardness FTIR spectra Total acidity Moisture pH Soluble protein content Hydrogel weight loss
Yogurt	Hydrogel blending	Plain yogurt	Total phenolic content
		C hydrogel	Antioxidant capacity
		PC hydrogel	
		GT hydrogel	
		XG hydrogel	

CHAPTER 3

RESULTS AND DISCUSSION

3.1 Characterization of Hydrogel Solutions

Physicochemical properties of hydrogel solutions affect the resulting hydrogel properties. Hydrogels having different characteristics may exert distinct release behaviors in various release media. Thus, rheological, dielectric, pH and zeta potential properties of the hydrogel solutions were analyzed.

3.1.1 Rheology Analysis

3.1.1.1 Flow Behavior Analysis

Shear rate ramp experiments of hydrogels solutions were conducted to determine the flow behaviors both in the presence and absence of BC. All hydrogel solutions contained WPI, an added polysaccharide (PC, GT or XG) and water. One set of hydrogels solutions included BC and the parallel set of hydrogel solutions did not include BC. By this way, effect of presence or absence of BC to flow behaviors were also investigated. In the presence of BC, C and PC hydrogel solutions exhibited Newtonian behavior. Apparent viscosity of PC solution was higher than that of C solution, 0.0206 Pa s and 0.0071 Pa s, respectively ($p < 0.05$) (Sahin & Sumnu, 2006). C and PC hydrogel solutions also exhibited similar flow characteristics in the absence of BC. Both C hydrogel solutions with 0.0071 Pa s and PC hydrogel solutions with 0.0203 Pa s apparent viscosity values, maintained their Newtonian characteristics. Presence or absence of BC did not affect the apparent viscosity values of these samples.

Table 3.1 Apparent viscosity values of Newtonian hydrogel solutions

Hydrogel Solutions	Apparent Viscosity (Pa s)
Control with BC	0.0071±0.0001 ^a
Control no BC	0.0071±0.0000 ^a
Pectin with BC	0.0206±0.0011 ^b
Pectin no BC	0.0203±0.0005 ^b

*Different small letters mean values are significantly different ($p < 0.05$).

In contrast, GT and XG hydrogel solutions demonstrated non-Newtonian flow behaviors for both BC including and not including samples. Apparent viscosities of these samples decreased when the applied shear rate was increased. Therefore, flow behaviors of these samples obeyed the Ostwald-de Waele equation, power law model (Sahin & Sumnu, 2006). BC including GT hydrogel solutions exerted shear – thinning (pseudoplastic) flow with a flow behavior index (n) value of 0.86. Consistency index (k) value of these solutions was 0.145 Pa s^{0.86}. GT solution that did not contain BC showed also pseudoplastic behavior with lower k and n values, 0.037 Pa s^{0.84} and 0.84, respectively ($p < 0.05$). For GT hydrogel solutions having pseudoplastic flow behavior, presence or absence of BC affected the flow characteristics. When BC was not present in the GT hydrogels solutions, resistance of these solutions to flow decreased (lower k) which was an expected situation due to the viscosity increasing nature of BC owing to its sugary content. However, GT solutions with no BC had a little more pseudoplastic character with respect to their BC including correspondents due to the lower n value (Bouyer et al., 2012).

Table 3.2 Flow parameters of Gum Tragacanth hydrogel solutions

Hydrogel Solutions	Consistency index ($k, Pa s$)	Flow behavior index (n)
Gum Tragacanth with BC	0.145±0.002 ^a	0.86±0.00 ^a
Gum Tragacanth no BC	0.037±0.001 ^b	0.84±0.00 ^b

*Columns with different letters are significantly different ($p < 0.05$)

XG hydrogel solutions also demonstrated non-Newtonian flow behaviors both with and without BC addition. XG hydrogel solutions also possessed a yield stress. The requirement of an initial stress to initiate the flow caused fitting of XG hydrogel solution data to Herschel – Bulkley model. The initial stress (τ_0), k and n values of BC containing XG solutions were 1.89 Pa, 3.61 Pa s^{0.28} and 0.28, respectively. Apparently, XG hydrogel solutions including BC had more pseudoplastic character with respect to other BC containing hydrogel solutions. This distinct flow behavior of XG hydrogel solutions could be due to the complex structure, enhanced entanglement and viscosity increasing effects of XG molecules in solutions. Removal of BC from XG hydrogel solutions changed neither the flow characteristics nor the τ_0 , k and n values of the solutions. Flow parameters of XG hydrogel solutions in the absence of BC were 1.42 Pa for τ_0 , 3.35 Pa s^{0.26} for k and 0.27 for n .

Table 3.3 Flow parameters of Xanthan Gum hydrogel solutions

Hydrogel Solutions	Yield Stress (Pa)	Consistency index ($k, Pa s$)	Flow behavior index (n)
Xanthan Gum with BC	1.89±0.24 ^a	3.61±0.12 ^a	0.28±0.01 ^a
Xanthan Gum no BC	1.42±0.01 ^a	3.35±0.27 ^a	0.27±0.01 ^a

*Columns with different letters are significantly different ($p < 0.05$)

Results showed that polymer type affected the flow behavior properties, dramatically. Moreover, presence or absence of BC changed the flow behavior of GT hydrogel solutions. BC was not effective in Newtonian solutions (C and PC hydrogel solutions) in terms of changing the apparent viscosity. XG hydrogel solutions also attained similar apparent flow characteristics with or without BC showing that XG was the dominant factor in determining the rheological properties of such solutions.

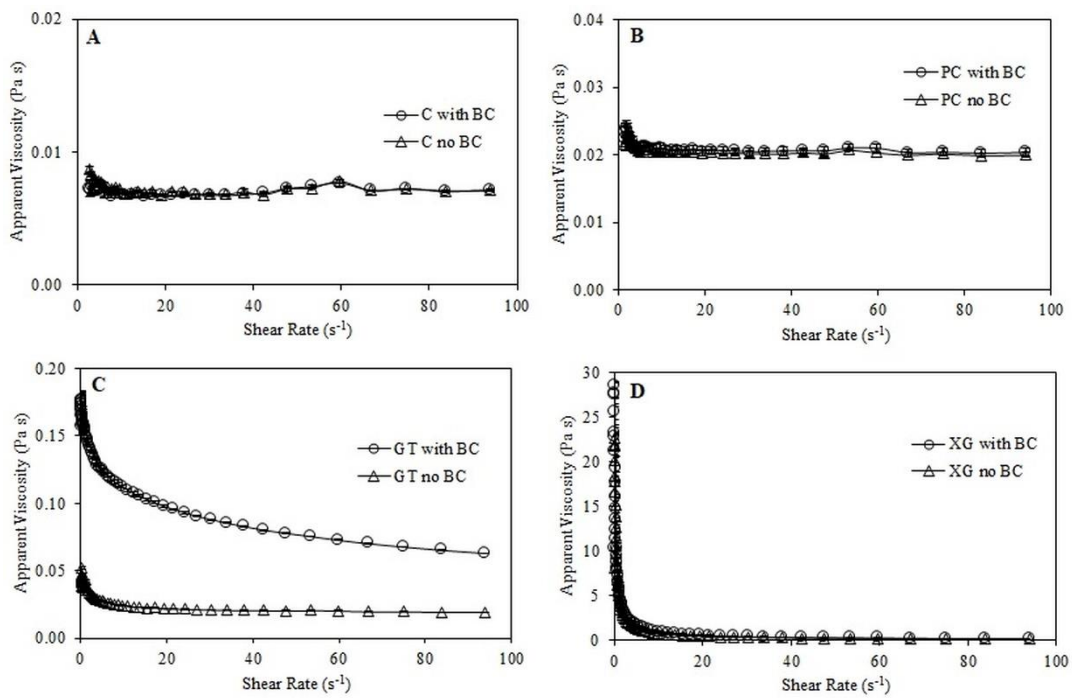


Figure 3.1. Flow curves of hydrogel solutions in the presence and absence of BC: A: Control, B: Pectin, C: Gum Tragacanth, D: Xanthan Gum

3.1.1.2 Amplitude Sweep Analysis

Amplitude sweep tests were performed at a fixed frequency and varying strains to determine the LVE region of the solutions where G' and G'' were expected to remain constant at varying strains. If the linearity of this region deviates larger than 5 %,

then the LVE of the sample is over (Abbastabar et al., 2015). Among the hydrogel solution samples, only GT and XG hydrogel solutions may have a LVE due to their non-Newtonian flow character. However, the shear – thinning character of GT solutions was not strong enough to give a LVE. Therefore, only XG hydrogel solutions (both in the presence and absence of BC) had a LVE due to their more pronounced pseudoplastic behavior. Length of the LVE of XG hydrogel solutions was long enough to assert a high polymer gel strength for XG samples since longer LVE regions are associated with increased polymer gel strength (Abbastabar et al., 2015).

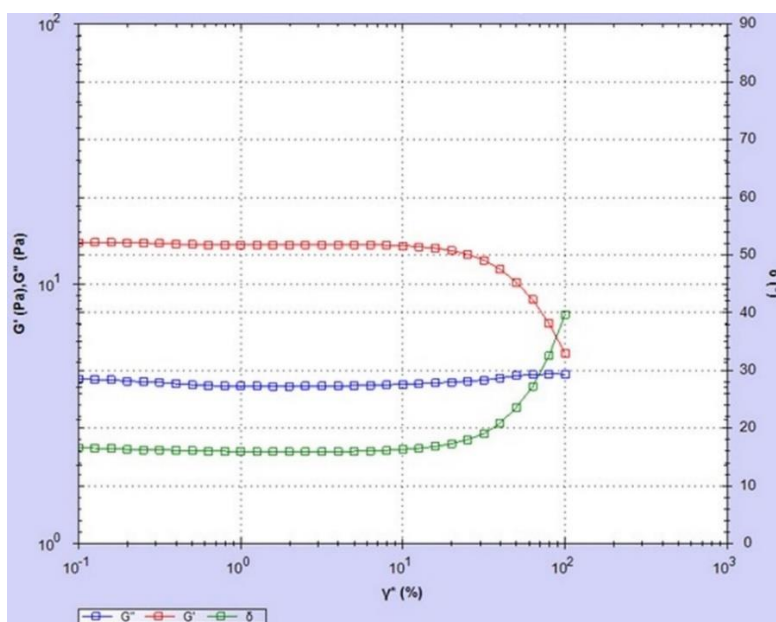


Figure 3.2. Amplitude sweep test graph of BC containing XG hydrogel solutions

3.1.1.3 Frequency Sweep Analysis

Frequency sweep test was applied to XG hydrogel solutions which were the only samples having a clear and sufficiently long LVE, both in the presence and absence of BC in the system (Fig. 3.3).

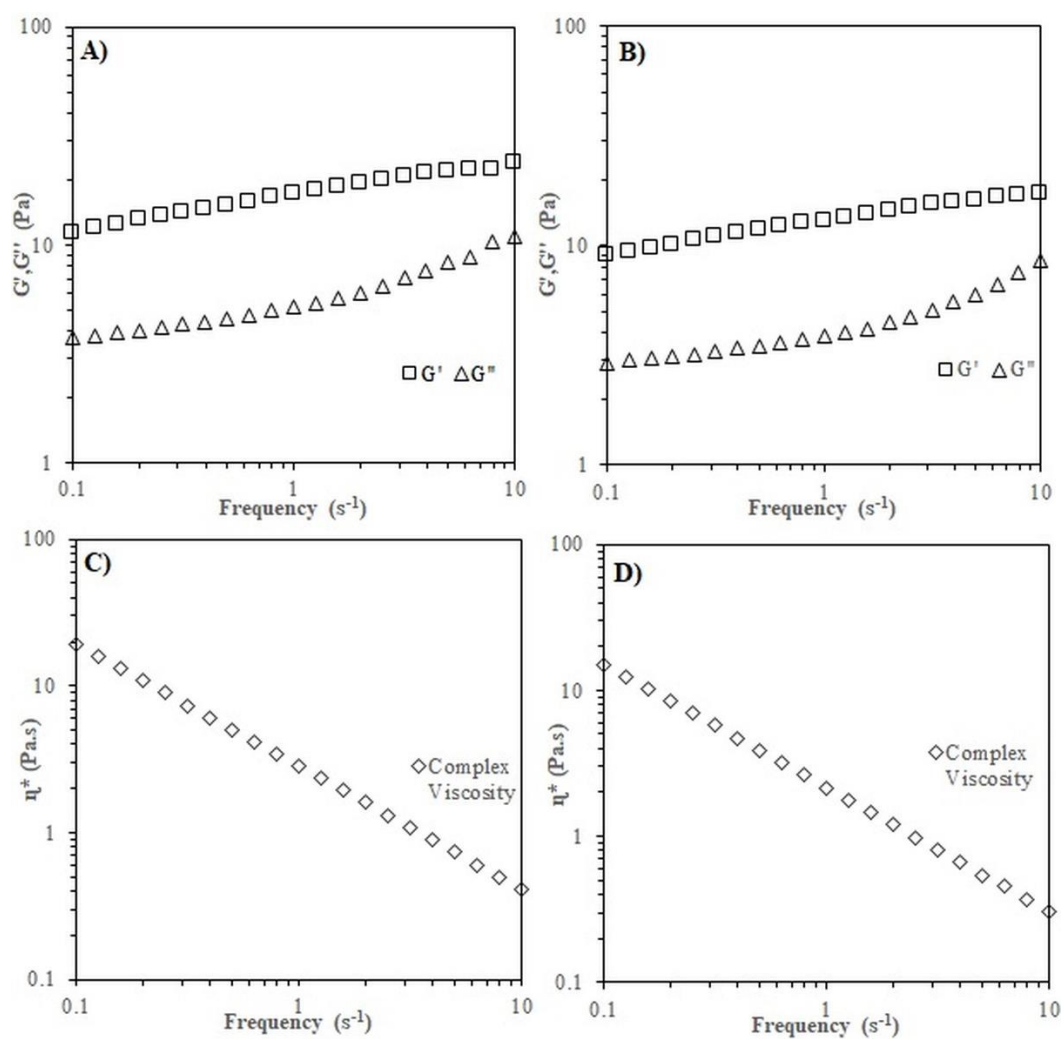


Figure 3.3. Frequency dependence of storage and loss moduli of xanthan hydrogel solutions: A: in the presence of BC, B: in the absence of BC and frequency dependence of complex viscosity of xanthan hydrogel solutions: C: in the presence of BC, D: in the absence of BC

The frequency sweep test characteristics of the solutions provide valuable information about the physical properties of the measured solutions (Doucet et al., 2001). These properties are also the precursors of the gel structure characteristics. The G' values of XG solutions, whether the solution contained BC or not, clearly predominated the G'' values over the entire frequency sweep range as seen in Fig 3.3. This produced a moderate to low values of loss tangent ($\tan \delta$, 0.46 – 0.30 with BC and $\tan \delta$, 0.49 – 0.29 without BC). Moreover, the complex viscosity decreased with increasing frequency. Frequency sweep tests indicated that XG hydrogel solutions had solid-like gel structures, that is solid-like characteristics of the solutions predominated over the liquid character (Tao et al., 2016). Decreasing trend of complex viscosity as frequency increased was an expected incidence due to aforementioned shear – thinning behavior of XG solutions.

3.1.1.4 Temperature Sweep Analysis

Temperature sweep measurements of the gel solutions were performed to understand the trend of gelling behaviors of the samples with increasing temperature (Fig. 3.4). For this purpose, changes in the storage and loss moduli of the solutions were investigated since the higher G' values with respect to G'' values were associated with the solid-like gel characteristics (Russ et al., 2013). During the linear temperature increment, a critical gelling point which could be defined as the point where G' of the solution was equal to or bigger than the G'' of the solution for the first time was tried to be detected for each sample (Shalla et al., 2017). BC containing C, PC, XG and GT hydrogel solutions had critical gelling temperatures of 79.4, 78.6, 78.0 and 75.8 °C, respectively (Fig. 3.4). Only addition of GT to WPI solutions decreased the critical gelling temperatures, significantly ($p < 0.05$). Presence of bassorin, the water swelling part of GT, could have provided GT hydrogel solutions an earlier gelation with respect to other polymer added solutions (Balaghi et al., 2011). C, PC and GT hydrogel solutions had similar temperature sweep profile trends since their G' were lower than their G'' in the beginning of the temperature sweep.

However, as the temperature increased further, G' also increased and at around 75 – 80 °C, their G' reached and even passed their G'' values. Finally, all these samples (C, PC and GT) possessed a more dominant G' profile at the end of the sweep. On the other hand, in accordance with the findings of the Abbastabar et al. (2015), XG hydrogel solutions had always a dominant solid-like behavior throughout the temperature sweep (Abbastabar et al., 2015). As the temperature increased up to 78 °C, G' of XG solutions showed a decreasing trend unlike other samples whose G' values had an increasing trend from the beginning of the experiment. Thus, the point where G' of XG hydrogel solutions started to increase again was considered as the critical gelling temperature (Shalla et al., 2017). The initial decrease in G' could be attributed to the highly pseudoplastic nature of XG hydrogel solutions. Temperature increment affected most probably the consistency index of XG hydrogel solutions which is a temperature dependent parameter that could be explained by an Arrhenius-type equation (Krokida et al., 2001). Presumably, k decreased along with the G' of the sample up to the critical gelling temperature resulting with a less resistance to flow due to the more linear alignments of XG molecules with the surrounding molecules (Kirtil & Oztop, 2016b). Since temperature sweep range reached and exceeded the denaturation temperature of WPI, protein unfolding was enhanced in the solution especially after 70 °C. Additionally, XG molecules also experienced some conformational changes at the elevated temperatures. Clearly, all these phenomena increased the interaction sites between WPI and XG molecules. Consequently, at around 78 °C, the system started to gain an increase in its solid structural character again, later giving a solid-like structure.

In the absence of BC, however, C, PC and GT hydrogel solutions could not reach a formerly defined critical gelling point in the temperature sweep interval. Only XG hydrogel solutions without BC reached this point towards the end of the experiment at around 83.3 °C (Fig. 3.5). Distinct structural conformations and its extended degree of interactions with WPI probably enabled XG hydrogel solutions to have an earlier critical gelling point with respect to others in the absence of BC (Zhang et al., 2014). Removal of BC from the solution systems caused a delayed gelling feature

and this confirmed the contribution of BC to faster gelling characteristics. Reasons include the viscosity increasing effect of BC and its carbohydrate containing composition *e. g.* 284.4 g/L sucrose, 145.9 g/L glucose and 129.0 g/L fructose which was determined specifically for the used BC by HPLC analysis. Without BC, C, PC and GT hydrogel solutions also formed gels but longer times were required.

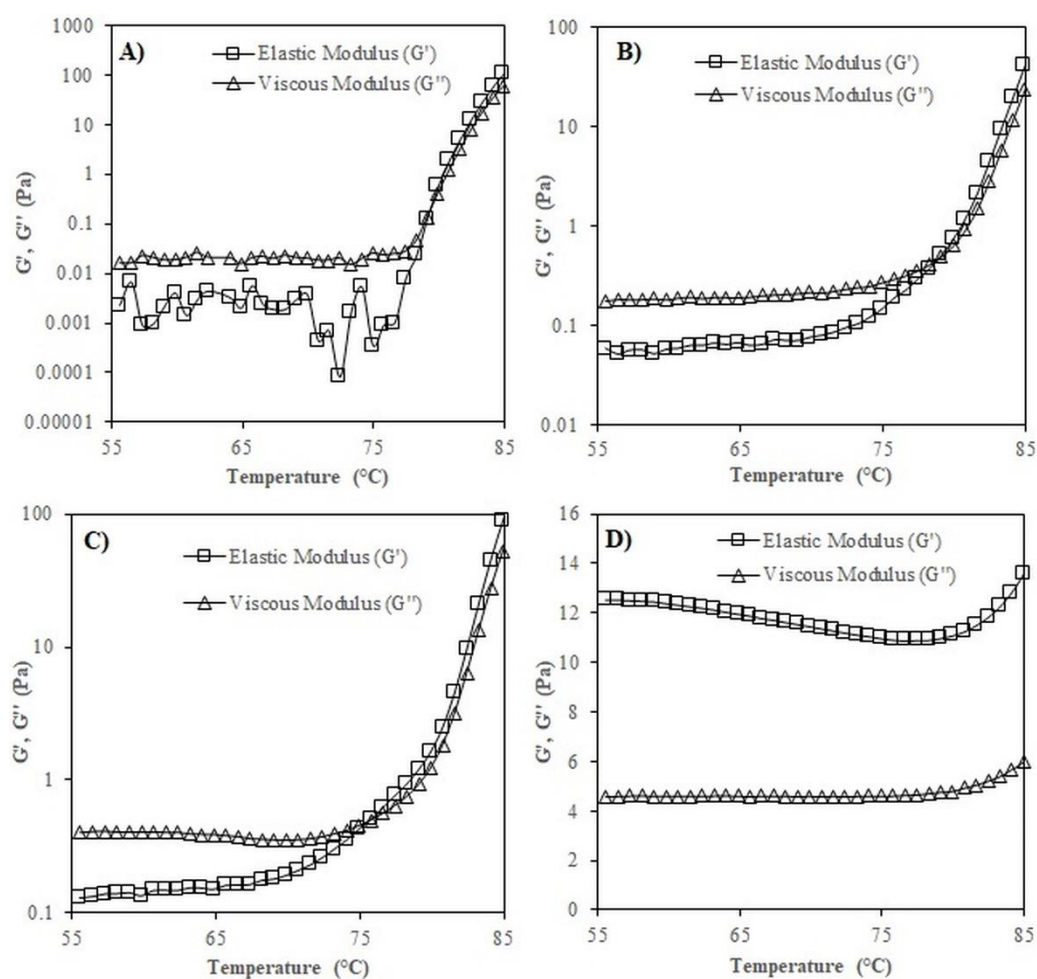


Figure 3.4. Temperature dependence of storage and loss moduli of A: Control, B: Pectin, C: Gum Tragacanth, D: Xanthan Gum hydrogel solutions, in the presence of BC

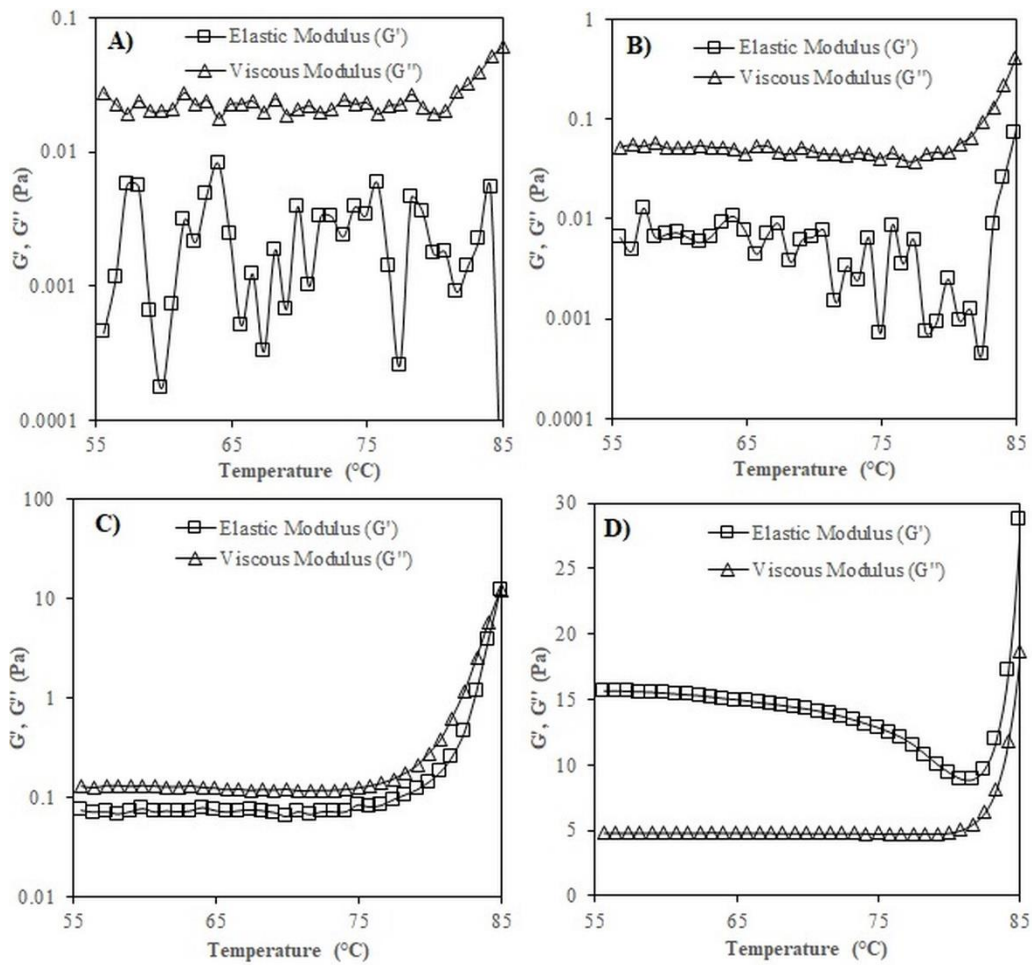


Figure 3.5. Temperature dependence of storage and loss moduli of A: Control, B: Pectin, C: Gum Tragacanth, D: Xanthan Gum hydrogel solutions, in the absence of BC

3.1.2 Dielectric Properties

Dielectric constant (ϵ') and dielectric loss factor (ϵ'') of a food material determine its microwave heating characteristics. ϵ' describes the ability of a material to store microwave energy. ϵ'' is the ability of a material to dissipate this microwave energy to heat (Sakiyan et al., 2007). Dielectric properties of hydrogel solutions showed variations as shown in Table 3.4. GT hydrogel solutions had lower dielectric constant

with respect to other hydrogels solutions ($p < 0.05$). This contributed to the more homogeneous microwave heating of GT hydrogel solutions due to the increased penetration depth (Calay et al., 1994). The reason could be the water soluble (tragacanthin) part of the GT molecule. The close ϵ'' of GT hydrogel solutions to ϵ'' of distilled water implies that microwave heating properties of GT hydrogel solutions are closer to distilled water than that of other hydrogels solutions. The lowest ϵ' of GT hydrogel solutions also suggests that GT bound water efficiently leaving less free water to increase the ϵ' of the solution.

Table 3.4 Dielectric properties of hydrogel solutions

Hydrogel Solutions	Dielectric Constant (ϵ')	Dielectric Loss Factor (ϵ'')
Distilled Water	77.9±0.8 ^a	9.6±0.2 ^c
Xanthan Gum	60.5±1.6 ^b	13.8±0.3 ^a
Control	60.1±0.9 ^b	13.6±0.2 ^a
Pectin	59.7±1.3 ^{bc}	13.6±0.3 ^a
Gum Tragacanth	55.7±0.7 ^c	12.4±0.1 ^b

*Columns with different letters are significantly different ($p < 0.05$)

The higher dielectric constant and dielectric loss factor values of the C, PC and XG hydrogel solutions showed that these solutions attained slightly faster heating rates during MW than GT hydrogel solutions. The differences between the dielectric properties of the hydrogel solutions may induce different responses to microwave heating. Therefore, hydrogels produced by MW may have different physicochemical characteristics. Pore size in the hydrogel polymer network, release rate of the encapsulated agent and the transverse relaxation profiles of the hydrogels are among these characteristics (Li et al., 2006).

3.1.3 Zeta Potential and pH Analysis

Zeta potential is defined as the overall charge that particles gain in a dispersion. Zeta potential measurements can be used to predict the stability of colloidal systems. Stability of a colloidal system depends on the sum of the electrical double layer repulsive and van der Waals attractive forces particles experiencing as they approach one another. Repulsive forces create an energy barrier preventing the approach of the two particles to one another and adhering together (Wu et al., 2018). Zeta potential measurements of the hydrogel solutions (both in the presence and absence of BC) were performed at neutral pH (7.0) (the approximate pH of the hydrogel solutions before heating) to understand the colloidal stability properties of the solutions (Table 3.5).

Table 3.5 Zeta potential values of the hydrogel forming solutions

Hydrogel Solutions	Without BC (mV)	With BC (mV)
Control	-31.10±0.23 ^a	-22.07±0.31 ^d
Pectin	-30.23±0.49 ^a	-19.00±0.30 ^e
Gum Tragacanth	-28.63±0.22 ^b	-18.50±0.30 ^e
Xanthan Gum	-28.57±0.23 ^b	-24.43±0.58 ^c

*Values with different letters are significantly different, in the whole table ($p < 0.05$)

When the zeta values of the hydrogel solutions without BC addition were examined, zeta potential values of C and PC solutions were detected as the lowest (more negative) ($p < 0.05$). Colloidal dispersions having zeta potential values higher than +30 mV and lower than -30 mV are considered as stable systems (Fan et al., 2017). Therefore, C and PC hydrogel solutions (without BC) could be defined as stable colloidal systems. All the polymers that were blended to WPI solutions in this study were anionic polysaccharides with low acid dissociation constants around 2.5 – 3.0. Thus, the pure PC, GT and XG solutions were reported to have negative zeta

potentials down to very low pH values such as 2.0 (Zeeb et al., 2018). After BC addition, zeta potentials of the hydrogel solutions increased (Table 3.5) due to the pH reduction caused by the nature of BC (Table 3.6). The same trend was also reported for WPI (with pI around 5.2) but pure WPI solutions started to have zero or positive zeta potentials at higher pH values (between 4.0 and 4.5) with respect to mentioned polymers. Thus, the presence of WPI in the gel solutions suppressed the real zeta potential decrease effect of the added polymer (Zeeb et al., 2018).

Table 3.6 pH values of the hydrogel solutions with and without BC

Hydrogel Solutions	<i>pH with BC</i>	<i>pH without BC</i>
Xanthan Gum	5.89±0.04 ^{a, A}	7.05±0.03 ^{a, B}
Gum Tragacanth	5.82±0.04 ^{a, C}	7.02±0.04 ^{a, D}
Control	5.72±0.04 ^{b, E}	6.95±0.01 ^{b, F}
Pectin	5.67±0.02 ^{b, E}	6.83±0.02 ^{c, G}

*Different small letters mean values are significantly different in each column ($p < 0.05$). Different capital letters mean values are significantly different in each row ($p < 0.05$).

Despite its high charge density, XG hydrogel solutions had higher zeta potentials (-28.57) in the unstable range than the C and PC samples (-31.10 for C and -30.23 for PC), in the absence of BC. The degree of polymer – WPI interactions obviously played a crucial role on the surface charge of such colloidal particles (Cheng et al., 2015). At pH 7.0, both WPI and XG have anionic structures and XG has an increased number of anionic groups due to its high charge density (Zhang et al., 2014). Positively charged protein regions also exist at the neutral pH and specific strong attractions take place between the WPI and XG molecules, even both polymers carry net negative charges. Probably, these enhanced attractions between WPI and XG molecules, contributed to the diminishing of the negativity of the surface charge of the complex. This increased the zeta potential (closer to zero) (Cheng et al., 2015).

The degree of WPI – PC interactions was not strong enough to increase the zeta potential of the system (Zeeb et al., 2018). In the case of GT, intermediate interaction capability of GT with WPI compared to PC and XG and presence of tragacanthin and bassorin parts determined the zeta values of these solutions. Only tragacanthin part of the GT molecule is effective on zeta potential, and this could have caused a decrease in the contribution to the surface negativity in GIT hydrogel solutions (Hajmohammadi et al., 2016).

Addition of BC increased the zeta potentials of all type of solutions ($p < 0.05$) (Table 3.5). Primary reason was the acidic nature of BC as can also be seen in the pH analysis (Table 3.6). BC diminished the surface negative charge densities of the particles. XG hydrogel solutions were affected less by the BC addition. XG samples demonstrated the least zeta potential increase and also had the lowest zeta potential (-24.43) with respect to other BC added samples ($p < 0.05$). In the presence of BC, XG hydrogel solutions exerted the highest colloidal stability and this finding was also related to the branched and highly charged density nature of the XG molecules. Despite the heavy protonation of the negatively charged parts with the introduction of BC, XG molecules still possessed higher negatively charged remaining parts with respect to WPI, PC and GT molecules. Therefore, the negative surface charge density of the particles belonging to XG containing solutions was higher than the others. This provided BC containing XG hydrogel solutions a better colloidal stability (closer to -30 mV). Hydrogel solutions were found to have different pH and zeta potential values. This phenomenon could affect the physicochemical properties of the resulting hydrogels after heating. For this reason, zeta potential characterization of the hydrogel forming solutions was important.

3.2 Controlled Release in Phosphate Buffer

Hydrogels produced by CV and MW were exposed to phosphate buffer at pH 7.0 for 24 h. Swelling ratios, BC release profiles, NMR relaxometry results, release

modellings and microstructure properties of the hydrogels were determined to investigate the controlled release from hydrogels in phosphate buffer.

3.2.1 Swelling Ratios

All hydrogels prepared by CV showed increasing swelling ratio (SR) profiles from the first 30 min to 24 h of the swelling experiments (Fig. 3.6). This implied that all CV hydrogels absorbed and retained some amount of solvent within their gel structures. On the other hand, MW hydrogels could not maintain their structures in pH 7.0 phosphate buffer and degraded to some extent during the 24 h swelling experiments. Clearly, MW hydrogels had weaker gel structures than the CV hydrogels. This was also in agreement with the visual and sensorial analysis of the MW hydrogels. Thus, only the SR of CV hydrogels was recorded. As shown in Figure 3.6, CV XG hydrogels had the highest SR (17.85%) at the end of 24 h ($p < 0.05$). Moreover, only CV XG hydrogels differed significantly from the CV C hydrogels which had the lowest SR (10.55%) ($p < 0.05$). SR's of CV PC (13.87%) and CV GT (10.88%) hydrogels did not differ from SR of CV C hydrogels.

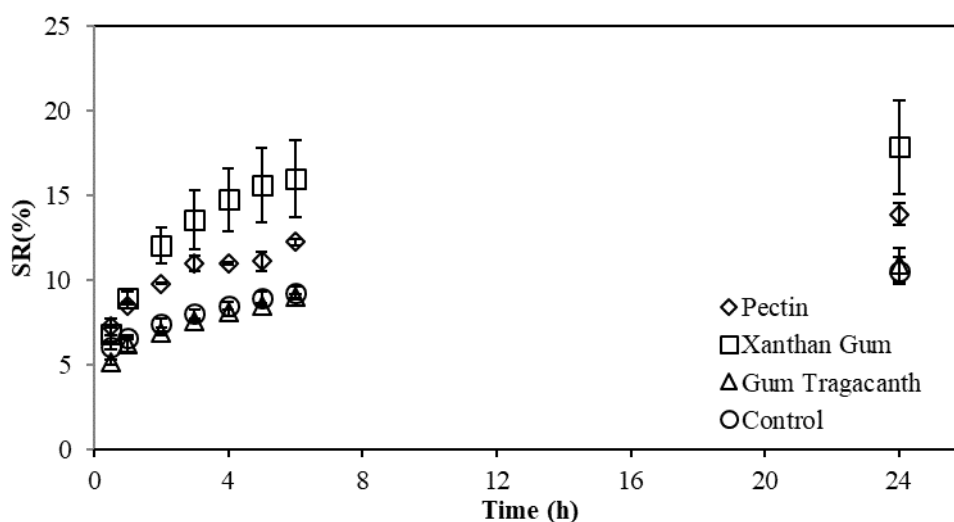


Figure 3.6. Swelling ratio profiles of conventionally heated hydrogels (0 – 24 h)

SR results suggest that addition of XG to WPI hydrogel increased the swelling ability. XG with a high molecular weight of 2000 kDa, is known for its high water holding capacity and viscosity increasing properties (García-Ochoa et al., 2000). Viscosity measurements of the hydrogel solutions by a vibro-viscometer also proved that XG increased the solution viscosity substantially (Table 3.7). XG was also reported to reduce the syneresis in curdlan – WPI solution over freeze thaw cycles (Shiroodi et al., 2015). SR results of XG including hydrogels were in agreement with this study. XG has a linear backbone composed of β -D-glucose units. XG is negatively charged at pH 7.0 due its negatively charged side chains containing an acetylated mannose, glucuronic acid residue and a pyruvic acid or a mannose residue, alternatively (Zasytkin et al., 1996). WPI having a pI around 5.2 is also negatively charged at pH 7.0 and high electrostatic repulsion is generated in WPI – XG complexes (Hatami et al., 2014). However, proteins have positively charged internal patches even at pH's higher than their pI and this makes possible for polysaccharide molecules to interact with WPI molecules in terms of electrostatic attractions. The large size and compact structure as well as the charge repulsion in the side chains of XG induced solutions with high viscosity and resulting gels were also capable of retaining larger amounts of solvent with respect to C hydrogels. This was expected because electrostatic repulsion of side chains contributes to solvent uptake characteristics (Hatami et al., 2014).

Table 3.7 Viscosities of BC containing hydrogel solutions

Hydrogel Solutions	Viscosity (Pa s)
Xanthan Gum	0.122±0.002 ^a
Gum Tragacanth	0.025±0.001 ^b
Pectin	0.014±0.001 ^c
Control	0.004±0.000 ^d

*Different small letters mean values are significantly ($p < 0.05$).

PC is also a branched, heterogeneous, anionic and structurally complex polysaccharide as XG (Mohnen, 2008). Galacturonic acid backbone of PC has side chains called rhamnose rich regions carrying natural sugars *e.g.* galactose, arabinose and xylose (Ventura & Bianco-Peled, 2015). The main reason for the differences in SR of CV PC and XG hydrogels originated from the different kind of residues located in the side chains of these polysaccharides. Each residue has distinct charge, bond forming and electrostatic interaction capacities with the environment. It was hypothesized that charge repulsion between PC residues was lower than the charge repulsion between XG residues at pH 7.0 thus CV PC hydrogels attained a lower SR. PC hydrogel solution viscosity was also lower than XG hydrogel solutions proving the viscosity effect on SR (Table 3.7).

GT is a highly acid resistant and heat stable hydrocolloid. GT is also a physical mixture of tragacanthin (water-soluble) and bassorin (water-swelling) parts (Balaghi et al., 2010). Balaghi et al. (2010) have also reported 1 % (w/v) bassorin dispersion at 25 °C showed a high viscosity gel-like structure whereas tragacanthin solution behaved like semi dilute to concentrated solution of entangled, random coil polymers. Therefore, tragacanthin and bassorin parts contributed differently to the swelling power of GT hydrogels in our study. Sugar composition of GT molecule includes mainly galacturonic acid, xylose, fucose, arabinose, galactose, glucose and traces of rhamnose. Presence of these sugars, especially galactose and arabinose residues, contributed to the liquid character of GT (Balaghi et al., 2011). The low SR of CV GT hydrogels, which was very close to SR of CV C hydrogels, can be attributed to the presence of tragacanthin in the GT hydrogels. Bassorin part of the GT molecules provided some gel-like characteristics to these hydrogels but that was not enough to attain a higher SR than the CV C hydrogels.

3.2.2 Release Profiles

Cumulative BC release profiles were determined for both CV and MW hydrogels. Figure 3.7 illustrates the BC release profile of CV hydrogels. According to Figure

3.7, all CV hydrogels exhibited similar release profiles up to 6 h of the experiment. The distinction in the release percentages of the hydrogels appeared between the 6 and 24 h of the experiment. At the end of 24 h, release rates of CV PC (37.16%), XG (32.79%) and GT (29.40%) hydrogels were lower than the release rate of CV C hydrogels (77.82%) ($p < 0.05$). Therefore, addition of polysaccharide to CV WPI hydrogels retarded the BC release in phosphate buffer after 1 day. Although CV XG hydrogels had the highest SR, they could also retard the BC release at the end of 24 h compared to CV C hydrogels. Generally, hydrogels having high SRs are expected to have high release rates (Oztop & McCarthy, 2011). But, CV XG hydrogels exerted an opposite behavior. Properties of BC, structure of XG and physicochemical properties of the release medium played a crucial role in the retarded release profile of CV XG hydrogels. pH of the BC was 3.42 and BC reduced the pH of the hydrogel solutions with respect to hydrogel solutions prepared without BC, as previously explained (Table 3.6). Thus, it was hypothesized that BC entrapment within the hydrogels may have provided further crosslinking between the BC and the gel internal structure through electrostatic attractions. According to the results presented in Table 3.6, XG and GT hydrogel solutions had the highest pH values with respect to other hydrogel solutions whether the solutions contained BC or not ($p < 0.05$). This could be related to the strong negative character of the XG molecules. The negatively charged branches of XG may have interacted with the positively charged parts of the BC leading to slow down in the release rates. Hydrogen bonding between anthocyanins and the internal gel structure was also important in terms of BC release rates since more hydrogen bonding between the encapsulated agent and the polysaccharide gel retards the release rate of the encapsulated agent (Ferreira et al., 2009). The long, branched, complex and strongly negative nature of XG side chains probably increased the hydrogen bonding of BC pigments to XG hydrogel structure. Retarded release of BC from CV XG hydrogels was also related to the enhanced helical chain entanglements of XG coils which is a common phenomenon for XG molecules in the solutions (García-Ochoa et al., 2000). Ionic nature of the release medium (phosphate buffer) was another factor that contributed to the retarded release

rates of CV XG hydrogels. The salts present in the phosphate buffer tend to strengthen the intermolecular associations between the XG molecules (Braga et al., 2006). As CV XG hydrogels spent more time in the buffer solution during the release experiment, screening of the electrostatic repulsions of the trisaccharide side chains took place. This also promoted helical backbone conformation in the XG molecules. Consequently, strength of the CV XG hydrogels increased which also caused a reduction in the BC release rate from these hydrogels.

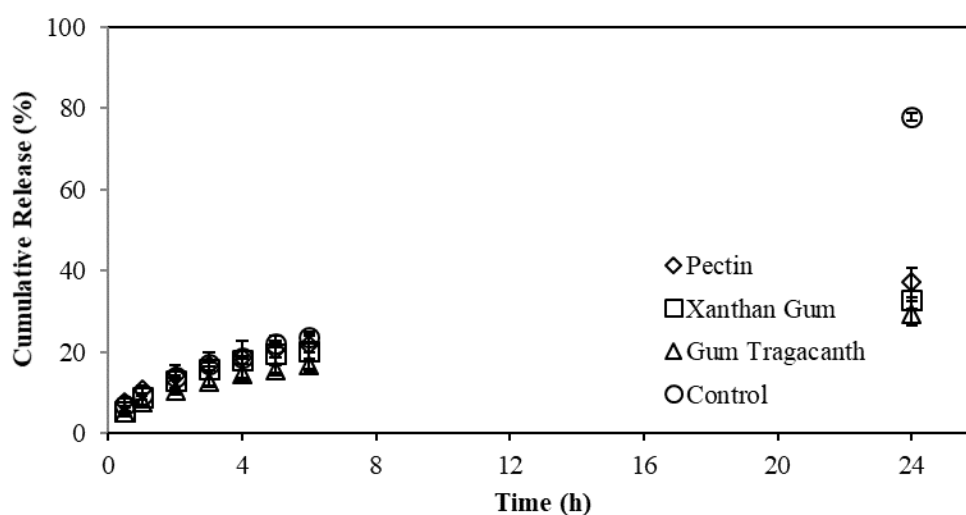


Figure 3.7. Release profiles of conventionally heated hydrogels (0 – 24 h)

CV PC and GT hydrogels also provided delayed release profiles after 1-day experiment as CV XG hydrogels (Table 3.7). However, retarded release profiles of CV PC and GT hydrogels were consistent with their low SR values contrary to CV XG hydrogels (Fig. 3.6). Retarded BC release profiles and low SR values of CV PC and GT hydrogels suggest that addition of these polysaccharides to WPI hydrogels contributed to the formation of additional junction zones within the WPI structure and formed three-dimensional gel networks. Interactions between the absorbed water and the CV GT hydrogel were enhanced probably by the water soluble part in GT.

Thus, BC molecules were in competition with water molecules to interact with the WPI – GT gel network. Unlike in XG hydrogels, BC pigments were not particularly preferred over water molecules by the internal structure of GT hydrogel. For this reason, similar BC release behaviors were observed for CV GT and XG hydrogels. In a previous study, a rapid decrease in the viscosity of tragacanthin was reported with the increase in the solution temperature (Mohammadifar et al., 2006). This also affected the release behavior of CV GT hydrogels since hydrogel solutions were heated at 90 °C for 30 min to obtain solid hydrogels in this study.

CV C hydrogels having the lowest hydrogel solution viscosity showed the fastest release profile suggesting that there was a reverse correlation between the viscosity of the hydrogel forming solutions and the release rates. Actually, CV C hydrogels followed a similar release profile to other hydrogels up to 6 h of the experiment. The reduced number of junction zones and interactions within the C gel matrix in the absence of a blended polysaccharide probably reduced the endurance of these hydrogels at prolonged times (24 h) in the phosphate buffer. Reasons for the release retardation of CV PC hydrogels were similar to GT case. PC mainly derives its negative charge at pH values higher than its pKa (2.9 – 3.2) from carboxylate groups like GT having a pKa around 3.0 (Nur et al., 2016; Ventura & Bianco-Peled, 2015). At pH 7.0, both polysaccharides are strongly negatively charged so that electrostatic and steric repulsions between the side chains affected significantly the release of encapsulated compound. Moreover, high hydrophilicity of PC branches contributed to the frequency of water – polysaccharide interactions resulting in diminished BC – polysaccharide interactions. However, this condition was not observed in XG hydrogels. On the contrary, BC molecules sufficiently interacted with XG molecules to slow down the release process despite the high SR which is normally the driving force for the faster release behavior. The difference mainly originates from the more compact and complex conformation of XG molecules (MW of 2000 kDa) than PC (MW of 150 kDa) and GT (MW of 850 kDa) molecules (Mohammadifar et al., 2006; Mohnen, 2008; Zasytkin et al., 1996). Side chain repulsions are also present in XG structure but rigid, close and complex conformation of XG molecules increased

interaction sites within the gel network. As a result, XG molecules triggered local aggregate formations in WPI continuous network (Li et al., 2006). This provided enhanced interactions between the BC molecules and the surrounding polymer network via more hydrogen bonding and electrostatic attractions. Therefore, high SR characteristic of CV XG hydrogels was overwhelmed by these conditions and release of BC from CV XG hydrogels in phosphate buffer (pH 7.0) was retarded.

Other than the type of the polysaccharide used, variations in the heating rate and mechanism are also important in obtaining hydrogels having different release properties. These factors affect the rheological and polymer interaction properties of the hydrogels (Li et al., 2006). For this reason, BC release profiles of MW hydrogels were also investigated and compared with CV hydrogels. Infrared Assisted Microwave Heating (MW) had distinct effects on the release behaviors of the MW hydrogels as shown in Figure 3.8.

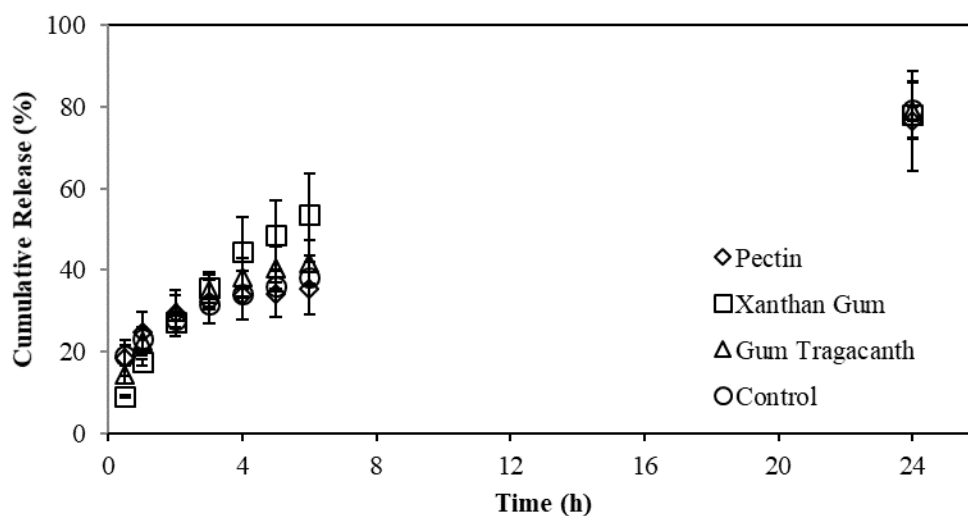


Figure 3.8. Release profiles of microwave heated hydrogels (0 – 24 h)

The first two striking marks in Figure 3.8 were the steep increase of the release rates in the early stages of the release experiment and the higher final release percentages at the end of 24 h with respect to CV hydrogels. Release rates of all hydrogels were similar throughout the experiment. At the end of 24 h, MW GT, XG, PC and C hydrogels had very close cumulative release rates 79.05 %, 78.09 %, 76.46 % and 79.12 %, respectively. This results suggest that under MW, release retarding property of the polymer added hydrogels was eliminated. Moreover, the distinct release profiles coming from polysaccharide addition was also eliminated. All MW hydrogels except for PC, started to show some differences in the release rates beginning from the 3 h of the experiment. After 6 h, all MW hydrogels including PC, showed another distinctive increase in the release rate up to 24 h. In contrast, CV hydrogels had shown a more gradual increase in their release rates in phosphate buffer. Obviously, MW weakened the gel structures and promoted structural defects within the gel structures due to volumetric heating. Consequently, MW resulted in faster release rates from the hydrogels. The final release rates of MW hydrogels indicated that all polysaccharide blended hydrogels attained higher release rates than their CV hydrogel counterparts in phosphate buffer ($p < 0.05$). On the other hand, MW C hydrogels showed a similar release profile to their CV correspondents from the early stages (2 h) of the experiment.

The mechanisms and heating rates of CV and MW are different. MW has a higher heating rate and the heating mechanism depends on the electromagnetic field variations causing instantaneous heat generation within the material because of the polarization of the chemical constituents (Liu & Kuo, 2011). Contrarily, CV provides heating by means of thermal conduction with a slower heating rate, thus a longer heating time. MW can provide a faster gelling for the protein solutions. The reduction in the heating time induces weaker, less homogeneous and coagulate-like gel structures since time to form a three-dimensional gel matrix is decreased (Gustaw & Mleko, 2007). Gustaw and Mleko (2007) reported that at pH 7.0, there were distinct differences between the CV and MW WPI gels. For instance, MW WPI gels had larger pores than the CV WPI gels. Protein denaturation via unfolding or protein

subunit dissociation and exposure of hydrophobic parts of the proteins during gelation are common for both types of heating mechanisms. But, CV promotes secondary aggregation after initial protein unfolding. This event contributes to stronger interactions within the gel network and higher gel strength. Since MW times are not long enough for the crosslinking of the free sulfhydryl groups residing in the protein structure, these free sulfhydryl groups induce subunit dis-aggregations leading to a more coagulate-like structure for the gels. On the contrary, CV enhances the crosslinking of the free sulfhydryl groups. MW also increases the exposure of the hydrophobic core residues promoting more protein disaggregation and unfolding. All in all, CV may generate WPI hydrogels with strong disulfide bonds, enhanced hydrophobic interactions between the molecules with a more compact and uniform gel network (Bi et al., 2015). Release results of MW hydrogels implied that presence of polysaccharides in WPI hydrogels did not have any effect on the release retardation. Their contribution to release retardation as in the case of CV hydrogels completely vanished. The reason for the similar release rates of CV and MW C hydrogels may have originated from the almost complete release of the encapsulated compound from the CV C gel matrix at the end of 24 h. Removal of the remaining small amount of BC was only possible after the partial degradation of the hydrogels since the remaining BC molecules were strongly bonded to the internal hydrogel structure. Accordingly, CV C hydrogels almost reached the maximum possible release amount so that their release rate enhancement in MW was lower than the other hydrogels.

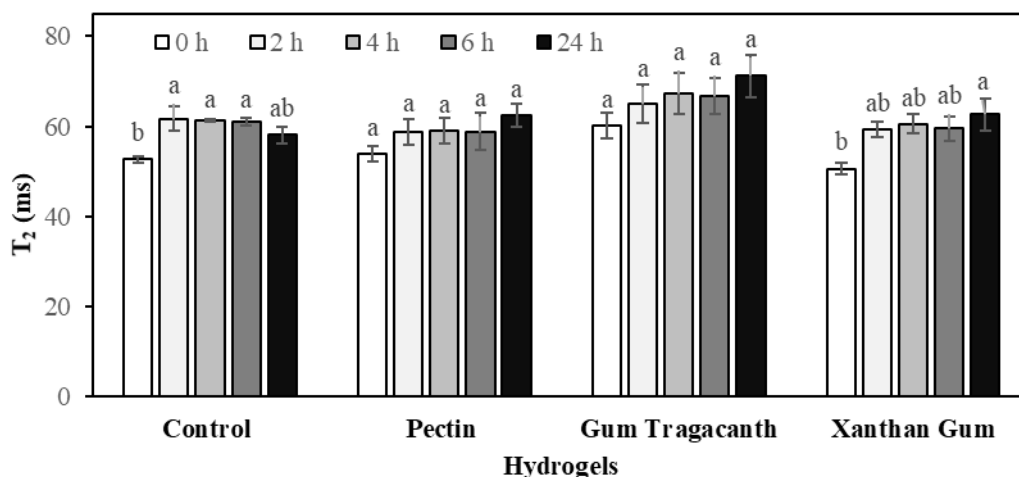
3.2.3 NMR Relaxometry Analysis

3.2.3.1 T₂ Analysis

NMR relaxometry enables non-destructive analysis of proton relaxation profiles of the food samples. Analysis of ¹H relaxation in food systems including hydrogels can be utilized to obtain information about the internal structures of these systems (Oztop

et al., 2014). T_2 (spin-spin relaxation time) is a useful parameter to interpret the water – polymer interactions in a gel system (Ozel, Uguz, et al., 2017). Presence of water in such systems gives rise to T_2 since liquids have higher T_2 than solids. In liquids, molecules are located further apart compared to the molecules of solid materials having a more closely packed conformation. Thus, the protons in solid substances diphas faster than the protons in liquid materials after the 90° RF pulse is turned off, giving lower T_2 (Hashemi et al., 2010).

T_2 values of hydrogels were measured before the solvent immersion of the hydrogels and throughout the 1-day release experiment. Initially, before exposing to release medium (phosphate buffer), CV XG hydrogels had the shortest T_2 (50.61 ms) among the other CV hydrogels ($p < 0.05$) (Fig. 3.9). Beginning from the 2 h of the release experiments, all CV hydrogels demonstrated similar T_2 values throughout the experiment. Therefore, T_2 profile of each hydrogel was investigated, separately. According to the results, only CV XG hydrogels achieved a longer T_2 at the end of the release experiments (24 h) with respect to their initial T_2 ($p < 0.05$) (Fig. 3.9).



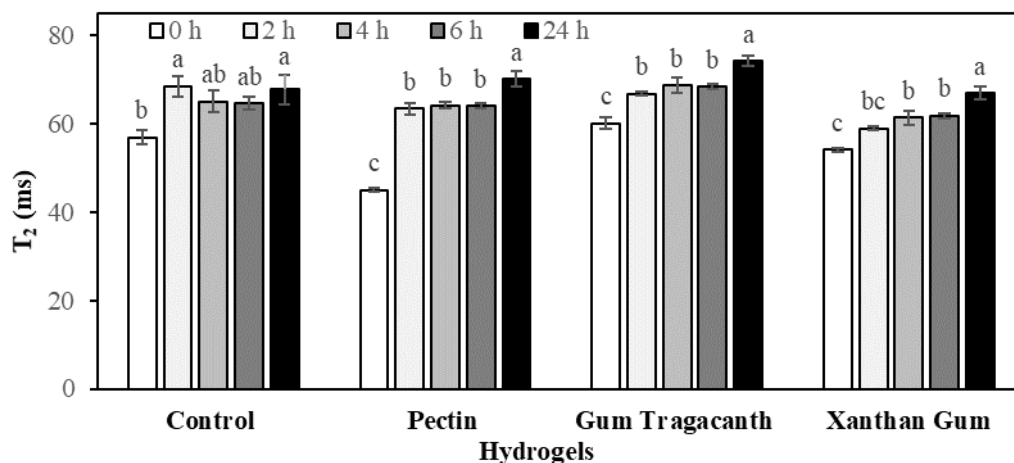
*Lettering was done for each hydrogel group, separately. Different small letters mean T_2 values are significantly different between 0 – 24 h ($p < 0.05$).

Figure 3.9. T_2 profiles of conventionally heated hydrogels

The increase in the T_2 of CV XG hydrogels at the end of the release experiment was in consistence with the high SR of the same set of hydrogels in 1-day experiment. Main factors contributing to the longer T_2 of CV XG hydrogels were the amount of water present in CV XG hydrogels and water – gel network interactions. CV XG hydrogels absorbed larger amount of solvent than CV C hydrogels which resulted in longer T_2 . A higher amount of water thus hydrogen molecules increased the T_2 (Oztop et al., 2010). Another reason was the abundance of BC – polymer interactions in CV XG hydrogels. This reduced the water – polymer interactions within the XG gel matrix. A considerable amount of absorbed water then remained in free-state leading to longer T_2 in CV XG hydrogels. CV C hydrogels attained a final T_2 (24 h) analogous to their initial T_2 . Although CV C hydrogels experienced some swelling in phosphate buffer, their high BC release rate affected the solvent – polymer interactions. Removal of excess amount of BC from CV C hydrogels through the end of the experiment provoked more water – polymer interactions within the CV C hydrogel. Interaction sites of the CV C hydrogel network were more available to water molecules after the release of BC. CV PC and GT hydrogels also exhibited stable T_2 profiles like CV C hydrogels during the 1-day experiment although they previously showed considerable SRs. Normally, an increase in SR should provide also a major increase in T_2 values since the presence of higher amounts of solvent in the hydrogels increases T_2 values. However, in the case of CV PC and GT hydrogels, absorbed water interacted with the surrounding polymer network more intensely than the water – polymer interactions in the other hydrogels. High hydrophilic side chain nature of the both polysaccharides (PC and GT) may have contributed to this phenomenon. Despite the high amount of solvent, water – polymer interactions predominated the transverse relaxation in these hydrogels.

MW had a crucial impact on the T_2 profiles of the hydrogels (Fig. 3.10). T_2 of the MW PC and GT hydrogels showed an increase beginning from the 2 h of the experiment contrary to their stable T_2 profiles of the CV counterparts ($p < 0.05$). MW XG hydrogels which had also a stable T_2 profile until the end of 6 h for their CV

correspondents, experienced longer T_2 beginning from 4 h. This change in the T_2 profile of MW XG hydrogels was also related to the dramatic increase in the release rates of MW XG hydrogels. The high ϵ'' of XG hydrogel solutions contributed to fast heating of these solutions and consequently the high release of MW XG hydrogels. Even a small increase in the heating rate can cause abrupt changes such as increased pore size in the gel network (Li et al., 2006). MW C hydrogels exerted a similar T_2 profile to their CV T_2 analogues except for the decrease in the final T_2 of CV C hydrogels. Although T_2 values of CV and MW hydrogels were similar to each other for each time interval except for the beginning of the experiment, MW hydrogels showed an increasing T_2 trend in their individual profiles. These results demonstrated that MW altered the water – polymer interactions and behaviors of solvent within the hydrogels. Early increasing tendency of T_2 for MW hydrogels suggested that MW hydrogels had weaker gel structures during solvent uptake allowing water molecules to present in a free state diffusing in and out through the hydrogels.



*Lettering was done for each hydrogel group, separately. Different small letters mean T_2 values are significantly different between 0 – 24 h ($p < 0.05$).

Figure 3.10. T_2 profiles of infrared assisted microwave heated hydrogels

3.2.3.2 SDC Analysis

SDC of water in hydrogels were determined to further investigate the properties of the CV and MW hydrogels (Table 3.8 and 3.9). Proton relaxation times provide information about the water present in hydrogels. However, there may be many distinct proton populations within the hydrogels. Therefore, direct SDC measurements of water can be introduced for more specific findings. The mobility of water protons and their self-diffusion throughout the matrix can be detected by SDC measurements. SDC of water is influenced by the presence of polymers and it can be reduced by the increase in the water – polymer interactions (Manetti et al., 2004). CV hydrogels revealed close SDC results before exposure to release medium. After 6 h solvent immersion, all CV hydrogels except for C hydrogels experienced an increase in their SDC values ($p < 0.05$). This increase in SDC was directly related to the water uptake of these CV hydrogels. As the amount of water absorbed increased, SDC of that hydrogel also increased. Solvent uptake did not alter the SDC of CV C hydrogels which was consistent with low SR of CV C samples. Only CV XG hydrogel attained a higher SDC ($1.67 \times 10^{-9} \text{ m}^2/\text{s}$) than CV C hydrogels ($1.45 \times 10^{-9} \text{ m}^2/\text{s}$) at 6 h ($p < 0.05$). CV PC and GT SDC values were in intermediate range 1.57 and $1.51 \times 10^{-9} \text{ m}^2/\text{s}$, respectively, at 6 h. These SDC results of CV hydrogels were identical to SR results, in terms of statistical analysis, proving that SR played a crucial role on the SDC values.

Table 3.8 SDC values of CV and MW hydrogels before exposing to release medium (0 h)

Hydrogels	CV SDC $\times 10^9$ 0 h (m^2/s)	MW SDC $\times 10^9$ 0 h (m^2/s)
Xanthan Gum	1.35 \pm 0.04 ^{a, A}	1.25 \pm 0.01 ^{a, A}
Gum Tragacanth	1.39 \pm 0.03 ^{a, A}	1.23 \pm 0.04 ^{a, B}
Control	1.33 \pm 0.02 ^{a, A}	1.26 \pm 0.04 ^{a, A}
Pectin	1.39 \pm 0.00 ^{a, A}	1.28 \pm 0.07 ^{a, A}

*Different small letters mean values are significantly different in each column ($p < 0.05$). Different capital letters mean values are significantly different in each row ($p < 0.05$).

MW hydrogels, contrary to CV hydrogels, did not show a significant increase in their SDC values at the end of 6 h solvent uptake process. Moreover, there was no difference between the SDC values of different MW hydrogels both at 0 h (prior to solvent exposure) and 6 h of the experiment. Stability in the MW hydrogel SDC values implied that, unlike CV hydrogels, MW hydrogels were not capable of retaining sufficient amount of water in their gel structures due to differences in their gel matrices. In addition, SDC comparison of CV and MW hydrogels showed that only SDC of CV XG hydrogels (at 6h) was higher than their MW counterparts ($p < 0.05$) (Table 3.9). Consequently, CV XG hydrogels with high SR and low release properties, were the most severely affected hydrogels by MW.

Table 3.9 SDC values of CV and MW hydrogels (6 h)

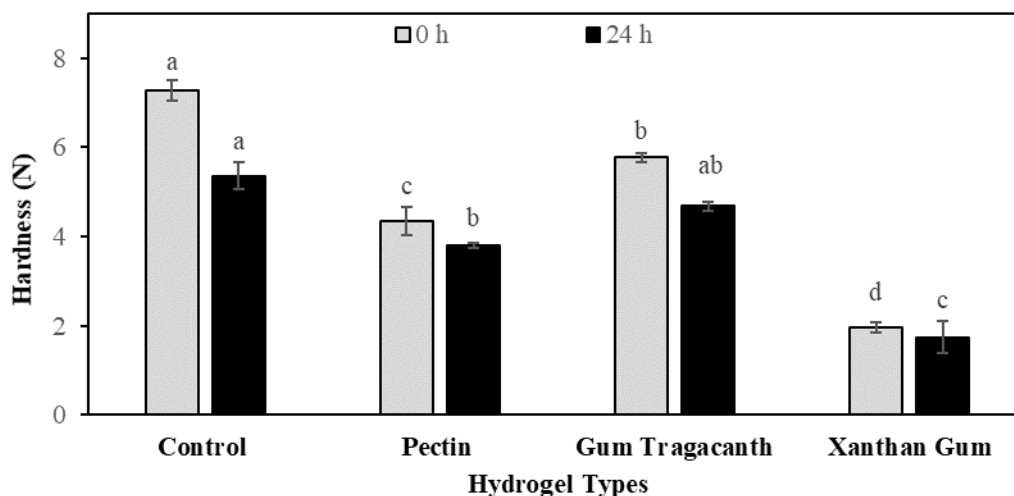
Hydrogels	CV SDC $\times 10^9$ 6 h (m^2/s)	MW SDC $\times 10^9$ 6 h (m^2/s)
Xanthan Gum	1.68 \pm 0.04 ^{a, A}	1.35 \pm 0.03 ^{a, B}
Gum Tragacanth	1.52 \pm 0.02 ^{ab, A}	1.39 \pm 0.05 ^{a, A}
Control	1.45 \pm 0.08 ^{b, A}	1.39 \pm 0.06 ^{a, A}
Pectin	1.57 \pm 0.05 ^{ab, A}	1.38 \pm 0.13 ^{a, A}

*Different small letters mean values are significantly different in each column ($p < 0.05$). Different capital letters mean values are significantly different in each row ($p < 0.05$).

3.2.4 Hardness Analysis

Hardness values of freshly produced CV hydrogels (0 h) and phosphate buffer treated CV hydrogels (24 h) were summarized in Figure 3.11. Freshly produced MW hydrogels were much softer than the CV hydrogels which could be easily noticed by simple sensorial observation. Moreover, MW hydrogels could not maintain their integrity over the 24 h release experiments in phosphate buffer and degraded to some extent. Therefore, hardness of MW hydrogels was not measured. Before exposing to phosphate buffer (0 h), hardness values of CV C, GT, PC and XG hydrogels were

measured as 7.27, 5.77, 4.34 and 1.97 N, respectively. Polymer addition to WPI hydrogels (C) resulted in softer hydrogel structures ($p < 0.05$). When an additional polymer was blended to the WPI hydrogels, added polymer also contributed to the interactions taking place within the gel matrix changing the extent of interactions between the WPI molecules (Turgeon & Beaulieu, 2001). Creation of more interaction sites within the WPI gel matrix ended up with softer gel structures. 24 h phosphate buffer treatment decreased the hardness of CV C and GT hydrogels ($p < 0.05$). On the other hand, hardness of CV PC and XG hydrogels remained stable after the release experiment. In general, polymer addition (PC and XG) prevented the softening of the gels in the release medium. However, the more liquid character of GT molecule induced lower hardness for the WPI based hydrogels in phosphate buffer ($p < 0.05$) (Balaghi et al., 2011). Despite its high hardness after the experiment, the most severe reduction in the hardness value was observed for the CV C hydrogels. This could be one of the reasons of the high release rate of CV C hydrogels. Obviously, CV C gel matrix loosened and became softer during the release experiment leading to more BC release in the absence of a blended polymer. The lowest hardness of CV XG hydrogels both before and after the release experiment could be associated with the high SR result of these hydrogels. Probably, intense XG – WPI interactions induced more interaction sites within the gel matrix compared to other WPI – polysaccharide hydrogels (Zhang et al., 2014). This may have provided a gel with more flexible structure leading to better swelling and low hardness.



*Lettering was done for each time (0 and 24 h), separately. Different small letters mean hardness values are significantly different at 0 h or 24 h ($p < 0.05$).

Figure 3.11. Hardness profiles of hydrogels in phosphate buffer

3.2.5 Release Modelling

Mathematical modelling of BC release from the hydrogels was performed using Fick's second law. Release data were fitted to analytical solution given in Eq. (4) to obtain the best estimated value for diffusivity, D , using MATLAB nonlinear curve fitting subroutine. Several factors such as composition of hydrogel (presence of any polymer and type of the polymer etc.), preparation technique, geometry of the gel (shape and size) and environmental conditions influence the release behavior (Zarzycki et al., 2010). Exterior diffusion, interior diffusion, desorption and chemical reactions are among the release mechanisms. In this study, SR of hydrogels has risen up to maximum 17.85 % thus, diffusion controlled mechanism has been considered. Therefore, interior diffusion throughout the polymeric matrix was explained by Fick's second law of diffusion. All fitted diffusion coefficient values for all hydrogel formulations were given in Table 3.10. D values of BC release from the hydrogels were found in the order of 10^{-10} m²/s. The results varied between 0.59×10^{-10} and 1.78×10^{-10} m²/s. However, due to the high variations between the D values of the

samples originating from the uniqueness of the each tested hydrogel, no significant difference was obtained between the samples ($p > 0.05$).

Table 3.10 Diffusion coefficients of CV and MW hydrogels

Hydrogels	CV $D \times 10^{10}$ (m^2/s)	MW $D \times 10^{10}$ (m^2/s)
Pectin	1.39±0.35 ^{a, A}	1.53±0.08 ^{a, A}
Xanthan Gum	2.29±1.52 ^{a, A}	1.17±0.33 ^{a, A}
Gum Tragacanth	1.13±0.03 ^{a, A}	1.53±1.37 ^{a, A}
Control	0.59±0.18 ^{a, A}	1.18±0.49 ^{a, A}

*Different small letters mean values are significantly different in each column ($p < 0.05$). Different capital letters mean values are significantly different in each row ($p < 0.05$).

3.2.6 Microstructure Analysis

SEM images of hydrogels revealed that addition and type of the polysaccharide used affected the hydrogel microstructures. Additionally, CV and MW caused striking characteristic microstructural differences in hydrogel matrices (Fig. 3.12). Firstly, all MW hydrogel images showed smoother and more coagulate-like structures with respect to their CV correspondents. CV C hydrogels had a homogeneous honeycomb-like gel structure whereas CV PC and XG hydrogels possessed clumpier and denser structures (Fig. 3.12A, C, E). Local aggregates could be observed more obviously in CV PC and CV XG hydrogels indicating high crosslinking density in these samples. In contrast to other CV samples, CV GT hydrogels exhibited a smooth, sheet-like gel network which was close to MW hydrogel images (Fig. 3.12G). Microstructural properties of CV GT justified the stable T_2 profile of GT hydrogels. CV XG hydrogels had homogeneous distribution of local aggregates (Fig. 3.12E). These closely packed and clumpy structure of CV XG hydrogels provided these hydrogels a high water holding capacity (high SR). CV PC hydrogels were similar to CV XG hydrogels but distribution of the aggregates was more

heterogeneous and size of the aggregates was bigger than the ones in CV XG hydrogel (Fig. 3.12C, E). This caused a more porous structure for CV PC hydrogels. When the image of MW C hydrogel was examined, it was observed that MW increased the pore size of the gel and the particulate structure became smoother (Fig. 3.12B). One of the reasons that led to a more porous structure in MW hydrogels was the internal pressure gradient produced by MW. Water transport from the interiors to the hydrogel surface was mainly driven by this pressure gradient, which adversely affected the gel structures. The effect of MW was even more severe on PC and XG hydrogels (Fig. 3.12D, F). Clumpy and dense microstructures of these hydrogels were lost after MW. Dramatic increase in the release rates of MW XG and PC hydrogels could be attributed to these microstructural changes induced by the heating type (MW). XG hydrogels clearly experienced the most severe alteration in the gel structure after MW (Fig. 3.12E, F). Slight differences between the CV GT and MW GT hydrogel images can be attributed to the water interaction properties of GT molecules. GT has a high affinity for water and water soluble parts of the GT molecules contributed to the coagulate-like structure of the respective hydrogels (Fig. 3.12G, H) (Balaghi et al., 2011).

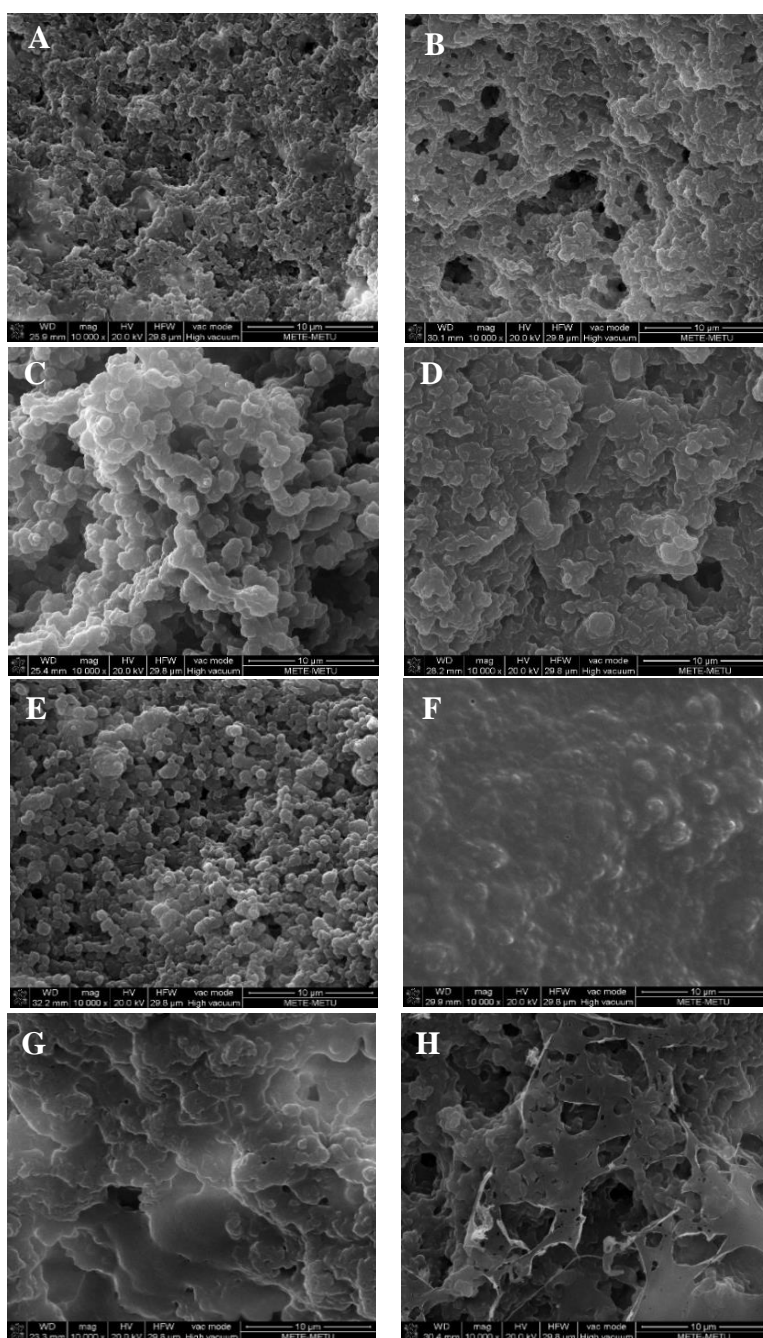


Figure 3.12. SEM images of hydrogels: A: CV C, B: MW C, C: CV PC, D: MW PC, E: CV XG, F: MW XG, G: CV GT, H: MW GT

3.3 Controlled Release in GIT

CV hydrogels were subjected to *in vitro* gastrointestinal digestion in order to understand the BC release characteristics of the hydrogels in simulated human GIT conditions. Release data were obtained for 2 h gastric and subsequent 6 h intestinal digestion (total 8 h gastrointestinal digestion). As previously mentioned, MW hydrogels were not suitable for *in vitro* gastrointestinal digestion. Therefore, CV C, CV PC, CV GT and CV XG hydrogels were denoted as C, PC, GT and XG hydrogels in the remainder of the manuscript. Cumulative release profiles in gastrointestinal digestion for 8 h revealed that both type of the release medium and polymer blending affected the release characteristics of the hydrogels (Fig. 3.13). Generally, hydrogels experienced faster release rates in SGF and gradual release in SIF. The overall gastrointestinal digestion (8 h) showed that PC hydrogels attained the highest cumulative release rate (96%) whereas XG hydrogels attained the lowest release rate (73%) ($p < 0.05$). C hydrogels had a final release of 88 % which was higher than XG (73%) and GT (79%) hydrogels ($p < 0.05$). Since gastric and intestinal digestion phases had distinct effects on the hydrogels, BC release properties of the hydrogels were investigated in SGF and SIF, separately.

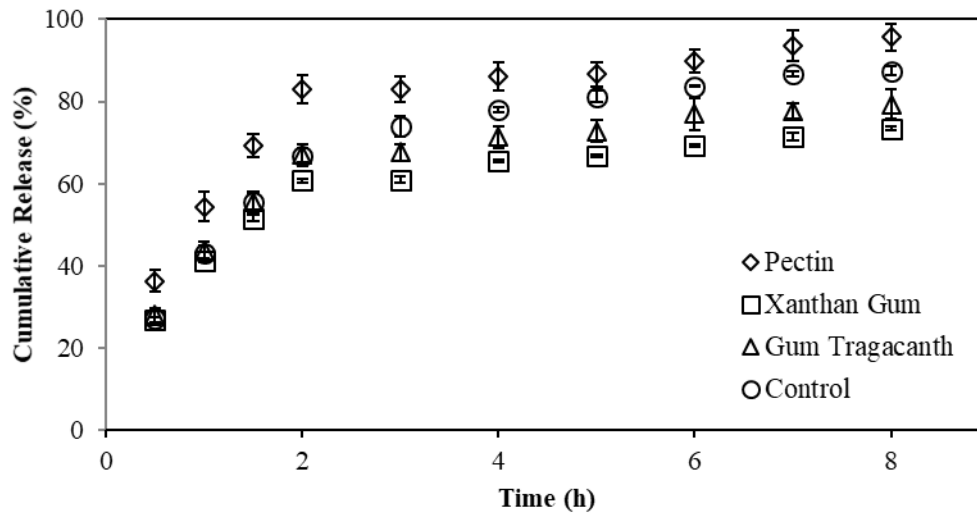


Figure 3.13. Cumulative release profiles of hydrogels in GIT (0 – 2 h gastric phase, 2 – 8 h intestinal phase)

3.3.1 Simulated Gastric Phase

3.3.1.1 Release Profiles

Release profiles of all hydrogels exhibited an increasing trend during the gastric digestion (Fig. 3.14). PC hydrogels attained the highest release rate (83%) ($p < 0.05$) in SGF than the GT (67%), C (67%) and XG (61%) hydrogels having similar release profiles. Electrostatic interactions between the proteins and polysaccharides in protein – polysaccharide complexes are highly dependent on the changes in pH (Santipanichwong et al., 2008). WPI having a pI around 5.2 and the blended polymers having pKa values around 2.5 – 3.5 were protonated in SGF (pH ~ 1.2), created a generally positively charged gel matrix (Joshi, Rawat, & Bohidar, 2018; Ozel et al., 2017). Suppression of the ionizable groups of WPI and the blended polymers at the highly acidic pH affected the release rates from these hydrogels. Extent of protonation depends on the type of the polymer used since charge density of the polymer determines the degree of protonation (Belscak-Cvitanovic et al.,

2015). However, polysaccharide blending was not able to retard the release of BC from the hydrogel matrices. Furthermore, addition of PC to WPI increased the release rate in SGF. Conformational behavior of PC molecules at a strongly acidic environment, chemical structure and physical properties of PC molecules could be among the reasons for this release behavior (Saldamli, 1998). Xu and Dumont (2015) also reported that polymer blending and polyelectrolyte complexation of canola and pea protein based composite hydrogels were not very effective to create structures for prolonged release applications in SGF (Xu & Dumont, 2015). Hydrogel solution viscosities were previously determined and PC hydrogel solution (including BC) had a lower viscosity with respect to GT and XG hydrogel solutions ($p < 0.05$) (Table 3.7). This gives an idea about the behavior of PC molecules in aqueous media. Generally, longer and bigger molecules tend to increase the solution viscosity. PC also has a lower molecular weight (50 – 150 kDa) than GT (~850 kDa) and XG (~2000 kDa) molecules supporting the viscosity results and also the smaller size of PC molecules compared to GT and XG molecules (Mohammadifar et al., 2006; Mohnen, 2008; Zasytkin et al., 1996). Despite the presence of side groups such as rhamnose, galactose, arabinose and xylose, the polymer structure of PC shows a more linear characteristic with respect to GT and XG molecules (Kyomugasho et al., 2015). Due to these properties, PC is not a highly acid resistant polymer and at extremely low pH values such as 1.2 (pH of SGF), hydrolysis of glycosidic linkages in the galacturonic acid backbone of PC could be observed (Saldamli, 1998). Moreover, with its lower molecular weight and more linear structure with respect to other blended polymers, PC is expected to have a lower charge density at acidic conditions with respect to GT and XG molecules (Mohnen, 2008; Zhang et al., 2014). Therefore, carboxylic groups of PC were not dissociated and almost complete protonation of PC molecules was achieved. Thus, negatively charged portions on the PC molecules were probably eliminated that would otherwise contribute to the crosslinking within the hydrogel matrix.

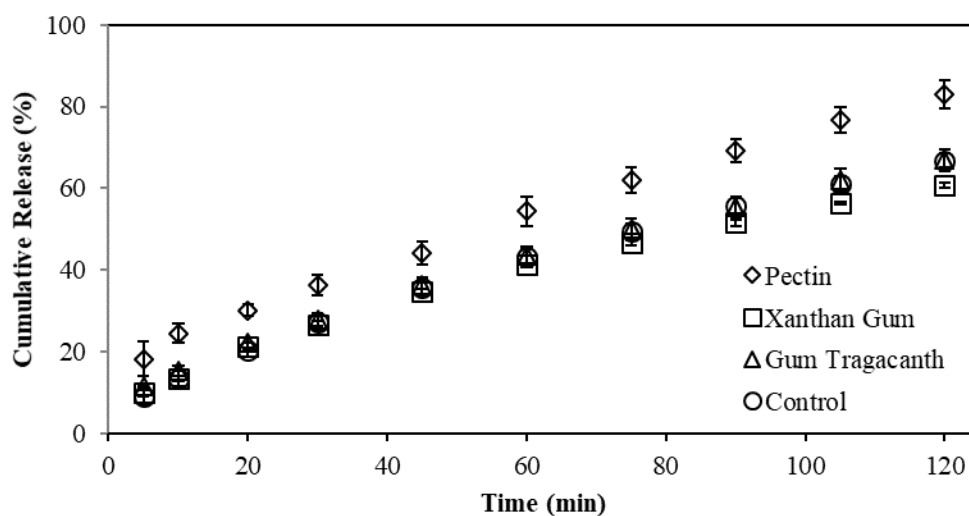


Figure 3.14. Release profiles of hydrogels in SGF

Contrary to PC, GT and XG polymers are known for their acid stable properties. GT is described as a highly acid resistant and heat stable hydrocolloid whereas XG is valued for its extraordinary acid resistance (Balaghi et al., 2011; Saldamli, 1998). Acid resistance of XG originates from the trisaccharide side chains containing α -D-mannopyranose, β -D-glucopyranose and β -D-mannopyranose that are linked to glucose units (Fabek et al., 2014). Some terminal mannose units are pyruvylated and some of the inner mannose units are acetylated. These trisaccharide chains interact with the main backbone and then the molecule gains a strongly rigid character in helical conformation. This structural conformation provides XG molecules a high acid resistance since the main cellulosic main backbone is protected. Thus, the likelihood of hydrolysis of the XG backbone is extremely diminished in strongly acidic conditions (Saldamli, 1998). Another factor contributing to the acid resistance of XG was the charge density of the polymer. XG has a branched and complex structure. XG structure contains a high number of charged side groups increasing the overall charge density of the polymer (Zhang et al., 2014). Ionization of carboxyl groups was suppressed and the negatively charged groups were protonated in acidic pH but due to the high density of the charged groups in XG, some parts may have

still remained negatively charged. Consequently, this may have contributed to further crosslinking between the blended polymer and positively charged WPI molecules in SGF (pH ~ 1.2). Charge density of PC is lower than both GT and XG molecules resulting in quick protonation of the ionizable groups of PC in acidic mediums. Therefore, PC – WPI gel network became weaker in SGF (Sriamornsak, 2003). On the other hand, negatively charged portions of GT and XG molecules contributed to the further crosslinking within the WPI gel matrix in SGF.

C hydrogels containing only WPI as the gelling agent also showed a similar release profile to GT and XG hydrogels. Strong crosslinking in the WPI gel network (*e. g.* disulfide linkages) in the absence of an additional polymer prevented the rapid BC release. Polymers are generally blended to protein hydrogels in order to retard the release of the encapsulated agent (Gunasekaran et al., 2007). However, this phenomenon depends on the type of the blended polymer and the nature of the release medium. If the blended polymer does not have strong crosslinking characteristics under the given release conditions, creation of new interaction sites between the added polymer and the continuous protein network may weaken the overall hydrogel matrix (Turgeon & Beaulieu, 2001). Therefore, homogeneity of the C hydrogel matrix provided a retarded BC release with respect to PC hydrogels under strong acidic conditions. Addition of PC, on the other hand, made the WPI hydrogels more susceptible to pepsin activity and low pH conditions due to the resulting structural inhomogeneity caused by PC degradation (Saldamli, 1998).

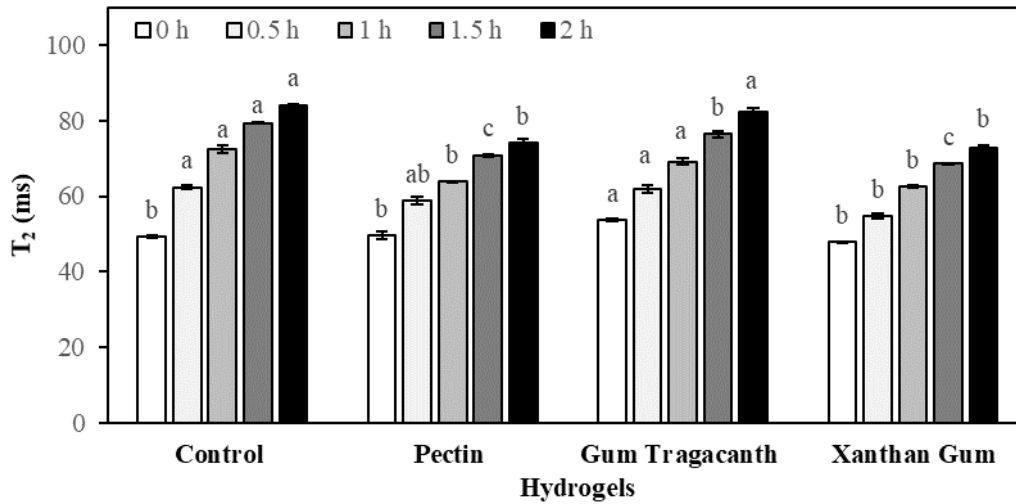
3.3.1.2 NMR Relaxometry Analysis

Undigested fresh (0 h) XG, C and PC hydrogels initially had similar T_2 values but fresh GT hydrogels had a longer T_2 than others before the gastric treatment ($p < 0.05$). T_2 values of all hydrogels increased after 2 h gastric digestion and attained T_2 values in the range of 73 – 84 ms ($p < 0.05$) (Fig. 3.15). One of the reasons behind this increasing trend was the strong acidic nature of the release medium (SGF, pH~1.2). At that low pH, hydrogen ion concentration increased in SGF giving longer

T_2 since T_2 depends on the hydrogen ion concentration (Oztop et al., 2010). Moreover, amino groups of the protein and carboxyl groups of the blended polymers were protonated at such acidic conditions (Xu & Dumont, 2015). The previous T_2 profiles of the CV hydrogels in phosphate buffer were more stable than the T_2 profiles of these hydrogels in SGF (Fig. 3.9). This difference in the T_2 profiles of the hydrogels in phosphate buffer and SGF emphasized the effect of release medium on transverse relaxation (Ozel et al., 2017).

Another factor contributing to the obtained T_2 profiles in SGF was the BC release behaviors of the hydrogels. When Figure 3.15 was examined, it was observed that PC and XG hydrogels attained shorter T_2 with respect to C and GT hydrogels ($p < 0.05$). The shorter T_2 (74 ms) of PC hydrogels was mainly because of the excess BC loss of these hydrogels in SGF. Transverse decays of all hydrogels were monoexponential showing the dominant effect of polymer – water interactions and fast exchange between different compartments. However, T_2 results also suggested that presence of BC and the interaction of the retained BC with the surrounding polymer network also affected the T_2 profiles in SGF. Under these acidic conditions, hydrogels did not experience any swelling that obstructed the excess penetration of SGF medium into the depths of the hydrogels. Retention of BC in the gel matrix increased the number of relaxing protons so that longer T_2 were observed for C and GT hydrogels which retarded BC release in SGF ($p < 0.05$). XG hydrogels also retarded BC release in SGF but they attained shorter T_2 compared to C and GT hydrogels ($p < 0.05$). Here, the state of the encapsulated agent (BC) in the hydrogel matrix determined the final T_2 (Manetti et al., 2004). Probably, enhanced interactions between the BC anthocyanins and XG hydrogel matrix via hydrogen bonding reduced the T_2 increasing effect of BC retention in the XG hydrogels. Highly branched and densely charged structure of XG created more interaction sites for BC within the polymer network than C, PC and GT hydrogels did. Thus, amount of the relaxing protons of bulk BC in free state was diminished (Ozel et al., 2017). In addition, absorption of SGF having the T_2 increasing effect, could not compensate the BC effect in XG hydrogels. This may have occurred due to the lower absorption

of the surrounding liquid into the XG hydrogel matrix with respect to other hydrogels. Sensorial observations were in agreement with this hypothesis since XG hydrogels exhibited a rigid gel structure at the end of gastric release which would definitely retard the absorption of SGF into the gel matrix.

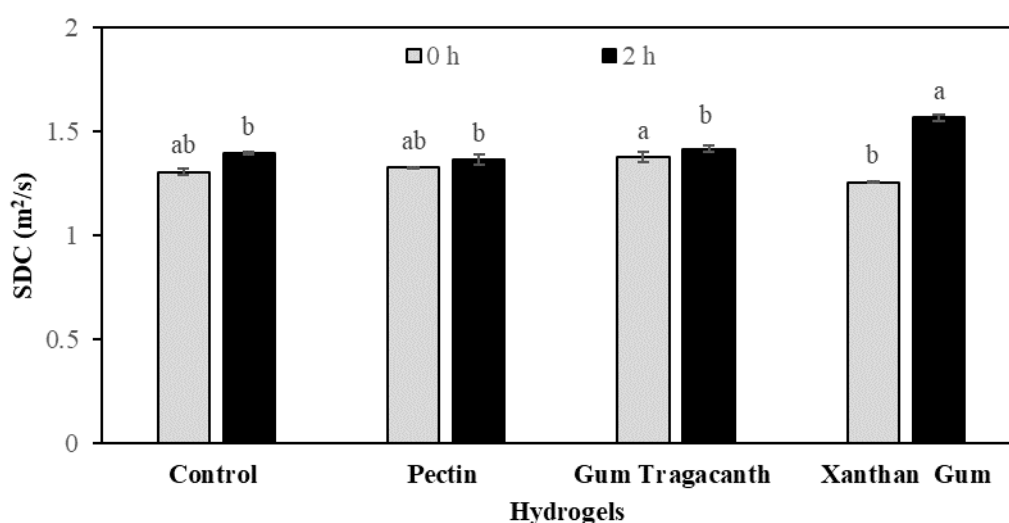


*Lettering was done for each time (0, 0.5, 1, 1.5 and 2 h), separately. Different small letters mean T₂ values are significantly different at each time ($p < 0.05$).

Figure 3.15. T₂ profiles of hydrogels in SGF

Mobility of water molecules and their self-diffusion throughout the gel matrix were determined by SDC measurements (Fig. 3.16). After the 2 h gastric treatment, only C and XG hydrogels experienced a significant increase in their SDC values ($p < 0.05$). SDC increase rates of C, GT, PC and XG hydrogels in SGF were 6, 3, 2 and 20 %, respectively. A dramatic increase in SDC of XG hydrogel was observed during 2 h SGF treatment. XG hydrogels also attained the highest SDC ($1.56 \times 10^{-9} \text{ m}^2/\text{s}$) after 2 h ($p < 0.05$) with respect to other hydrogels. C, PC and GT hydrogels had similar but lower SDC values with respect to XG hydrogels at the end of the gastric digestion ($p < 0.05$). The considerably high SDC of XG hydrogels after the gastric treatment was the result of the enhanced interactions between the XG hydrogel

matrix and BC. These interactions lowered the degree of polymer – water interactions which were effective on the SDC of water. An increased polymer – water interaction reduces the SDC of water (Manetti et al., 2004). Moreover, state of the water in the gel matrix is more effective than the amount of water present in the gel matrix in terms of determining the SDC (Ozel et al., 2017). Therefore, the increased XG – BC and reduced XG – water interactions in XG hydrogels hypothesis was supported by the SDC results.



*Lettering was done for each time (0 and 2 h), separately. Different small letters mean T_2 values are significantly different at 0 h or 2 h ($p < 0.05$).

Figure 3.16. SDC profiles hydrogels in SGF

3.3.1.3 Release Modelling

BC release from hydrogels in SGF was mathematically modeled using Fick’s second law. Release data in SGF were fitted to Eq. (4) (Crank, 1975). Since hydrogels did not swell in SGF, diffusion controlled mechanism was considered. Fick’s second law of diffusion was used to explain the interior diffusion throughout the polymeric matrix. PC hydrogels with the highest release rate had D value of 11.10×10^{-10} which was higher than the D values of the release retarding C and GT hydrogels ($p < 0.05$).

This suggests a positive correlation between the BC release rates and diffusion coefficients in SGF. However, D value of XG hydrogels was intermediate resembling statistically to other hydrogels ($p > 0.05$). The specific interactions between the XG hydrogel matrix and the encapsulated BC molecules may have induced such a result for the diffusion coefficient of XG hydrogels. All fitted values of diffusion coefficients for the release experiments in SGF were given in Table 3.11.

Table 3.11 Diffusion coefficient of hydrogels in SGF

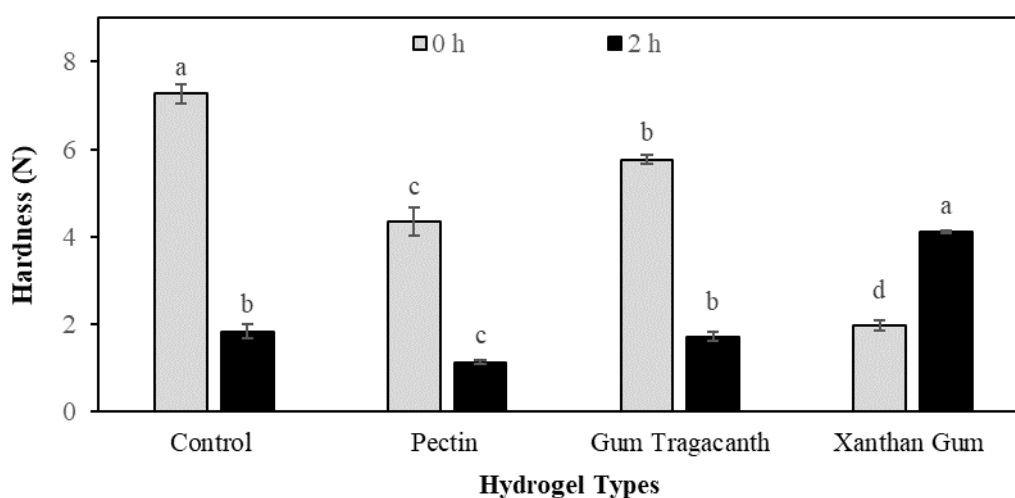
Hydrogels	Diffusion Coefficient $\times 10^{10}$ (m^2/s)
Control	9.68 \pm 0.04 ^b
Pectin	11.10 \pm 0.16 ^a
Gum Tragacanth	9.63 \pm 0.37 ^b
Xanthan Gum	10.32 \pm 0.47 ^{ab}

*Different small letters mean values are significantly different ($p < 0.05$).

3.3.1.4 Hardness Analysis

Exposure of the hydrogels to SGF for 2 h decreased the hydrogel hardness values except for XG hydrogels ($p < 0.05$) (Fig. 3.17). The final release rates and the hardness values of the hydrogels in SGF were in correlation. PC hydrogels having the lowest hardness after gastric treatment attained faster BC release among the others and XG hydrogels with the final hardest structure retarded the BC release ($p < 0.05$). C and GT hydrogels attained intermediate hardness values after 2 h SGF treatment. There were some reasons for the increased hardness of XG hydrogels in acidic conditions such as the molecular charge density and structural conformation of the XG polymer (García-Ochoa et al., 2000). XG has a high number of ionizable groups and this led to a higher charge density with respect to PC and GT polysaccharides. PC has a more linear structure and GT has also side chains but its molecular weight is lower and molecule size is smaller (Balaghi et al., 2011;

Mohnen, 2008). Thus, higher degree of interactions in the WPI polymer matrix was induced by XG molecules even in such low pH conditions. Additionally, the low pH configurations in XG such as the interactions of trisaccharide side chains with the main cellulosic backbone induced a rigid conformation. All these distinct properties of XG generated stronger WPI – XG interactions, thus gels with a higher strength (Zhang et al., 2014).



*Lettering was done for each time (0 and 2 h), separately. Different small letters mean hardness values are significantly different at 0 h or 2 h ($p < 0.05$).

Figure 3.17. Hardness profiles of hydrogels in SGF

3.3.1.5 FTIR Analysis

FTIR spectra of raw ingredients (dry WPI, PC, GT and XG powders), fresh hydrogels prior to SGF treatment (0 h) and SGF treated hydrogels (2 h) were analyzed (Fig. 3.18). WPI powder showed distinct absorption bands at specific wavenumbers (Fig. 3.18A). Firstly, the two peaks with low spectral intensities located in the range of $1200 - 1400 \text{ cm}^{-1}$ are related to the amide III bonds including the vibrations in the C – N plane and N – H groups of the peptide bonds (Muyonga

et al., 2004). Secondly, the peaks with higher spectral intensities between 1500 and 1600 cm^{-1} belong to amide II band representing the vibrations of C – N linkages and bending vibrations of N – H groups around 1500 cm^{-1} . Amide I band representing the C = O stretching vibrations around 1633 cm^{-1} was also responsible for the narrow peaks in this region (Díaz et al., 2016; Xu & Dumont, 2015). Amide I band is related to the protein secondary structure and C = O vibrations in the protein backbone (Bandeekar, 1992). This band determines the nature of the hydrogen bonds involved in C = O and N – H groups of the peptide linkages. Amide I region is sensitive to conformational changes in the secondary structures of proteins indicating mainly the intermolecular β -sheet structures of aggregated proteins. Hydrogen bond strength and the geometry of secondary structures also have impacts on the amide I band (Lefèvre & Subirade, 1999). Presence and high intensity of the amide I in the hydrogels was due to the presence of WPI and higher amount of WPI was associated with higher band intensity in this region. Moreover, the location of the amide I peak in WPI powder suggested a β -sheet protein structure. If this peak moves towards the wavenumbers of 1640 – 1650 cm^{-1} , it means that a transition from β -sheet to random coil protein structure takes place (Zand-Rajabi & Madadlou, 2016). The small peak between 2800 and 3000 cm^{-1} in the WPI powder indicated the –CH group stretching vibrations (Tonyali et al., 2018). Finally, the broad peak between 3000 and 3600 cm^{-1} is attributed to the stretching vibrations of total free and bonded O – H and N – H groups (Ebrahimi et al., 2016; Lozano-Vazquez et al., 2015).

Analysis of PC powder resulted in a different spectrum due to the polysaccharide characteristics of the PC (Fig. 3.18B). The peak around 1040 cm^{-1} which was not observed in WPI powder originates from the C – O stretching (Ebrahimi et al., 2016). This peak could originate from sugar glycosidic bond and C – O – C in the sugar ring. Besides, this peak could be associated with the presence of carboxylic acid units implying the polysaccharide existence (Simi & Abraham, 2010). Galacturonic acid, glucose, galactan and arabinogalactan residues may contribute to the absorbance intensity of this band (Blanco-Pascual et al., 2014). The small peak around 1732 cm^{-1} is also abundantly observed in polysaccharides and originates from the carbonyl

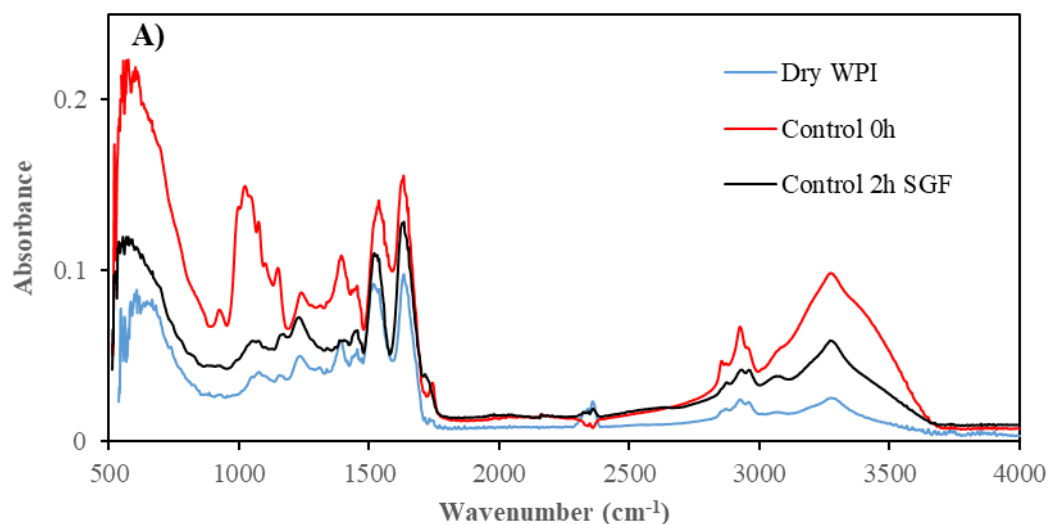
groups of $-\text{COOH}$ (Hosseini et al., 2014). This peak was not observed in dry WPI. Dry PC had a very small $-\text{CH}$ peak close to 3000 cm^{-1} and a broad peak between 3000 and 3600 cm^{-1} like WPI powder. Despite little differences, GT powder had a similar absorption spectrum to PC powder (Fig. 3.18C). One of the distinctions in dry GT spectrum was the small peak around 1618 cm^{-1} representing the asymmetrical $\text{C}=\text{O}$ stretching vibrations of the carboxylate anion. Another distinction was the shape of the $\text{O}-\text{H}$ peak. A broader and slightly lower intensity band was observed in this region for GT powder. The same peak was sharper in dry PC but the positions of the peaks were very close around 3331 and 3346 cm^{-1} for PC and GT powders, respectively. Although the spectrum of XG powder was also similar to the spectra of the other polysaccharides, some distinctions were present. The broader $\text{O}-\text{H}$ peak with a lower spectral intensity and the lower peak intensity at the peak responsible for the $\text{C}-\text{O}$ were observed in dry XG. The lower peak intensity at 1040 cm^{-1} could be attributed to the distinct side groups in XG structure.

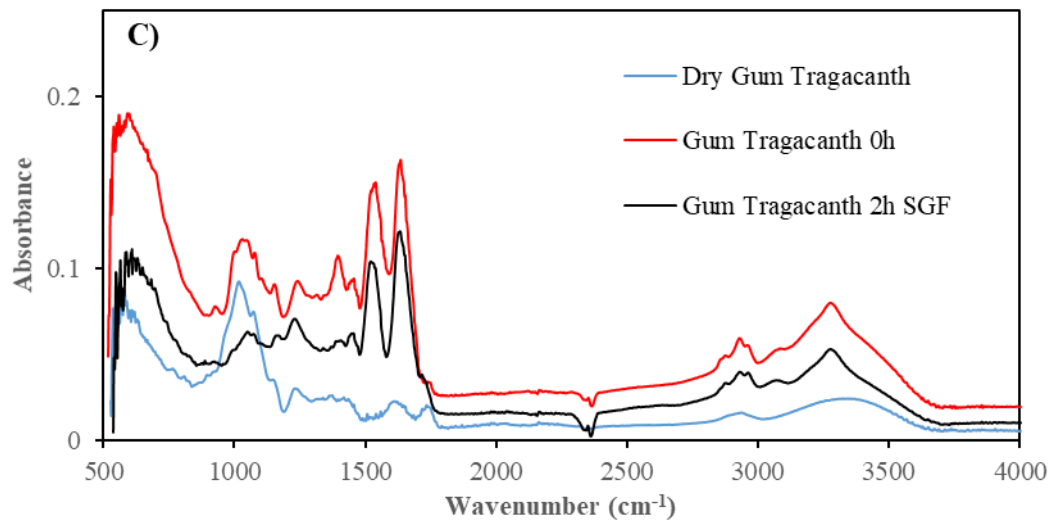
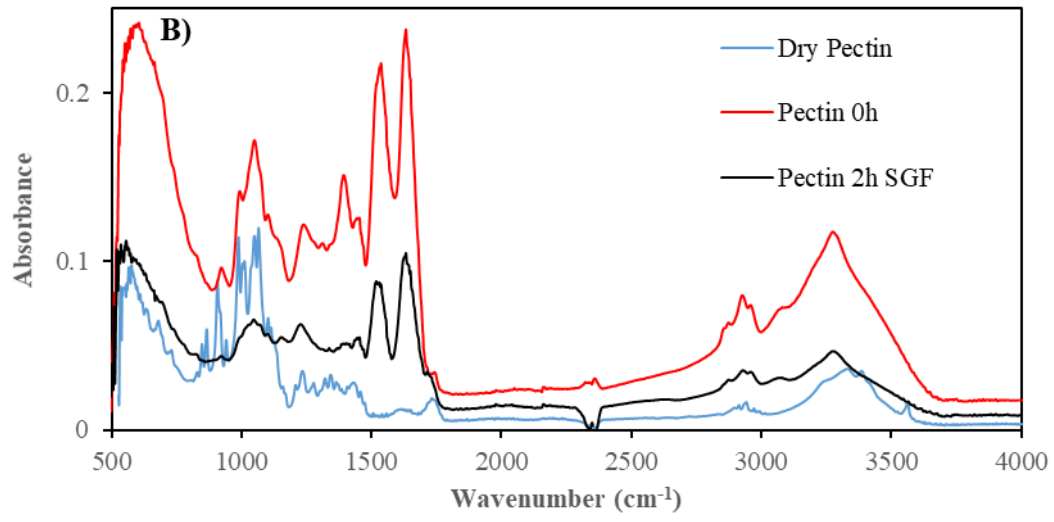
All hydrogels attained higher peak intensities than their powder form correspondents (Fig. 3.18). For instance, higher spectral intensities as well as sharper peaks representing the $\text{O}-\text{H}$ band were observed in fresh hydrogels with respect to absorbance spectra of dry WPI, PC, GT and XG ingredients. The increase in the spectral intensity of this range implies more hydrogen bonding which is one of the main characteristics of polymer gelation. Protein unfolding during gelation and interactions between the WPI and the added polymer also contributed to the intensity increase in this range. The sharper $\text{O}-\text{H}$ peak characteristic came from the introduction of solvent during gel preparation. In the presence of a solvent, the bending of $\text{O}-\text{H}$ linkages changed and a sharper spectrum was obtained (Raut et al., 2004). The increase in the $\text{O}-\text{H}$ band of XG hydrogel was lower than the other hydrogel types mainly originated from the different gelling characteristics WPI-XG system during gelation. These characteristics were mainly related to the rigid and branched molecular structure and big molecule size of XG. The interactions between the WPI and XG molecules were more intense than the other WPI-polysaccharide systems. Therefore, hydration of the WPI-XG gel matrix was retarded. In addition

to O – H bands, hydrogels also showed higher intensities for the other bands with respect to their powder forms demonstrating increased bond formations due to gelation process. However, XG hydrogels also showed slight intensity increments in other bands similar to change in O – H peaks. PC, GT and XG hydrogels showed amide bands due to presence of WPI. For C hydrogels, the already existing amide spectra in WPI form were enhanced with gelation. Moreover, the lacking band at 1040 cm^{-1} for dry WPI was observed in its gel form although C hydrogels do not contain any additional polymer. The reason was the addition of BC into the WPI solution before gelation. Units responsible for this peak such as glucose and its isomers were introduced into the system by BC addition since BC contains different sugar units.

2 h SGF treatment of hydrogels decreased the intensity of absorbance bands except for XG hydrogels (Fig. 3.18). The most severe reductions in the spectral intensities were observed for the PC hydrogels which also had a faster BC release profile in SGF. GT and C hydrogels experienced minor losses in their absorption peaks compared to PC hydrogels in SGF. After 2 h in SGF, PC spectrum showed that the peaks ($1400 - 1500\text{ cm}^{-1}$ and $1600 - 1700\text{ cm}^{-1}$) responsible for the presence of WPI were diminished extremely supporting the high BC release rate of PC hydrogels in acidic conditions (Fig. 3.18B). Under gastric digestion conditions, PC could not form strong interactions with WPI in the gel matrix. Thus, amide bands lost their absorbance intensities and PC – WPI hydrogel matrix became more susceptible to proteolysis. Interestingly, an increase in the absorbance intensities for all bands of XG hydrogel was observed after gastric treatment (Fig. 3.18D). The high hardness value of SGF treated XG hydrogels was confirmed by the higher and sharper amide band intensities after SGF treatment. In this way, the intense WPI – XG interactions and resulting rigid structure was supported by FTIR analysis. XG polymer may have prevented the protein degradation in SGF more efficiently with respect to other blended polymers (Zhang et al., 2014). Additionally, the O – H band of XG hydrogel became sharper and its absorbance intensity increased. Other hydrogels especially PC hydrogels having the highest BC release rate experienced a decreased O – H band

intensity. Retention of BC in the XG hydrogel matrix enhanced the hydrogen bonding between the gel matrix and BC. Molecular characteristics of XG *e. g.* high charge density, played a crucial role in the increase of the absorbance intensity of this spectrum since C and GT hydrogels also retarded the BC release but they still lost absorbance intensity in their O – H bands (Fig. 3.18A, C). The number of protonated carbonyl and other side groups of XG molecule was much higher than the other polymers. This increased the density of interactions within the XG hydrogel matrix due to the interactions such as hydrogen bonding between the carbonyl groups of BC molecules and the protonated sites of the XG polymer. The extensive loss in the O – H band absorbance intensity of PC hydrogels after gastric treatment manifested the predominant role of BC retention of hydrogels in determining the characteristics of this peak. PC hydrogels could not form as many hydrogen bonds with BC as the other hydrogels did in their gel networks which led to higher BC release from the PC hydrogels during SGF treatment.





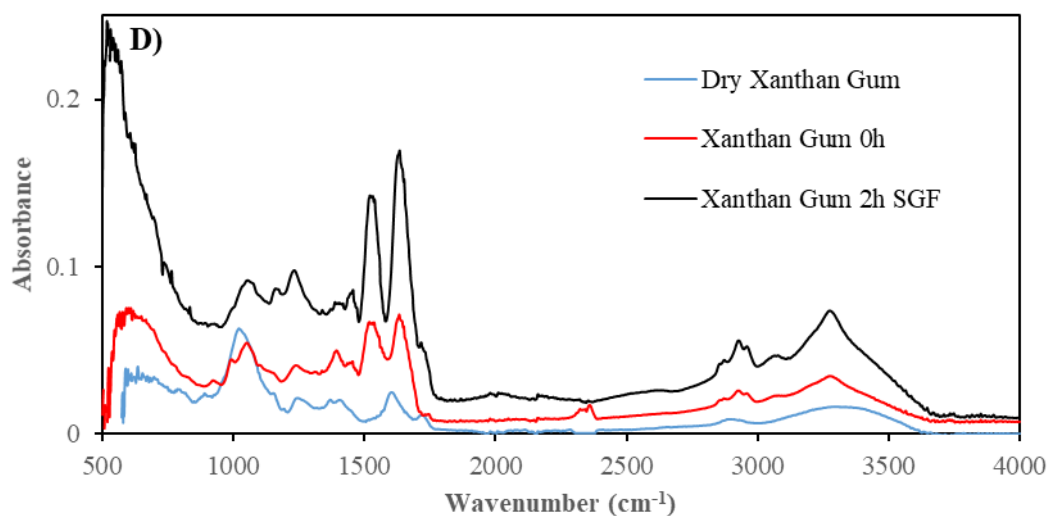


Figure 3.18. FTIR spectra of dry powders, hydrogels before SGF treatment (0 h) and hydrogels after 2 h SGF treatment: A: Control, B: Pectin, C: Gum Tragacanth, D: Xanthan Gum

3.3.1.6 Total Acidity, pH and Moisture Analysis

All hydrogels experienced an increase in their total acidity values after 2 h gastric treatment ($p < 0.05$) (Table 3.12). Prior to SGF treatment, all hydrogels had similar total acidity values. After exposure to SGF, PC hydrogels had the highest total acidity (1.32 g citric acid/100 g gel) with respect to other hydrogels ($p < 0.05$). PC hydrogels could not retard the BC release in SGF as previously explained. Therefore, WPI – PC gel polymer matrix had probably some structural defects during gastric treatment. These structural defects may have provided a more permeable environment for the gastric juice through the PC hydrogel network. Consequently, PC hydrogels had the highest total acidity at the end of the gastric digestion. In addition to release profiles, total acidity measurements also had similarities with the hardness measurements of the samples after SGF treatment. XG hydrogels having the hardest gel structures after SGF treatment also had the lowest total acidity after 2 h exposure to SGF ($p < 0.05$). The firm structure of XG hydrogels probably did not allow the gastric juice to penetrate into the depths of the gel network as other

hydrogels did during the gastric treatment. C and GT hydrogels attained moderate values for both the total acidity and hardness measurements. PC hydrogels with weaker and softer gel structures, reached the highest total acidity value at the end of the gastric digestion. Thus, decrease in the gel strength could be associated with the increased total acidity of the gels.

Table 3.12 Total acidity values of hydrogels before and after gastric treatment

Hydrogels	<i>Before SGF Treatment</i> (g Citric Acid/100 g Gel)	<i>After SGF Treatment</i> (g Citric Acid/100 g Gel)
Control	0.29±0.01 ^a	1.29±0.01 ^b
Pectin	0.31±0.02 ^a	1.32±0.01 ^a
Gum Tragacanth	0.29±0.02 ^a	1.30±0.01 ^b
Xanthan Gum	0.30±0.06 ^a	1.18±0.01 ^c

*Different small letters mean values are significantly different in each column ($p < 0.05$).

Changes in the moisture contents and pH values of the hydrogels during gastric digestion was summarized in Table 3.13. Moisture contents of all hydrogels showed some increase in SGF. XG (11.88%) and GT (9.74%) hydrogels retained more moisture in their gel matrices than PC (8.85%) and C (6.36%) hydrogels ($p < 0.05$). The final moisture contents of the hydrogels cannot directly be attributed to the amount of gastric juice retained within the gel matrices since these hydrogels also contained a considerable amount of water that was added during the gel preparation (~80%). Clearly, addition of polymer to WPI increased the moisture retention capabilities of these heat induced hydrogels (Table 3.13). This was mainly achieved by more crosslinking within the hydrogel matrices with the incorporation of an additional polymer. However, addition of PC did not result in higher moisture increase with respect to C hydrogels contrary to GT and XG addition. Due to adverse

effects of acidic release medium on WPI – PC gel network, PC hydrogels could not provide a higher moisture retention than C hydrogels.

The most severe pH reductions in hydrogels were observed for C and XG hydrogels (Table 3.13). C hydrogels had final pH around 2.5 showing that there was a great degree of protonation for these samples. The pI of WPI is around 5.2 so that the protonation of C started earlier than the polymer added hydrogels (Hatami et al., 2014). At pH 1.2, a great majority of WPI structure was protonated in the absence of any low pKa possessing additional polymer. However, addition of PC and GT decreased the pH reduction of WPI hydrogels. These blended polymers remained negatively charged for longer time periods than the WPI molecules due to their lower acid dissociation constants with respect to WPI (Ozel et al., 2017). Nevertheless, XG hydrogels also having low pKa, did not experience a low pH reduction like other polysaccharide blended hydrogels and attained lower final pH values close to C hydrogels. The reason was the higher charge density of XG molecules compared to PC and GT molecules. Although XG carried some negatively charged parts within its structure at such a low pH, abundance of the negatively charged side groups of XG enhanced overall protonation in the system. These properties led to lower pH values for XG hydrogels after 2 h SGF treatment. The reverse correlation between the XG hydrogel total acidity (lowest final acidity) and the pH (highest pH drop) originated from the differences between the nature of these two measurements. pH is the measure of hydrogen ion activity in a solution whereas total acidity is the measure of total hydrogen ion concentration within a system. Therefore, a change in pH may not always induce an equivalent change in total acidity. The low total acidity of XG hydrogels was related to the amount of acidic medium in the hydrogel network while high reduction in pH was caused by the substantially protonated structure of the WPI – XG polymer matrix. Consequently, the complex and strong interactions in WPI – XG hydrogel matrix increased the gel strength in SGF and this resulted in lower gastric juice presence in the XG hydrogels leading to a lower total acidity value.

Table 3.13 Moisture increase and pH reduction ratios of hydrogels during gastric treatment

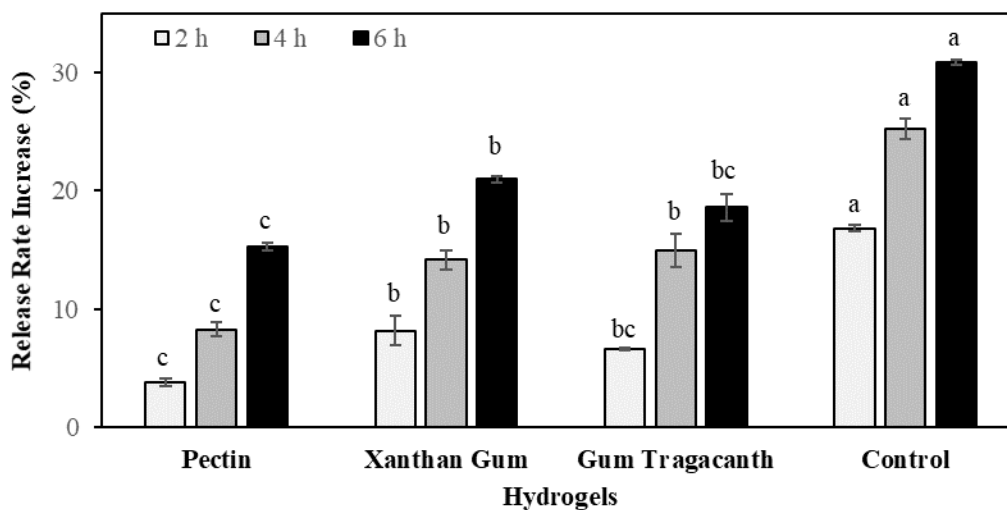
Hydrogels	Moisture Increase (%)	pH Reduction (%)
Control	6.36±0.07 ^c	58.16±0.01 ^a
Pectin	8.85±0.10 ^{bc}	49.46±0.03 ^b
Gum Tragacanth	9.74±0.03 ^{ab}	49.01±0.02 ^b
Xanthan Gum	11.88±0.08 ^a	55.09±0.03 ^a

*Different small letters mean values are significantly different in each column ($p < 0.05$).

3.3.2 Simulated Intestinal Phase

3.3.2.1 Release Profiles

Hydrogels were exposed to intestinal digestion subsequent to gastric digestion. All hydrogels had distinct release profiles in SIF. Figure 3.19 illustrates the percent increase in the release rates of the hydrogels with respect to their final release rates right after 2 h SGF treatment. During 6 h intestinal digestion, C hydrogels reached the highest increase in BC release ratio as 31 % ($p < 0.05$). XG, GT and PC hydrogels exerted lower increments in release rates 21 %, 19 % and 15 %, respectively ($p < 0.05$). These results showed that addition of polymer to WPI retarded the BC release in SIF. The pH of the SIF (6.8) was higher than both pI of the WPI and pKa of the blended polysaccharides so that the polysaccharides and WPI carried net negative charges in SIF. Under these conditions, indeed, chain relaxation mechanism due to excess charge repulsion would have been the dominant mechanism but the presence of KH_2PO_4 salt in SIF prevented this phenomenon (Argin et al., 2014). Ionic strength of the SIF medium was 0.05 M and this created a charge screening effect diminishing the effect of the electro-repulsive forces.



*Lettering was done for each time (2, 4 and 6 h), separately. Different small letters mean release rate increase values are significantly different at 2, 4 or 6 h ($p < 0.05$).

Figure 3.19. BC release rate increase (%) of hydrogels during 6 h SIF treatment with respect to their final release rates after 2 h SGF treatment

Crosslinking among the polymer chains is an important requirement for gelation and stability of the gels. In WPI hydrogels, crosslinking could take place via disulfide linkages, electrostatic interactions, hydrophobic interactions and hydrogen bonding. If polysaccharides are present in the hydrogel system, electrostatic interactions are expected to contribute to the crosslinking interactions, intensively. It was previously shown that in WPI hydrogels at alkaline pH, significant swelling was observed due to strong charge repulsion between the polypeptide chains (Oztop et al., 2010). Accordingly, at high pH conditions such as the SIF medium used in this study, high charge repulsion would loosen the gel network. However, the ionic strength of the SIF did not allow loosening of the gel networks by decreasing the repulsive forces between the ionized groups. The reduction in the repulsive forces within the hydrogel networks enhanced the proximity between the molecules and crosslinking density was increased via both hydrogen bonding and electrostatic attraction interactions in SIF (Jones & McClements, 2010). Thus, ions in the release medium enhanced the crosslinking within the hydrogel networks. Each hydrogel had different charge

densities depending on the polymer used. Therefore, they possessed different crosslinking densities which affected their BC release behaviors in SIF. C hydrogels having only WPI as the gelling agent had lower charge density with respect to polysaccharide added hydrogels. At pH 6.8, all added polysaccharides having pKa around 3.0 contributed to the abundance of the negatively charged portions of the gel networks. Consequently, C hydrogels experienced lower crosslinking within their molecular structures leading to higher BC release rate in SIF. PC, GT and XG molecules with negatively charged side groups induced more intense crosslinking and their hydrogels retarded BC release in SIF ($p < 0.05$).

Charge screening effect was not the only factor that influenced the release characteristics of the hydrogels in SIF. Hydrogen bonding interactions between the internal hydrogel polymer network surrounding the encapsulated agent and the anthocyanins of BC also played a crucial role in determining the release features of the hydrogels. Combination of WPI network with polysaccharides created more interaction sites between BC anthocyanin molecules and gel network particularly via hydrogen bonding that retarded BC release (Ferreira et al., 2009). Another factor that affected the release profiles of the hydrogels was the presence of pancreatin enzyme in SIF which caused degradation of hydrogels due to its proteolytic activity. Pancreatic activity of the enzyme eroded the hydrogels to some extent in SIF and the degree of erosion affected the release properties of the hydrogels. Rapid BC release rates of the C hydrogels could also be induced by the enzyme activity. Owing to the lower crosslinking density within the C hydrogels in SIF, pancreatin enzyme may have induced plenty of structural defects in C hydrogels by breaking the peptide bonds between the amino acids and disulfide bonds formed between the protein units during heat denaturation eventually leading to higher BC release rate. PC hydrogels demonstrated a retarded release profile in SIF despite the lower crosslinking density of PC hydrogels due to the less branched and lower charge density characteristics of the PC molecules ($p < 0.05$) (Fig. 3.19). This condition could have been prompted by the fast release behavior of PC hydrogels in gastric phase. Most of the bulk BC molecules located in the cavities within the PC hydrogel matrix were released in

SGF. Since the remaining BC was embedded in the depths of the gel matrix, PC hydrogels slowly released the rest of the BC. The remaining BC molecules after SGF treatment were probably strongly interacting with the surrounding polymer network which reinforced the PC hydrogel network through hydrogen bonding during the SIF treatment. As a consequence, GT and XG hydrogels with enhanced capacity to interact with BC anthocyanins and high crosslinking density within their gel networks could not retard BC release in SIF as much as PC hydrogels did. Nonetheless, GT and XG hydrogels retarded BC release in SIF with respect to C hydrogels ($p < 0.05$) (Fig. 3.19).

After the whole *in vitro* gastrointestinal digestion for 8 h, PC hydrogels attained the highest release rate (96%) ($p < 0.05$) due to their extensive BC release in SGF. On the other hand, C hydrogels reached a higher cumulative release rate (88%) than XG and GT hydrogels ($p < 0.05$) despite their similar retarded BC release profiles in SGF. The enhanced BC release behavior of C hydrogels in SIF led to this result. When the contributions of SGF and SIF release profiles to overall release rates were compared, it was obvious that all hydrogels achieved higher release rates in SGF. There were two fundamental reasons for the observed release trend relevant to the nature of the release media. Firstly, although SGF medium had an ionic strength of 0.034 M which was not much lower than the ionic strength of SIF (0.05 M), charge screening effect was much stronger in SIF medium. The strong acidic pH in SGF forced the carboxylic acid groups to remain in undissociated form and amino groups to be protonated residing in the hydrogels. For this reason, positive charge distribution was dominant within the hydrogel matrices in SGF so that crosslinking density throughout the hydrogel networks during SGF treatment was not as intense as in the case of SIF treatment (Wang, Chen, An, Chang, & Song, 2018). Secondly, impacts of pepsin and pancreatin enzymes were different in terms of their proteolytic activity which originated from their distinct specifications. Characteristics of β -Lg molecule of WPI regarding its susceptibility or resistance to digestive enzymes (pepsin and pancreatin) also affected the digestibility of the hydrogels (Souza et al., 2012).

3.3.2.2 Soluble Protein Contents in Digestion Media

Protein contents of the release media (SGF and SIF) were determined in order to determine the protein losses of the hydrogels during *in vitro* digestion in GIT. As shown in Table 3.14, protein contents were considerably lower in SGF with respect to SIF. One of the reasons for the lower protein loss of hydrogels in SGF was the resistance of native β -Lg which is the main globular protein of WPI to pepsin activity. Although β -Lg becomes susceptible to pepsin activity after unfolding by thermal denaturation, a small proportion of native β -Lg could still be observed even after heat induced denaturation treatment at 140 °C, 20 s and 80 °C, 30 min (Dissanayake et al., 2013; Ju & Kilara, 1998). In this case, hydrogel solutions were subjected to heat treatment at 90 °C for 30 min so that there may be some native β -Lg presence in the formed hydrogels. Conversion rate of β -Lg is accelerated with increase in pH (Hoffmann & Van Mil, 1997). At a critical pH around 7.5, β -Lg molecules undergo a conformational transformation known as *Tanford* transition during thermal denaturation (Tanford et al., 1959). This new association increases the reactivity of thiol groups and enhances the thiol – disulfide exchange reactions. These reactions accelerate native β -Lg denaturation rate (Hoffmann & Van Mil, 1997). Although both non-covalent (physical aggregation) and covalent interactions (thiol-disulfide exchange reactions) could contribute to the denaturation of native β -Lg at pH values also lower than 7.5, final pH of the hydrogel solutions were around 6.5, therefore thiol mediated reactions were not extremely enhanced in this case. These factors may have led to a slower native β -Lg denaturation rate which would end up with presence of small amount of native β -Lg in the hydrogels. Other than the remnants of native β -Lg, strong acidic condition of SGF also contributed to the low protein loss of the hydrogels during gastric digestion. Suppression of the ionizable groups within the hydrogel matrices created more compact gel structures which hindered the penetration of pepsin enzyme and reduced the pepsin activity. Comparison of the hydrogel types in SGF revealed that presence of polysaccharide in the WPI hydrogel matrix could not reduce the protein loss of the hydrogels in SGF

(Table 3.14). This result indicated that the interactions between proteins without any intervention by another polymer provided a better protection for proteins from getting hydrolyzed by pepsin SGF. Yang et al. (2015) reported that addition of hsian-tsaio gum to soy protein based films during film preparation by heating at 80 °C, 30 min, weakened the interactions among the hydrophobic amino acid residues of soy protein isolate because of the presence of bulk hydrophilic part in hsian-tsaio gum (Yang et al., 2015). A higher protein loss observed for GT hydrogels in SGF (2.21 mg BSA/mL) ($p < 0.05$) was also related to the decrease in the interactions between the proteins in the gel network. Moreover, water soluble parts of the GT molecules contributed to the liquid character of the GT hydrogels which also increased the protein loss of these hydrogels during gastric treatment (Balaghi et al., 2010). PC hydrogels also lost high protein similar to GT hydrogels. PC hydrogels were the only samples that attained faster release rate than C hydrogels mainly because of the weakening of the continuous WPI gel network. As a result of this weakened hydrogel structure, possibility of pepsin enzyme to reach the cleavage sites of the proteins was increased. XG addition also reduced interactions between proteins and caused a relatively higher protein loss from its hydrogels with respect to C hydrogels ($p < 0.05$). Nonetheless, XG hydrogels lost lower amount of protein in SGF with respect to other polymer blended hydrogels ($p < 0.05$). This was due to the intense interactions between the WPI and XG molecules. These interactions provided a firmer gel structure for XG hydrogels compared to PC and GT hydrogels. Therefore, penetration of pepsin into the XG hydrogel structure was retarded despite the diminished degree of interactions between the proteins. Under the extreme acidic conditions of SGF where crosslinking between the polymers and proteins were minimized, disulfide, hydrogen and hydrophobic interactions among the protein molecules restrained pepsin activity. In the absence of any polymer that would constitute polymer – protein interactions and expose more protein cleavage sites to pepsin for hydrolysis, C hydrogels lost the lowest amount of protein from their matrices in SGF ($p < 0.05$).

Table 3.14 Soluble protein contents of the release media after gastric digestion (SGF 2 h) and overall gastrointestinal digestion (SIF 8 h) caused by the protein losses of respective hydrogels.

Hydrogels	Protein Content in SGF (2 h) (mg BSA/mL)	Protein Content in SIF (8 h) (mg BSA/mL)
Control	1.40±0.04 ^c	4.72±0.06 ^b
Pectin	2.23±0.05 ^a	4.91±0.03 ^b
Gum Tragacanth	2.21±0.03 ^a	5.31±0.09 ^a
Xanthan Gum	1.73±0.06 ^b	4.45±0.16 ^c

*Different small letters mean values are significantly different in each column ($p < 0.05$).

After 2 h gastric digestion and subsequent 6 h intestinal digestion (8 h gastrointestinal digestion), SIF contained higher protein contents for all hydrogels with respect to protein contents in SGF. Clearly, pancreatic activity was more effective than pepsin activity on hydrogels. Takagi et al. (2003) claimed that β -Lg was more labile in pancreatin containing SIF than pepsin containing SGF. After preheating (100 °C, 5 min) of β -Lg solution, β -Lg exerted stability in SGF but it was easily digested in SIF (Takagi et al., 2003). In addition, *in vitro* digestibility studies of bovine milk whey protein demonstrated that β -Lg could be hydrolyzed by pancreatin both in native and heat denatured form (Kitabatake & Kinekawa, 1998). Pancreatin has a specific proteolytic activity mainly due to the presence of trypsin in its content. Trypsin can hydrolyze peptide bonds with distinct specificities. Trypsin action is mainly focused on the peptide links involving the carboxylic groups of arginine and lysine (Beaulieu et al., 2002). Amino acid composition analysis of β -Lg revealed a considerably high proportion of lysine and arginine (Stein & Moore, 1949). Although all hydrogels experienced high protein degradation in SIF, the most severe protein loss was observed for GT hydrogels ($p < 0.05$). As happened in gastric phase, liquid character of GT enabled pancreatin enzyme to reach proteins interacting with GT molecules in these hydrogels during SIF treatment. The outcome

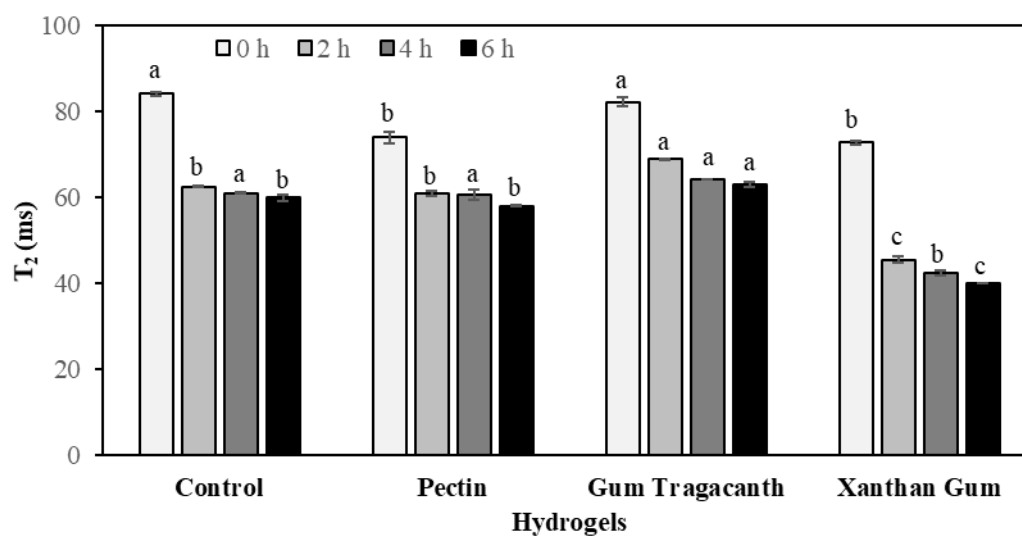
was the loss of more protein from the GT hydrogels (Table 3.14). XG hydrogels retarded the protein loss with respect to other hydrogels ($p < 0.05$). Since the crosslinking mechanism was more pronounced in SIF, XG molecules promoted denser polymer – protein interactions resulting in lower protein degradation within the hydrogels. After SGF treatment, a glassy layer around XG hydrogels was observed. Helical structural conformation of XG molecules which was formed via interactions of its trisaccharide side chains with the cellulosic backbone in acidic conditions induced such an observation (Saldamli, 1998). This rigid surface probably maintained its presence for some time during SIF treatment and reduced the penetration of pancreatin through the XG hydrogel. On the other hand, protein loss values of C and PC hydrogels in SIF were at intermediate levels. In intestinal conditions, C hydrogels could not prevent protein degradation due to lack of enhanced crosslinking interactions in the absence of an additional polymer. PC hydrogels could not also reduce the protein loss with respect to C hydrogels. Structural characteristics and molecular conformations of PC molecules could not provide a sufficient crosslinking density within the WPI gel matrix. As a result, only XG blended hydrogels were able to reduce the rate of protein loss in SIF with respect to C hydrogels ($p < 0.05$).

3.3.2.3 NMR Relaxometry Analysis

When SGF treated hydrogels were placed in SIF for subsequent digestion, T_2 values decreased as shown in Figure 3.20 and remained lower relative to their SGF correspondents throughout the intestinal digestion ($p < 0.05$). The sudden reduction of T_2 's could be attributed to the nature of the SIF medium. Contrary to high hydrogen ion concentration in acidic SGF that triggered longer spin-spin relaxation times, SIF with a pH around 6.8 had lower overall hydrogen ion concentration (Oztop et al., 2010). Additionally, hydrogels lost considerable amounts of BC in SGF so that the lower BC content of hydrogels in SIF also induced shorter T_2 profiles. At the end of the overall gastrointestinal digestion (8 h) (2 h gastric phase and 6 h

intestinal phase) GT hydrogels attained the longest T_2 ($p < 0.05$) (Fig. 3.20). Retarded release profile of GT hydrogels in SIF was one of the reasons for this longer T_2 . In addition, liquid character of GT molecules helped GT hydrogels compensate the lost BC content with the absorption of release medium into the hydrogel matrix. The absorbed SIF also allowed pancreatic activity to increase by reaching the interior cleavage sites within the GT hydrogel which increased the protein loss of GT hydrogels in SIF as previously explained (Table 3.14). However, XG hydrogels with a retarded release profile in SIF attained the shortest T_2 after SIF treatment ($p < 0.05$). This T_2 profile of XG claimed that the lost amount of BC could not be equilibrated by the absorption of release medium into the XG hydrogels. Highly cross-linked gel network and relatively harder outer surface of the XG hydrogels did not permit an adequate amount of SIF penetration into the hydrogel network. This resulted in shorter T_2 for XG hydrogels after the overall gastrointestinal digestion.

Although C hydrogels attained the fastest BC release rate in SIF, they apparently compensated BC loss to some level by absorbing a certain amount of SIF. In this way, the amount of liquid residing within the C hydrogel was balanced. Low crosslinking density of C hydrogels in intestinal conditions increased the penetration of SIF into the hydrogel matrix. Therefore, T_2 of C hydrogels did not experience a severe decrease during SIF treatment, contrary to XG hydrogels. Because of the limited BC release and absorption of SIF of PC hydrogels, T_2 of PC hydrogels remained at an intermediate level between GT and XG hydrogels.



*Lettering was done for each time (0, 2, 1, 4 and 6 h), separately. Different small letters mean T_2 values are significantly different at each time ($p < 0.05$).

Figure 3.20. T_2 profiles of hydrogels in SIF (0 h: T_2 after SGF digestion, 6 h: T_2 after the 6 h SIF digestion subsequent to SGF digestion)

3.3.2.4 FTIR Analysis

FTIR analysis was performed in order to understand the physicochemical changes that took place within the hydrogels during SIF treatment. For this purpose, FTIR spectra of hydrogels that were subjected to 2 h gastric digestion and complete 8 h gastrointestinal digestion (2 h SGF then 6 h SIF treatment) were compared (Fig. 3.21). Generally, absorption bands of SIF treated samples that were previously exposed to SGF showed increments with respect to the bands obtained after only SGF treatment. A couple of new absorption peaks were also detected for the hydrogels after SIF treatment. Despite some similar patterns and identical positions of the peaks at specific wavenumbers, each hydrogel possessed distinct absorption band features.

Intestinal digestion following the gastric digestion caused an increase in the amide band intensities of all hydrogels indicating the effect of pancreatic activity during SIF treatment (Fig. 3.21). The spectral intensity increase in the amide I regions was

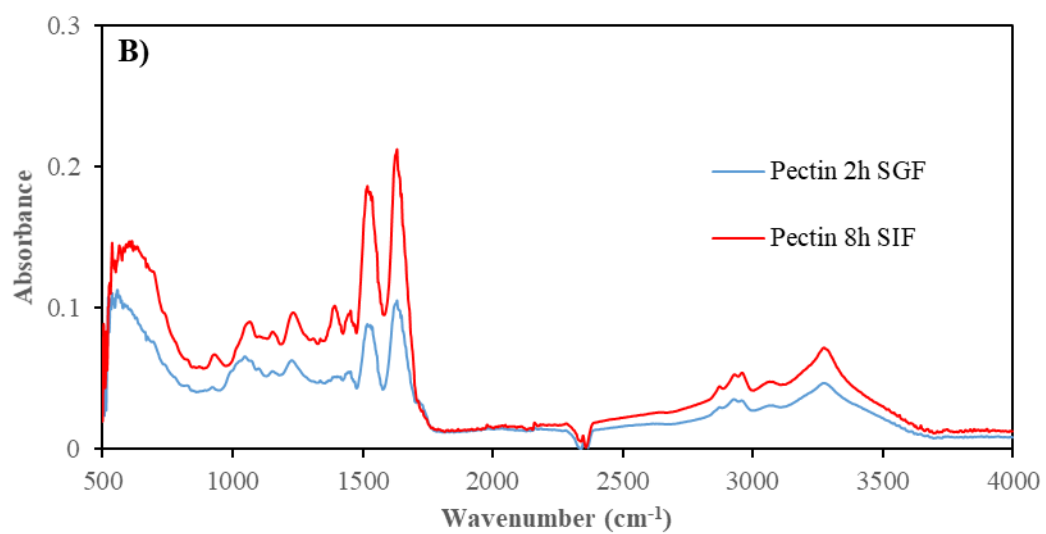
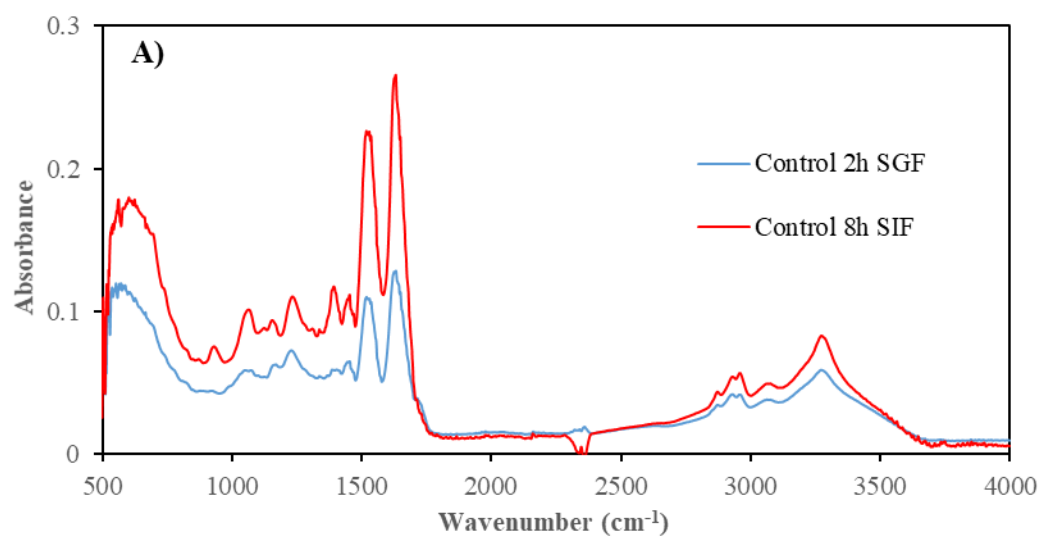
related to the final structures of proteins in freeze-dried hydrogels. Changes in the secondary structure geometry of the proteins were induced by the increase in the structural mobility of the proteins during intestinal digestion. These changes were also prompted by the degradation of the protein parts of the hydrogels. N – H groups of the peptide bonds present in the unfolded polypeptides formed hydrogen bonds with the aqueous solvent increasing the protein dissolution in SIF treatment (Dong et al., 1996). These factors increased the vibrations of amide I band. The higher amide I spectral intensity was also the result of the increased number of free amino groups formed due to the hydrolysis of the peptide linkages (Su et al., 2010). Other factors that may have contributed to the higher intensities for amide I bands of the hydrogels after SIF treatment were the protein amount and heating effect. Shape of the amide I peak around 1633 cm^{-1} representing the complete protein aggregation is also important in terms of protein secondary structure characteristics. For instance, a smooth singular peak in amide I region represents a more disordered secondary structure. Lefèvre and Subirade (1999) have reported that heating of β -Lg solutions (1 – 10 % w/w) at $85\text{ }^{\circ}\text{C}$ broadened the amide I peak located between 1600 and 1700 cm^{-1} by eliminating the other peaks present in that region. Effect of heating was enhanced by longer heating times (Lefèvre & Subirade, 1999). Amide I bands of the SIF treated hydrogels showed the features of this amide I band. One distinct peak in this region with increased peak intensity after intestinal digestion suggested a more disordered secondary structure for all hydrogels. Increase in the spectral intensities of amide II and amide III regions of the hydrogels after SIF treatment with respect to only SGF treatment were also prompted by the hydrolysis of the peptide bonds. N – H and C – N vibrations around 1519 cm^{-1} were enhanced by more intense hydrogen bonding between these groups and the aqueous release medium. Similar effect of proteolysis was also observed for amide III region. An additional peak around 1394 cm^{-1} appeared after intestinal digestion for all hydrogels. The increase in the free state vibrations of N – H and C – N groups after the breaking of long polypeptide chains probably created this peak (Ebrahimi et al., 2016). Another peak that arose for all hydrogels after SIF treatment was the peak between 930 and 933 cm^{-1} .

Skeleton C – C vibrations were responsible for this peak (Ebrahimi et al., 2016). After SGF treatment, the intensity of C – C stretching located in the relatively longer protein molecules was probably not high enough to reveal a peak in that region. However, extensive breaking of the peptide bonds during intestinal digestion enabled C – C groups to vibrate freely leading to another peak between 930 and 933 cm^{-1} .

A rising trend for the spectral intensity of O – H bands around 3275 cm^{-1} was observed after SIF treatment of the hydrogels with respect to only SGF treated samples, except for XG hydrogels. Formation of intermolecular hydrogen bonding with the carbonyl groups of the peptide linkages contributed to the enhancement of this band. Retention of BC in the hydrogels and the level of bound water present in the SIF treated freeze-dried hydrogels were the other factors that altered the intensity and shape of the O – H bands. Slightly higher O – H band intensities of C, PC and GT hydrogels suggested that these hydrogels formed more hydrogen bonds with the surrounding aqueous release medium during intestinal digestion (Fig. 3.21A – C). As FTIR spectroscopy analysis revealed, these hydrogels had higher amounts of strongly bound water in their structures after the gastrointestinal digestion. Contribution of free –OH and –NH groups may have also been higher for these samples with respect to XG hydrogels. Dissolution rate of proteins from C, PC and GT hydrogels were higher than XG hydrogels in SIF proving this claim ($p < 0.05$) (Table 3.14). Apart from their higher absorbance values in O – H region, C, PC and GT hydrogels also possessed wider bands in this region compared to XG hydrogels. Broadened O – H bands of these hydrogels emerged from the increase in the number of –OH groups involved in hydrogen bonding with respect to free –OH groups (Fattahi et al., 2013). The reason for this phenomenon could be the differences between the degree of ionization of the ionizable groups of the polymers residing in the hydrogels. Intense interactions between XG molecules and WPI in SIF resulted in a lower degree of ionization throughout the XG hydrogel matrix. This may have reduced the amount of bound water in the XG hydrogels after gastrointestinal digestion. Despite the severe BC loss of C hydrogels in SIF, these hydrogels still experienced a mild increase in the intensity of the –OH band after the SIF treatment

(Fig. 3.21A). Severe BC loss from the C hydrogel matrices clearly decreased the hydrogen bonding interactions but these interactions were compensated within the hydrogel after the intestinal digestion so that an increase in the –OH band could be observed. Probably, hydrogen bonding intensity of the C gel matrix was balanced by the enhanced hydrogen bonding interactions between the gel matrix and the aqueous release medium. Thus, C hydrogels had a high final level of bound water at the end of the SIF treatment and the effect of BC loss was compensated. GT hydrogels experienced a lower BC release rate with respect to C hydrogels in SIF ($p < 0.05$). In addition to slow BC release rate, high protein loss of GT hydrogels induced enhanced hydrogen bonding interactions between the hydrogel polymer matrix and SIF which contributed to the higher intensity of –OH band of GT hydrogels (Fig. 3.21C). Similar to GT hydrogels, slow release behavior of PC hydrogels combined with the protein degradation in SIF readily ensured the spectral intensity increase in –OH band (Fig. 3.21B). Other FTIR spectra differences between XG hydrogels and the other hydrogels were in the amide bands. Despite the considerable absorbance increases in the amide bands of C, PC and GT hydrogels after SIF treatment, XG hydrogels showed subtle absorbance increases in the amide bands especially in amide II and amide III regions. These changes in the amide region of XG hydrogels verified the intense interactions between the XG molecules and the WPI protein network that decreased the hydrolysis of the proteins as previously demonstrated in Table 3.14.

Absorbance values of symmetric –CH stretching peak at 2960 cm^{-1} increased for all hydrogels except for XG hydrogels, after SIF treatment (Fig. 3.21). The change in this peak was due to the boosted degree of the disordered hydrocarbon chains during SIF treatment (Kodati & Lafleur, 1993). Dissolution of proteins taking place during SIF treatment increased the hydration of the polar groups and responsible peaks at 2960 and 3064 cm^{-1} were enhanced for C, PC and GT hydrogels (Fig. 3.21A – C). Stability of these peaks in XG hydrogels was also in agreement with the retarded protein degradation behavior of XG hydrogels during intestinal digestion with respect to other samples (Fig. 3.21D).



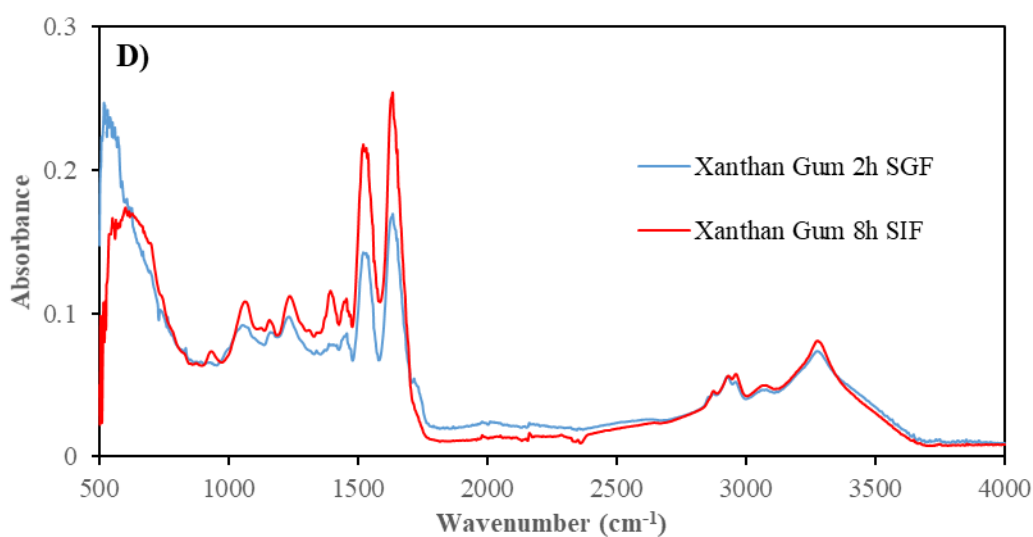
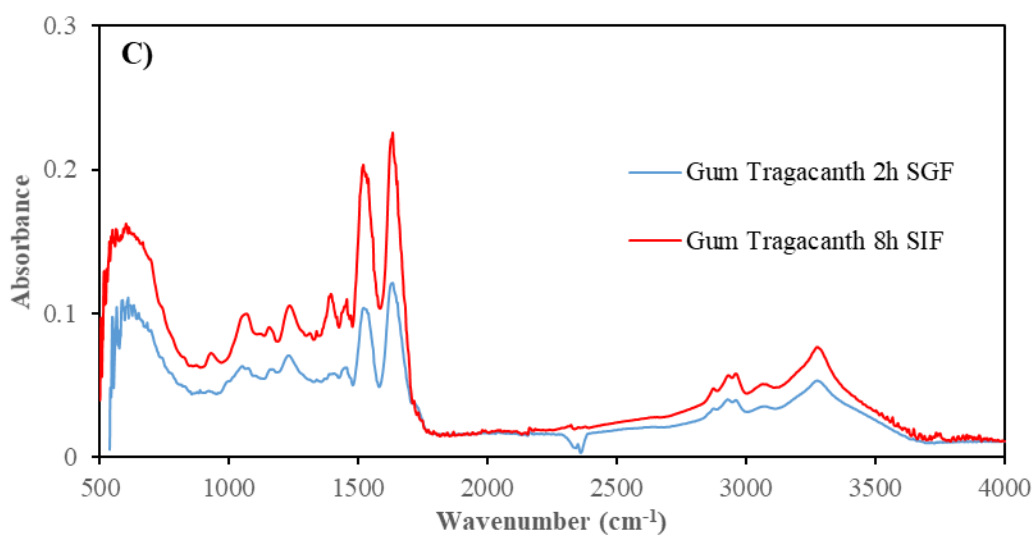
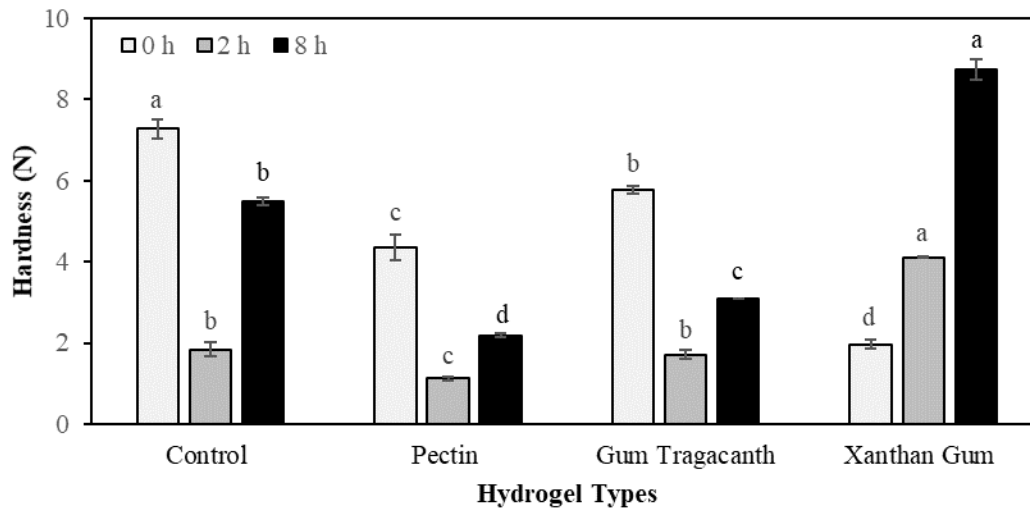


Figure 3.21. FTIR spectra of hydrogels after 2 h SGF digestion (2 h SGF) and 8 h gastrointestinal digestion (2 h SGF + 6 h SIF treatment) (8 h SIF): A: Control, B: Pectin, C: Gum Tragacanth, D: Xanthan Gum

3.3.2.5 Hardness Analysis

Hardness values of hydrogels were demonstrated in Figure 3.22. All hydrogels experienced an increase in their hardness values in SIF treatment with respect to their

hardness values after SGF treatment ($p < 0.05$). Ionic nature of SIF made intense crosslinking interactions possible within the hydrogels in contrast to SGF which contributed to the strengthening of the hydrogels in SIF (Jones & McClements, 2010). Hardening of the hydrogels during SIF treatment could not be prevented by the high protein degradation. At the end of the 8 h gastrointestinal digestion, XG hydrogels attained the hardest gel structures (8.73 N) ($p < 0.05$) (Fig. 3.22). The weakest hydrogel structure after gastrointestinal digestion was observed for PC hydrogels (2.19 N) ($p < 0.05$). There was a negative correlation between the final hardness values of the hydrogels and their respective cumulative release rates during gastrointestinal treatment. XG hydrogels with the lowest cumulative release rate (73.43 %) had the hardest gel structure whereas PC hydrogels with the highest cumulative release rate (95 %) had the weakest gel structure at the end of the *in vitro* GIT digestion ($p < 0.05$). Therefore, it can be concluded that higher gel strength retarded the BC release during gastrointestinal digestion. In addition to these findings, XG hydrogels also followed a different hardness trend during the whole digestion experiment with respect to other hydrogels. Hardness of XG hydrogels increased continuously in gastrointestinal digestion whereas all other hydrogels had softer gel structures after gastric digestion ($p < 0.05$) (Fig. 3.22). Distinct hardness profile of XG hydrogels originated from the molecular and charge characteristics of XG molecules. Enhanced crosslinking between the XG molecules and WPI, particularly in SIF, resulted in such hardness profile for XG hydrogels during gastrointestinal digestion experiments. Increasing hardness trend of XG hydrogels was also supported by the shortest T_2 ($p < 0.05$), stable $-OH$ band characteristics and the lowest protein loss ($p < 0.05$) results during SIF treatment.



*Lettering was done for each time (0, 2 and 8 h), separately. Different small letters mean hardness values are significantly different at 0, 2 or 8 h ($p < 0.05$).

Figure 3.22. Hardness profiles of hydrogels in gastrointestinal digestion: 0 h: Before any treatment, 2 h: After SGF treatment, 8 h: After gastrointestinal digestion (2 h SGF + 6 h SIF)

3.3.2.6 Release Trend in SIF

Release trends of the previously SGF treated hydrogels during 6 h SIF treatment were estimated as shown in Figure 3.23. Release mechanisms of protein based delivery systems depend on the nature and amount of the encapsulated agent, protein composition, type and composition of the any other blended polymer, release media and the geometry of the delivery tool. Four mechanisms, namely diffusion, swelling – shrinkage, erosion and fragmentation mainly govern the release phenomenon (Fathi et al., 2018). In this study, release data in SIF showed an irregular behavior. Additionally, substantial reductions in the hydrogel dimensions were detected after SIF digestion. Therefore, the release behaviors of the hydrogels could not also be identified by the power law model. It was clear that BC release of the hydrogels in SIF was mainly driven by the enzymatic erosion of the hydrogels in the presence of pancreatin digestive enzyme (Ozel et al., 2018). Chen and Subirade (2006) have also

stated that the mechanism of riboflavin release from whey protein – alginate microspheres in pancreatin containing SIF was the erosion of the microspheres. Additionally, they have also concluded that a fitting release model cannot be identified for this process (Chen & Subirade, 2006). The gradual size reductions of the hydrogels in SIF suggested that hydrogels experienced heterogeneous erosion which took place mainly on the hydrogel surfaces. Contrary to heterogeneous erosion, homogeneous erosion (also known as bulk erosion) do not induce a remarkable size reduction in the hydrogels and sizes of the hydrogels remain almost constant. In homogeneous erosion case, the external digestion medium would penetrate into the gel system by breaking the physical and chemical bonds so that the erosion would take place in the bulk volume of the gel (Zhang, Yang, Chow, & Wang, 2003). However, size reduction of the hydrogels in our case suggested a surface erosion mechanism. Hydrogels mostly eroded at the external boundary during SIF treatment. This proposed erosion model was also compatible with the high protein degradation of the hydrogels in SIF.

According to Figure 3.23, hydrogels did not release a considerable amount of BC except for C hydrogels, within the first hour of the SIF treatment. Primary reason for this trend was the dominant effect of charge screening which eliminated the effect of charge repulsions within the hydrogels. All polymer blended hydrogels (PC, GT and XG hydrogels) experienced higher degrees of crosslinking with respect to C hydrogels which experienced more charge repulsions within their matrices, in the beginning of the intestinal digestion. Nevertheless, pancreatic activity predominated the release behaviors of the hydrogels which induced severe erosion on the gel surfaces, starting from the second hour of the experiment (Fig. 3.23). Consequently, hydrogels exerted a burst release behavior in SIF due to the substantial increase in the degradation of hydrogel matrices (Wang et al., 2018). Direct contact of pancreatin with proteins on the hydrogel surfaces dramatically changed the initial release trends of the hydrogels in SIF (Xu & Dumont, 2015).

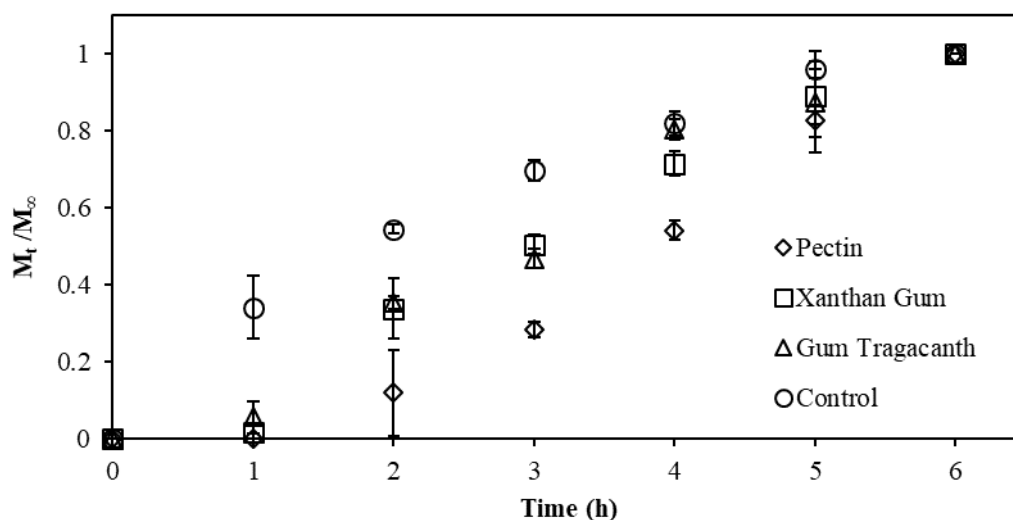


Figure 3.23. Release trends of hydrogels in SIF

3.3.2.7 Weight Loss of Hydrogels in SIF

All hydrogels had reduced weights after the intestinal treatment as shown in Table 3.15. Although XG hydrogels experienced the lowest protein loss during SIF treatment compared to other hydrogels, they showed the highest weight loss rate in SIF ($p < 0.05$) (Table 3.15). Thus, weight loss of the hydrogels in SIF was not only the result of protein degradation during intestinal treatment. Contrary to XG hydrogels, GT hydrogels lost the highest amount of protein in SIF ($p < 0.05$). However, GT hydrogels experienced a lower weight loss with respect to XG hydrogels ($p < 0.05$). Since XG and GT hydrogels showed similar BC release profiles in SIF, the difference in their weight loss values originated from their interactions with the release medium during the intestinal digestion. Transverse relaxation time and weight loss results were compared in order to understand this effect. The longest final T_2 of GT hydrogels and the shortest final T_2 of XG hydrogels after SIF treatment explained the distinct weight loss characteristics of these hydrogels. GT hydrogels were able to compensate their weight loss due to BC release and protein degradation by absorption of an adequate amount of release medium into their gel matrices.

Nevertheless, XG hydrogels could not absorb enough SIF in the intestinal phase so that they experienced a severe weight loss despite their retarded BC release profile and low protein loss features. These findings were also verified by the FTIR results. XG hydrogels had stable –OH band characteristic while other hydrogels had broadened and higher intensity –OH bands after SIF treatment, as previously explained. Presence of lower amounts of liquid in the XG hydrogels induced rare hydroxyl group vibrations within the XG hydrogels after the intestinal digestion (Ebrahimi et al., 2016). PC hydrogels having intermediate protein loss level in SIF also attained an intermediate weight loss ratio as expected. The low weight loss ratio of C hydrogels originated from the high absorption rate of surrounding release medium into the gel matrix in the absence of an additional polymer in SIF conditions (Table 3.15). Rapid BC release of C hydrogels in SIF was compensated by this way which reduced the weight loss of these hydrogels.

Table 3.15 Weight loss ratios of hydrogels in SIF

Hydrogels	<i>Weight Loss in SIF (%)</i>
Control	33.30±1.79 ^c
Pectin	38.74±1.47 ^b
Gum Tragacanth	32.00±1.12 ^c
Xanthan Gum	43.63±1.42 ^a

*Different small letters mean values are significantly different ($p < 0.05$).

3.3.2.8 Microstructure Analysis

SEM images of the hydrogels after gastric and overall gastrointestinal digestions were compared in Figure 3.24. Type of the exposed media and polymer addition had distinct effects on the hydrogel morphologies. SGF treatment affected the distribution of the aggregates formed within the hydrogels but hydrogels maintained their structurally integrated continuous matrices after the gastric digestion. After gastric phase, C hydrogels had relatively big and hexahedral shaped aggregates (Fig.

3.24A). These aggregates on the closely packed smooth surface were attributed to the sucrose crystals coming from the sucrose containing BC interacting with the whey protein network (Harnkarnsujarit & Charoenrein, 2011; Ozel et al., 2018). Previously it was reported that whey proteins acted as nuclei prompting primary heterogeneous nucleation of lactose (Sánchez-García et al., 2019). Additionally, presence of rhombohedral crystals of trehalose on the whey protein film surfaces was also reported in the literature (Pérez et al., 2016). SGF treated GT hydrogels possessed intense and smaller sized hexahedral aggregates (Fig. 3.24E). XG hydrogels had even smaller sized aggregates with greater intensity after gastric digestion (Fig. 3.24G). In accordance with their microstructural characteristics, XG hydrogels were the hardest gels after the gastric phase ($p < 0.05$). SGF treated PC hydrogels, on the other hand, demonstrated loose and heterogeneous distribution of coarse particles with irregular orientations (Fig. 3.24C). These microstructural observations of SGF treated PC hydrogels were in agreement with the weakest gel strength of these hydrogels after gastric treatment ($p < 0.05$).

SIF treatment subsequent to gastric phase created clumpy structures for all hydrogels with different extents depending on the addition and type of the polymer. Enhanced intermolecular interactions between the blended polymers and WPI which were induced by the nature of SIF were the main reasons for this observation (Fig. 3.24). In the absence of an additional polymer, C hydrogels had a milder network with prominent defects within the gel network at the end of the gastrointestinal digestion which probably caused the rapid BC release of these hydrogels during the intestinal phase (Fig. 3.24B). Impact of polymer blending to WPI hydrogels was observed in terms of presence of more distinct aggregates within the hydrogel matrices of PC, GT and XG hydrogels after SIF treatment (Fig. 3.24D, F, H). Moreover, pancreatic activity produced discontinuities within the all SIF treated hydrogel structures. Formed cavities and cracks in the gel networks were the result of the proteolytic activity of pancreatin which caused excess protein loss from the hydrogels. Size distribution of the aggregates was mostly narrowed by whey protein molecules in SIF due to the alteration in pH (Sánchez-García et al., 2019). Despite the severe

protein degradation, hardening of the hydrogels in SIF suggested that smaller size distribution of the aggregates as well as the clumpy microstructures predominated the final physical characteristics of the hydrogels.

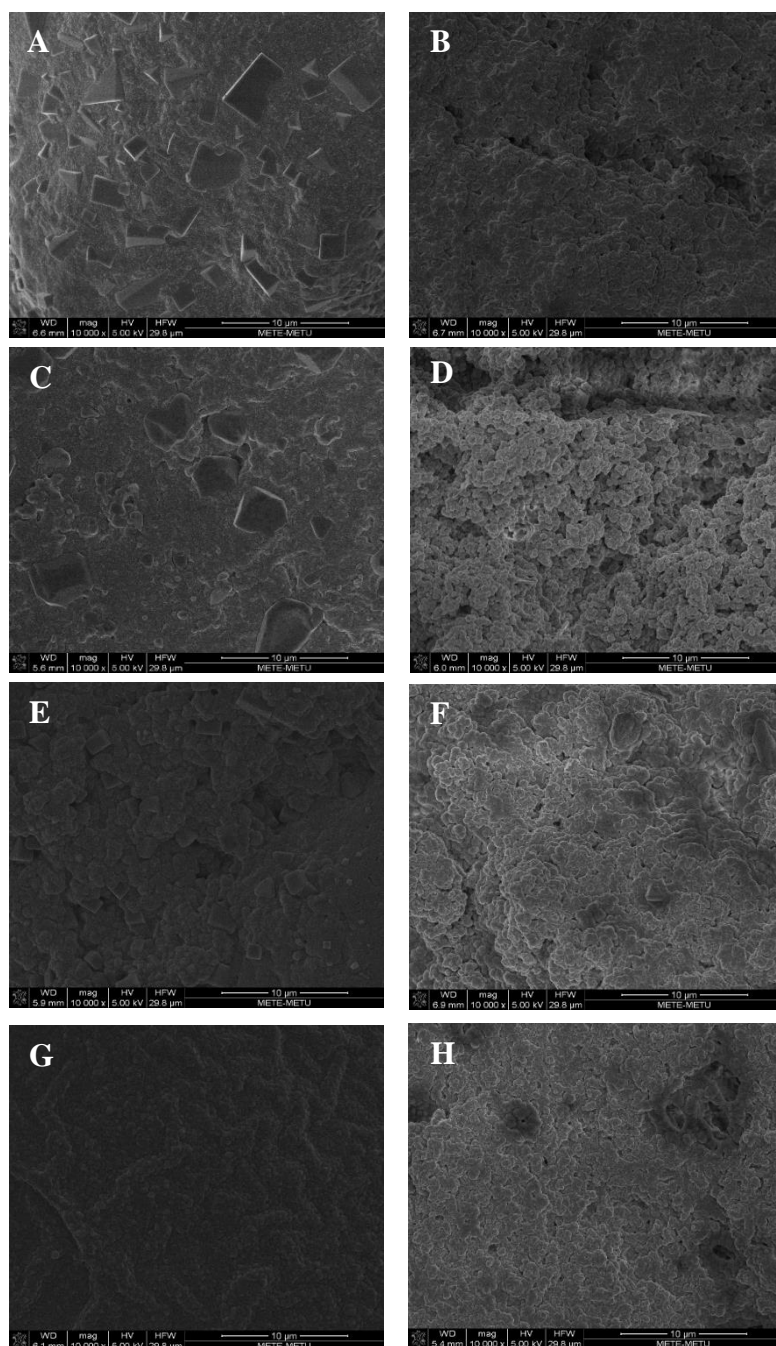


Figure 3.24. SEM images of hydrogels: A: Only SGF treated C, B: SGF + SIF treated C, C: Only SGF treated PC, D: SGF + SIF treated PC, E: Only SGF treated GT, F: SGF + SIF treated GT, G: Only SGF treated XG, H: SGF + SIF treated XG

3.4 Application of Hydrogels in Yogurt

CV hydrogels were placed in yogurt samples and stored for four weeks at 4 °C in order to determine the stability of the total phenolic contents and antioxidant capacities of the yogurt samples during this application. BC loaded hydrogel addition to plain yogurt increased both the total phenolic content and antioxidant capacity of the yogurt samples (Table 3.16 – 3.17) ($p < 0.05$). C hydrogel containing yogurt samples had the highest total phenolic content after one-week storage ($p < 0.05$). C hydrogels with no additional polysaccharide in their structures probably released a little bit more BC into the yogurt matrix within the first week. Polymer blended PC, GT and XG hydrogels imparted similar total phenolic contents in the yogurt samples after one-week storage. After four-week storage, yogurt samples containing BC loaded C, PC, GT and XG hydrogels maintained their total phenolic contents. However, the yogurt sample with no hydrogel application experienced a decrease (5.2 % loss) in its total phenolic content ($p < 0.05$) (Table 3.16). These results suggested that hydrogels continued BC release in yogurt samples during the storage period and compensated the degraded phenolic compounds.

Table 3.16 Total phenolic contents of the yogurt samples in the presence and absence of the hydrogels

Yogurt Sample	1 week (mg GAE/mL sample)	4 weeks (mg GAE/mL sample)
Plain Yogurt	0.847±0.006 ^{c, A}	0.803±0.006 ^{b, B}
Control	1.030±0.030 ^{a, A}	1.040±0.010 ^{a, A}
Pectin	0.937±0.040 ^{b, A}	0.930±0.046 ^{ab, A}
Gum Tragacanth	0.937±0.012 ^{b, A}	0.940±0.082 ^{ab, A}
Xanthan Gum	0.963±0.015 ^{b, A}	0.920±0.078 ^{ab, A}

*Different small letters mean values are significantly different in each column ($p < 0.05$). Different capital letters mean values are significantly different in each row ($p < 0.05$).

Antioxidant results showed that total phenolic and antioxidant contents were in correlation except for XG hydrogel containing samples (Table 3.17). Generally, high total phenolic content induces high antioxidant capacity (Ersus Bilek et al., 2017; Guldiken et al., 2018). C hydrogel applied yogurt sample had the highest antioxidant capacity in compliance with its highest total phenolic content at the end of the first week of the storage ($p < 0.05$). Hydrogel-free yogurt showed very little antioxidant capacity even after one-week storage. Interestingly, XG hydrogel containing yogurt also had a very low antioxidant capacity with respect to other hydrogel containing samples after one-week ($p < 0.05$). Most likely, enhanced interactions of BC anthocyanins with the XG molecules reduced their antioxidant capabilities (Ozel et al., 2017). In contrast to stable total phenolic profiles of the hydrogel blended yogurt samples, they experienced lower antioxidant capacity values after four-week storage ($p < 0.05$). Antioxidant capacity losses of C, PC, GT and XG hydrogel blended yogurt samples in three weeks were 15.2, 8.3, 7.5 and 21.5 %, respectively. Although hydrogel application to yogurt maintained most of the imparted antioxidant capacity, storage conditions were more detrimental for the antioxidant content. Moreover, plain yogurt sample lost its antioxidant capacity completely after four-week storage (Table 3.17).

Table 3.17 Antioxidant capacity of the yogurt samples in the presence and absence of the hydrogels

Yogurt Sample	1 week (mg Trolox/mL sample)	4 weeks (mg Trolox/mL sample)
Plain Yogurt	0.024±0.001 ^c	-
Control	0.541±0.002 ^{a, A}	0.459±0.003 ^{a, B}
Pectin	0.483±0.003 ^{c, A}	0.443±0.024 ^{a, B}
Gum Tragacanth	0.508±0.013 ^{b, A}	0.470±0.010 ^{a, B}
Xanthan Gum	0.079±0.010 ^{d, A}	0.062±0.007 ^{b, A}

*Different small letters mean values are significantly different in each column ($p < 0.05$). Different capital letters mean values are significantly different in each row ($p < 0.05$).

Total phenolic content of BC is composed of flavonoids and phenolic acids (Ersus Bilek et al., 2017). Phenolic acids *e.g.* chlorogenic acid constitute the majority of the BC phenolics (FronD et al., 2019). There is also a considerable anthocyanin presence in BC which contributes to the total phenolic content (up to 40 – 50%) (Kirca et al., 2006). Both chlorogenic acid and cyanidin-3-xylosyl-galactoside (main anthocyanin in BC) have antioxidant properties (Chen et al., 2020; FronD et al., 2019). Since chlorogenic acid is the most abundant antioxidant compound in BC, chlorogenic acid is mainly responsible for the antioxidant capacity in BC (FronD et al., 2019). Therefore, total phenolic content and antioxidant capacity of the hydrogel applied yogurt samples depended on the degradation stability of these compounds during storage.

The main factors influencing the stability of antioxidant capacity in food samples during storage are temperature, ingredients of the food material *e.g.* water, fat and dietary fiber contents, pH, oxygen, light, water and microbial activities (Ścibisz et al., 2019). Acylated anthocyanins are more stable in storage conditions than the non-acylated ones (Algarra et al., 2014). BC anthocyanins are mostly in acylated form giving them more stability against environmental conditions (Türkyilmaz & Özkan, 2012). Hydrogel containing samples experienced some antioxidant capacity loss after the four-week storage. One of the reasons could be the high water content of yogurt. Yogurt includes around 88 % (w/w) water which would induce hydrolytic reactions for the compounds (Ścibisz et al., 2019). Since BC has been reported to preserve most of its phenolic acid content during storage at 4 °C, mostly degradation of BC anthocyanins determined the final antioxidant capacity values of the samples (Kamiloglu et al., 2015b). Majority of the BC anthocyanins are in glycoside form meaning that at least one sugar moiety is attached to the anthocyanin molecule (Kamiloglu et al., 2015a). In the presence of high amount of water, molecular mobility is increased and degradation rate of the chemical constituents may be enhanced (Akhavan Mahdavi et al., 2016). Hydrolysis of the glycoside linkages of such antioxidant molecules could be one of the main reasons for the reduced antioxidant capacity of the hydrogel containing yogurt samples during storage.

Interactions between the phenolic compounds and the compounds in yogurt *e.g.* proteins, dietary fiber, may affect the polyphenol solubility and availability (Kamiloglu et al., 2015b). In this way, antioxidant potentials of the respective compounds may have been affected. Actually, protein – anthocyanin complexation, self – association of the anthocyanin molecules, co-pigmentation of anthocyanins with other phenolics and presence of fat in the food matrix contribute to the stability of the antioxidant capacity of BC in a food product (Ścibisz et al., 2019). For instance, fat in yogurt protects especially the acylated anthocyanins from degradation. Wallace and Giusti (2008) claimed a protective role of fat content on acylated anthocyanins in yogurt via mostly inter/intra-molecular co-pigmentation and self-association reactions of anthocyanins (Wallace & Giusti, 2008). Thus, presence of 2 – 2.5 % (w/w) fat in our yogurt samples may have prevented the further degradation of the BC anthocyanins during storage. However, presence of oxygen increases the degradation rate of the anthocyanins (Ścibisz et al., 2019). Oxygen was not removed from the containers of the yogurt samples and this may have affected the antioxidant capacity of the aliquots, negatively. Moreover, lactic acid bacteria in yogurt could produce hydrogen peroxide which would accelerate the anthocyanin degradation (Jaroni & Brashears, 2000).

Protection of total phenolic content and antioxidant capacity of the food products which were blended with a high polyphenol containing material is an important subject for the food industry. Therefore, encapsulation of such phytochemicals is gaining interest. Akhavan Mahdavi et al. (2016) demonstrated that encapsulation of barberry anthocyanins by spray drying with gum Arabic – maltodextrin combination increased the storage stability of these compounds (Akhavan Mahdavi et al., 2016). Additionally, storage at refrigeration temperatures was always associated with good stability of the acylated anthocyanins (Akhavan Mahdavi et al., 2016; Kamiloglu et al., 2015a; Kirca et al., 2006). Similarly, we have encapsulated BC in WPI based hydrogels and provided controlled release of the BC into the yogurt matrix during storage at the refrigeration temperature. Hydrogel blending protected the total phenolic contents of the samples. Despite some loss, most of the antioxidant

activities were also preserved. However, blending of XG hydrogel to yogurt could not provide a high antioxidant capacity even in the early stages of the storage. Therefore, XG hydrogels were not suitable to be used for such applications. The soft initial structure of XG hydrogels and the distinct interactions between the BC anthocyanins and XG molecules may have induced this result. Consequently, C, PC and GT hydrogels successfully protected the total phenolic content and antioxidant capacity of the yogurt samples by controlled release of the encapsulated BC into the food matrix during storage.

CHAPTER 4

CONCLUSIONS AND RECOMMENDATIONS

In this study, composite whey protein hydrogels were produced by blending PC, GT and XG polysaccharides to WPI. Conventional water bath heating (CV) and infrared assisted microwave heating (MW) were implemented to produce the hydrogels. Hydrogels with no added polysaccharide were also produced (C). BC was encapsulated in these hydrogels for controlled release purposes in different release media. Before the controlled release experiments, physico-chemical characteristics of the hydrogel solutions were analyzed. C and PC hydrogel solutions had Newtonian flow behaviors whereas GT and XG hydrogel solutions exerted pseudoplastic flow character. Flow behaviors, pH, zeta potential, dielectric properties and critical gelling temperatures of the hydrogel solutions were found to be effective in the respective physico-chemical characteristics and release behaviors of the produced hydrogels.

Firstly, CV and MW hydrogels were exposed to phosphate buffer at pH 7.0 for one day. For the CV samples, polymer blending retarded the release rates. However, polymer blending to MW samples did not retard the release rates and all hydrogels released BC rapidly. NMR relaxation, texture, release modelling and SEM analyses of the hydrogels revealed the effect of polymer blending, heating type and solvent exposure on the physico-chemical properties of the hydrogels. For instance, CV hydrogels had more stable T_2 profiles than MW hydrogels. Moreover, MW hydrogels could not maintain their physical integrity in the phosphate buffer due to their soft structures. Although we have demonstrated that MW could be used to produce protein based hydrogels for controlled release applications, their physical characteristics were not suitable for the GIT experiments and food applications.

Secondly, only CV hydrogels were subjected to *in vitro* simulated gastrointestinal conditions. All hydrogels attained higher release rates in gastric phase compared to

intestinal phase. PC hydrogels released BC faster in SGF with respect to other hydrogels. Release modelling of the hydrogels in the stomach phase suggested a Fickian diffusion from the hydrogels similar to the case in the phosphate buffer release experiments. On the other hand, polymer blending retarded the release rates in SIF treatment. However, PC hydrogel attained the highest cumulative release rate at the end of the overall GIT digestion due its enhanced BC release rate in the stomach phase. C, GT and XG hydrogels had similar final release rates in simulated GIT. FTIR analysis showed that each hydrogel had distinct bonding characteristics in different release media. FTIR spectra also showed that proteolytic activity of pepsin and pancreatin produced different responses on the hydrogels. Effects of blended polysaccharides were also investigated by the FTIR experiments. It was also found that pancreatin activity was much more effective in terms of protein digestion with respect to pepsin activity. Therefore, surface erosion of the hydrogels in SIF caused a burst release from the hydrogels which could not be described by the Fickian diffusion. Gastrointestinal digestion also induced distinct textural characteristics for the different hydrogels. GIT experiments showed that all hydrogels were able to provide a controlled BC release in simulated gastrointestinal conditions to some extent.

Finally, CV hydrogels were blended into the full – fat yogurt samples for the food application of the hydrogels. Yogurt samples were stored at 4 °C for four weeks. All hydrogels provided better total phenolic contents and antioxidant activities with respect to plain yogurt with no blended hydrogel. During four-week storage, hydrogel blended yogurts preserved their total phenolic contents. All hydrogels maintained gradual BC release in yogurt and compensated the degraded phenolic compounds. Nevertheless, yogurt samples experienced some antioxidant capacity loss during storage. Nonetheless, most of the antioxidant capacity was preserved except for the XG hydrogel blended yogurt samples. XG hydrogels were not suitable for the yogurt application. These results showed that C, PC and GT hydrogels were successfully applied to yogurt samples for storage purposes.

All in all, this study demonstrated that composite whey protein hydrogels could be used for controlled release applications in phosphate buffer, *in vitro* simulated GIT conditions and food matrices such as yogurt. However, there are also some aspects that could be considered for the future studies. For instance, the static digestion model used in this study could be replaced by more realistic *in vitro* digestion models such as semi-dynamic models. These models are also able to simulate even the shaking character of the stomach phase. Removal of specific volumes of gastric juice at predetermined time intervals that simulate gastric emptying rate can also contribute to the accuracy of the experiments. Additionally, new protein-polysaccharide combinations can be tried and/or the concentration of the biopolymers used can be changed to further delay the release of BC in the gastric phase. In this way, the rate of BC delivered to the intestinal phase will be increased, resulting in a higher degree of bioavailability of this bioactive substance.

REFERENCES

- Abae, A., Mohammadian, M., & Jafari, S. M. (2017). Whey and soy protein-based hydrogels and nano-hydrogels as bioactive delivery systems. *Trends in Food Science and Technology*, 70(October), 69–81. <https://doi.org/10.1016/j.tifs.2017.10.011>
- Abbastabar, B., Azizi, M. H., Adnani, A., & Abbasi, S. (2015). Determining and modeling rheological characteristics of quince seed gum. *Food Hydrocolloids*, 43, 259–264. <https://doi.org/10.1016/j.foodhyd.2014.05.026>
- Ahmed, E. M. (2015). Hydrogel: Preparation, characterization, and applications: A review. *Journal of Advanced Research*, 6(2), 105–121. <https://doi.org/10.1016/j.jare.2013.07.006>
- Akhavan Mahdavi, S., Jafari, S. M., Assadpour, E., & Ghorbani, M. (2016). Storage stability of encapsulated barberry's anthocyanin and its application in jelly formulation. *Journal of Food Engineering*, 181, 59–66. <https://doi.org/10.1016/j.jfoodeng.2016.03.003>
- Akhtar, S., Rauf, A., Imran, M., Qamar, M., Riaz, M., & Mubarak, M. S. (2017). Black carrot (*Daucus carota* L.), dietary and health promoting perspectives of its polyphenols: A review. *Trends in Food Science and Technology*, 66, 36–47. <https://doi.org/10.1016/j.tifs.2017.05.004>
- Algarra, M., Fernandes, A., Mateus, N., de Freitas, V., Esteves da Silva, J. C. G., & Casado, J. (2014). Anthocyanin profile and antioxidant capacity of black carrots (*Daucus carota* L. ssp. *sativus* var. *atrorubens* Alef.) from Cuevas Bajas, Spain. *Journal of Food Composition and Analysis*, 33(1), 71–76. <https://doi.org/10.1016/j.jfca.2013.11.005>
- Altin, G., Gültekin-Özgiiven, M., & Ozcelik, B. (2018). Liposomal dispersion and powder systems for delivery of cocoa hull waste phenolics via Ayran (drinking yoghurt): Comparative studies on in-vitro bioaccessibility and antioxidant capacity. *Food Hydrocolloids*, 81, 364–370. <https://doi.org/10.1016/j.foodhyd.2018.02.051>
- Arab, F., Alemzadeh, I., & Maghsoudi, V. (2011). Determination of antioxidant component and activity of rice bran extract. *Scientia Iranica*, 18(6), 1402–1406. <https://doi.org/10.1016/j.scient.2011.09.014>
- Argin, S., Kofinas, P., & Lo, Y. M. (2014). The cell release kinetics and the swelling behavior of physically crosslinked xanthan-chitosan hydrogels in simulated gastrointestinal conditions. *Food Hydrocolloids*, 40, 138–144. <https://doi.org/10.1016/j.foodhyd.2014.02.018>
- Arrondo, J. L. R., Muga, A., Castresana, J., & Goni, F. M. (1993). Quantitative

- studies of the structure of proteins in solution by fourier-transform infrared spectroscopy. *Progress in Biophysics & Molecular Biology*, 59(1), 23–56.
- Arts, I. C. W., & Hollman, P. C. H. (2005). Polyphenols and disease risk in epidemiologic studies 1 – 4. *American Journal of Clinical Nutrition*, 81, 317–325.
- Aspinall, G. O., & Baillie, J. (1963). Gum tragacanth. Part I. Fractionation of the gum and the structure of tragacanthic acid. *Gum Tragacanth. Part I. Fractionation of the Gum and the Structure of Tragacanthic Acid*, 1702, 1702–1714.
- Balaghi, S., Mohammadifar, M. A., & Zargaraan, A. (2010). Physicochemical and Rheological Characterization of Gum Tragacanth Exudates from Six Species of Iranian Astragalus. *Food Biophysics*, 5(1), 59–71. <https://doi.org/https://doi.org/10.1007/s11483-009-9144-5>
- Balaghi, S., Mohammadifar, M. A., Zargaraan, A., Gavlighi, H. A., & Mohammadi, M. (2011). Compositional analysis and rheological characterization of gum tragacanth exudates from six species of Iranian Astragalus. *Food Hydrocolloids*, 25(7), 1775–1784. <https://doi.org/10.1016/j.foodhyd.2011.04.003>
- Bandekar, J. (1992). Amide modes and protein conformation. *Biochemica et Biophysica Acta*, 1120(2), 123–143. [https://doi.org/10.1016/0167-4838\(92\)90261-B](https://doi.org/10.1016/0167-4838(92)90261-B)
- Barbut, S., & Foegeding, E. A. (1993). Ca²⁺-Induced Gelation of Pre-heated Whey Protein Isolate. *Journal of Food Science*, 58(4), 867–871. <https://doi.org/10.1111/j.1365-2621.1993.tb09379.x>
- Bateman, L., Ye, A., & Singh, H. (2011). Re-formation of fibrils from hydrolysates of β -lactoglobulin fibrils during in vitro gastric digestion. *Journal of Agricultural and Food Chemistry*, 59(17), 9605–9611. <https://doi.org/10.1021/jf2020057>
- Beaulieu, L., Savoie, L., Paquin, P., & Subirade, M. (2002). Elaboration and characterization of whey protein beads by an emulsification/cold gelation process: Application for the protection of retinol. *Biomacromolecules*, 3(2), 239–248. <https://doi.org/10.1021/bm010082z>
- Belscak-Cvitanovic, A., Komes, D., Karlović, S., Djaković, S., Špoljarić, I., Mršić, G., & Ježek, D. (2015). Improving the controlled delivery formulations of caffeine in alginate hydrogel beads combined with pectin, carrageenan, chitosan and psyllium. *Food Chemistry*, 167, 378–386. <https://doi.org/10.1016/j.foodchem.2014.07.011>
- Berthomieu, C., & Hienerwadel, R. (2009). Fourier transform infrared (FTIR) spectroscopy. *Photosynthesis Research*, 101, 157–170.

<https://doi.org/10.1007/s11120-009-9439-x>

- Betz, M., & Kulozik, U. (2011a). Microencapsulation of bioactive bilberry anthocyanins by means of whey protein gels. *Procedia Food Science*, *1*, 2047–2056. <https://doi.org/10.1016/j.profoo.2011.10.006>
- Betz, M., & Kulozik, U. (2011b). Whey protein gels for the entrapment of bioactive anthocyanins from bilberry extract. *International Dairy Journal*, *21*(9), 703–710. <https://doi.org/10.1016/j.idairyj.2011.04.003>
- Betz, M., Steiner, B., Schantz, M., Oidtmann, J., Mäder, K., Richling, E., & Kulozik, U. (2012). Antioxidant capacity of bilberry extract microencapsulated in whey protein hydrogels. *Food Research International*, *47*(1), 51–57. <https://doi.org/10.1016/j.foodres.2012.01.010>
- Bi, W., Zhao, W., Li, X., Ge, W., Muhammad, Z., Wang, H., & Du, L. (2015). Study on microwave-accelerated casein protein grafted with glucose and β -cyclodextrin to improve the gel properties. *International Journal of Food Science and Technology*, *50*(6), 1429–1435. <https://doi.org/10.1111/ijfs.12794>
- Biehler, E., & Bohn, T. (2010). Methods for Assessing Aspects of Carotenoid Bioavailability. *Current Nutrition & Food Science*, *6*(1), 44–69. <https://doi.org/10.2174/157340110790909545>
- Blanco-Pascual, N., Montero, M. P., & Gómez-Guillén, M. C. (2014). Antioxidant film development from unrefined extracts of brown seaweeds *Laminaria digitata* and *Ascophyllum nodosum*. *Food Hydrocolloids*, *37*, 100–110. <https://doi.org/10.1016/j.foodhyd.2013.10.021>
- Bouayed, J., Hoffmann, L., & Bohn, T. (2011). Total phenolics, flavonoids, anthocyanins and antioxidant activity following simulated gastro-intestinal digestion and dialysis of apple varieties: Bioaccessibility and potential uptake. *Food Chemistry*, *128*(1), 14–21. <https://doi.org/10.1016/j.foodchem.2011.02.052>
- Bouyer, E., Mekhloufi, G., Rosilio, V., Grossiord, J. L., & Agnely, F. (2012). Proteins, polysaccharides, and their complexes used as stabilizers for emulsions: Alternatives to synthetic surfactants in the pharmaceutical field? *International Journal of Pharmaceutics*, *436*(1–2), 359–378. <https://doi.org/10.1016/j.ijpharm.2012.06.052>
- Braga, A. L. M., Azevedo, A., Julia Marques, M., Menossi, M., & Cunha, R. L. (2006). Interactions between soy protein isolate and xanthan in heat-induced gels: The effect of salt addition. *Food Hydrocolloids*, *20*(8), 1178–1189. <https://doi.org/10.1016/j.foodhyd.2006.01.003>
- Brand-Williams, W., Cuvelier, M. E., & Berset, C. (1995). Use of a free radical method to evaluate antioxidant activity. *LWT - Food Science and Technology*, *28*(1), 25–30. [https://doi.org/10.1016/S0023-6438\(95\)80008-5](https://doi.org/10.1016/S0023-6438(95)80008-5)

- Britten, M., & Giroux, H. J. (2001). Acid-induced gelation of whey protein polymers: Effects of pH and calcium concentration during polymerization. *Food Hydrocolloids*, 15(4–6), 609–617. [https://doi.org/10.1016/S0268-005X\(01\)00049-2](https://doi.org/10.1016/S0268-005X(01)00049-2)
- Bryant, C M, & McClements, D. J. (2000). Influence of xanthan gum on physical characteristics of heat-denatured whey protein solutions and gels. *Food Hydrocolloids*, 14(4), 383–390. [https://doi.org/10.1016/S0268-005X\(00\)00018-7](https://doi.org/10.1016/S0268-005X(00)00018-7)
- Bryant, Cory M., & McClements, D. J. (1998). Molecular basis of protein functionality with special consideration of cold-set gels derived from heat-denatured whey. *Trends in Food Science and Technology*, 9(4), 143–151. [https://doi.org/10.1016/S0924-2244\(98\)00031-4](https://doi.org/10.1016/S0924-2244(98)00031-4)
- Buffler, C. R. (1993). *Microwave Cooking and Processing*. Springer US.
- Cabrita, L., Fossen, T., & Andersen, Ø. M. (2000). Colour and stability of the six common anthocyanidin 3-glucosides in aqueous solutions. *Food Chemistry*, 68(1), 101–107. [https://doi.org/10.1016/S0308-8146\(99\)00170-3](https://doi.org/10.1016/S0308-8146(99)00170-3)
- Cai, J., Yang, J., Wang, C., Hu, Y., Lin, J., & Fan, L. (2010). Structural Characterization and Antimicrobial Activity of Chitosan (CS-40)/Nisin Complexes. *Journal of Applied Polymer Science*, 116, 3702–3707. <https://doi.org/10.1002/app.31936>
- Calay, R. K., Newborough, M., Probert, D., & Calay, P. S. (1994). Predictive equations for the dielectric properties of foods. *International Journal of Food Science & Technology*, 29(6), 699–713. <https://doi.org/10.1111/j.1365-2621.1994.tb02111.x>
- Çam, M., İçyer, N. C., & Erdoğan, F. (2014). Pomegranate peel phenolics: Microencapsulation, storage stability and potential ingredient for functional food development. *LWT - Food Science and Technology*, 55(1), 117–123. <https://doi.org/10.1016/j.lwt.2013.09.011>
- Cardoso, C., Afonso, C., Lourenço, H., Costa, S., & Nunes, M. L. (2015). Bioaccessibility assessment methodologies and their consequences for the risk-benefit evaluation of food. *Trends in Food Science and Technology*, 41(1), 5–23. <https://doi.org/10.1016/j.tifs.2014.08.008>
- Cemeroglu, B. (2010). *Gıda Analizleri* (B. Cemeroglu (ed.); 2nd ed.). Gıda Teknolojisi Dernegi Press.
- Chen, Liang, Xin, X., Feng, H., Li, S., Cao, Q., Wang, X., & Vriesekoop, F. (2020). Isolation and identification of anthocyanin component in the fruits of *Acanthopanax sessiliflorus* (Rupr. & Maxim.) seem. By means of high speed counter current chromatography and evaluation of its antioxidant activity. *Molecules*, 25(8), 5–10. <https://doi.org/10.3390/molecules25081781>

- Chen, Lingyun, & Subirade, M. (2006). Alginate-whey protein granular microspheres as oral delivery vehicles for bioactive compounds. *Biomaterials*, 27(26), 4646–4654. <https://doi.org/10.1016/j.biomaterials.2006.04.037>
- Cheng, J., Ma, Y., Li, X., Yan, T., & Cui, J. (2015). Effects of milk protein-polysaccharide interactions on the stability of cream mix model systems. *Food Hydrocolloids*, 45, 327–336. <https://doi.org/10.1016/j.foodhyd.2014.11.027>
- Cilla, A., González-Sarrías, A., Tomás-Barberán, F. A., Espín, J. C., & Barberá, R. (2009). Availability of polyphenols in fruit beverages subjected to in vitro gastrointestinal digestion and their effects on proliferation, cell-cycle and apoptosis in human colon cancer Caco-2 cells. *Food Chemistry*, 114(3), 813–820. <https://doi.org/10.1016/j.foodchem.2008.10.019>
- Crank, J. (1975). *The Mathematics of Diffusion* (2nd ed.). Oxford University Press.
- Cussler, E. L. (2009). *Diffusion: Mass transfer in fluid systems* (3rd Ed). Cambridge University Press.
- De la Fuente, M. A., Singh, H., & Hemar, Y. (2002). Recent advances in the characterisation of heat-induced aggregates and intermediates of whey proteins. *Trends in Food Science and Technology*, 13(8), 262–274. [https://doi.org/10.1016/S0924-2244\(02\)00133-4](https://doi.org/10.1016/S0924-2244(02)00133-4)
- Díaz, O., Candia, D., & Cobos, Á. (2016). Effects of ultraviolet radiation on properties of films from whey protein concentrate treated before or after film formation. *Food Hydrocolloids*, 55, 189–199. <https://doi.org/10.1016/j.foodhyd.2015.11.019>
- Dima, C., Assadpour, E., Dima, S., & Jafari, S. M. (2020). Bioavailability of nutraceuticals: Role of the food matrix, processing conditions, the gastrointestinal tract, and nanodelivery systems. *Comprehensive Reviews in Food Science and Food Safety*, 19, 954–994. <https://doi.org/10.1111/1541-4337.12547>
- Dissanayake, M., Ramchandran, L., Donkor, O. N., & Vasiljevic, T. (2013). Denaturation of whey proteins as a function of heat, pH and protein concentration. *International Dairy Journal*, 31(2), 93–99. <https://doi.org/10.1016/j.idairyj.2013.02.002>
- Dong, A., Matsuura, J., Allison, S. D., Chrisman, E., Manning, M. C., & Carpenter, J. F. (1996). Infrared and circular dichroism spectroscopic characterization of structural differences between β -lactoglobulin A and B. *Biochemistry*, 35(5), 1450–1457. <https://doi.org/10.1021/bi9518104>
- Doublier, J. L., Garnier, J., Renard, D., & Sanchez, C. (2000). Protein-polysaccharide interactions. *Current Opinion in Colloid and Interface Science*, 5, 202–214. [https://doi.org/10.1016/S1359-0294\(00\)00054-6](https://doi.org/10.1016/S1359-0294(00)00054-6)

- Doucet, D., Gauthier, S. F., & Foegeding, E. A. (2001). Rheological Characterization of a Gel Formed During Extensive Enzymatic Hydrolysis. *Journal of Food Science*, 66(5), 711–715. <https://doi.org/10.1111/j.1365-2621.2001.tb04626.x>
- Downham, A., & Collins, P. (2000). Colouring our foods in the last and next millennium. *International Journal of Food Science and Technology*, 35(1), 5–22. <https://doi.org/10.1046/j.1365-2621.2000.00373.x>
- Ebrahimi, S. E., Koocheki, A., Milani, E., & Mohebbi, M. (2016). Interactions between *Lepidium perfoliatum* seed gum - Grass pea (*Lathyrus sativus*) protein isolate in composite biodegradable film. *Food Hydrocolloids*, 54, 302–314. <https://doi.org/10.1016/j.foodhyd.2015.10.020>
- Ersus Bilek, S., Yılmaz, F. M., & Özkan, G. (2017). The effects of industrial production on black carrot concentrate quality and encapsulation of anthocyanins in whey protein hydrogels. *Food and Bioproducts Processing*, 102, 72–80. <https://doi.org/10.1016/j.fbp.2016.12.001>
- Esatbeyoglu, T., Rodríguez-Werner, M., Schlösser, A., Liehr, M., Ipharraguerre, I., Winterhalter, P., & Rimbach, G. (2016). Fractionation of Plant Bioactives from Black Carrots (*Daucus carota* subspecies *sativus* varietas *atrorubens* Alef.) by Adsorptive Membrane Chromatography and Analysis of Their Potential Anti-Diabetic Activity. *Journal of Agricultural and Food Chemistry*, 64(29), 5901–5908. <https://doi.org/10.1021/acs.jafc.6b02292>
- Fabek, H., Messerschmidt, S., Brulport, V., & Goff, H. D. (2014). The effect of invitro digestive processes on the viscosity of dietary fibres and their influence on glucose diffusion. *Food Hydrocolloids*, 35, 718–726. <https://doi.org/10.1016/j.foodhyd.2013.08.007>
- Fan, Y., Yi, J., Zhang, Y., & Yokoyama, W. (2017). Improved Chemical Stability and Antiproliferative Activities of Curcumin-Loaded Nanoparticles with a Chitosan Chlorogenic Acid Conjugate. *Journal of Agricultural and Food Chemistry*, 65(49), 10812–10819. <https://doi.org/10.1021/acs.jafc.7b04451>
- Fathi, M., Donsi, F., & McClements, D. J. (2018). Protein-Based Delivery Systems for the Nanoencapsulation of Food Ingredients. *Comprehensive Reviews in Food Science and Food Safety*, 17(4), 920–936. <https://doi.org/10.1111/1541-4337.12360>
- Fattahi, A., Petrini, P., Munarin, F., Shokoohinia, Y., Golozar, M. A., Varshosaz, J., & Tanzi, M. C. (2013). Polysaccharides derived from tragacanth as biocompatible polymers and Gels. *Journal of Applied Polymer Science*, 129(4), 2092–2102. <https://doi.org/10.1002/app.38931>
- Ferreira, D. S., Faria, A. F., Grosso, C. R. F., & Mercadante, A. Z. (2009). Encapsulation of Blackberry Anthocyanins by Thermal Gelation of Curdlan. *Journal of the Brazilian Chemical Society*, 20(10), 1908–1915.

- Fronđ, A. D., Iuhas, C. I., Stirbu, I., Leopold, L., Socaci, S., Andreea, S., Ayvaz, H., Andreea, S., Mihai, S., Diaconeasa, Z., & Carmen, S. (2019). Phytochemical characterization of five edible purple-reddish vegetables: Anthocyanins, flavonoids, and phenolic acid derivatives. *Molecules*, 24(8). <https://doi.org/10.3390/molecules24081536>
- Fuchsman, C. H. (1980). *Peat, Industrial Chemistry and Technology* (1st ed.). ACADEMIC PRESS LTD-ELSEVIER SCIENCE LTD.
- García-Ochoa, F., Santos, V. E., Casas, J. A., & Gómez, E. (2000). Xanthan gum: Production, recovery, and properties. *Biotechnology Advances*, 18(7), 549–579. [https://doi.org/10.1016/S0734-9750\(00\)00050-1](https://doi.org/10.1016/S0734-9750(00)00050-1)
- Garti, N., & Reichman, D. (1993). Hydrocolloids as Food Emulsifiers and Stabilizers. *Food Structure*, 12(4), 411–426. <http://digitalcommons.usu.edu/foodmicrostructurehttp://digitalcommons.usu.edu/foodmicrostructure/vol12/iss4/3>
- Gavlighi, H. A., Michalak, M., Meyer, A. S., & Mikkelsen, J. D. (2013). Enzymatic depolymerization of gum tragacanth: Bifidogenic potential of low molecular weight oligosaccharides. *Journal of Agricultural and Food Chemistry*, 61(6), 1272–1278. <https://doi.org/10.1021/jf304795f>
- Gbassi, G. K., Vandamme, T., Yolou, F. S., & Marchioni, E. (2011). In vitro effects of pH, bile salts and enzymes on the release and viability of encapsulated *Lactobacillus plantarum* strains in a gastrointestinal tract model. *International Dairy Journal*, 21(2), 97–102. <https://doi.org/10.1016/j.idairyj.2010.09.006>
- Graf, B. A., Milbury, P. E., & Blumberg, J. B. (2005). Mini-Review Flavonols, Flavones, Flavanones, and Human Health: Epidemiological Evidence. *Journal of Medicinal Food*, 8(3), 281–290.
- Gude, V. G., Patil, P., Martinez-Guerra, E., Deng, S., & Nirmalakhandan, N. (2013). Microwave energy potential for large scale biodiesel production. *Sustainable Chemical Process*, 1(5). <https://doi.org/10.1186/2043-7129-1-5>
- Guldiken, B., Gibis, M., Boyacioglu, D., Capanoglu, E., & Weiss, J. (2018). Physical and chemical stability of anthocyanin-rich black carrot extract-loaded liposomes during storage. *Food Research International*, 108(September 2017), 491–497. <https://doi.org/10.1016/j.foodres.2018.03.071>
- Gunasekaran, S., Ko, S., & Xiao, L. (2007). Use of whey proteins for encapsulation and controlled delivery applications. *Journal of Food Engineering*, 83(1), 31–40. <https://doi.org/10.1016/j.jfoodeng.2006.11.001>
- Guo, J., & Kaletunç, G. (2016). Dissolution kinetics of pH responsive alginate-pectin hydrogel particles. *Food Research International*, 88, 129–139. <https://doi.org/10.1016/j.foodres.2016.05.020>
- Guo, Q., Bellissimo, N., & Rousseau, D. (2017). Role of gel structure in controlling

- in vitro intestinal lipid digestion in whey protein emulsion gels. *Food Hydrocolloids*, 69, 264–272. <https://doi.org/10.1016/j.foodhyd.2017.01.037>
- Gustaw, W., & Mleko, S. (2007). Gelation of whey proteins by microwave heating. *Milchwissenschaft-Milk Science International*, 62(4), 439–442.
- Hajmohammadi, A., Pirouzifard, M. K., Shahedi, M., & Alizadeh, M. (2016). Enrichment of a fruit-based beverage in dietary fiber using basil seed: Effect of Carboxymethyl cellulose and Gum Tragacanth on stability. *LWT - Food Science and Technology*, 74, 84–91. <https://doi.org/10.1016/j.lwt.2016.07.033>
- Harnkarnsujarit, N., & Charoenrein, S. (2011). Effect of water activity on sugar crystallization and β -carotene stability of freeze-dried mango powder. *Journal of Food Engineering*, 105(4), 592–598. <https://doi.org/10.1016/j.jfoodeng.2011.03.026>
- Hashemi, R. H., Bradley, W. G., & Lisanti, C. J. (2010). *MRI: The basics* (3rd ed.). Lippincott Williams and Wilkins.
- Hatami, M., Nejatian, M., Mohammadifar, M. A., & Pourmand, H. (2014). Milk protein-gum tragacanth mixed gels: Effect of heat-treatment sequence. *Carbohydrate Polymers*, 101(1), 1068–1073. <https://doi.org/10.1016/j.carbpol.2013.10.004>
- Havea, P., Singh, H., & Creamer, L. K. (2001). A-Lactalbumin and Bovine Serum Albumin in a Whey Protein Concentrate Environment. *Journal of Dairy Research*, 68(2001), 483–497.
- Hébrard, G., Hoffart, V., Beyssac, E., Cardot, J. M., Alric, M., & Subirade, M. (2010). Coated whey protein/alginate microparticles as oral controlled delivery systems for probiotic yeast. *Journal of Microencapsulation*, 27(4), 292–302. <https://doi.org/10.3109/02652040903134529>
- Hoffman, M. A. M., & Van Mil, P. J. J. M. (1999). Heat-induced aggregation of β -lactoglobulin as a function of pH. *Journal of Agricultural and Food Chemistry*, 47(5), 1898–1905. <https://doi.org/10.1021/jf980886e>
- Hoffmann, M. A. M., & Van Mil, P. J. J. M. (1997). Heat-Induced Aggregation of β -Lactoglobulin: Role of the Free Thiol Group and Disulfide Bonds. *Journal of Agricultural and Food Chemistry*, 45(8), 2942–2948. <https://doi.org/10.1021/jf960789q>
- Hosseini, S. M., Hosseini, H., Mohammadifar, M. A., German, J. B., Mortazavian, A. M., Mohammadi, A., Khosravi-Darani, K., Shojaee-Aliabadi, S., & Khaksar, R. (2014). Preparation and characterization of alginate and alginate-resistant starch microparticles containing nisin. *Carbohydrate Polymers*, 103(1), 573–580. <https://doi.org/10.1016/j.carbpol.2013.12.078>
- Jaroni, D., & Brashears, M. M. (2000). Production of hydrogen peroxide by *Lactobacillus delbrueckii* subsp. *lactis* as Influenced by media used for

- propagation of cells. *Journal of Food Science*, 65(6), 1033–1036. <https://doi.org/10.1111/j.1365-2621.2000.tb09412.x>
- Je Lee, S., & Rosenberg, M. (2000). Whey Protein-based Microcapsules Prepared by Double Emulsification and Heat Gelation. *LWT - Food Science and Technology*, 33(2), 80–88. <https://doi.org/10.1006/fstl.1999.0619>
- Jones, O. G., & McClements, D. J. (2010). Biopolymer Nanoparticles from Heat-Treated Electrostatic Protein-Polysaccharide Complexes: Factors Affecting Particle Characteristics. *Journal of Food Science*, 75(2). <https://doi.org/10.1111/j.1750-3841.2009.01512.x>
- Joshi, N., Rawat, K., & Bohidar, H. B. (2018). pH and ionic strength induced complex coacervation of Pectin and Gelatin A. *Food Hydrocolloids*, 74, 132–138. <https://doi.org/10.1016/j.foodhyd.2017.08.011>
- Ju, Z. Y., & Kilara, A. (1998). Effects of Preheating on Properties of Aggregates and of Cold-Set Gels of Whey Protein Isolate. *Journal of Agricultural and Food Chemistry*, 46(9), 3604–3608. <https://doi.org/10.1021/jf980392h>
- Kalab, M., Allan-Wojtas Paula, & Miller, S. (1995). Microscopy and other imaging techniques in food structure analysis. *Trends in Food Science and Technology*, 6(June). [https://doi.org/10.1016/S0924-2244\(00\)89052-4](https://doi.org/10.1016/S0924-2244(00)89052-4)
- Kamiloglu, S., Pasli, A. A., Ozcelik, B., Van Camp, J., & Capanoglu, E. (2015a). Colour retention, anthocyanin stability and antioxidant capacity in black carrot (*Daucus carota*) jams and marmalades: Effect of processing, storage conditions and in vitro gastrointestinal digestion. *Journal of Functional Foods*, 13(October 2014), 1–10. <https://doi.org/10.1016/j.jff.2014.12.021>
- Kamiloglu, S., Pasli, A. A., Ozcelik, B., Van Camp, J., & Capanoglu, E. (2015b). Influence of different processing and storage conditions on in vitro bioaccessibility of polyphenols in black carrot jams and marmalades. *Food Chemistry*, 186, 74–82. <https://doi.org/10.1016/j.foodchem.2014.12.046>
- Kamiloglu, S., van Camp, J., & Capanoglu, E. (2017). Black carrot polyphenols: effect of processing, storage and digestion—an overview. *Phytochemistry Reviews*, 17(2), 1–17. <https://doi.org/10.1007/s11101-017-9539-8>
- Kammerer, D., Carle, R., & Schieber, A. (2003). Detection of peonidin and pelargonidin glycosides in black carrots (*Daucus carota* ssp. *sativus* var. *atrorubens* Alef.) by high-performance liquid chromatography/electrospray ionization mass spectrometry. *Rapid Communications in Mass Spectrometry*, 17(21), 2407–2412. <https://doi.org/10.1002/rcm.1212>
- Kammerer, D., Carle, R., & Schieber, A. (2004). Quantification of anthocyanins in black carrot extracts (*Daucus carota* ssp. *sativus* var. *atrorubens* Alef.) and evaluation of their color properties. *European Food Research and Technology*, 219(5), 479–486. <https://doi.org/10.1007/s00217-004-0976-4>

- Kaszuba, M., Corbett, J., Watson, F. M., & Jones, A. (2010). High-concentration zeta potential measurements using light-scattering techniques. *Philosophical Transactions of the Royal Society A: Mathematical, Physical and Engineering Sciences*, 368(1927), 4439–4451. <https://doi.org/10.1098/rsta.2010.0175>
- Kirca, Ayşegül, & Cemeroglu, B. (2003). Degradation kinetics of anthocyanins in blood orange juice and concentrate. *Food Chemistry*, 81(4), 583–587. [https://doi.org/10.1016/S0308-8146\(02\)00500-9](https://doi.org/10.1016/S0308-8146(02)00500-9)
- Kirca, Aysegul, Ozkan, M., & Cemeroglu, B. (2006). Stability of black carrot anthocyanins in various fruit juices and nectars. *Food Chemistry*, 97, 598–605. <https://doi.org/10.1016/j.foodchem.2005.05.036>
- Kirtil, E., & Oztop, M. H. (2016a). ¹H Nuclear Magnetic Resonance Relaxometry and Magnetic Resonance Imaging and Applications in Food Science and Processing. In *Food Engineering Reviews* (Vol. 8, Issue 1, pp. 1–22). <https://doi.org/10.1007/s12393-015-9118-y>
- Kirtil, E., & Oztop, M. H. (2016b). Characterization of emulsion stabilization properties of quince seed extract as a new source of hydrocolloid. *Food Research International*, 85, 84–94. <https://doi.org/10.1016/j.foodres.2016.04.019>
- Kitabatake, N., & Kinekawa, Y. I. (1998). Digestibility of Bovine Milk Whey Protein and β -Lactoglobulin in Vitro and in Vivo. *Journal of Agricultural and Food Chemistry*, 46(12), 4917–4923. <https://doi.org/10.1021/jf9710903>
- Kodati, V. R., & Lafleur, M. (1993). Comparison between orientational and conformational orders in fluid lipid bilayers. *Biophysical Journal*, 64(1), 163–170. [https://doi.org/10.1016/S0006-3495\(93\)81351-1](https://doi.org/10.1016/S0006-3495(93)81351-1)
- Krawitzky, M., Arias, E., Peiro, J. M., Negueruela, A. I., Val, J., & Oria, R. (2014). Determination of color, antioxidant activity, and phenolic profile of different fruit tissue of spanish verde doncella apple cultivar. *International Journal of Food Properties*, 17(10), 2298–2311. <https://doi.org/10.1080/10942912.2013.792829>
- Krokida, M. K., Maroulis, Z. B., & Saravacos, G. D. (2001). Rheological Properties of Fluid Fruit and Vegetable Puree Products: Compilation of Literature Data. *International Journal of Food Properties*, 4(2), 179–200. <https://doi.org/10.1081/JFP-100105186>
- Krstonošić, V., Dokić, L., Nikolić, I., & Milanović, M. (2015). Influence of xanthan gum on oil-in-water emulsion characteristics stabilized by OSA starch. *Food Hydrocolloids*, 45, 9–17. <https://doi.org/10.1016/j.foodhyd.2014.10.024>
- Kuck, L. S., & Noreña, C. P. Z. (2016). Microencapsulation of grape (*Vitis labrusca* var. Bordo) skin phenolic extract using gum Arabic, polydextrose, and partially hydrolyzed guar gum as encapsulating agents. *Food Chemistry*, 194, 569–576.

<https://doi.org/10.1016/j.foodchem.2015.08.066>

- Kumar, D. D., Mann, B., Pothuraju, R., Sharma, R., Bajaj, R., & Minaxi. (2016). Formulation and characterization of nanoencapsulated curcumin using sodium caseinate and its incorporation in ice cream. *Food and Function*, 7(1), 417–424. <https://doi.org/10.1039/c5fo00924c>
- Kyomugasho, C., Willemsen, K. L. D. D., Christiaens, S., Van Loey, A. M., & Hendrickx, M. E. (2015). Microscopic evidence for Ca²⁺ mediated pectin-pectin interactions in carrot-based suspensions. *Food Chemistry*, 188, 126–136. <https://doi.org/10.1016/j.foodchem.2015.04.135>
- Le, X. T., Rioux, L. E., & Turgeon, S. L. (2017). Formation and functional properties of protein–polysaccharide electrostatic hydrogels in comparison to protein or polysaccharide hydrogels. *Advances in Colloid and Interface Science*, 239, 127–135. <https://doi.org/10.1016/j.cis.2016.04.006>
- Lefèvre, T., & Subirade, M. (1999). Structural and interaction properties of β-lactoglobulin as studied by FTIR spectroscopy. *International Journal of Food Science and Technology*, 34(5–6), 419–428. <https://doi.org/10.1046/j.1365-2621.1999.00311.x>
- Li, J., Ould Eleya, M. M., & Gunasekaran, S. (2006). Gelation of whey protein and xanthan mixture: Effect of heating rate on rheological properties. *Food Hydrocolloids*, 20(5), 678–686. <https://doi.org/10.1016/j.foodhyd.2005.07.001>
- Li, Jessie, Ye, A., Lee, S. J., & Singh, H. (2013). Physicochemical behaviour of WPI-stabilized emulsions in in vitro gastric and intestinal conditions. *Colloids and Surfaces B: Biointerfaces*, 111, 80–87. <https://doi.org/10.1016/j.colsurfb.2013.05.034>
- Liang, L., Wu, X., Zhao, T., Zhao, J., Li, F., Zou, Y., Mao, G., & Yang, L. (2012). In vitro bioaccessibility and antioxidant activity of anthocyanins from mulberry (*Morus atropurpurea* Roxb.) following simulated gastro-intestinal digestion. *Food Research International*, 46(1), 76–82. <https://doi.org/10.1016/j.foodres.2011.11.024>
- Liang, X., Ma, C., Yan, X., Zeng, H., McClements, D. J., Liu, X., & Liu, F. (2020). Structure, rheology and functionality of whey protein emulsion gels: Effects of double cross-linking with transglutaminase and calcium ions. *Food Hydrocolloids*, 102(December 2019), 105569. <https://doi.org/10.1016/j.foodhyd.2019.105569>
- Lin, C. C., & Metters, A. T. (2006). Hydrogels in controlled release formulations: Network design and mathematical modeling. *Advanced Drug Delivery Reviews*, 58(12–13), 1379–1408. <https://doi.org/10.1016/j.addr.2006.09.004>
- Liu, H. H., & Kuo, M. I. (2011). Effect of microwave heating on the viscoelastic property and microstructure of soy protein isolate gel. *Journal of Texture*

- Studies*, 42(1), 1–9. <https://doi.org/10.1111/j.1745-4603.2010.00262.x>
- Lowry, O. H., Rosebrough, N. J., Farr, A. L., & Randall, R. J. (1951). The folin by oliver. *Journal of Biological Chemistry*, 275, 265–275. <http://linkinghub.elsevier.com/retrieve/pii/S0003269784711122>
- Lozano-Vazquez, G., Lobato-Calleros, C., Escalona-Buendia, H., Chavez, G., Alvarez-Ramirez, J., & Vernon-Carter, E. J. (2015). Effect of the weight ratio of alginate-modified tapioca starch on the physicochemical properties and release kinetics of chlorogenic acid containing beads. *Food Hydrocolloids*, 48, 301–311. <https://doi.org/10.1016/j.foodhyd.2015.02.032>
- Lu, M., Li, Z., Liang, H., Shi, M., Zhao, L., Li, W., Chen, Y., Wu, J., Wang, S., Chen, X., Yuan, Q., & Li, Y. (2015). Controlled release of anthocyanins from oxidized konjac glucomannan microspheres stabilized by chitosan oligosaccharides. *Food Hydrocolloids*, 51, 476–485. <https://doi.org/10.1016/j.foodhyd.2015.05.036>
- Manetti, C., Casciani, L., & Pescosolido, N. (2004). LF-NMR water self-diffusion and relaxation time measurements of hydrogel contact lenses interacting with artificial tears. *Journal of Biomaterials Science, Polymer Edition*, 15(3), 331–342. <https://doi.org/10.1163/156856204322977210>
- Markakis, P. (1982). Stability of Anthocyanins in Foods. In *Anthocyanins as Food Colors* (pp. 163–178). Academic Press Inc.
- McClements, D. J. (2017). Recent progress in hydrogel delivery systems for improving nutraceutical bioavailability. *Food Hydrocolloids*, 68, 238–245. <https://doi.org/10.1016/j.foodhyd.2016.05.037>
- McClements, D. J., & Gumus, C. E. (2016). Natural emulsifiers-Biosurfactants, phospholipids, biopolymers and colloidal particles: Molecular and physicochemical basis of functional performance. *Advances in Colloid and Interface Science*, 234, 3–26. <https://doi.org/10.1016/j.cis.2016.03.002>
- McDougall, G. J., Dobson, P., Smith, P., Blake, A., & Stewart, D. (2005). Assessing potential bioavailability of raspberry anthocyanins using an in vitro digestion system. *Journal of Agricultural and Food Chemistry*, 53(15), 5896–5904. <https://doi.org/10.1021/jf050131p>
- Mession, J. L., Chihi, M. L., Sok, N., & Saurel, R. (2015). Effect of globular pea proteins fractionation on their heat-induced aggregation and acid cold-set gelation. *Food Hydrocolloids*, 46, 233–243. <https://doi.org/10.1016/j.foodhyd.2014.11.025>
- Metzger, B. T., & Barnes, D. M. (2009). Polyacetylene diversity and bioactivity in orange market and locally grown colored carrots (*Daucus carota* L). *Journal of Agricultural and Food Chemistry*, 57(23), 11134–11139. <https://doi.org/10.1021/jf9025663>

- Mikac, U., Sepe, A., Kristl, J., & Baumgartner, S. (2010). A new approach combining different MRI methods to provide detailed view on swelling dynamics of xanthan tablets influencing drug release at different pH and ionic strength. *Journal of Controlled Release*, 145(3), 247–256. <https://doi.org/10.1016/j.jconrel.2010.04.018>
- Mohammadifar, M. A., Musavi, S. M., Kiumarsi, A., & Williams, P. A. (2006). Solution properties of targacanthin (water-soluble part of gum tragacanth exudate from *Astragalus gossypinus*). *International Journal of Biological Macromolecules*, 38(1), 31–39. <https://doi.org/10.1016/j.ijbiomac.2005.12.015>
- Mohnen, D. (2008). Pectin structure and biosynthesis. *Current Opinion in Plant Biology*, 11(3), 266–277. <https://doi.org/10.1016/j.pbi.2008.03.006>
- Montilla, E. C., Arzaba, M. R., Hillebrand, S., & Winterhalter, P. (2011). Anthocyanin composition of black carrot (*Daucus carota* ssp. *sativus* var. *atrorubens* Alef.) Cultivars antonina, beta sweet, deep purple, and purple haze. *Journal of Agricultural and Food Chemistry*, 59(7), 3385–3390. <https://doi.org/10.1021/jf104724k>
- Mostafavi, F. S., Kadkhodae, R., Emadzadeh, B., & Koocheki, A. (2016). Preparation and characterization of tragacanth-locust bean gum edible blend films. *Carbohydrate Polymers*, 139, 20–27. <https://doi.org/10.1016/j.carbpol.2015.11.069>
- Muhammad, D. R. A., Saputro, A. D., Rottiers, H., Van de Walle, D., & Dewettinck, K. (2018). Physicochemical properties and antioxidant activities of chocolates enriched with engineered cinnamon nanoparticles. *European Food Research and Technology*, 244(7), 1185–1202. <https://doi.org/10.1007/s00217-018-3035-2>
- Muhammadifar, M., Musavi, S., & Williams, P. A. (2007). Study of complex coacervation between β -lactoglobulin and tragacanthin (soluble part of gum tragacanth). *Milchwissenschaft-Milk Science International*, 62(4), 389–392.
- Mun, S., Kim, Y. R., & McClements, D. J. (2015). Control of β -carotene bioaccessibility using starch-based filled hydrogels. *Food Chemistry*, 173, 454–461. <https://doi.org/10.1016/j.foodchem.2014.10.053>
- Munialo, D. C., Linden, E. Van Der, Ako, K., Nieuwland, M., As, H. Van, & Jongh, H. H. J. De. (2016). Food Hydrocolloids The effect of polysaccharides on the ability of whey protein gels to either store or dissipate energy upon mechanical deformation. *Food Hydrocolloids*, 52, 707–720. <https://doi.org/10.1016/j.foodhyd.2015.08.013>
- Muyonga, J. H., Cole, C. G. B., & Duodu, K. G. (2004). Characterisation of acid soluble collagen from skins of young and adult Nile perch (*Lates niloticus*). *Food Chemistry*, 85(1), 81–89. <https://doi.org/10.1016/j.foodchem.2003.06.006>

- Naczka, M., Grant, S., Zadernowski, R., & Barre, E. (2006). Protein precipitating capacity of phenolics of wild blueberry leaves and fruits. *Food Chemistry*, 96(4), 640–647. <https://doi.org/10.1016/j.foodchem.2005.03.017>
- Naczka, Marian, & Shahidi, F. (2004). Extraction and analysis of phenolics in food. *Journal of Chromatography A*, 1054(1–2), 95–111. <https://doi.org/10.1016/j.chroma.2004.08.059>
- Nogueira, G. F., Prata, A. S., & Grosso, C. R. F. (2017). Alginate and whey protein based-multilayered particles: production, characterisation and resistance to pH, ionic strength and artificial gastric/intestinal fluid. *Journal of Microencapsulation*, 34(2), 151–161. <https://doi.org/10.1080/02652048.2017.1310945>
- Nur, M., Ramchandran, L., & Vasiljevic, T. (2016). Tragacanth as an oral peptide and protein delivery carrier: Characterization and mucoadhesion. *Carbohydrate Polymers*, 143, 223–230. <https://doi.org/10.1016/j.carbpol.2016.01.074>
- Osawa, Y. (1982). Copigmentation of Anthocyanins. In *Anthocyanins as Food Colors* (pp. 41–65). Academic Press Inc.
- Owens, C., Griffin, K., Houryieh, H., & Williams, K. (2018). Creaming and oxidative stability of fish oil-in-water emulsions stabilized by whey protein-xanthan-locust bean complexes: Impact of pH. *Food Chemistry*, 239, 314–322. <https://doi.org/10.1016/j.foodchem.2017.06.096>
- Ozel, B., Aydin, O., Grunin, L., & Oztop, M. H. (2018). Physico-Chemical Changes of Composite Whey Protein Hydrogels in Simulated Gastric Fluid Conditions [Research-article]. *Journal of Agricultural and Food Chemistry*, 66(36), 9542–9555. <https://doi.org/10.1021/acs.jafc.8b02829>
- Ozel, B., Aydin, O., & Oztop, M. H. (2020). In vitro digestion of polysaccharide including whey protein isolate hydrogels. *Carbohydrate Polymers*, 229(July 2019), 115469. <https://doi.org/10.1016/j.carbpol.2019.115469>
- Ozel, B., Cikrikci, S., Aydin, O., & Oztop, M. H. (2017). Polysaccharide blended whey protein isolate-(WPI) hydrogels: A physicochemical and controlled release study. *Food Hydrocolloids*, 71, 35–46. <https://doi.org/10.1016/j.foodhyd.2017.04.031>
- Ozel, B., Uguz, S. S., Kilercioglu, M., Grunin, L., & Oztop, M. H. (2017). Effect of different polysaccharides on swelling of composite whey protein hydrogels: A low field (LF) NMR relaxometry study. *Journal of Food Process Engineering*, 40(3), 1–9. <https://doi.org/10.1111/jfpe.12465>
- Oztop, M. H., & McCarthy, K. L. (2011). Mathematical modeling of swelling in high moisture whey protein gels. *Journal of Food Engineering*, 106(1), 53–59. <https://doi.org/10.1016/j.jfoodeng.2011.04.007>
- Oztop, M. H., McCarthy, K. L., McCarthy, M. J., & Rosenberg, M. (2012). Uptake

- of Divalent Ions (Mn +2 and Ca +2) by Heat-Set Whey Protein Gels. *Journal of Food Science*, 77(2), 68–73. <https://doi.org/10.1111/j.1750-3841.2011.02541.x>
- Oztop, M. H., McCarthy, K. L., McCarthy, M. J., & Rosenberg, M. (2014). Monitoring the effects of divalent ions (Mn+2 and Ca+2) in heat-set whey protein gels. *LWT - Food Science and Technology*, 56(1), 93–100. <https://doi.org/10.1016/j.lwt.2013.10.043>
- Oztop, M. H., Rosenberg, M., Rosenberg, Y., McCarthy, K. L., & McCarthy, M. J. (2010). Magnetic resonance imaging (MRI) and relaxation spectrum analysis as methods to investigate swelling in whey protein gels. *Journal of Food Science*, 75(8), 508–515. <https://doi.org/10.1111/j.1750-3841.2010.01788.x>
- Pakzad, H., Alemzadeh, I., & Kazemi, A. (2013). Encapsulation of peppermint oil with arabic gum-gelatin by complex coacervation method. *International Journal of Engineering, Transactions B: Applications*, 26(8), 807–814. <https://doi.org/10.5829/idosi.ije.2013.26.08b.01>
- Peanparkdee, M., & Iwamoto, S. (2020). Encapsulation for Improving in Vitro Gastrointestinal Digestion of Plant Polyphenols and Their Applications in Food Products. *Food Reviews International*, 00(00), 1–19. <https://doi.org/10.1080/87559129.2020.1733595>
- Pérez, L. M., Piccirilli, G. N., Delorenzi, N. J., & Verdini, R. A. (2016). Effect of different combinations of glycerol and/or trehalose on physical and structural properties of whey protein concentrate-based edible films. *Food Hydrocolloids*, 56, 352–359. <https://doi.org/10.1016/j.foodhyd.2015.12.037>
- Petzold, G., Gianelli, M. P., Bugueño, G., Celan, R., Pavez, C., & Orellana, P. (2014). Encapsulation of liquid smoke flavoring in ca-alginate and ca-alginate-chitosan beads. *Journal of Food Science and Technology*, 51(1), 183–190. <https://doi.org/10.1007/s13197-013-1090-z>
- Phillips, G. O., & Williams, P. A. (2009). *Handbook of Hydrocolloids* (2nd ed.). Woodhead Publishing.
- Prabakaran, S., & Damodaran, S. (1997). Thermal Unfolding of β -Lactoglobulin: Characterization of Initial Unfolding Events Responsible for Heat-Induced Aggregation. *Journal of Agricultural and Food Chemistry*, 45(11), 4303–4308. <https://doi.org/10.1021/jf970269a>
- Ralet, M.-C., Dronnet, V., Buchholt, H. C., & Thibault, J.-F. (2011). Enzymatically and chemically de-esterified lime pectins: Physico-chemical characterisation, polyelectrolyte behaviour and calcium binding properties. *Carbohydrate Research*, 336, 117–125. <https://doi.org/10.1039/9781847551672-00055>
- Rashidinejad, A., Birch, E. J., Sun-Waterhouse, D., & Everett, D. W. (2016). Effect of liposomal encapsulation on the recovery and antioxidant properties of green

- tea catechins incorporated into a hard low-fat cheese following in vitro simulated gastrointestinal digestion. *Food and Bioproducts Processing*, 100, 238–245. <https://doi.org/10.1016/j.fbp.2016.07.005>
- Raut, U., Loeffler, M. J., Vidal, R. A., & Baragiola, R. A. (2004). The OH stretch infrared band of water ice and its temperature and radiation dependence. *Lunar and Planetary Science XXXV*, 395, 2003–2004.
- Rein, M. (2005). *Copigmentation reactions and color stability of berry anthocyanins*. University of Helsinki.
- Rezvani, E., Schleining, G., & Taherian, A. R. (2012). Assessment of physical and mechanical properties of orange oil-in-water beverage emulsions using response surface methodology. *LWT - Food Science and Technology*, 48(1), 82–88. <https://doi.org/10.1016/j.lwt.2012.02.025>
- Roefs, S. P. F. M., & De Kruif, K. G. (1994). A Model for the Denaturation and Aggregation of β -Lactoglobulin. *European Journal of Biochemistry*, 226(3), 883–889. <https://doi.org/10.1111/j.1432-1033.1994.00883.x>
- Russ, N., Zielbauer, B. I., Koynov, K., & Vilgis, T. A. (2013). Influence of Nongelling Hydrocolloids on the Gelation of Agarose. *Biomacromolecules*, 14(11), 4116–4124. <https://doi.org/10.1021/bm4012776>
- Sahin, S., & Sumnu, S. G. (2006). *Physical Properties of Foods* (D. R. Heldman (ed.)). Springer Science.
- Sakiyan, O., Sumnu, G., Sahin, S., & Meda, V. (2007). Investigation of dielectric properties of different cake formulations during microwave and infrared-microwave combination baking. *Journal of Food Science*, 72(4). <https://doi.org/10.1111/j.1750-3841.2007.00325.x>
- Salami, S., Rondeau-Mouro, C., van Duynhoven, J., & Mariette, F. (2013). PFG-NMR self-diffusion in casein dispersions: Effects of probe size and protein aggregate size. *Food Hydrocolloids*, 31(2), 248–255. <https://doi.org/10.1016/j.foodhyd.2012.10.020>
- Saldamli, I. (1998). *Gida Kimyasi* (I. Saldamli (ed.)). Hacettepe University Press.
- Sánchez-García, Y. I., Gutiérrez-Méndez, N., Orozco-Mena, R. E., Ramos-Sánchez, V. H., & Leal-Ramos, M. Y. (2019). Individual and combined effect of pH and whey proteins on lactose crystallization. *Food Research International*, 116(January 2018), 455–461. <https://doi.org/10.1016/j.foodres.2018.08.061>
- Santipanichwong, R., Suphantharika, M., Weiss, J., & McClements, D. J. (2008). Core-shell biopolymer nanoparticles produced by electrostatic deposition of beet pectin onto heat-denatured β -lactoglobulin aggregates. *Journal of Food Science*, 73(6). <https://doi.org/10.1111/j.1750-3841.2008.00804.x>
- Sarkar, A., Goh, K. K. T., Singh, R. P., & Singh, H. (2009). Behaviour of an oil-in-

- water emulsion stabilized by β -lactoglobulin in an in vitro gastric model. *Food Hydrocolloids*, 23(6), 1563–1569. <https://doi.org/10.1016/j.foodhyd.2008.10.014>
- Ścibisz, I., Ziarno, M., & Mitek, M. (2019). Color stability of fruit yogurt during storage. *Journal of Food Science and Technology*, 56(4), 1997–2009. <https://doi.org/10.1007/s13197-019-03668-y>
- Shalla, A. H., Rangreez, T. A., Rizvi, M. A., Yaseen, Z., & Kabir-ud-Din. (2017). Strength and sorption capacity modulation of carboxymethylcellulose hydrogels in presence of ester-bonded gemini surfactants. *Journal of Molecular Liquids*, 238, 215–224. <https://doi.org/10.1016/j.molliq.2017.04.125>
- Shiroodi, S. G., Mohammadifar, M. A., Gorji, E. G., Ezzatpanah, H., & Zohouri, N. (2012). Influence of gum tragacanth on the physicochemical and rheological properties of kashk. *Journal of Dairy Research*, 79(1), 93–101. <https://doi.org/10.1017/S0022029911000872>
- Shiroodi, S. G., Rasco, B. A., & Lo, Y. M. (2015). Influence of Xanthan-Curdlan Hydrogel Complex on Freeze-Thaw Stability and Rheological Properties of Whey Protein Isolate Gel over Multiple Freeze-Thaw Cycle. *Journal of Food Science*, 80(7), E1498–E1505. <https://doi.org/10.1111/1750-3841.12915>
- Si, L., Zhao, Y., Huang, J., Li, S., Zhai, X., & Li, G. (2009). Calcium pectinate gel bead intended for oral protein delivery: Preparation improvement and formulation development. *Chemical and Pharmaceutical Bulletin*, 57(7), 663–667. <https://doi.org/10.1248/cpb.57.663>
- Siepmann, J., & Peppas, N. A. (2001). Modeling of drug release from delivery systems based on hydroxypropyl methylcellulose (HPMC). *Advanced Drug Delivery Reviews*, 48(2–3), 139–157. [https://doi.org/10.1016/S0169-409X\(01\)00112-0](https://doi.org/10.1016/S0169-409X(01)00112-0)
- Simi, C. K., & Abraham, T. E. (2010). Transparent xyloglucan-chitosan complex hydrogels for different applications. *Food Hydrocolloids*, 24(1), 72–80. <https://doi.org/10.1016/j.foodhyd.2009.08.007>
- Souza, F. N., Gebara, C., Ribeiro, M. C. E., Chaves, K. S., Gigante, M. L., & Grosso, C. R. F. (2012). Production and characterization of microparticles containing pectin and whey proteins. *Food Research International*, 49(1), 560–566. <https://doi.org/10.1016/j.foodres.2012.07.041>
- Sperber, B. L. H. M., Schols, H. A., Cohen Stuart, M. A., Norde, W., & Voragen, A. G. J. (2009). Influence of the overall charge and local charge density of pectin on the complex formation between pectin and β -lactoglobulin. *Food Hydrocolloids*, 23(3), 765–772. <https://doi.org/10.1016/j.foodhyd.2008.04.008>
- Sriamornsak, P. (2003). Chemistry of pectin and its pharmaceutical uses: a review. *Silpakorn University International Journal*, 3(1–2), 207–228.

<https://doi.org/10.5458/jag.54.211>

- Stein, W. H., & Moore, S. (1949). Amino acid composition of beta lactoglobulin and bovine serum albumin. *Journal of Biological Chemistry*, *178*, 79–91.
- Stintzing, F. C., & Carle, R. (2004). Functional properties of anthocyanins and betalains in plants, food, and in human nutrition. *Trends in Food Science and Technology*, *15*(1), 19–38. <https://doi.org/10.1016/j.tifs.2003.07.004>
- Su, J. F., Huang, Z., Yuan, X. Y., Wang, X. Y., & Li, M. (2010). Structure and properties of carboxymethyl cellulose/soy protein isolate blend edible films crosslinked by Maillard reactions. *Carbohydrate Polymers*, *79*(1), 145–153. <https://doi.org/10.1016/j.carbpol.2009.07.035>
- Tagliazucchi, D., Verzelloni, E., Bertolini, D., & Conte, A. (2010). In vitro bio-accessibility and antioxidant activity of grape polyphenols. *Food Chemistry*, *120*(2), 599–606. <https://doi.org/10.1016/j.foodchem.2009.10.030>
- Taherian, A. R., Lacasse, P., Bisakowski, B., Pelletier, M., Lanctôt, S., & Fustier, P. (2017). Rheological and thermogelling properties of commercial chitosan/ β -glycerophosphate: Retention of hydrogel in water, milk and UF-milk. *Food Hydrocolloids*, *63*, 635–645. <https://doi.org/10.1016/j.foodhyd.2016.09.031>
- Takagi, K., Teshima, R., Okunuki, H., & Sawada, J. (2003). Comparative Study of in Vitro Digestibility of Food Proteins and Effect of Preheating on the Digestion. *Biological & Pharmaceutical Bulletin*, *26*(7), 969–973. <https://doi.org/10.1248/bpb.26.969>
- Tanford, C., Bunville, L. G., & Nozaki, Y. (1959). The Reversible Transformation of β -Lactoglobulin at pH 7.5. *Journal of the American Chemical Society*, *81*(15), 4032–4036. <https://doi.org/10.1021/ja01524a054>
- Tao, Y., Zhang, R., Xu, W., Bai, Z., Zhou, Y., Zhao, S., Xu, Y., & Yu, D. (2016). Rheological behavior and microstructure of release-controlled hydrogels based on xanthan gum crosslinked with sodium trimetaphosphate. *Food Hydrocolloids*, *52*, 923–933. <https://doi.org/10.1016/j.foodhyd.2015.09.006>
- Thakur, N., Raigond, P., Singh, Y., Mishra, T., Singh, B., Lal, M. K., & Dutt, S. (2020). Recent updates on bioaccessibility of phytonutrients. *Trends in Food Science and Technology*, *97*(January), 366–380. <https://doi.org/10.1016/j.tifs.2020.01.019>
- Tonyali, B., Cikrikci, S., & Oztop, M. H. (2018). Physicochemical and microstructural characterization of gum tragacanth added whey protein based films. *Food Research International*, *105*(June 2017), 1–9. <https://doi.org/10.1016/j.foodres.2017.10.071>
- Turabi, E., Sumnu, G., & Sahin, S. (2010). Quantitative analysis of macro and micro-structure of gluten-free rice cakes containing different types of gums baked in different ovens. *Food Hydrocolloids*, *24*(8), 755–762.

<https://doi.org/10.1016/j.foodhyd.2010.04.001>

- Turgeon, S. L., & Beaulieu, M. (2001). Improvement and modification of whey protein gel texture using polysaccharides. *Food Hydrocolloids*, *15*(4–6), 583–591. [https://doi.org/10.1016/S0268-005X\(01\)00064-9](https://doi.org/10.1016/S0268-005X(01)00064-9)
- Türkyilmaz, M., & Özkan, M. (2012). Kinetics of anthocyanin degradation and polymeric colour formation in black carrot juice concentrates during storage. *International Journal of Food Science and Technology*, *47*(11), 2273–2281. <https://doi.org/10.1111/j.1365-2621.2012.03098.x>
- Ullah, F., Othman, M. B. H., Javed, F., Ahmad, Z., & Akil, H. M. (2015). Classification, processing and application of hydrogels: A review. *Materials Science and Engineering C*, *57*, 414–433. <https://doi.org/10.1016/j.msec.2015.07.053>
- Vantaraki, C. (2019). *Counter action of urea-induced protein denaturation by Trimethylamine N-oxide*. Uppsala University.
- Ventura, I., & Bianco-Peled, H. (2015). Small-angle X-ray scattering study on pectin-chitosan mixed solutions and thermoreversible gels. *Carbohydrate Polymers*, *123*, 122–129. <https://doi.org/10.1016/j.carbpol.2015.01.025>
- Verheul, M., Roefs, S. P. F. M., & De Kruif, K. G. (1998). Kinetics of Heat-Induced Aggregation of β Lactoglobulin. *Journal of Agricultural and Food Chemistry*, *46*(3), 896–903. <https://doi.org/10.1021/jf970751t>
- Vernon-Parry, K. D. (2000). Scanning Electron Microscopy : an Introduction. *III-Vs Review*, *13*(4), 40–44. [https://doi.org/10.1016/S0961-1290\(00\)80006-X](https://doi.org/10.1016/S0961-1290(00)80006-X)
- Villanueva-Carvajal, A., Dominguez-Lopez, A., Bernal-Martínez, L. R., & Díaz-Bandera, D. (2013). Hibiscus sabdariffa L. confesctionery gels, in vitro digestion, antioxidant activity and phenolic compounds quantification: A nutraceutical application. *International Journal of Food Science and Technology*, *48*(12), 2659–2667. <https://doi.org/10.1111/ijfs.12262>
- Wallace, T. C., & Giusti, M. M. (2008). Determination of color, pigment, and phenolic stability in yogurt systems colored with nonacylated anthocyanins from *Berberis boliviana* L. as compared to other natural/synthetic colorants. *Journal of Food Science*, *73*(4). <https://doi.org/10.1111/j.1750-3841.2008.00706.x>
- Wang, H., Gao, X. D., Zhou, G. C., Cai, L., & Yao, W. B. (2008). In vitro and in vivo antioxidant activity of aqueous extract from *Choerospondias axillaris* fruit. *Food Chemistry*, *106*(3), 888–895. <https://doi.org/10.1016/j.foodchem.2007.05.068>
- Wang, L., Liu, H. M., Xie, A. J., Wang, X. De, Zhu, C. Y., & Qin, G. Y. (2018). Chinese quince (*Chaenomeles sinensis*) seed gum: Structural characterization. *Food Hydrocolloids*, *75*, 237–245.

<https://doi.org/10.1016/j.foodhyd.2017.08.001>

- Wang, Y. W., Chen, L. Y., An, F. P., Chang, M. Q., & Song, H. B. (2018). A novel polysaccharide gel bead enabled oral enzyme delivery with sustained release in small intestine. *Food Hydrocolloids*, 84(May), 68–74. <https://doi.org/10.1016/j.foodhyd.2018.05.039>
- Wichchukit, S., Oztop, M. H., McCarthy, M. J., & McCarthy, K. L. (2013). Whey protein/alginate beads as carriers of a bioactive component. *Food Hydrocolloids*, 33(1), 66–73. <https://doi.org/10.1016/j.foodhyd.2013.02.013>
- Williams, M., & Hrazdina, G. (1979). Anthocyanins as food colorants: Effect of pH on the formation of anthocyanin - rutin complexes. *Journal of Food Science*, 44(1), 66–68.
- Williams, P. D., Oztop, M. H., McCarthy, M. J., McCarthy, K. L., & Lo, Y. M. (2011). Characterization of water distribution in xanthan-curdlan hydrogel complex using magnetic resonance imaging, nuclear magnetic resonance relaxometry, rheology, and scanning electron microscopy. *Journal of Food Science*, 76(6), 472–478. <https://doi.org/10.1111/j.1750-3841.2011.02227.x>
- Wu, T., Huang, J., Jiang, Y., Hu, Y., Ye, X., Liu, D., & Chen, J. (2018). Formation of hydrogels based on chitosan/alginate for the delivery of lysozyme and their antibacterial activity. *Food Chemistry*, 240, 361–369. <https://doi.org/10.1016/j.foodchem.2017.07.052>
- Wüstenberg, T. (2015). *Cellulose and Cellulose Derivatives in the Food Industry: Fundamentals and Applications* (1st ed.). Wiley-VCH Verlag GmbH & Co. KGaA. <https://doi.org/10.1002/9783527682935>
- Xiong, Y. L., Dawson, K. A., & Wan, L. (1993). Thermal Aggregation of β -Lactoglobulin: Effect of pH, Ionic Environment, and Thiol Reagent. *Journal of Dairy Science*, 76(1), 70–77. [https://doi.org/10.3168/jds.s0022-0302\(93\)77324-5](https://doi.org/10.3168/jds.s0022-0302(93)77324-5)
- Xu, M., & Dumont, M. J. (2015). Evaluation of the stability of pea and canola protein-based hydrogels in simulated gastrointestinal fluids. *Journal of Food Engineering*, 165, 52–59. <https://doi.org/10.1016/j.jfoodeng.2015.04.033>
- Yang, H., Li, J. G., Wu, N. F., Fan, M. M., Shen, X. L., Chen, M. T., Jiang, A. M., & Lai, L. S. (2015). Effect of hsian-tsao gum (HG) content upon rheological properties of film-forming solutions (FFS) and physical properties of soy protein/hsian-tsao gum films. *Food Hydrocolloids*, 50, 211–218. <https://doi.org/10.1016/j.foodhyd.2015.03.028>
- Yildiz, F. (2010). *Advances in Food Biochemistry* (F. Yildiz (ed.); 1st ed.). CRC Press.
- Zand-Rajabi, H., & Madadlou, A. (2016). Caffeine-loaded whey protein hydrogels reinforced with gellan and enriched with calcium chloride. *International Dairy*

Journal, 56, 38–44. <https://doi.org/10.1016/j.idairyj.2015.12.011>

- Zarzycki, R., Modrzejewska, Z., Nawrotek, K., & Lek, U. (2010). Drug Release From Hydrogel Matrices. *Ecological Chemistry and Engineering S*, 17(2), 117–136.
- Zasytkin, D. V, Dumay, E., & Cheftel, J. C. (1996). Pressure- and heat-induced gelation of mixed β -lactoglobulin/xanthan solutions. *Food Hydrocolloids*, 10(2), 203–211. [https://doi.org/10.1016/S0268-005X\(96\)80036-1](https://doi.org/10.1016/S0268-005X(96)80036-1)
- Zeeb, B., Mi-Yeon, L., Gibis, M., & Weiss, J. (2018). Growth phenomena in biopolymer complexes composed of heated WPI and pectin. *Food Hydrocolloids*, 74, 53–61. <https://doi.org/10.1016/j.foodhyd.2017.07.026>
- Zhang, M. P., Yang, Z. C., Chow, L. L., & Wang, C. H. (2003). Simulation of drug release from biodegradable polymeric microspheres with bulk and surface erosions. *Journal of Pharmaceutical Sciences*, 92(10), 2040–2056. <https://doi.org/10.1002/jps.10463>
- Zhang, S., Zhang, Z., & Vardhanabhuti, B. (2014). Effect of charge density of polysaccharides on self-assembled intragastric gelation of whey protein/polysaccharide under simulated gastric conditions. *Food Funct.*, 5(8), 1829–1838. <https://doi.org/10.1039/C4FO00019F>
- Zhang, Z., Decker, E. A., & McClements, D. J. (2014). Encapsulation, protection, and release of polyunsaturated lipids using biopolymer-based hydrogel particles. *Food Research International*, 64, 520–526. <https://doi.org/10.1016/j.foodres.2014.07.020>
- Zhang, Z., Zhang, R., Chen, L., Tong, Q., & McClements, D. J. (2015). Designing hydrogel particles for controlled or targeted release of lipophilic bioactive agents in the gastrointestinal tract. *European Polymer Journal*, 72, 698–716. <https://doi.org/10.1016/j.eurpolymj.2015.01.013>
- Zhang, Z., Zhang, R., & McClements, D. J. (2017). Control of protein digestion under simulated gastrointestinal conditions using biopolymer microgels. *Food Research International*, 100(August), 86–94. <https://doi.org/10.1016/j.foodres.2017.08.037>

APPENDICES

A. Statistical Analysis

Table A.1 One way Analysis of Variance (ANOVA) and Tukey's comparison test for the apparent viscosity (Pa s) values of BC containing different hydrogel solutions

Source	DF	SS	MS	F	P
sample	3	26811.34	8937.11	11554.25	0.000
Error	8	6.19	0.77		
Total	11	26817.53			

S = 0.8795 R-Sq = 99.98% R-Sq(adj) = 99.97%

Grouping Information Using Tukey Method and 95.0% Confidence

sample	N	Mean	Grouping
Xanthan	3	122.000	A
Tragacanth	3	25.267	B
Pectin	3	14.000	C
Control	3	3.587	D

Means that do not share a letter are significantly different.

Table A.2 General linear model and Tukey's comparison test for the apparent viscosity (Pa s) vs hydrogel solution; solution type of the C and PC hydrogel solutions

Factor	Type	Levels	Values
Hydrogel Solution	fixed	2	Control; Pectin
Solution Type	fixed	2	no BC; with BC

Source	DF	Seq SS	Adj SS	Adj MS
F				
Hydrogel Solution	1	0,0004473	0,0004267	0,0004267
1026,13				
Solution Type	1	0,0000001	0,0000001	0,0000001
0,14				
Hydrogel Solution*Solution Type	1	0,0000001	0,0000001	0,0000001
0,25				
Error	6	0,0000025	0,0000025	0,0000004
Total	9	0,0004500		

Source	P
Hydrogel Solution	0,000
Solution Type	0,721
Hydrogel Solution*Solution Type	0,633
Error	
Total	

S = 0,000644866 R-Sq = 99,45% R-Sq(adj) = 99,17%

Grouping Information Using Tukey Method and 95,0% Confidence

Hydrogel			
Solution	N	Mean	Grouping
Pectin	5	0,020437	A
Control	5	0,007103	B

Means that do not share a letter are significantly different.

Grouping Information Using Tukey Method and 95,0% Confidence

Solution			
Type	N	Mean	Grouping
with BC	6	0,013848	A
no BC	4	0,013692	A

Means that do not share a letter are significantly different.

Grouping Information Using Tukey Method and 95,0% Confidence

Hydrogel Solution				
Solution	Type	N	Mean	Grouping
Pectin	with BC	3	0,020620	A
Pectin	no BC	2	0,020255	A
Control	no BC	2	0,007130	B
Control	with BC	3	0,007077	B

Means that do not share a letter are significantly different.

Table A.3 One way Analysis of Variance (ANOVA) and Tukey's comparison test for the consistency index values (k, Pa s) of GT hydrogel solutions in the presence and absence of BC

Source	DF	SS	MS	F	P
solution type	1	0,0118168	0,0118168	4667,85	0,000
Error	2	0,0000051	0,0000025		
Total	3	0,0118218			

S = 0,001591 R-Sq = 99,96% R-Sq(adj) = 99,94%

Grouping Information Using Tukey Method and 95.0% Confidence

solution type	N	Mean	Grouping
with BC	2	0,14545	A
without BC	2	0,03675	B

Means that do not share a letter are significantly different.

Table A.4 One way Analysis of Variance (ANOVA) and Tukey's comparison test for the flow behavior index values (n) of GT hydrogel solutions in the presence and absence of BC

Source	DF	SS	MS	F	P
solution type	1	0,0003667	0,0003667	30,40	0,031
Error	2	0,0000241	0,0000121		
Total	3	0,0003908			

S = 0,003473 R-Sq = 93,83% R-Sq(adj) = 90,74%

Grouping Information Using Tukey Method and 95.0% Confidence

solution type	N	Mean	Grouping
with BC	2	0,858550	A
without BC	2	0,839400	B

Means that do not share a letter are significantly different.

Table A.5 One way Analysis of Variance (ANOVA) and Tukey's comparison test for the yield stress values (Pa) of XG hydrogel solutions in the presence and absence of BC

Source	DF	SS	MS	F	P
solution type	1	0,2158	0,2158	7,48	0,112
Error	2	0,0577	0,0288		
Total	3	0,2734			

S = 0,1698 R-Sq = 78,91% R-Sq(adj) = 68,37%

Grouping Information Using Tukey Method and 95.0% Confidence

solution type	N	Mean	Grouping
with BC	2	1,8885	A
without BC	2	1,4240	A

Means that do not share a letter are significantly different.

Table A.6 One way Analysis of Variance (ANOVA) and Tukey's comparison test for the consistency index values (k, Pa s) of XG hydrogel solutions in the presence and absence of BC

Source	DF	SS	MS	F	P
solution type	1	0,0679	0,0679	1,58	0,336
Error	2	0,0860	0,0430		
Total	3	0,1539			

S = 0,2074 R-Sq = 44,10% R-Sq(adj) = 16,15%

Grouping Information Using Tukey Method and 95.0% Confidence

solution type	N	Mean	Grouping
with BC	2	3,6140	A
without BC	2	3,3535	A

Means that do not share a letter are significantly different.

Table A.7 One way Analysis of Variance (ANOVA) and Tukey's comparison test for the flow behavior index values (n) of XG hydrogel solutions in the presence and absence of BC

Source	DF	SS	MS	F	P
solution type	1	0,0002465	0,0002465	3,74	0,193
Error	2	0,0001317	0,0000658		
Total	3	0,0003781			

S = 0,008113 R-Sq = 65,18% R-Sq(adj) = 47,78%

Grouping Information Using Tukey Method and 95.0% Confidence

solution type	N	Mean	Grouping
with BC	2	0,284250	A
without BC	2	0,268550	A

Means that do not share a letter are significantly different.

Table A.8 One way Analysis of Variance (ANOVA) and Tukey's comparison test for the critical gelling temperatures (°C) of the different BC containing hydrogel solutions

Source	DF	SS	MS	F	P
sample	3	21,69	7,23	4,17	0,047
Error	8	13,87	1,73		
Total	11	35,56			

S = 1,317 R-Sq = 60,99% R-Sq(adj) = 46,36%

Grouping Information Using Tukey Method and 95.0% Confidence

sample	N	Mean	Grouping
Control	3	79,397	A
Pectin	3	78,570	A B
Xanthan	3	77,993	A B
Tragacanth	3	75,770	B

Means that do not share a letter are significantly different.

Table A.9 One way Analysis of Variance (ANOVA) and Tukey's comparison test for the dielectric constant values of the different BC containing hydrogel solutions and distilled water

Source	DF	SS	MS	F	P
sample	4	599.27	149.82	122.31	0.000
Error	5	6.12	1.22		
Total	9	605.40			

S = 1.107 R-Sq = 98.99% R-Sq(adj) = 98.18%

Grouping Information Using Tukey Method and 95.0% Confidence

sample	N	Mean	Grouping
Distilled Water	2	77.868	A
Xanthan	2	60.537	B
Control	2	60.122	B
Pectin	2	59.739	B C
Tragacanth	2	55.664	C

Means that do not share a letter are significantly different.

Table A.10 One way Analysis of Variance (ANOVA) and Tukey's comparison test for the dielectric loss factor values of the different BC containing hydrogel solutions and distilled water

Source	DF	SS	MS	F	P
sample	4	24.9724	6.2431	95.92	0.000
Error	5	0.3254	0.0651		
Total	9	25.2978			

S = 0.2551 R-Sq = 98.71% R-Sq(adj) = 97.68%

Grouping Information Using Tukey Method and 95.0% Confidence

sample	N	Mean	Grouping
Xanthan	2	13.8288	A
Control	2	13.5953	A
Pectin	2	13.5463	A
Tragacanth	2	12.4176	B
Distilled Water	2	9.5906	C

Means that do not share a letter are significantly different.

Table A.11 General linear model and Tukey's comparison test for the absolute zeta potential (mV) vs BC presence; hydrogel solution type (C, PC, GT & XG)

Factor	Type	Levels	Values
BC Presence	fixed	2	With BC; Without BC
Solution Type	fixed	4	Control; Pectin; Tragacanth; Xanthan

Analysis of Variance for Zeta Potential, using Adjusted SS for Tests

Source	DF	Seq SS	Adj SS	Adj MS	F	P
BC Presence	1	447,207	447,207	447,207	1958,57	0,000
Solution Type	3	39,343	39,343	13,114	57,44	0,000
BC Presence*Solution Type	3	44,130	44,130	14,710	64,42	0,000
Error	16	3,653	3,653	0,228		
Total	23	534,333				

S = 0,477842 R-Sq = 99,32% R-Sq(adj) = 99,02%

Grouping Information Using Tukey Method and 95,0% Confidence

BC Presence	N	Mean	Grouping
Without BC	12	29,63	A
With BC	12	21,00	B

Means that do not share a letter are significantly different.

Grouping Information Using Tukey Method and 95,0% Confidence

Solution Type	N	Mean	Grouping
Control	6	26,58	A
Xanthan	6	26,50	A
Pectin	6	24,62	B
Tragacanth	6	23,57	C

Means that do not share a letter are significantly different.

Grouping Information Using Tukey Method and 95,0% Confidence

BC Presence	Solution Type	N	Mean	Grouping
Without BC	Control	3	31,10	A
Without BC	Pectin	3	30,23	A
Without BC	Tragacanth	3	28,63	B
Without BC	Xanthan	3	28,57	B
With BC	Xanthan	3	24,43	C
With BC	Control	3	22,07	D
With BC	Pectin	3	19,00	E
With BC	Tragacanth	3	18,50	E

Means that do not share a letter are significantly different.

Table A.12 One way Analysis of Variance (ANOVA) and Tukey's comparison test for the pH values of the different BC containing hydrogel solutions

Source	DF	SS	MS	F	P
sample	3	0.09050	0.03017	23.25	0.000
Error	8	0.01038	0.00130		
Total	11	0.10088			

S = 0.03602 R-Sq = 89.71% R-Sq(adj) = 85.85%

Grouping Information Using Tukey Method and 95,0% Confidence

sample	N	Mean	Grouping
xanthan	3	5.89222	A
tragacanth	3	5.82000	A
control	3	5.72111	B
pectin	3	5.66778	B

Means that do not share a letter are significantly different.

Table A.13 One way Analysis of Variance (ANOVA) and Tukey's comparison test for the pH values of the different hydrogel solutions in the absence of BC

Source	DF	SS	MS	F	P
sample	3	0.085433	0.028478	45.90	0.000
Error	8	0.004963	0.000620		
Total	11	0.090396			

S = 0.02491 R-Sq = 94.51% R-Sq(adj) = 92.45%

Grouping Information Using Tukey Method and 95,0% Confidence

sample	N	Mean	Grouping
xanthan	3	7.04667	A
tragacanth	3	7.02000	A
control	3	6.94667	B
pectin	3	6.82889	C

Means that do not share a letter are significantly different.

Table A.14 One way Analysis of Variance (ANOVA) and Tukey's comparison test for the pH values of the PC hydrogel solutions in the absence and presence of BC

Source	DF	SS	MS	F	P
sample	1	2.022269	2.022269	4152.19	0.000
Error	4	0.001948	0.000487		
Total	5	2.024217			

S = 0.02207 R-Sq = 99.90% R-Sq(adj) = 99.88%

Grouping Information Using Tukey Method and 95,0% Confidence

sample	N	Mean	Grouping
Pectin without BC	3	6.8289	A
Pectin with BC	3	5.6678	B

Means that do not share a letter are significantly different.

Table A.15 One way Analysis of Variance (ANOVA) and Tukey's comparison test for the pH values of the GT hydrogel solutions in the absence and presence of BC

Source	DF	SS	MS	F	P
sample	1	2.16000	2.16000	1450.75	0.000
Error	4	0.00596	0.00149		
Total	5	2.16596			

S = 0.03859 R-Sq = 99.73% R-Sq(adj) = 99.66%

Grouping Information Using Tukey Method and 95,0% Confidence

sample	N	Mean	Grouping
Tragacanth without BC	3	7.0200	A
Tragacanth with BC	3	5.8200	B

Means that do not share a letter are significantly different.

Table A.16 One way Analysis of Variance (ANOVA) and Tukey's comparison test for the pH values of the C hydrogel solutions in the absence and presence of BC

Source	DF	SS	MS	F	P
sample	1	2.252980	2.252980	2952.93	0.000
Error	4	0.003052	0.000763		
Total	5	2.256031			

S = 0.02762 R-Sq = 99.86% R-Sq(adj) = 99.83%

Grouping Information Using Tukey Method and 95,0% Confidence

sample	N	Mean	Grouping
Control without BC	3	6.9467	A
Control with BC	3	5.7211	B

Means that do not share a letter are significantly different.

Table A.17 One way Analysis of Variance (ANOVA) and Tukey's comparison test for the pH values of the XG hydrogel solutions in the absence and presence of BC

Source	DF	SS	MS	F	P
sample	1	1.99911	1.99911	1823.52	0.000
Error	4	0.00439	0.00110		
Total	5	2.00350			

S = 0.03311 R-Sq = 99.78% R-Sq(adj) = 99.73%

Grouping Information Using Tukey Method and 95,0% Confidence

sample	N	Mean	Grouping
Xanthan without BC	3	7.0467	A
Xanthan with BC	3	5.8922	B

Means that do not share a letter are significantly different.

Table A.18 One way Analysis of Variance (ANOVA) and Tukey's comparison test for the swelling ratios (%) of the CV hydrogels in phosphate buffer at 6 h

Source	DF	SS	MS	F	P
sample	3	94,98	31,66	7,91	0,009
Error	8	32,04	4,00		
Total	11	127,01			

S = 2,001 R-Sq = 74,78% R-Sq(adj) = 65,32%

Grouping Information Using Tukey Method and 95,0% Confidence

sample	N	Mean	Grouping
Xanthan	3	15,965	A
Pectin	3	12,247	A B
Control	3	9,231	B
Tragacanth	3	9,037	B

Means that do not share a letter are significantly different.

Table A.19 One way Analysis of Variance (ANOVA) and Tukey's comparison test for the swelling ratios (%) of the CV hydrogels in phosphate buffer at 24 h

Source	DF	SS	MS	F	P
sample	3	103,28	34,43	4,80	0,034
Error	8	57,37	7,17		
Total	11	160,64			

S = 2,678 R-Sq = 64,29% R-Sq(adj) = 50,90%

Grouping Information Using Tukey Method and 95,0% Confidence

sample	N	Mean	Grouping
Xanthan	3	17,847	A
Pectin	3	13,870	A B
Tragacanth	3	10,875	A B
Control	3	10,553	B

Means that do not share a letter are significantly different.

Table A.20 One way Analysis of Variance (ANOVA) and Tukey's comparison test for the change in the swelling ratios (%) of the CV PC hydrogels in phosphate buffer during 24 h experiment

Source	DF	SS	MS	F	P
Time	7	90.373	12.910	27.51	0.000
Error	16	7.509	0.469		
Total	23	97.882			

S = 0.6850 R-Sq = 92.33% R-Sq(adj) = 88.97%

Grouping Information Using Tukey Method and 95,0% Confidence

Time	N	Mean	Grouping
24.0	3	13.8705	A
6.0	3	12.2471	A B
5.0	3	11.0946	B C
4.0	3	10.9790	B C
3.0	3	10.9609	B C
2.0	3	9.7931	C D
1.0	3	8.5000	D E
0.5	3	7.2629	E

Means that do not share a letter are significantly different.

Table A.21 One way Analysis of Variance (ANOVA) and Tukey's comparison test for the change in the swelling ratios (%) of the CV XG hydrogels in phosphate buffer during 24 h experiment

Source	DF	SS	MS	F	P
Time	7	294.25	42.04	4.43	0.007
Error	16	151.71	9.48		
Total	23	445.95			

S = 3.079 R-Sq = 65.98% R-Sq(adj) = 51.10%

Grouping Information Using Tukey Method and 95,0% Confidence

Time	N	Mean	Grouping
24.0	3	17.847	A
6.0	3	15.965	A B
5.0	3	15.604	A B
4.0	3	14.749	A B C
3.0	3	13.543	A B C
2.0	3	12.058	A B C
1.0	3	8.943	B C
0.5	3	6.788	C

Means that do not share a letter are significantly different.

Table A.22 One way Analysis of Variance (ANOVA) and Tukey's comparison test for the change in the swelling ratios (%) of the CV C hydrogels in phosphate buffer during 24 h experiment

Source	DF	SS	MS	F	P
Time	7	44.574	6.368	16.04	0.000
Error	16	6.353	0.397		
Total	23	50.928			

S = 0.6302 R-Sq = 87.52% R-Sq(adj) = 82.07%

Grouping Information Using Tukey Method and 95,0% Confidence

Time	N	Mean	Grouping
24.0	3	10.5532	A
6.0	3	9.2309	A B
5.0	3	8.9358	A B
4.0	3	8.5067	B
3.0	3	7.9968	B C
2.0	3	7.4533	B C D
1.0	3	6.6114	C D
0.5	3	6.0772	D

Means that do not share a letter are significantly different.

Table A.23 One way Analysis of Variance (ANOVA) and Tukey's comparison test for the change in the swelling ratios (%) of the CV GT hydrogels in phosphate buffer during 24 h experiment

Source	DF	SS	MS	F	P
Time	7	66.188	9.455	20.18	0.000
Error	16	7.496	0.469		
Total	23	73.684			

S = 0.6845 R-Sq = 89.83% R-Sq(adj) = 85.38%

Grouping Information Using Tukey Method and 95,0% Confidence

Time	N	Mean	Grouping
24.0	3	10.8752	A
6.0	3	9.0365	A B
5.0	3	8.4779	B C
4.0	3	8.0629	B C D
3.0	3	7.5354	B C D
2.0	3	6.8699	C D E
1.0	3	6.1866	D E
0.5	3	5.1513	E

Means that do not share a letter are significantly different.

Table A.24 One way Analysis of Variance (ANOVA) and Tukey's comparison test for the viscosity values (cP) of the hydrogel solutions

Source	DF	SS	MS	F	P
sample	3	26811.34	8937.11	11554.25	0.000
Error	8	6.19	0.77		
Total	11	26817.53			

S = 0.8795 R-Sq = 99.98% R-Sq(adj) = 99.97%

Grouping Information Using Tukey Method and 95,0% Confidence

sample	N	Mean	Grouping
Xanthan	3	122.000	A
Tragacanth	3	25.267	B
Pectin	3	14.000	C
Control	3	3.587	D

Means that do not share a letter are significantly different.

Table A.25 One way Analysis of Variance (ANOVA) and Tukey's comparison test for the release rates (%) of the different CV hydrogels in phosphate buffer at 24 h

Source	DF	SS	MS	F	P
sample	3	3206,5	1068,8	51,57	0,000
Error	6	124,4	20,7		
Total	9	3330,9			

S = 4,553 R-Sq = 96,27% R-Sq(adj) = 94,40%

Grouping Information Using Tukey Method and 95,0% Confidence

sample	N	Mean	Grouping
Control	2	77,818	A
Pectin	3	37,155	B
Xanthan	3	32,792	B
Tragacanth	2	29,397	B

Means that do not share a letter are significantly different.

Table A.26 One way Analysis of Variance (ANOVA) and Tukey's comparison test for the release rates (%) of the different MW hydrogels in phosphate buffer at 24 h

Source	DF	SS	MS	F	P
sample	3	11	4	0.03	0.991
Error	7	742	106		
Total	10	753			

S = 10.30 R-Sq = 1.40% R-Sq(adj) = 0.00%

Grouping Information Using Tukey Method and 95,0% Confidence

sample	N	Mean	Grouping
Control	3	79.12	A
Tragacanth	3	79.05	A
Xanthan	3	78.09	A
Pectin	2	76.46	A

Means that do not share a letter are significantly different.

Table A.27 General linear model and Tukey's comparison test for the release rates (%) vs hydrogel type (C, PC, GT, XG); heating type (CV, MW) in phosphate buffer at 24 h

Factor	Type	Levels	Values
sample	fixed	4	Control; Pectin; Tragacanth; Xanthan
heating type	fixed	2	conv; mw

Analysis of Variance for R at 24h, using Adjusted SS for Tests

Source	DF	Seq SS	Adj SS	Adj MS	F	P
sample	3	2078.6	1954.2	651.4	9.77	0.001
heating type	1	6092.1	5803.3	5803.3	87.03	0.000
sample*heating type	3	1801.2	1801.2	600.4	9.00	0.002
Error	13	866.8	866.8	66.7		
Total	20	10838.6				

S = 8.16576 R-Sq = 92.00% R-Sq(adj) = 87.70%

Grouping Information Using Tukey Method and 95.0% Confidence

sample	N	Mean	Grouping
Control	5	78.47	A
Pectin	5	56.81	B
Xanthan	6	55.44	B
Tragacanth	5	54.22	B

Means that do not share a letter are significantly different.

Grouping Information Using Tukey Method and 95.0% Confidence

heating			
type	N	Mean	Grouping
mw	11	78.18	A
conv	10	44.29	B

Means that do not share a letter are significantly different.

Grouping Information Using Tukey Method and 95.0% Confidence

heating				
sample	type	N	Mean	Grouping
Control	mw	3	79.12	A
Tragacanth	mw	3	79.05	A
Xanthan	mw	3	78.09	A
Control	conv	2	77.82	A
Pectin	mw	2	76.46	A
Pectin	conv	3	37.15	B
Xanthan	conv	3	32.79	B
Tragacanth	conv	2	29.40	B

Means that do not share a letter are significantly different.

Table A.28 One way Analysis of Variance (ANOVA) and Tukey's comparison test for the change in the release rates (%) of the CV PC hydrogels in phosphate buffer during 24 h experiment

Source	DF	SS	MS	F	P
Time	7	1704.4	243.5	23.97	0.000
Error	16	162.6	10.2		
Total	23	1867.0			

S = 3.188 R-Sq = 91.29% R-Sq(adj) = 87.48%

Grouping Information Using Tukey Method and 95,0% Confidence

Time	N	Mean	Grouping
24.0	3	37.155	A
6.0	3	21.876	B
5.0	3	20.368	B
4.0	3	18.551	B C
3.0	3	16.681	B C
2.0	3	14.157	B C D
1.0	3	10.641	C D
0.5	3	7.478	D

Means that do not share a letter are significantly different.

Table A.29 One way Analysis of Variance (ANOVA) and Tukey's comparison test for the change in the release rates (%) of the CV XG hydrogels in phosphate buffer during 24 h experiment

Source	DF	SS	MS	F	P
Time	7	1445.7	206.5	5.27	0.003
Error	16	627.5	39.2		
Total	23	2073.2			

S = 6.262 R-Sq = 69.73% R-Sq(adj) = 56.49%

Grouping Information Using Tukey Method and 95,0% Confidence

Time	N	Mean	Grouping
24.0	3	32.792	A
6.0	3	20.045	A B
5.0	3	19.447	A B
4.0	3	17.890	A B
3.0	3	15.648	A B
2.0	3	13.095	B
1.0	3	8.935	B
0.5	3	5.369	B

Means that do not share a letter are significantly different.

Table A.30 One way Analysis of Variance (ANOVA) and Tukey's comparison test for the change in the release rates (%) of the CV GT hydrogels in phosphate buffer during 24 h experiment

Source	DF	SS	MS	F	P
Time	7	2230.0	318.6	8.88	0.000
Error	16	574.2	35.9		
Total	23	2804.3			

S = 5.991 R-Sq = 79.52% R-Sq(adj) = 70.56%

Grouping Information Using Tukey Method and 95,0% Confidence

Time	N	Mean	Grouping
24.0	3	38.702	A
6.0	3	16.760	B
5.0	3	15.312	B
4.0	3	14.491	B
3.0	3	12.581	B
2.0	3	10.557	B
1.0	3	7.486	B
0.5	3	5.193	B

Means that do not share a letter are significantly different.

Table A.31 One way Analysis of Variance (ANOVA) and Tukey's comparison test for the change in the release rates (%) of the CV C hydrogels in phosphate buffer during 24 h experiment

Source	DF	SS	MS	F	P
Time	7	7737.8	1105.4	27.91	0.000
Error	16	633.6	39.6		
Total	23	8371.4			

S = 6.293 R-Sq = 92.43% R-Sq(adj) = 89.12%

Grouping Information Using Tukey Method and 95,0% Confidence

Time	N	Mean	Grouping
24.0	3	67.716	A
6.0	3	23.506	B
5.0	3	21.960	B
4.0	3	18.516	B
3.0	3	16.988	B
2.0	3	14.024	B
1.0	3	9.405	B
0.5	3	6.877	B

Means that do not share a letter are significantly different.

Table A.32 One way Analysis of Variance (ANOVA) and Tukey's comparison test for the change in the release rates (%) of the MW PC hydrogels in phosphate buffer during 24 h experiment

Source	DF	SS	MS	F	P
Time	7	4648.2	664.0	6.91	0.001
Error	15	1441.9	96.1		
Total	22	6090.1			

S = 9.804 R-Sq = 76.32% R-Sq(adj) = 65.28%

Grouping Information Using Tukey Method and 95,0% Confidence

Time	N	Mean	Grouping
24.0	2	76.46	A
6.0	3	35.54	B
5.0	3	34.35	B
4.0	3	33.91	B
3.0	3	32.34	B
2.0	3	29.57	B
1.0	3	24.76	B
0.5	3	18.60	B

Means that do not share a letter are significantly different.

Table A.33 One way Analysis of Variance (ANOVA) and Tukey's comparison test for the change in the release rates (%) of the MW XG hydrogels in phosphate buffer during 24 h experiment

Source	DF	SS	MS	F	P
Time	7	10076.2	1439.5	14.57	0.000
Error	16	1580.7	98.8		
Total	23	11657.0			

S = 9.940 R-Sq = 86.44% R-Sq(adj) = 80.51%

Grouping Information Using Tukey Method and 95,0% Confidence

Time	N	Mean	Grouping
24.0	3	78.09	A
6.0	3	53.66	A B
5.0	3	48.53	B
4.0	3	44.46	B C
3.0	3	35.85	B C D
2.0	3	27.32	B C D
1.0	3	17.54	C D
0.5	3	9.19	D

Means that do not share a letter are significantly different.

Table A.34 One way Analysis of Variance (ANOVA) and Tukey's comparison test for the change in the release rates (%) of the MW GT hydrogels in phosphate buffer during 24 h experiment

Source	DF	SS	MS	F	P
Time	7	7700.5	1100.1	16.89	0.000
Error	16	1041.9	65.1		
Total	23	8742.3			

S = 8.069 R-Sq = 88.08% R-Sq(adj) = 82.87%

Grouping Information Using Tukey Method and 95,0% Confidence

Time	N	Mean	Grouping
24.0	3	79.051	A
6.0	3	41.743	B
5.0	3	40.360	B
4.0	3	38.293	B
3.0	3	35.066	B C
2.0	3	29.934	B C
1.0	3	22.570	B C
0.5	3	14.527	C

Means that do not share a letter are significantly different.

Table A.35 One way Analysis of Variance (ANOVA) and Tukey's comparison test for the change in the release rates (%) of the MW C hydrogels in phosphate buffer during 24 h experiment

Source	DF	SS	MS	F	P
Time	7	7183.3	1026.2	38.35	0.000
Error	16	428.1	26.8		
Total	23	7611.5			

S = 5.173 R-Sq = 94.38% R-Sq(adj) = 91.91%

Grouping Information Using Tukey Method and 95,0% Confidence

Time	N	Mean	Grouping
24.0	3	79.116	A
6.0	3	38.121	B
5.0	3	36.099	B C
4.0	3	34.249	B C
3.0	3	31.633	B C D
2.0	3	27.830	B C D
1.0	3	23.271	C D
0.5	3	19.256	D

Means that do not share a letter are significantly different.

Table A.36 One way Analysis of Variance (ANOVA) and Tukey's comparison test for the transverse relaxation times (T₂, ms) of the different CV hydrogels at 0 h

Source	DF	SS	MS	F	P
sample	3	150.14	50.05	5.38	0.025
Error	8	74.40	9.30		
Total	11	224.54			

S = 3.050 R-Sq = 66.87% R-Sq(adj) = 54.44%

Grouping Information Using Tukey Method and 95,0% Confidence

sample	N	Mean	Grouping
Tragacanth	3	60.097	A
Pectin	3	53.921	A B
Control	3	52.646	A B
Xanthan	3	50.616	B

Means that do not share a letter are significantly different.

Table A.37 One way Analysis of Variance (ANOVA) and Tukey's comparison test for the transverse relaxation times (T_2 , ms) of the different CV hydrogels in phosphate buffer at 24 h

Source	DF	SS	MS	F	P
sample	3	269.6	89.9	2.62	0.123
Error	8	274.8	34.3		
Total	11	544.4			

S = 5.861 R-Sq = 49.52% R-Sq(adj) = 30.59%

Grouping Information Using Tukey Method and 95,0% Confidence

sample	N	Mean	Grouping
Tragacanth	3	71.131	A
Xanthan	3	62.624	A
Pectin	3	62.488	A
Control	3	58.036	A

Means that do not share a letter are significantly different.

Table A.38 One way Analysis of Variance (ANOVA) and Tukey's comparison test for the transverse relaxation times (T_2 , ms) of the different MW hydrogels at 0 h

Source	DF	SS	MS	F	P
sample	3	379.14	126.38	38.89	0.000
Error	8	26.00	3.25		
Total	11	405.14			

S = 1.803 R-Sq = 93.58% R-Sq(adj) = 91.18%

Grouping Information Using Tukey Method and 95,0% Confidence

sample	N	Mean	Grouping
Tragacanth	3	60.109	A
Control	3	56.856	A B
Xanthan	3	54.153	B
Pectin	3	45.007	C

Means that do not share a letter are significantly different.

Table A.39 One way Analysis of Variance (ANOVA) and Tukey's comparison test for the transverse relaxation times (T_2 , ms) of the different MW hydrogels in phosphate buffer at 24 h

Source	DF	SS	MS	F	P
sample	3	93.7	31.2	2.44	0.140
Error	8	102.6	12.8		
Total	11	196.3			

S = 3.581 R-Sq = 47.75% R-Sq(adj) = 28.15%

Grouping Information Using Tukey Method and 95,0% Confidence

sample	N	Mean	Grouping
Tragacanth	3	74.118	A
Pectin	3	70.044	A
Control	3	67.696	A
Xanthan	3	66.946	A

Means that do not share a letter are significantly different.

Table A.40 General linear model and Tukey's comparison test for the transverse relaxation times (T_2 , ms) vs hydrogel type (C, PC, GT, XG); heating type (CV, MW) at 0 h

Factor	Type	Levels	Values
sample	fixed	4	Control, Pectin, Tragacanth, Xanthan
heating type	fixed	2	conv, mw

Analysis of Variance for T2 at 0h, using Adjusted SS for Tests

Source	DF	Seq SS	Adj SS	Adj MS	F	P
sample	3	365.224	365.224	121.741	19.40	0.000
heating type	1	0.500	0.500	0.500	0.08	0.781
sample*heating type	3	164.059	164.059	54.686	8.72	0.001
Error	16	100.394	100.394	6.275		
Total	23	630.177				

S = 2.50492 R-Sq = 84.07% R-Sq(adj) = 77.10%

Grouping Information Using Tukey Method and 95.0% Confidence

sample	N	Mean	Grouping
Tragacanth	6	60.10	A
Control	6	54.75	B
Xanthan	6	52.38	B C
Pectin	6	49.46	C

Means that do not share a letter are significantly different.

Grouping Information Using Tukey Method and 95.0% Confidence

heating			
type	N	Mean	Grouping
conv	12	54.32	A
mw	12	54.03	A

Means that do not share a letter are significantly different.

Grouping Information Using Tukey Method and 95.0% Confidence

heating				
sample	type	N	Mean	Grouping
Tragacanth	mw	3	60.11	A
Tragacanth	conv	3	60.10	A
Control	mw	3	56.86	A B
Xanthan	mw	3	54.15	A B
Pectin	conv	3	53.92	A B
Control	conv	3	52.65	B
Xanthan	conv	3	50.62	B C
Pectin	mw	3	45.01	C

Means that do not share a letter are significantly different.

Table A.41 General linear model and Tukey's comparison test for the transverse relaxation times (T_2 , ms) vs hydrogel type (C, PC, GT, XG); heating type (CV, MW) in phosphate buffer at 24 h

Factor	Type	Levels	Values
sample	fixed	4	Control, Pectin, Tragacanth, Xanthan
heating type	fixed	2	conv, mw

Analysis of Variance for T2 at 24h, using Adjusted SS for Tests

Source	DF	Seq SS	Adj SS	Adj MS	F	P
sample	3	321.85	321.85	107.28	4.55	0.017
heating type	1	225.55	225.55	225.55	9.56	0.007
sample*heating type	3	41.46	41.46	13.82	0.59	0.633
Error	16	377.36	377.36	23.58		
Total	23	966.21				

S = 4.85642 R-Sq = 60.94% R-Sq(adj) = 43.86%

Grouping Information Using Tukey Method and 95.0% Confidence

sample	N	Mean	Grouping
Tragacanth	6	72.62	A
Pectin	6	66.27	A B
Xanthan	6	64.78	A B
Control	6	62.87	B

Means that do not share a letter are significantly different.

Grouping Information Using Tukey Method and 95.0% Confidence

heating			
type	N	Mean	Grouping
mw	12	69.70	A
conv	12	63.57	B

Means that do not share a letter are significantly different.

Grouping Information Using Tukey Method and 95.0% Confidence

heating				
sample	type	N	Mean	Grouping
Tragacanth	mw	3	74.12	A
Tragacanth	conv	3	71.13	A B
Pectin	mw	3	70.04	A B
Control	mw	3	67.70	A B
Xanthan	mw	3	66.95	A B
Xanthan	conv	3	62.62	A B
Pectin	conv	3	62.49	A B
Control	conv	3	58.04	B

Means that do not share a letter are significantly different.

Table A.42 One way Analysis of Variance (ANOVA) and Tukey’s comparison test for the change in the transverse relaxation times (T_2 , ms) of the CV PC hydrogels in phosphate buffer during 24 h experiment

Source	DF	SS	MS	F	P
Time	4	111.7	27.9	1.13	0.398
Error	10	248.1	24.8		
Total	14	359.8			

S = 4.981 R-Sq = 31.04% R-Sq(adj) = 3.45%

Grouping Information Using Tukey Method and 95.0% Confidence

Time	N	Mean	Grouping
24	3	62.488	A
4	3	58.990	A
6	3	58.838	A
2	3	58.679	A
0	3	53.921	A

Means that do not share a letter are significantly different

Table A.43 One way Analysis of Variance (ANOVA) and Tukey's comparison test for the change in the transverse relaxation times (T_2 , ms) of the CV XG hydrogels in phosphate buffer during 24 h experiment

Source	DF	SS	MS	F	P
Time	4	254.1	63.5	3.70	0.042
Error	10	171.5	17.2		
Total	14	425.7			

S = 4.142 R-Sq = 59.70% R-Sq(adj) = 43.58%

Grouping Information Using Tukey Method and 95.0% Confidence

Time	N	Mean	Grouping
24	3	62.624	A
4	3	60.488	A B
6	3	59.517	A B
2	3	59.256	A B
0	3	50.616	B

Means that do not share a letter are significantly different.

Table A.44 One way Analysis of Variance (ANOVA) and Tukey's comparison test for the change in the transverse relaxation times (T_2 , ms) of the CV C hydrogels in phosphate buffer during 24 h experiment

Source	DF	SS	MS	F	P
Time	4	174.67	43.67	6.26	0.009
Error	10	69.80	6.98		
Total	14	244.47			

S = 2.642 R-Sq = 71.45% R-Sq(adj) = 60.03%

Grouping Information Using Tukey Method and 95.0% Confidence

Time	N	Mean	Grouping
2	3	61.660	A
4	3	61.394	A
6	3	61.030	A
24	3	58.036	A B
0	3	52.646	B

Means that do not share a letter are significantly different.

Table A.45 One way Analysis of Variance (ANOVA) and Tukey's comparison test for the change in the transverse relaxation times (T_2 , ms) of the CV GT hydrogels in phosphate buffer during 24 h experiment

Source	DF	SS	MS	F	P
Time	4	192.7	48.2	0.94	0.482
Error	10	514.8	51.5		
Total	14	707.5			

S = 7.175 R-Sq = 27.24% R-Sq(adj) = 0.00%

Grouping Information Using Tukey Method and 95.0% Confidence

Time	N	Mean	Grouping
24	3	71.131	A
4	3	67.288	A
6	3	66.707	A
2	3	65.041	A
0	3	60.097	A

Means that do not share a letter are significantly different.

Table A.46 One way Analysis of Variance (ANOVA) and Tukey's comparison test for the change in the transverse relaxation times (T_2 , ms) of the MW PC hydrogels in phosphate buffer during 24 h experiment

Source	DF	SS	MS	F	P
Time	4	1084.87	271.22	74.12	0.000
Error	10	36.59	3.66		
Total	14	1121.46			

S = 1.913 R-Sq = 96.74% R-Sq(adj) = 95.43%

Grouping Information Using Tukey Method and 95.0% Confidence

Time	N	Mean	Grouping
24	3	70.044	A
4	3	64.155	B
6	3	64.019	B
2	3	63.339	B
0	3	45.007	C

Means that do not share a letter are significantly different.

Table A.47 One way Analysis of Variance (ANOVA) and Tukey's comparison test for the change in the transverse relaxation times (T_2 , ms) of the MW XG hydrogels in phosphate buffer during 24 h experiment

Source	DF	SS	MS	F	P
Time	4	259.50	64.88	18.76	0.000
Error	10	34.58	3.46		
Total	14	294.08			

S = 1.860 R-Sq = 88.24% R-Sq(adj) = 83.54%

Grouping Information Using Tukey Method and 95.0% Confidence

Time	N	Mean	Grouping
24	3	66.946	A
6	3	61.800	B
4	3	61.339	B
2	3	58.960	B C
0	3	54.153	C

Means that do not share a letter are significantly different.

Table A.48 One way Analysis of Variance (ANOVA) and Tukey's comparison test for the change in the transverse relaxation times (T_2 , ms) of the MW C hydrogels in phosphate buffer during 24 h experiment

Source	DF	SS	MS	F	P
Time	4	255.0	63.8	3.98	0.035
Error	10	160.1	16.0		
Total	14	415.1			

S = 4.001 R-Sq = 61.44% R-Sq(adj) = 46.01%

Grouping Information Using Tukey Method and 95.0% Confidence

Time	N	Mean	Grouping
2	3	68.508	A
24	3	67.696	A
4	3	65.049	A B
6	3	64.632	A B
0	3	56.856	B

Means that do not share a letter are significantly different.

Table A.49 One way Analysis of Variance (ANOVA) and Tukey's comparison test for the change in the transverse relaxation times (T_2 , ms) of the MW GT hydrogels in phosphate buffer during 24 h experiment

Source	DF	SS	MS	F	P
Time	4	303.24	75.81	21.18	0.000
Error	10	35.80	3.58		
Total	14	339.04			

S = 1.892 R-Sq = 89.44% R-Sq(adj) = 85.22%

Grouping Information Using Tukey Method and 95.0% Confidence

Time	N	Mean	Grouping
24	3	74.118	A
4	3	68.685	B
6	3	68.396	B
2	3	66.783	B
0	3	60.109	C

Means that do not share a letter are significantly different.

Table A.50 One way Analysis of Variance (ANOVA) and Tukey's comparison test for the self-diffusion coefficient ($SDC \times 10^9$, m^2/s) of the different CV hydrogels at 0 h

Source	DF	SS	MS	F	P
sample	3	0.005633	0.001878	2.20	0.231
Error	4	0.003415	0.000854		
Total	7	0.009048			

S = 0.02922 R-Sq = 62.25% R-Sq(adj) = 33.94%

Grouping Information Using Tukey Method and 95.0% Confidence

sample	N	Mean	Grouping
Tragacanth	2	1.39130	A
Pectin	2	1.38920	A
Xanthan	2	1.34940	A
Control	2	1.32900	A

Means that do not share a letter are significantly different.

Table A.51 One way Analysis of Variance (ANOVA) and Tukey's comparison test for the self-diffusion coefficient (SDC x 10⁹, m²/s) of the different CV hydrogels in phosphate buffer at 6 h

Source	DF	SS	MS	F	P
sample	3	0.05425	0.01808	6.71	0.049
Error	4	0.01078	0.00270		
Total	7	0.06503			

S = 0.05193 R-Sq = 83.42% R-Sq(adj) = 70.98%

Grouping Information Using Tukey Method and 95.0% Confidence

sample	N	Mean	Grouping
Xanthan	2	1.67695	A
Pectin	2	1.57415	A B
Tragacanth	2	1.51665	A B
Control	2	1.45295	B

Means that do not share a letter are significantly different.

Table A.52 One way Analysis of Variance (ANOVA) and Tukey's comparison test for the self-diffusion coefficient (SDC x 10⁹, m²/s) of the different MW hydrogels at 0 h

Source	DF	SS	MS	F	P
sample	3	0.00278	0.00093	0.41	0.755
Error	4	0.00905	0.00226		
Total	7	0.01184			

S = 0.04758 R-Sq = 23.52% R-Sq(adj) = 0.00%

Grouping Information Using Tukey Method and 95.0% Confidence

sample	N	Mean	Grouping
Pectin	2	1.27885	A
Control	2	1.25915	A
Xanthan	2	1.25030	A
Tragacanth	2	1.22690	A

Means that do not share a letter are significantly different.

Table A.53 One way Analysis of Variance (ANOVA) and Tukey's comparison test for the self-diffusion coefficient (SDC x 10⁹, m²/s) of the different MW hydrogels in phosphate buffer at 6 h

Source	DF	SS	MS	F	P
sample	3	0.00236	0.00079	0.14	0.933
Error	4	0.02301	0.00575		
Total	7	0.02537			

S = 0.07584 R-Sq = 9.31% R-Sq(adj) = 0.00%

Grouping Information Using Tukey Method and 95.0% Confidence

sample	N	Mean	Grouping
Tragacanth	2	1.39065	A
Control	2	1.38940	A
Pectin	2	1.38000	A
Xanthan	2	1.34815	A

Means that do not share a letter are significantly different.

Table A.54 General linear model and Tukey's comparison test for the self-diffusion coefficient (SDC x 10⁹, m²/s) vs hydrogel type (C, PC, GT, XG); heating type (CV, MW) at 0 h

Factor	Type	Levels	Values
sample	fixed	4	Control, Pectin, Tragacanth, Xanthan
heating type	fixed	2	conv, mw

Analysis of Variance for SDC at 0h, using Adjusted SS for Tests

Source	DF	Seq SS	Adj SS	Adj MS	F	P
sample	3	0.003730	0.003730	0.001243	0.80	0.529
heating type	1	0.049217	0.049217	0.049217	31.58	0.000
sample*heating type	3	0.004687	0.004687	0.001562	1.00	0.440
Error	8	0.012470	0.012470	0.001559		
Total	15	0.070104				

S = 0.0394805 R-Sq = 82.21% R-Sq(adj) = 66.65%

Grouping Information Using Tukey Method and 95.0% Confidence

sample	N	Mean	Grouping
Pectin	4	1.334	A
Tragacanth	4	1.309	A
Xanthan	4	1.300	A
Control	4	1.294	A

Means that do not share a letter are significantly different.

Grouping Information Using Tukey Method and 95.0% Confidence

```
heating
type      N   Mean  Grouping
conv     8  1.365   A
mw       8  1.254   B
```

Means that do not share a letter are significantly different.

Grouping Information Using Tukey Method and 95.0% Confidence

```
          heating
sample   type  N   Mean  Grouping
Tragacanth conv  2  1.391  A
Pectin   conv  2  1.389  A
Xanthan  conv  2  1.349  A B
Control  conv  2  1.329  A B
Pectin   mw   2  1.279  A B
Control  mw   2  1.259  A B
Xanthan  mw   2  1.250  A B
Tragacanth mw  2  1.227  B
```

Means that do not share a letter are significantly different.

Table A.55 General linear model and Tukey's comparison test for the self-diffusion coefficient ($SDC \times 10^9, m^2/s$) vs hydrogel type (C, PC, GT, XG); heating type (CV, MW) in phosphate buffer at 6 h

```
Factor      Type  Levels  Values
sample      fixed    4  Control, Pectin, Tragacanth, Xanthan
heating type fixed    2  conv, mw
```

Analysis of Variance for SDC at 6h, using Adjusted SS for Tests

Source	DF	Seq SS	Adj SS	Adj MS	F	P
sample	3	0.017805	0.017805	0.005935	1.41	0.311
heating type	1	0.126914	0.126914	0.126914	30.04	0.001
sample*heating type	3	0.038804	0.038804	0.012935	3.06	0.091
Error	8	0.033793	0.033793	0.004224		
Total	15	0.217317				

S = 0.0649937 R-Sq = 84.45% R-Sq(adj) = 70.84%

Grouping Information Using Tukey Method and 95.0% Confidence

```
sample      N   Mean  Grouping
Xanthan     4  1.513  A
Pectin      4  1.477  A
Tragacanth  4  1.454  A
Control     4  1.421  A
```

Means that do not share a letter are significantly different.

Grouping Information Using Tukey Method and 95.0% Confidence

heating			
type	N	Mean	Grouping
conv	8	1.555	A
mw	8	1.377	B

Means that do not share a letter are significantly different.

Grouping Information Using Tukey Method and 95.0% Confidence

heating				
sample	type	N	Mean	Grouping
Xanthan	conv	2	1.677	A
Pectin	conv	2	1.574	A B
Tragacanth	conv	2	1.517	A B
Control	conv	2	1.453	A B
Tragacanth	mw	2	1.391	B
Control	mw	2	1.389	B
Pectin	mw	2	1.380	B
Xanthan	mw	2	1.348	B

Means that do not share a letter are significantly different.

Table A.56 One way Analysis of Variance (ANOVA) and Tukey’s comparison test for the change in the self-diffusion coefficient (SDC x 10⁹, m²/s) of the CV PC hydrogels in phosphate buffer during 6 h experiment

Source	DF	SS	MS	F	P
Time	1	0.03421	0.03421	32.18	0.030
Error	2	0.00213	0.00106		
Total	3	0.03633			

S = 0.03261 R-Sq = 94.15% R-Sq(adj) = 91.22%

Grouping Information Using Tukey Method and 95.0% Confidence

Time	N	Mean	Grouping
6	2	1.57415	A
0	2	1.38920	B

Means that do not share a letter are significantly different.

Table A.57 One way Analysis of Variance (ANOVA) and Tukey's comparison test for the change in the self-diffusion coefficient (SDC x 10⁹, m²/s) of the CV XG hydrogels in phosphate buffer during 6 h experiment

Source	DF	SS	MS	F	P
Time	1	0.10729	0.10729	53.47	0.018
Error	2	0.00401	0.00201		
Total	3	0.11130			

S = 0.04480 R-Sq = 96.39% R-Sq(adj) = 94.59%

Grouping Information Using Tukey Method and 95.0% Confidence

Time	N	Mean	Grouping
6	2	1.67695	A
0	2	1.34940	B

Means that do not share a letter are significantly different.

Table A.58 One way Analysis of Variance (ANOVA) and Tukey's comparison test for the change in the self-diffusion coefficient (SDC x 10⁹, m²/s) of the CV GT hydrogels in phosphate buffer during 6 h experiment

Source	DF	SS	MS	F	P
Time	1	0.015713	0.015713	20.85	0.045
Error	2	0.001507	0.000754		
Total	3	0.017220			

S = 0.02745 R-Sq = 91.25% R-Sq(adj) = 86.87%

Grouping Information Using Tukey Method and 95.0% Confidence

Time	N	Mean	Grouping
6	2	1.51665	A
0	2	1.39130	B

Means that do not share a letter are significantly different.

Table A.59 One way Analysis of Variance (ANOVA) and Tukey's comparison test for the change in the self-diffusion coefficient (SDC x 10⁹, m²/s) of the CV C hydrogels in phosphate buffer during 6 h experiment

Source	DF	SS	MS	F	P
Time	1	0.01536	0.01536	4.69	0.163
Error	2	0.00655	0.00328		
Total	3	0.02192			

S = 0.05724 R-Sq = 70.10% R-Sq(adj) = 55.15%

Grouping Information Using Tukey Method and 95.0% Confidence

Time	N	Mean	Grouping
6	2	1.45295	A
0	2	1.32900	A

Means that do not share a letter are significantly different.

Table A.60 One way Analysis of Variance (ANOVA) and Tukey's comparison test for the change in the self-diffusion coefficient (SDC x 10⁹, m²/s) of the MW PC hydrogels in phosphate buffer during 6 h experiment

Source	DF	SS	MS	F	P
Time	1	0.0102	0.0102	0.95	0.432
Error	2	0.0215	0.0107		
Total	3	0.0317			

S = 0.1037 R-Sq = 32.25% R-Sq(adj) = 0.00%

Grouping Information Using Tukey Method and 95.0% Confidence

Time	N	Mean	Grouping
6	2	1.3800	A
0	2	1.2788	A

Means that do not share a letter are significantly different.

Table A.61 One way Analysis of Variance (ANOVA) and Tukey's comparison test for the change in the self-diffusion coefficient (SDC x 10⁹, m²/s) of the MW XG hydrogels in phosphate buffer during 6 h experiment

Source	DF	SS	MS	F	P
Time	1	0.009575	0.009575	15.85	0.058
Error	2	0.001208	0.000604		
Total	3	0.010783			

S = 0.02458 R-Sq = 88.80% R-Sq(adj) = 83.19%

Grouping Information Using Tukey Method and 95.0% Confidence

Time	N	Mean	Grouping
6	2	1.34815	A
0	2	1.25030	A

Means that do not share a letter are significantly different.

Table A.62 One way Analysis of Variance (ANOVA) and Tukey's comparison test for the change in the self-diffusion coefficient (SDC x 10⁹, m²/s) of the MW GT hydrogels in phosphate buffer during 6 h experiment

Source	DF	SS	MS	F	P
Time	1	0.02681	0.02681	11.88	0.075
Error	2	0.00451	0.00226		
Total	3	0.03133			

S = 0.04750 R-Sq = 85.59% R-Sq(adj) = 78.39%

Grouping Information Using Tukey Method and 95.0% Confidence

Time	N	Mean	Grouping
6	2	1.39065	A
0	2	1.22690	A

Means that do not share a letter are significantly different.

Table A.63 One way Analysis of Variance (ANOVA) and Tukey's comparison test for the change in the self-diffusion coefficient (SDC x 10⁹, m²/s) of the MW C hydrogels in phosphate buffer during 6 h experiment

Source	DF	SS	MS	F	P
Time	1	0.01697	0.01697	7.00	0.118
Error	2	0.00485	0.00242		
Total	3	0.02181			

S = 0.04923 R-Sq = 77.78% R-Sq(adj) = 66.67%

Grouping Information Using Tukey Method and 95.0% Confidence

Time	N	Mean	Grouping
6	2	1.38940	A
0	2	1.25915	A

Means that do not share a letter are significantly different.

Table A.64 One way Analysis of Variance (ANOVA) and Tukey's comparison test for the hardness values (N) of the different CV hydrogels at 0 h

Source	DF	SS	MS	F	P
sample	3	30,5347	10,1782	120,07	0,000
Error	4	0,3391	0,0848		
Total	7	30,8738			

S = 0,2912 R-Sq = 98,90% R-Sq(adj) = 98,08%

Grouping Information Using Tukey Method and 95.0% Confidence

sample	N	Mean	Grouping
Control	2	7,2688	A
Tragacanth	2	5,7668	B
Pectin	2	4,3409	C
Xanthan	2	1,9660	D

Means that do not share a letter are significantly different.

Table A.65 One way Analysis of Variance (ANOVA) and Tukey's comparison test for the hardness values (N) of the different CV hydrogels in phosphate buffer at 24 h

Source	DF	SS	MS	F	P
sample	3	14,785	4,928	42,44	0,002
Error	4	0,464	0,116		
Total	7	15,250			

S = 0,3408 R-Sq = 96,95% R-Sq(adj) = 94,67%

Grouping Information Using Tukey Method and 95.0% Confidence

sample	N	Mean	Grouping
Control	2	5,3544	A
Tragacanth	2	4,6792	A B
Pectin	2	3,8093	B
Xanthan	2	1,7408	C

Means that do not share a letter are significantly different.

Table A.66 One way Analysis of Variance (ANOVA) and Tukey's comparison test for the change in the hardness values (N) of the CV PC hydrogels in phosphate buffer during 24 h experiment

Source	DF	SS	MS	F	P
Time	1	0,283	0,283	2,79	0,237
Error	2	0,203	0,101		
Total	3	0,485			

S = 0,3183 R-Sq = 58,24% R-Sq(adj) = 37,36%

Grouping Information Using Tukey Method and 95.0% Confidence

Time	N	Mean	Grouping
0	2	4,3409	A
24	2	3,8093	A

Means that do not share a letter are significantly different.

Table A.67 One way Analysis of Variance (ANOVA) and Tukey's comparison test for the change in the hardness values (N) of the CV XG hydrogels in phosphate buffer during 24 h experiment

Source	DF	SS	MS	F	P
Time	1	0,051	0,051	0,36	0,608
Error	2	0,279	0,139		
Total	3	0,329			

S = 0,3734 R-Sq = 15,39% R-Sq(adj) = 0,00%

Grouping Information Using Tukey Method and 95.0% Confidence

Time	N	Mean	Grouping
0	2	1,9660	A
24	2	1,7408	A

Means that do not share a letter are significantly different.

Table A.68 One way Analysis of Variance (ANOVA) and Tukey's comparison test for the change in the hardness values (N) of the CV GT hydrogels in phosphate buffer during 24 h experiment

Source	DF	SS	MS	F	P
Time	1	1,1830	1,1830	64,93	0,015
Error	2	0,0364	0,0182		
Total	3	1,2194			

S = 0,1350 R-Sq = 97,01% R-Sq(adj) = 95,52%

Grouping Information Using Tukey Method and 95.0% Confidence

Time	N	Mean	Grouping
0	2	5,7668	A
24	2	4,6792	B

Means that do not share a letter are significantly different.

Table A.69 One way Analysis of Variance (ANOVA) and Tukey's comparison test for the change in the hardness values (N) of the CV C hydrogels in phosphate buffer during 24 h experiment

Source	DF	SS	MS	F	P
Time	1	3,665	3,665	25,66	0,037
Error	2	0,286	0,143		
Total	3	3,951			

S = 0,3780 R-Sq = 92,77% R-Sq(adj) = 89,15%

Grouping Information Using Tukey Method and 95.0% Confidence

Time	N	Mean	Grouping
0	2	7,2688	A
24	2	5,3544	B

Means that do not share a letter are significantly different.

Table A.70 One way Analysis of Variance (ANOVA) and Tukey's comparison test for the diffusion coefficient values (m²/s) of the different CV hydrogels in phosphate buffer

Source	DF	SS	MS	F	P
CV Sample	3	3.575	1.192	3.14	0.096
Error	7	2.653	0.379		
Total	10	6.228			

S = 0.6157 R-Sq = 57.40% R-Sq(adj) = 39.14%

Grouping Information Using Tukey Method and 95.0% Confidence

CV Sample	N	Mean	Grouping
Xanthan	2	2.2900	A
Pectin	3	1.3900	A
Tragacanth	3	1.1300	A
Control	3	0.5887	A

Means that do not share a letter are significantly different.

Table A.71 One way Analysis of Variance (ANOVA) and Tukey's comparison test for the diffusion coefficient values (m^2/s) of the different MW hydrogels in phosphate buffer

Source	DF	SS	MS	F	P
MW Sample	3	0.333	0.111	0.18	0.910
Error	7	4.428	0.633		
Total	10	4.761			

S = 0.7954 R-Sq = 6.99% R-Sq(adj) = 0.00%

Grouping Information Using Tukey Method and 95.0% Confidence

MW Sample	N	Mean	Grouping
Tragacanth	3	1.5267	A
Pectin	3	1.5267	A
Control	3	1.1800	A
Xanthan	2	1.1735	A

Means that do not share a letter are significantly different.

Table A.72 One way Analysis of Variance (ANOVA) and Tukey's comparison test for the diffusion coefficient values (m^2/s) of the CV and MW C hydrogels in phosphate buffer

Source	DF	SS	MS	F	P
Polymer Type	1	0,525	0,525	3,75	0,125
Error	4	0,560	0,140		
Total	5	1,085			

S = 0,3742 R-Sq = 48,35% R-Sq(adj) = 35,44%

Grouping Information Using Tukey Method and 95.0% Confidence

Polymer Type	N	Mean	Grouping
control mw	3	1,1800	A
control cv	3	0,5887	A

Means that do not share a letter are significantly different.

Table A.73 One way Analysis of Variance (ANOVA) and Tukey's comparison test for the diffusion coefficient values (m^2/s) of the CV and MW PC hydrogels in phosphate buffer

Source	DF	SS	MS	F	P
Polymer Type	1	0,0280	0,0280	0,42	0,553
Error	4	0,2679	0,0670		
Total	5	0,2959			

S = 0,2588 R-Sq = 9,47% R-Sq(adj) = 0,00%

Grouping Information Using Tukey Method and 95.0% Confidence

Polymer Type	N	Mean	Grouping
pectin mw	3	1,5267	A
pectin cv	3	1,3900	A

Means that do not share a letter are significantly different.

Table A.74 One way Analysis of Variance (ANOVA) and Tukey's comparison test for the diffusion coefficient values (m^2/s) of the CV and MW GT hydrogels in phosphate buffer

Source	DF	SS	MS	F	P
Polymer Type	1	0.236	0.236	0.25	0.645
Error	4	3.809	0.952		
Total	5	4.045			

S = 0.9758 R-Sq = 5.83% R-Sq(adj) = 0.00%

Grouping Information Using Tukey Method and 95.0% Confidence

Polymer Type	N	Mean	Grouping
tragacanth mw	3	1.5267	A
tragacanth cv	3	1.1300	A

Means that do not share a letter are significantly different.

Table A.75 One way Analysis of Variance (ANOVA) and Tukey's comparison test for the diffusion coefficient values (m^2/s) of the CV and MW XG hydrogels in phosphate buffer

Source	DF	SS	MS	F	P
Polymer Type	1	1,25	1,25	1,02	0,419
Error	2	2,44	1,22		
Total	3	3,69			

S = 1,106 R-Sq = 33,77% R-Sq(adj) = 0,66%

Grouping Information Using Tukey Method and 95.0% Confidence

Polymer Type	N	Mean	Grouping
xanthan cv	2	2,290	A
xanthan mw	2	1,174	A

Means that do not share a letter are significantly different.

Table A.76 One way Analysis of Variance (ANOVA) and Tukey's comparison test for the cumulative release rates (%) of the CV hydrogels in GIT (8 h)

Source	DF	SS	MS	F	P
Hydrogel	3	565.073	188.358	516.31	0.000
Error	4	1.459	0.365		
Total	7	566.532			

S = 0.6040 R-Sq = 99.74% R-Sq(adj) = 99.55%

Grouping Information Using Tukey Method and 95.0% Confidence

Hydrogel	N	Mean	Grouping
Pectin	2	95.715	A
Control	2	87.470	B
Gum Tragacanth	2	79.360	C
Xanthan Gum	2	73.430	D

Means that do not share a letter are significantly different.

Table A.77 One way Analysis of Variance (ANOVA) and Tukey's comparison test for the cumulative release rates (%) of the CV hydrogels in SGF (2 h)

Source	DF	SS	MS	F	P
sample	3	820,9	273,6	16,53	0,001
Error	8	132,4	16,6		
Total	11	953,3			

S = 4,068 R-Sq = 86,11% R-Sq(adj) = 80,90%

Grouping Information Using Tukey Method and 95.0% Confidence

sample	N	Mean	Grouping
Pectin	3	82,999	A
Tragacanth	3	66,917	B
Control	3	66,853	B
Xanthan	3	60,679	B

Means that do not share a letter are significantly different.

Table A.78 One way Analysis of Variance (ANOVA) and Tukey's comparison test for the transverse relaxation times (T_2 , ms) of the different CV hydrogels before gastric treatment

Source	DF	SS	MS	F	P
Sample	3	38,431	12,810	18,97	0,008
Error	4	2,701	0,675		
Total	7	41,131			

S = 0,8217 R-Sq = 93,43% R-Sq(adj) = 88,51%

Grouping Information Using Tukey Method and 95.0% Confidence

Sample	N	Mean	Grouping
Tragacanth	2	53,750	A
Pectin	2	49,515	B
Control	2	49,270	B
Xanthan	2	47,895	B

Means that do not share a letter are significantly different.

Table A.79 One way Analysis of Variance (ANOVA) and Tukey's comparison test for the transverse relaxation times (T_2 , ms) of the different CV hydrogels after gastric treatment (2 h)

Source	DF	SS	MS	F	P
Sample	3	196,82	65,61	40,91	0,002
Error	4	6,41	1,60		
Total	7	203,23			

S = 1,266 R-Sq = 96,84% R-Sq(adj) = 94,48%

Grouping Information Using Tukey Method and 95.0% Confidence

Sample	N	Mean	Grouping
Control	2	84,120	A
Tragacanth	2	82,235	A
Pectin	2	73,970	B
Xanthan	2	72,795	B

Means that do not share a letter are significantly different.

Table A.80 One way Analysis of Variance (ANOVA) and Tukey's comparison test for the change in the transverse relaxation times (T_2 , ms) of the CV PC hydrogels in SGF during 2 h experiment

Source	DF	SS	MS	F	P
Time	4	759,42	189,85	128,04	0,000
Error	5	7,41	1,48		
Total	9	766,83			

S = 1,218 R-Sq = 99,03% R-Sq(adj) = 98,26%

Grouping Information Using Tukey Method and 95.0% Confidence

Time	N	Mean	Grouping
2h	2	73,970	A
1.5h	2	70,745	A
1h	2	63,870	B
0.5h	2	58,815	C
0h	2	49,515	D

Means that do not share a letter are significantly different.

Table A.81 One way Analysis of Variance (ANOVA) and Tukey's comparison test for the change in the transverse relaxation times (T_2 , ms) of the CV XG hydrogels in SGF during 2 h experiment

Source	DF	SS	MS	F	P
Time	4	816,988	204,247	601,66	0,000
Error	5	1,697	0,339		
Total	9	818,685			

S = 0,5826 R-Sq = 99,79% R-Sq(adj) = 99,63%

Grouping Information Using Tukey Method and 95.0% Confidence

Time	N	Mean	Grouping
2h	2	72,795	A
1.5h	2	68,565	B
1h	2	62,580	C
0.5h	2	54,800	D
0h	2	47,895	E

Means that do not share a letter are significantly different.

Table A.82 One way Analysis of Variance (ANOVA) and Tukey's comparison test for the change in the transverse relaxation times (T_2 , ms) of the CV C hydrogels in SGF during 2 h experiment

Source	DF	SS	MS	F	P
Time	4	1557,085	389,271	574,20	0,000
Error	5	3,390	0,678		
Total	9	1560,474			

S = 0,8234 R-Sq = 99,78% R-Sq(adj) = 99,61%

Grouping Information Using Tukey Method and 95.0% Confidence

Time	N	Mean	Grouping
2h	2	84,120	A
1.5h	2	79,330	B
1h	2	72,355	C
0.5h	2	62,375	D
0h	2	49,270	E

Means that do not share a letter are significantly different.

Table A.83 One way Analysis of Variance (ANOVA) and Tukey's comparison test for the change in the transverse relaxation times (T_2 , ms) of the CV GT hydrogels in SGF during 2 h experiment

Source	DF	SS	MS	F	P
Time	4	1023,26	255,81	163,25	0,000
Error	5	7,83	1,57		
Total	9	1031,09			

S = 1,252 R-Sq = 99,24% R-Sq(adj) = 98,63%

Grouping Information Using Tukey Method and 95.0% Confidence

Time	N	Mean	Grouping
2h	2	82,235	A
1.5h	2	76,390	B
1h	2	69,105	C
0.5h	2	61,945	D
0h	2	53,750	E

Means that do not share a letter are significantly different.

Table A.84 One way Analysis of Variance (ANOVA) and Tukey's comparison test for the self-diffusion coefficients (SDC, m²/s) of the different CV hydrogels before gastric treatment

Source	DF	SS	MS	F	P
sample	3	0,014800	0,004933	10,96	0,021
Error	4	0,001800	0,000450		
Total	7	0,016600			

S = 0,02121 R-Sq = 89,16% R-Sq(adj) = 81,02%

Grouping Information Using Tukey Method and 95.0% Confidence

sample	N	Mean	Grouping
Tragacanth	2	1,37500	A
Pectin	2	1,32500	A B
Control	2	1,30500	A B
Xanthan	2	1,25500	B

Means that do not share a letter are significantly different.

Table A.85 One way Analysis of Variance (ANOVA) and Tukey's comparison test for the self-diffusion coefficients (SDC, m²/s) of the different CV hydrogels after gastric treatment (2 h)

Source	DF	SS	MS	F	P
sample	3	0,047600	0,015867	28,85	0,004
Error	4	0,002200	0,000550		
Total	7	0,049800			

S = 0,02345 R-Sq = 95,58% R-Sq(adj) = 92,27%

Grouping Information Using Tukey Method and 95.0% Confidence

sample	N	Mean	Grouping
Xanthan	2	1,56500	A
Tragacanth	2	1,41500	B
Control	2	1,39500	B
Pectin	2	1,36500	B

Means that do not share a letter are significantly different.

Table A.86 One way Analysis of Variance (ANOVA) and Tukey's comparison test for the change in the self-diffusion coefficients (SDC, m²/s) of the CV PC hydrogels in SGF during 2 h experiment

Source	DF	SS	MS	F	P
Time	1	0,001600	0,001600	2,46	0,257
Error	2	0,001300	0,000650		
Total	3	0,002900			

S = 0,02550 R-Sq = 55,17% R-Sq(adj) = 32,76%

Grouping Information Using Tukey Method and 95.0% Confidence

Time	N	Mean	Grouping
2	2	1,36500	A
0	2	1,32500	A

Means that do not share a letter are significantly different.

Table A.87 One way Analysis of Variance (ANOVA) and Tukey's comparison test for the change in the self-diffusion coefficients (SDC, m²/s) of the CV XG hydrogels in SGF during 2 h experiment

Source	DF	SS	MS	F	P
Time	1	0,096100	0,096100	384,40	0,003
Error	2	0,000500	0,000250		
Total	3	0,096600			

S = 0,01581 R-Sq = 99,48% R-Sq(adj) = 99,22%

Grouping Information Using Tukey Method and 95.0% Confidence

Time	N	Mean	Grouping
2	2	1,56500	A
0	2	1,25500	B

Means that do not share a letter are significantly different.

Table A.88 One way Analysis of Variance (ANOVA) and Tukey's comparison test for the change in the self-diffusion coefficients (SDC, m²/s) of the CV GT hydrogels in SGF during 2 h experiment

Source	DF	SS	MS	F	P
Time	1	0,001600	0,001600	1,88	0,304
Error	2	0,001700	0,000850		
Total	3	0,003300			

S = 0,02915 R-Sq = 48,48% R-Sq(adj) = 22,73%

Grouping Information Using Tukey Method and 95.0% Confidence

Time	N	Mean	Grouping
2	2	1,41500	A
0	2	1,37500	A

Means that do not share a letter are significantly different.

Table A.89 One way Analysis of Variance (ANOVA) and Tukey's comparison test for the change in the self-diffusion coefficients (SDC, m²/s) of the CV C hydrogels in SGF during 2 h experiment

Source	DF	SS	MS	F	P
Time	1	0,008100	0,008100	32,40	0,030
Error	2	0,000500	0,000250		
Total	3	0,008600			

S = 0,01581 R-Sq = 94,19% R-Sq(adj) = 91,28%

Grouping Information Using Tukey Method and 95.0% Confidence

Time	N	Mean	Grouping
2	2	1,39500	A
0	2	1,30500	B

Means that do not share a letter are significantly different.

Table A.90 One way Analysis of Variance (ANOVA) and Tukey's comparison test for the diffusion coefficient values (m²/s) of the CV hydrogels in SGF (2 h)

Source	DF	SS	MS	F	P
sample	3	3,134	1,045	8,23	0,015
Error	6	0,762	0,127		
Total	9	3,895			

S = 0,3563 R-Sq = 80,45% R-Sq(adj) = 70,67%

Grouping Information Using Tukey Method and 95.0% Confidence

sample	N	Mean	Grouping
Pectin	2	11,1025	A
Xanthan	3	10,3285	A B
Control	2	9,6844	B
Tragacanth	3	9,6367	B

Means that do not share a letter are significantly different.

Table A.91 One way Analysis of Variance (ANOVA) and Tukey's comparison test for the hardness values (N) of the CV hydrogels after gastric treatment (2 h)

Source	DF	SS	MS	F	P
sample	3	10,3587	3,4529	163,26	0,000
Error	4	0,0846	0,0211		
Total	7	10,4433			

S = 0,1454 R-Sq = 99,19% R-Sq(adj) = 98,58%

Grouping Information Using Tukey Method and 95.0% Confidence

sample	N	Mean	Grouping
Xanthan	2	4,1105	A
Control	2	1,8349	B
Tragacanth	2	1,7156	B
Pectin	2	1,1223	C

Means that do not share a letter are significantly different.

Table A.92 One way Analysis of Variance (ANOVA) and Tukey's comparison test for the total acidity values (g citric acid/100 g gel) of the CV hydrogels before gastric treatment

Source	DF	SS	MS	F	P
sample	3	0,000974	0,000325	3,05	0,092
Error	8	0,000851	0,000106		
Total	11	0,001825			

S = 0,01032 R-Sq = 53,36% R-Sq(adj) = 35,87%

Grouping Information Using Tukey Method and 95.0% Confidence

sample	N	Mean	Grouping
Pectin	3	0,30554	A
Xanthan	3	0,30404	A
Control	3	0,28836	A
Tragacanth	3	0,28548	A

Means that do not share a letter are significantly different.

Table A.93 One way Analysis of Variance (ANOVA) and Tukey's comparison test for the total acidity values (g citric acid/100 g gel) of the CV hydrogels after gastric treatment (2 h)

Source	DF	SS	MS	F	P
sample	3	0,0373753	0,0124584	284,10	0,000
Error	8	0,0003508	0,0000439		
Total	11	0,0377261			

S = 0,006622 R-Sq = 99,07% R-Sq(adj) = 98,72%

Grouping Information Using Tukey Method and 95.0% Confidence

sample	N	Mean	Grouping
Pectin	3	1,32021	A
Tragacanth	3	1,29725	B
Control	3	1,28954	B
Xanthan	3	1,17611	C

Means that do not share a letter are significantly different.

Table A.94 One way Analysis of Variance (ANOVA) and Tukey's comparison test for the reduction of the pH (%) of the CV hydrogels in SGF during 2 h experiment

Source	DF	SS	MS	F	P
sample	3	118,82	39,61	21,91	0,006
Error	4	7,23	1,81		
Total	7	126,05			

S = 1,345 R-Sq = 94,26% R-Sq(adj) = 89,96%

Grouping Information Using Tukey Method and 95.0% Confidence

sample	N	Mean	Grouping
Control	2	58,158	A
Xanthan	2	55,091	A
Pectin	2	49,457	B
Tragacanth	2	49,012	B

Means that do not share a letter are significantly different.

Table A.95 One way Analysis of Variance (ANOVA) and Tukey's comparison test for the increase of the moisture content (%) of the CV hydrogels in SGF during 2 h experiment

Source	DF	SS	MS	F	P
sample	3	31,354	10,451	20,83	0,007
Error	4	2,007	0,502		
Total	7	33,360			

S = 0,7083 R-Sq = 93,98% R-Sq(adj) = 89,47%

Grouping Information Using Tukey Method and 95.0% Confidence

sample	N	Mean	Grouping
Xanthan	2	11,8797	A
Tragacanth	2	9,7400	A B
Pectin	2	8,8533	B C
Control	2	6,3566	C

Means that do not share a letter are significantly different.

Table A.96 One way Analysis of Variance (ANOVA) and Tukey's comparison test for the increase in the release rates (%) of the CV hydrogels in SIF (2 h) with respect to their final release rates after gastric treatment

Source	DF	SS	MS	F	P
sample	3	189.068	63.023	73.22	0.001
Error	4	3.443	0.861		
Total	7	192.512			

S = 0.9278 R-Sq = 98.21% R-Sq(adj) = 96.87%

Grouping Information Using Tukey Method and 95.0% Confidence

sample	N	Mean	Grouping
Control	2	16.831	A
Xanthan	2	8.147	B
Tragacanth	2	6.601	B C
Pectin	2	3.821	C

Means that do not share a letter are significantly different.

Table A.97 One way Analysis of Variance (ANOVA) and Tukey's comparison test for the increase in the release rates (%) of the CV hydrogels in SIF (4 h) with respect to their final release rates after gastric treatment

Source	DF	SS	MS	F	P
sample	3	301.23	100.41	49.49	0.000
Error	5	10.15	2.03		
Total	8	311.37			

S = 1.424 R-Sq = 96.74% R-Sq(adj) = 94.79%

Grouping Information Using Tukey Method and 95.0% Confidence

sample	N	Mean	Grouping
Control	2	25.276	A
Tragacanth	2	14.936	B
Xanthan	3	14.173	B
Pectin	2	8.283	C

Means that do not share a letter are significantly different.

Table A.98 One way Analysis of Variance (ANOVA) and Tukey's comparison test for the increase in the release rates (%) of the CV hydrogels in SIF (6 h) with respect to their final release rates after gastric treatment

Source	DF	SS	MS	F	P
sample	3	268.651	89.550	112.83	0.000
Error	4	3.175	0.794		
Total	7	271.825			

S = 0.8909 R-Sq = 98.83% R-Sq(adj) = 97.96%

Grouping Information Using Tukey Method and 95.0% Confidence

sample	N	Mean	Grouping
Control	2	30.845	A
Xanthan	2	21.009	B
Tragacanth	2	18.587	B C
Pectin	2	15.313	C

Means that do not share a letter are significantly different.

Table A.99 One way Analysis of Variance (ANOVA) and Tukey's comparison test for the soluble protein contents (mg BSA/mL) of the CV hydrogel containing SGF release media at the end of the gastric treatment

Source	DF	SS	MS	F	P
Sample	3	1,45087	0,48362	233,07	0,000
Error	8	0,01660	0,00208		
Total	11	1,46747			

S = 0,04555 R-Sq = 98,87% R-Sq(adj) = 98,44%

Grouping Information Using Tukey Method and 95.0% Confidence

Sample	N	Mean	Grouping
Pectin	3	2,23000	A
Tragacanth	3	2,21333	A
Xanthan	3	1,72667	B
Control	3	1,40333	C

Means that do not share a letter are significantly different.

Table A.100 One way Analysis of Variance (ANOVA) and Tukey's comparison test for the soluble protein contents (mg BSA/mL) of the CV hydrogel containing SIF release media at the end of the intestinal treatment

Source	DF	SS	MS	F	P
Sample	3	1,16108	0,38703	40,17	0,000
Error	8	0,07707	0,00963		
Total	11	1,23815			

S = 0,09815 R-Sq = 93,78% R-Sq(adj) = 91,44%

Grouping Information Using Tukey Method and 95.0% Confidence

Sample	N	Mean	Grouping
Tragacanth	3	5,3079	A
Pectin	3	4,9124	B
Control	3	4,7225	B
Xanthan	3	4,4535	C

Means that do not share a letter are significantly different.

Table A.101 One way Analysis of Variance (ANOVA) and Tukey's comparison test for the transverse relaxation times (T_2 , ms) of the CV hydrogels after SIF treatment (6 h)

Source	DF	SS	MS	F	P
Sample	3	650,776	216,925	402,03	0,000
Error	4	2,158	0,540		
Total	7	652,934			

S = 0,7346 R-Sq = 99,67% R-Sq(adj) = 99,42%

Grouping Information Using Tukey Method and 95.0% Confidence

Sample	N	Mean	Grouping
Tragacanth	2	63,160	A
Control	2	59,965	B
Pectin	2	58,085	B
Xanthan	2	40,000	C

Means that do not share a letter are significantly different.

Table A.102 One way Analysis of Variance (ANOVA) and Tukey's comparison test for the change in the transverse relaxation times (T_2 , ms) of the CV C hydrogels during SIF treatment (6 h)

Source	DF	SS	MS	F	P
Time	3	794.161	264.720	626.06	0.000
Error	4	1.691	0.423		
Total	7	795.852			

S = 0.6503 R-Sq = 99.79% R-Sq(adj) = 99.63%

Grouping Information Using Tukey Method and 95.0% Confidence

Time	N	Mean	Grouping
0	2	84.120	A
2	2	62.595	B
4	2	61.075	B
6	2	59.965	B

Means that do not share a letter are significantly different.

Table A.103 One way Analysis of Variance (ANOVA) and Tukey's comparison test for the change in the transverse relaxation times (T_2 , ms) of the CV PC hydrogels during SIF treatment (6 h)

Source	DF	SS	MS	F	P
Time	3	307.36	102.45	60.96	0.001
Error	4	6.72	1.68		
Total	7	314.08			

S = 1.296 R-Sq = 97.86% R-Sq(adj) = 96.25%

Grouping Information Using Tukey Method and 95.0% Confidence

Time	N	Mean	Grouping
0	2	73.970	A
2	2	60.990	B
4	2	60.590	B
6	2	58.085	B

Means that do not share a letter are significantly different.

Table A.104 One way Analysis of Variance (ANOVA) and Tukey's comparison test for the change in the transverse relaxation times (T_2 , ms) of the CV GT hydrogels during SIF treatment (6 h)

Source	DF	SS	MS	F	P
Time	3	459.808	153.269	224.97	0.000
Error	4	2.725	0.681		
Total	7	462.533			

S = 0.8254 R-Sq = 99.41% R-Sq(adj) = 98.97%

Grouping Information Using Tukey Method and 95.0% Confidence

Time	N	Mean	Grouping
0	2	82.235	A
2	2	68.935	B
4	2	64.275	C
6	2	63.160	C

Means that do not share a letter are significantly different.

Table A.105 One way Analysis of Variance (ANOVA) and Tukey's comparison test for the change in the transverse relaxation times (T_2 , ms) of the CV XG hydrogels during SIF treatment (6 h)

Source	DF	SS	MS	F	P
Time	3	1394.922	464.974	693.81	0.000
Error	4	2.681	0.670		
Total	7	1397.603			

S = 0.8186 R-Sq = 99.81% R-Sq(adj) = 99.66%

Grouping Information Using Tukey Method and 95.0% Confidence

Time	N	Mean	Grouping
0	2	72.795	A
2	2	45.580	B
4	2	42.355	B C
6	2	40.000	C

Means that do not share a letter are significantly different.

Table A.106 One way Analysis of Variance (ANOVA) and Tukey's comparison test for the hardness values (N) of the CV hydrogels after SIF treatment (6 h)

Source	DF	SS	MS	F	P
sample	3	51,2588	17,0863	471,92	0,000
Error	4	0,1448	0,0362		
Total	7	51,4036			

S = 0,1903 R-Sq = 99,72% R-Sq(adj) = 99,51%

Grouping Information Using Tukey Method and 95.0% Confidence

sample	N	Mean	Grouping
Xanthan	2	8,7282	A
Control	2	5,4965	B
Tragacanth	2	3,0932	C
Pectin	2	2,1879	D

Means that do not share a letter are significantly different.

Table A.107 One way Analysis of Variance (ANOVA) and Tukey's comparison test for the change in the hardness values (N) of the CV PC hydrogels during SIF treatment (6 h)

Source	DF	SS	MS	F	P
Time	1	1,13538	1,13538	192,88	0,005
Error	2	0,01177	0,00589		
Total	3	1,14715			

S = 0,07672 R-Sq = 98,97% R-Sq(adj) = 98,46%

Grouping Information Using Tukey Method and 95.0% Confidence

Time	N	Mean	Grouping
6	2	2,1879	A
0	2	1,1223	B

Means that do not share a letter are significantly different.

Table A.108 One way Analysis of Variance (ANOVA) and Tukey's comparison test for the change in the hardness values (N) of the CV XG hydrogels during SIF treatment (6 h)

Source	DF	SS	MS	F	P
Time	1	21,3236	21,3236	350,10	0,003
Error	2	0,1218	0,0609		
Total	3	21,4454			

S = 0,2468 R-Sq = 99,43% R-Sq(adj) = 99,15%

Grouping Information Using Tukey Method and 95.0% Confidence

Time	N	Mean	Grouping
6	2	8,7282	A
0	2	4,1105	B

Means that do not share a letter are significantly different.

Table A.109 One way Analysis of Variance (ANOVA) and Tukey's comparison test for the change in the hardness values (N) of the CV GT hydrogels during SIF treatment (6 h)

Source	DF	SS	MS	F	P
Time	1	1,8978	1,8978	187,37	0,005
Error	2	0,0203	0,0101		
Total	3	1,9181			

S = 0,1006 R-Sq = 98,94% R-Sq(adj) = 98,42%

Grouping Information Using Tukey Method and 95.0% Confidence

Time	N	Mean	Grouping
6	2	3,0932	A
0	2	1,7156	B

Means that do not share a letter are significantly different.

Table A.110 One way Analysis of Variance (ANOVA) and Tukey's comparison test for the change in the hardness values (N) of the CV C hydrogels during SIF treatment (6 h)

Source	DF	SS	MS	F	P
Time	1	13,4078	13,4078	354,81	0,003
Error	2	0,0756	0,0378		
Total	3	13,4834			

S = 0,1944 R-Sq = 99,44% R-Sq(adj) = 99,16%

Grouping Information Using Tukey Method and 95.0% Confidence

Time	N	Mean	Grouping
6	2	5,4965	A
0	2	1,8349	B

Means that do not share a letter are significantly different.

Table A.111 One way Analysis of Variance (ANOVA) and Tukey's comparison test for the weight loss values (%) of the CV hydrogels during 6h SIF treatment

Source	DF	SS	MS	F	P
Sample	3	256,88	85,63	39,59	0,000
Error	8	17,30	2,16		
Total	11	274,18			

S = 1,471 R-Sq = 93,69% R-Sq(adj) = 91,32%

Grouping Information Using Tukey Method and 95.0% Confidence

Sample	N	Mean	Grouping
Xanthan	3	43,630	A
Pectin	3	38,737	B
Control	3	33,297	C
Tragacanth	3	32,003	C

Means that do not share a letter are significantly different.

Table A.112 One way Analysis of Variance (ANOVA) and Tukey's comparison test for the total phenolic contents (mg Gallic acid/mL sample) of the yogurt samples at the end of the first week of the storage

Source	DF	SS	MS	F	P
Sample	4	0.052027	0.013007	22.17	0.000
Error	10	0.005867	0.000587		
Total	14	0.057893			

S = 0.02422 R-Sq = 89.87% R-Sq(adj) = 85.81%

Grouping Information Using Tukey Method and 95.0% Confidence

Sample	N	Mean	Grouping
Control	3	1.03000	A
Xanthan	3	0.96333	B
Tragacanth	3	0.93667	B
Pectin	3	0.93667	B
Yogurt with no hydrogel	3	0.84667	C

Means that do not share a letter are significantly different.

Table A.113 One way Analysis of Variance (ANOVA) and Tukey's comparison test for the total phenolic contents (mg Gallic acid/mL sample) of the yogurt samples at the end of the fourth week of the storage

Source	DF	SS	MS	F	P
Sample	4	0.08487	0.02122	7.06	0.006
Error	10	0.03007	0.00301		
Total	14	0.11493			

S = 0.05483 R-Sq = 73.84% R-Sq(adj) = 63.38%

Grouping Information Using Tukey Method and 95.0% Confidence

Sample	N	Mean	Grouping
Control	3	1.04000	A
Tragacanth	3	0.94000	A B
Pectin	3	0.93000	A B

Xanthan	3	0.92000	A B
Yogurt with no hydrogel	3	0.80333	B

Means that do not share a letter are significantly different.

Table A.114 One way Analysis of Variance (ANOVA) and Tukey's comparison test for the antioxidant capacities (mg Trolox/mL sample) of the yogurt samples at the end of the first week of the storage

Source	DF	SS	MS	F	P
Sample	4	0.7694031	0.1923508	3358.86	0.000
Error	10	0.0005727	0.0000573		
Total	14	0.7699757			

S = 0.007567 R-Sq = 99.93% R-Sq(adj) = 99.90%

Grouping Information Using Tukey Method and 95.0% Confidence

Sample	N	Mean	Grouping
Control	3	0.54100	A
Tragacanth	3	0.50833	B
Pectin	3	0.48333	C
Xanthan	3	0.07933	D
Yogurt with no hydrogel	3	0.02367	E

Means that do not share a letter are significantly different.

Table A.115 One way Analysis of Variance (ANOVA) and Tukey's comparison test for the antioxidant capacities (mg Trolox/mL sample) of the yogurt samples at the end of the fourth week of the storage

Source	DF	SS	MS	F	P
Sample	4	0.662003	0.165501	1156.27	0.000
Error	10	0.001431	0.000143		
Total	14	0.663434			

S = 0.01196 R-Sq = 99.78% R-Sq(adj) = 99.70%

Grouping Information Using Tukey Method and 95.0% Confidence

Sample	N	Mean	Grouping
Tragacanth	3	0.47000	A
Control	3	0.45933	A
Pectin	3	0.44300	A
Xanthan	3	0.06167	B
Yogurt with no hydrogel	3	0.00000	C

Means that do not share a letter are significantly different.

Table A.116 One way Analysis of Variance (ANOVA) and Tukey's comparison test for the change in the total phenolic contents (mg Gallic acid/mL sample) of the CV C hydrogel containing yogurt samples during storage (1 – 4 weeks)

Source	DF	SS	MS	F	P
Week	1	0.000150	0.000150	0.30	0.613
Error	4	0.002000	0.000500		
Total	5	0.002150			

S = 0.02236 R-Sq = 6.98% R-Sq(adj) = 0.00%

Grouping Information Using Tukey Method and 95.0% Confidence

Week	N	Mean	Grouping
4	3	1.04000	A
1	3	1.03000	A

Means that do not share a letter are significantly different.

Table A.117 One way Analysis of Variance (ANOVA) and Tukey's comparison test for the change in the total phenolic contents (mg Gallic acid/mL sample) of the CV PC hydrogel containing yogurt samples during storage (1 – 4 weeks)

Source	DF	SS	MS	F	P
Week	1	0.00007	0.00007	0.04	0.859
Error	4	0.00747	0.00187		
Total	5	0.00753			

S = 0.04320 R-Sq = 0.88% R-Sq(adj) = 0.00%

Grouping Information Using Tukey Method and 95.0% Confidence

Week	N	Mean	Grouping
1	3	0.93667	A
4	3	0.93000	A

Means that do not share a letter are significantly different.

Table A.118 One way Analysis of Variance (ANOVA) and Tukey's comparison test for the change in the total phenolic contents (mg Gallic acid/mL sample) of the CV GT hydrogel containing yogurt samples during storage (1 – 4 weeks)

Source	DF	SS	MS	F	P
Week	1	0.00002	0.00002	0.00	0.948
Error	4	0.01367	0.00342		
Total	5	0.01368			

S = 0.05845 R-Sq = 0.12% R-Sq(adj) = 0.00%

Grouping Information Using Tukey Method and 95.0% Confidence

Week	N	Mean	Grouping
4	3	0.94000	A
1	3	0.93667	A

Means that do not share a letter are significantly different.

Table A.119 One way Analysis of Variance (ANOVA) and Tukey's comparison test for the change in the total phenolic contents (mg Gallic acid/mL sample) of the CV XG hydrogel containing yogurt samples during storage (1 – 4 weeks)

Source	DF	SS	MS	F	P
Week	1	0.00282	0.00282	0.89	0.399
Error	4	0.01267	0.00317		
Total	5	0.01548			

S = 0.05627 R-Sq = 18.19% R-Sq(adj) = 0.00%

Grouping Information Using Tukey Method and 95.0% Confidence

Week	N	Mean	Grouping
1	3	0.96333	A
4	3	0.92000	A

Means that do not share a letter are significantly different.

Table A.120 One way Analysis of Variance (ANOVA) and Tukey's comparison test for the change in the total phenolic contents (mg Gallic acid/mL sample) of the yogurt samples with no blended hydrogel during storage (1 – 4 weeks)

Source	DF	SS	MS	F	P
Week	1	0.0028167	0.0028167	84.50	0.001
Error	4	0.0001333	0.0000333		
Total	5	0.0029500			

S = 0.005774 R-Sq = 95.48% R-Sq(adj) = 94.35%

Grouping Information Using Tukey Method and 95.0% Confidence

Week	N	Mean	Grouping
1	3	0.846667	A
4	3	0.803333	B

Means that do not share a letter are significantly different.

Table A.121 One way Analysis of Variance (ANOVA) and Tukey's comparison test for the change in the antioxidant capacities (mg Trolox/mL sample) of the CV C hydrogel containing yogurt samples during storage (1 – 4 weeks)

Source	DF	SS	MS	F	P
Week	1	0.0100042	0.0100042	1500.62	0.000
Error	4	0.0000267	0.0000067		
Total	5	0.0100308			

S = 0.002582 R-Sq = 99.73% R-Sq(adj) = 99.67%

Grouping Information Using Tukey Method and 95.0% Confidence

Week	N	Mean	Grouping
1	3	0.541000	A
4	3	0.459333	B

Means that do not share a letter are significantly different.

Table A.122 One way Analysis of Variance (ANOVA) and Tukey's comparison test for the change in the antioxidant capacities (mg Trolox/mL sample) of the CV PC hydrogel containing yogurt samples during storage (1 – 4 weeks)

Source	DF	SS	MS	F	P
Week	1	0.002440	0.002440	8.69	0.042
Error	4	0.001123	0.000281		
Total	5	0.003563			

S = 0.01675 R-Sq = 68.49% R-Sq(adj) = 60.61%

Grouping Information Using Tukey Method and 95.0% Confidence

Week	N	Mean	Grouping
1	3	0.48333	A
4	3	0.44300	B

Means that do not share a letter are significantly different.

Table A.123 One way Analysis of Variance (ANOVA) and Tukey's comparison test for the change in the antioxidant capacities (mg Trolox/mL sample) of the CV GT hydrogel containing yogurt samples during storage (1 – 4 weeks)

Source	DF	SS	MS	F	P
Week	1	0.002204	0.002204	15.40	0.017
Error	4	0.000573	0.000143		

Total 5 0.002777

S = 0.01197 R-Sq = 79.38% R-Sq(adj) = 74.22%

Grouping Information Using Tukey Method and 95.0% Confidence

Week	N	Mean	Grouping
1	3	0.50833	A
4	3	0.47000	B

Means that do not share a letter are significantly different.

Table A.124 One way Analysis of Variance (ANOVA) and Tukey's comparison test for the change in the antioxidant capacities (mg Trolox/mL sample) of the CV XG hydrogel containing yogurt samples during storage (1 – 4 weeks)

Source	DF	SS	MS	F	P
Week	1	0.0004682	0.0004682	6.66	0.061
Error	4	0.0002813	0.0000703		
Total	5	0.0007495			

S = 0.008386 R-Sq = 62.46% R-Sq(adj) = 53.08%

Grouping Information Using Tukey Method and 95.0% Confidence

Week	N	Mean	Grouping
1	3	0.079333	A
4	3	0.061667	A

Means that do not share a letter are significantly different.

CURRICULUM VITAE

Surname, Name: Özel, Barış

EDUCATION

Degree	Institution	Year of Graduation
BS	METU Food Engineering	2013
High School	Ödemiş Anadolu Öğretmen High School, İzmir	2008

WORK EXPERIENCE

Year	Place	Enrollment
2014-Present	METU Dept. of Food Eng.	Research Assistant
2019-2020	University of Massachusetts Amherst	Visiting Researcher
2014	Ahi Evran University	Research Assistant

FOREIGN LANGUAGES

Advanced English, Intermediate German

PUBLICATIONS

1. **Ozel, B.** "Organogels", In M. Miao, L. Chen & D. J. McClements (Eds.), *Bioactive Delivery Systems for Lipophilic Nutraceuticals: Formulation, Fabrication, and Application*. Royal Society of Chemistry (in press)
2. **Ozel, B.**, Oztop, M. H. "Rheology of food hydrogels, and organogels", In J. Ahmed & S. Basu (Eds.), *Advances in Food Rheology and Its Applications* (2nd ed., pp. 657-684). Cambridge, MA: Woodhead Publishing (2023)
3. Tirpanci, B., **Ozel, B.**, Oztop, M. H., Alpas, H. "Stability of acidified milk drinks: Comparison of high hydrostatic pressure (HHP) and thermal treatments", *International Dairy Journal*, 147, 105512 (2023)
4. Kalayci, A., **Ozel, B.**, Oztop, M. H., Alpas, H. "Investigation of the effects of high hydrostatic pressure on the functional properties of pea protein isolate", *Journal of Food Process Engineering*, e14243 (2022)

5. Uguz, S. S., **Ozel, B.**, Grunin, L., Ozvural, E. B., Oztop, M. H. "Non-conventional time domain (TD)-NMR approaches for food quality: Case of gelatin-based candies as a model food", *Molecules*, 27(19), 6745 (2022)
6. **Ozel, B.**, McClements, D. J., Arikan, C., Kaner, O., Oztop, M. H. "Challenges in dried whey powder production: Quality problems", *Food Research International*, 160, 111682 (2022)
7. Okur, I., **Ozel, B.**, Ucbas, D., Grunin, L., Sezer Okur, P., Alpas, H., Ide, S., Oztop, M. H. "Nuclear magnetic resonance (NMR) study of palm kernel stearin: Effects of cooling rate on crystallization behaviour", *LWT-Food Science and Technology*, 155, 113001 (2022)
8. **Ozel, B.**, Kruk, D., Wojciechowski, M., Osuch, M., Oztop, M. H. "Water dynamics in whey-protein-based composite hydrogels by means of NMR relaxometry", *International Journal of Molecular Sciences*, 22(18), 9672 (2021)
9. Elik, A., Kocak Yanik, D., **Ozel, B.**, Oztop, M. H., Gogus, F. "The effects of pectin and wax on the characteristics of oil-in-water (O/W) emulsions", *Journal of Food Science*, 86(7), 3148-3158 (2021)
10. **Ozel, B.**, Oztop, M. H. "A quick look to the use of time domain nuclear magnetic resonance relaxometry and magnetic resonance imaging for food quality applications", *Current Opinion in Food Science*, 41, 122-129 (2021)
11. Akkaya, S., **Ozel, B.**, Kocak Yanik, D., Oztop, M. H., Gogus, F. "Physical characterization of high methoxyl pectin and sunflower oil wax emulsions: A low-field ¹H NMR relaxometry study", *Journal of Food Science*, 86(1), 120-128 (2021)
12. **Ozel B.**, Zhang Z., He L., and McClements D. J. "Digestion of Animal- and Plant-Based Proteins Encapsulated in κ -Carrageenan/Protein Beads Under Simulated Gastrointestinal Conditions", *Food Research International*, 137, 109662 (2020)
13. Alacik Develioglu I., **Ozel B.**, Oztop, M. H., and Sahin, S. "NMR Relaxometry and Magnetic Resonance Imaging as Tools to Determine the Emulsifying Characteristics of Quince Seed Powder in Emulsions and Hydrogels", *International Journal of Biological Macromolecules*, 164, 2051-2061 (2020)
14. **Ozel B.**, Aydin O., and Oztop, M. H. "In vitro Digestion of Polysaccharide Including Whey Protein Isolate Hydrogels", *Carbohydrate Polymers*, 229, 115469 (2020)
15. Okur I., **Ozel B.**, Oztop M. H., and Alpas H. "Effect of High Hydrostatic Pressure in Physicochemical Properties and in vitro Digestibility of Cornstarch by Nuclear Magnetic Resonance Relaxometry", *Journal of Food Process Engineering*, 42(6), e13168 (2019)

16. **Ozel B.**, Aydin O., Grunin L., and Oztop M. H. "Physico-chemical Changes of Composite Whey Protein Hydrogels in Simulated Gastric Fluid Conditions", *Journal of Agricultural and Food Chemistry*, 66(36), 9542-9555 (2018)
17. Sevdin S., **Ozel B.**, Yucel U., Oztop M. H. and Alpas H. "High Hydrostatic Pressure Induced Changes on Palm Stearin Emulsions", *Journal of Food Engineering*, 229, 65-71 (2018)
18. **Ozel B.**, Dag D., Kilercioglu M., Sumnu S. G., and Oztop M. H. "NMR Relaxometry as a Tool to Understand the Effect of Microwave Heating on Starch-Water Interactions and Gelatinization Behavior", *LWT-Food Science and Technology*, 83, 10-17 (2017)
19. **Ozel B.**, Cikrikci S., Aydin O., and Oztop M. H. "Polysaccharide Blended Whey Protein Isolate-(WPI) Hydrogels: A Physicochemical and Controlled Release Study", *Food Hydrocolloids*, 71, 35-46 (2017)
20. **Ozel B.**, Uguz S. S., Kilercioglu M., Grunin L., and Oztop M. H. "Effect of Different Polysaccharides on Swelling of Composite Whey Protein Hydrogels: A Low Field (LF) NMR Relaxometry Study", *Journal of Food Process Engineering*, 40(3), e12465 (2017)
21. Kilercioglu M., **Ozel B.**, and Oztop M. H. "Characterization and Comparison of Turkish Table Olive Varieties with NMR Relaxometry and Magnetic Resonance Imaging", *Gida/The Journal of Food*, 41(2), 61-67 (2016)
22. Kilercioglu M., **Ozel B.**, Karacam C. H., Pocan P., and Oztop M. H. "Yüksek Sıcaklığın ve Nemli Ortamın Fındıktaki Su ve Yağ Dağılımına Olan Etkisinin Manyetik Rezonans Görüntüleme (MRG) ve NMR Relaksometre Teknikleri ile Belirlenmesi", *Gida/The Journal of Food*, 40(3), 141-148 (2015)

HOBBIES

Philosophy, History, Football, Basketball, Music, Video games